

**KWAME NKRUMAH UNIVERSITY OF SCIENCE AND TECHNOLOGY
COLLEGE OF ENGINEERING FACULTY OF MECHANICAL AND
CHEMICAL ENGINEERING DEPARTMENT OF MATERIALS
ENGINEERING**

KNUST

**THERMALLY ACTIVATED CLAY AND BIOMASS MIXTURES AS
SUPPLEMENTARY CEMENTITIOUS MATERIALS FOR SUSTAINABLE
CONSTRUCTION IN GHANA**

By

MARK BEDIAKO (BSc. (Hons), MPhil)

**A THESIS SUBMITTED IN PARTIAL FULFILMENT OF THE
REQUIREMENTS FOR THE AWARD OF DEGREE OF DOCTOR OF
PHILOSOPHY IN MATERIALS ENGINEERING**



MAY 2015

KNUST



Abstract

The concept of sustainable development is probably one of the most significant gifts of the 21st century to human kind in pursuit of benign environment, sound economic growth and a peaceful society. Many researchers have reported that there is gross lack of respect for the ecosystem and other factors that support quality of life for human beings and this seriously threatens mankind in this millennium on earth. Currently the global emphasis on sustainability has urged many engineers to design products and provide services that incorporate the concepts of sustainability. The cement industry is among the industries whose activities have negative impact on sustainability due to its huge economic, ecological and societal footprint. In recent times the cement industry has become fully aware of these negative impacts and has currently positioned itself to address these footprints. This study sought to formulate cementitious materials as partial replacement of cement estimated to have lesser footprint on the economy, environment and society compared to the use of only Portland cement for construction. The formulated cementitious materials were prepared using clay and waste biomass at different replacement levels by mass of clay powder. The waste biomass used for the study included palm kernel shells, rice husk, maize cob and sawdust. These biomass materials were selected because of their elemental silica and calorific values which had the potential to impact positively on the properties of calcined clay. Formulated clay and waste biomass were used to form pellets which were thermally activated in an electric furnace and used to replace Portland cement at percentages between 10% and 40% by weight. The experimental approach for this study was segmented into six different phases and they included biomass characterization, optimum temperature of clay calcination and dosage determination, maximum clay/biomass mixture and optimum dosage

determination, influence of calcined clay and clay/biomass mixture on Portland cement hydration and pozzolanic reaction, durability studies and sustainability analysis. The maximum clay/biomass mixture and optimum dosage increasing effect determination were performed using the compressive strength machine whereas the thermogravimetric analyzer and the nuclear magnetic angle machine were used to investigate the influence of calcined clay and clay/biomass on cement. Durability studies performed in this work focused on shrinkage and sorptivity analysis. The results from the study showed that complete calcination of clays was achieved at 800°C, and therefore attained optimum performance in terms of strength. The maximum strength activity indices obtained for mortar mixtures involving Portland cement and calcined clay/biomass mixture were at 20% and 1.5% replacement of clay with palm kernel shells and sawdust respectively whereas that of rice husk and maize cob were at 2% replacement by weight of clay. 20 wt% calcined clay, calcined clay/palm kernel shells, calcined clay/maize cob and calcined clay/sawdust, and 30 wt% of calcined clay/rice husk pozzolans produced the optimum strengths. At optimum values, thermogravimetric and MAS NMR analysis were performed using their formulated binder paste. The thermal gravimetric analysis showed that calcined clay/rice husk paste mixture indicated a higher degree of pozzolanic reaction than the calcined clay paste mixture at all periods. The degree of pozzolanic reaction of the other calcined products remained sluggish at earlier periods however indicated a consumption pattern higher than the calcined clay paste system. At 28 days calcined clay/palm kernel shells and clay/sawdust mixtures showed similar lime consumption pattern like calcined clay paste system. The analysis by the MAS ^{29}Si and ^{27}Al NMR also indicated the formation of increased polymerized materials and stable monosulphates respectively, confirming strength enhancement of cement-pozzolan system than only Portland cement system. The

results obtained from the shrinkage studies indicated insignificant effect with regards to Portland cement and calcined clay mortar mixtures. However, with sorptivity analysis, there were significant effects with regards to the type of calcined products used for the mortar mixture formulation. Generally, all the calcined products showed a lower initial and secondary sorptivity coefficient values than the control which indicated a higher resistance to ingress of ions. Calcined products that included clay/palm kernel shells and clay/maize cob indicated a higher sorptivity coefficient values than calcined clay mortar mixture whereas that of calcined clay/rice husk and clay/sawdust had lower initial and secondary sorptivity values. The study showed that the use of the supplementary cementitious materials investigated could save between 9% and 14% on cement utilization which will mean a significant cost reduction of cement importation. Moreover, the inclusion of the selected biomass in the supplementary cementitious materials (SCMs) production could also save the country between \$0.12 million and \$1.59 million depending on the type of biomass.

KNUST

Dedication

I dedicate this work to my departed father Edward Bediako and sister Flora Bediako who unfortunately couldn't see the academic success of his son and her senior brother.



Acknowledgement

First and foremost, I would like to thank the Almighty God who through his son Jesus Christ provides all things to his children who diligently seek him. Within the period of this study, the Lord Jesus Christ has been the source of my strength and the one who empowered me with heavenly wisdom to finish this PhD thesis. May the name of the most-high be praised

My second thanks go to my supervisors, Prof. S.K.Y. Gawu and Dr. A.A. Adjaottor for the confidence and belief they have reposed in me over the years.

Thirdly I would like to extend my heartfelt gratitude to Dr. John Tristan Kevern of the University of Missouri-Kansas City, United States. Dr. Kevern offered me the opportunity in the university and acted as an external supervisor for my work. I salute you Sir for the wonderful hospitality you showed to me whilst carrying my thesis project in the United States.

Fourthly, I would like to thank Emerald publishers for granting me an African Engineering Research Award which provided a significant financial relief to me whilst pursuing my thesis in the United States.

Last but not the least, I would like to express my sincere gratitude to my wife Hannah Okyere Bediako, my mother Madam Beatrice Brayie and my siblings Jones and Nancy Bediako for their financial support and encouragements.

Lastly, I would like to acknowledge two important persons, Dr. Eugene Atiemo and Mr. Augustine Boateng for their tremendous effort and roles played for the success of this PhD program.

Table of Contents

Abstract	ii
Dedication	v
Acknowledgement	vi
Table of Contents	vii
List of Figures	xi
List of Appendices	xvii
1.0 Introduction	1
1.1 Background	1
1.2 Statement of Problem	4
1.2.1 The construction industry dimension	4
1.2.2 The Biomass industry dimension	11
1.3 Objectives of the study	12
1.4 Research hypothesis	12
1.5 Research significance	13
1.6 Justification of the study	14
1.7 Scope of the study	14
CHAPTER TWO	16
2.0 Literature Review	16
2.1 Sustainability and Sustainable Development: the use of the term from literature	16
2.2 Sustainable Development: History and Emergence	16
2.2.1 History	16
2.2.2 Emergence	18
2.3 What is Sustainability?	20
2.3.1 The commonalities between the definitions of sustainability	24
2.3.2 The Brundtland Commission's Definition: Ambiguities versus Commonalities	24
2.4 Principles and pillars of sustainable development	25
2.4.1 Principles	25
2.4.2 Pillars	26
2.5 The construction industry and sustainability	27

2.6 Sustainable development practices in the global construction industry	29
2.7 The Biomass industry	29
2.7.1 What is Biomass?	29
2.7.2 Classification of Biomass	30
2.7.3 Composition of Biomass	30
2.7.4 Some examples of biomass feedstock and their usage around the globe.....	34
2.8 The Ghanaian biomass	35
2.9 Potential biomass feedstock considered for pozzolan production in Ghana	37
2.10 Thermal decomposition of solid biomass	38
2.10.1 General mechanism	38
2.11 Biomass characterization and ash properties	40
2.11.1 Palm kernel shells	41
2.11.2 Maize residues	43
2.11.3 Rice Husk	44
2.11.4 Saw dust	48
2.11.5 Chemical composition of biomass ashes.....	49
2.12 Introduction to pozzolana	49
2.12.1 What is Pozzolana?	52
2.12.2 Types of pozzolana	52
2.12.3 The benefits of using pozzolanic materials	53
2.12.4 Pozzolan utilization in Ghana	54
2.13 The cement industry	56
2.13.1 Production of Portland cement	56
2.13.2 Properties of Portland cement: Chemical, mineralogical and physical	57
2.13.3 Reaction of cement compounds	59
2.13.4 Mechanism of Portland cement hydration	62
2.13.5 Microstructure of the hydrated phases of cement	64
2.14 Pozzolan reaction	69
2.15 Clays and clay pozzolana production	70
2.15.1 Clay	70
2.15.2 Types of clay minerals	71
2.15.3 Clay layer	72

2.15.4 Clay pozzolana production	78
2.15.5 Degree of dehydroxylation based on calcination temperatures	78
2.15.6 Degree of dehydroxylation based on calcination time	80
2.16 Characterization of pozzolana.....	81
2.16.1 Classification based on chemistry or mineralogy	81
2.16.2 Classification based on performance	91
2.17 Pozzolanic activity of clay pozzolana	93
2.17.1 Pozzolana strength activity index	94
2.17.2 Optimum temperature determination of calcined clays using strength activity index	95
2.18 Influence of clay pozzolana in cement matrix	95
2.18.1 Physical properties of cement paste and mortar	95
2.18.2 Analysis of the hydrated phases of cement and blended pozzolana cement ..	102
2.18.3 Microstructure of hydrated phases	115
2.19 Durability studies of cement and pozzolana based system	117
2.19.1 Shrinkage of cementitious mortars	118
2.19.2 Water Sorptivity.....	120
CHAPTER THREE	122
3.0 Materials and Methods	122
3.1 Materials	122
3.1.1. Portland cements	122
3.1.2 Clay	122
3.1.3 Biomass	124
3.1.4 Sand.....	124
3.2 Experimental approach	125
3.3 Test methods	129
3.3.1 Formation of clay/biomass pellets	129
3.3.2 Test on biomass samples	130
3.3.3. Calcination of samples and pulverization	131
3.3.4 Test on raw and calcined powder materials	131
3.3.5 Strength test on mortars	132

3.3.6 Test on cementitious binder paste.....	133
3.3.6 Durability test	136
CHAPTER FOUR	140
4.0 RESULTS AND DISCUSSIONS	140
4.1 Properties of selected biomass	140
4.1.1. Mineralogical composition	140
4.1.2 Chemical composition	142
4.2 Properties of raw and calcined clay	144
4.2.1 Thermal gravimetric analysis of powder clay	144
4.2.2 Mineralogical composition	148
4.2.3 MAS NMR analysis	150
4.3 Optimum calcination temperature and replacement level of calcined clay	154
4.3.1 Optimal temperature determination	154
4.3.2 Obtaining the optimal replacement level	156
4.4 Determination of maximum clay/biomass proportions based on strength activity index	158
4.5 Optimum replacement of Calcined clay/biomass mixes	163
4.5.1 Comparison of compressive strength of control and optimum mixes	167
4.6 Consistency and setting times of optimum mixtures	167
4.7 Test on hydrated phases.....	169
4.7.1 Calcium hydroxide content and degree of pozzolanic reaction	169
4.7.2 MAS NMR analysis	173
4.8 Durability studies	180
4.8.1 Shrinkage	180
4.8.2 Water Sorptivity	185
4.9 Sustainability analysis	189
5.1 Conclusion	193
5.2 Recommendations	196
REFERENCES	198

List of Figures

Figure 2.1: Thermal decomposition of palm kernel shells (Okoreigwe and Shaffron,

2012)	43
Figure 2.2: TG/DTG graph of corn residuum	46
Figure 2.3: DTA graph of corn residuum	46
Figure 2.4: Thermochemical conversion of rice husk (Mansaray and Ghaly, 1998)	47
Figure 2.5: Thermochemical process of sawdust pyrolysis (Gao et al, 2013)	49
Figure 2.6: X-ray diffraction analysis of unhydrated cement (Jain, 2012)	59
Figure 2.7: Schematic illustration of the microstructure development of OPC (Scrivener, 1984)	66
Figure 2.8: 1-day old cement grain (Diamond, 2004 and Kjellsen and Justnes, 2004)	68
Figure 2.9: Microstructure of alite cured for 14 days at room temperature (Costoya Fernandez, 2008)	68
Figure 2.10: Microstructure of a 100-day old cement paste (Diamond, 2004)	69
Figure 2.11 Sheet components of clay mineral (Erberl, 1984)	72
Figure 2.12: Structure of 1:1 layer (Anon, 2001)	73
Figure 2.13: A structure of 2:1 clay mineral (Kurecic and Smole, 2012)	73
Figure 2.14: Process cycle for clay formation (Eberl, 1984)	77
Figure 2.15: Differential thermal analysis of kaolinite, illite and montmorillonite clay structures (Fernandez et al, 2011)	80
Figure 2.16: Dehydroxylation of calcined clays at different temperatures and time (Ilic et al, 2010)	81
Figure 2.17: Hump structure between 2 theta= 15-35 of metakaolin (750°C) (AL-Salami et al, 2013).....	85
Figure 2.18: X-ray diffraction patterns of fired clays at different temperature (Samet et al, 2007)	86
Figure 2.19: NMR spectras of kaolinite (a), illite (b) and montmorillonite (c) (Fernandez et al, 2013).....	88
Figure 2.20: Si MAS NMR spectra for calcined kaolinitc clay between 600 and 800°C (Maia et al, 2014)	90
Figure 2.21: DTG curves for raw and calcined kaolinite, illite and montmorillonite clay structures	90
Figure 2.22: XRD patterns of white cement and calcined kaolin hydrated pastes at 28 days (AL-Salami et al, 2013)	105

Figure 2.23: TG/DTA of cement and 15% silica paste cured at 24 hrs and 28 days (Esteves, 2014)	107
Figure 2.24: Al NMR spectra of anhydrous blends and pastes at 28 days (Fernandez et al, 2011).....	111
Figure 2.25: Spectrum of chemical shift regions of different Si tetrahedral, Q ⁿ showing the number of Si atoms connected to the central Si atom (Maclaren and White, 2003).	113
Figure 2.26: Si MAS NMR spectra of the hydration products of a blend of 80% OPC/20% MK ordinary 1, 7, 36 and 100days (Brough et al, 1996).	114
Figure 2.27: Hydrated cement paste containing pozzolanic fly ash (Antiohos et al, 2006)	116
Figure 2.28: SEM of 28 days hydrated 20% pozzolana (RHA) blended cement (Jain, 2012).....	117
Figure 2.29: Crystals of hydrated cement-pozzolana (fly ash) system at 90 days and EDX analysis (Antiohos et al, 2006)	117
Figure 3.1. Map showing the location of Nyamabekeyere in Ashanti region	123
Figure 3.2: Biomass waste, a. Palm kernel shells, b. rice husk, c. maize cob, d. sawdust	124
Figure 3.3: Flow chart for the experimental approach	128
Figure 3.4: Schematic diagram of sorptivity experiment (After ASTM C1885)	139
Figure 4.1: X ray diffraction analysis of biomass ashes: A-palm kernel; B-rice husk; C-miaze cob; D-sawdust	141
Figure 4.2(a): TGA analysis of powdered clay	146
Figure 4.2(b): DTA analysis of powdered clay	147
Figure 4.3: XRD overlay of raw clay and calcined clay at 600°C, 800°C and 1000°C	149
Figure 4.4: ²⁷ Al solid state MAS NMR of raw and calcined clays	152
Figure 4.5: ²⁹ Si solid state MAS NMR of raw and calcined clays	153
Figure 4.6 Optimum temperature for thermally activated clay	155
Figure 4.7: Compressive strength test of mortars containing calcined clay pozzolana (800°C)	157
Figure 4.8: Pozzolan strength activity index of cement and clay/palm kernel shell pozzolana	160
Figure 4.9: Pozzolana strength activity index of cement and rice husk pozzolana	161
Figure 4.10: Pozzolana strength activity index of cement and maize cobs	162

Figure 4.11: Pozzolana strength activity index of cement and sawdust	163
Figure 4.12: Compressive strength of mortar with varying calcined clay/palm kernel shells	164
Figure 4.13: Compressive strength of mortar with varying calcined clay/rice husk pozzolan	165
Figure 4.14: Compressive strength of mortar with varying calcined clay/maize cobs pozzolan	166
Figure 4.15: Compressive strength of mortars with varying calcined clay/sawdust pozzolan	166
Figure 4.16: CH consumption of control, calcined clay and calcined clay/palm kernel shells	170
Figure 4.17: CH consumption of control, calcined clay and calcined clay/rice husk.	171
Figure 4.18: CH consumption of control, calcined clay and calcined clay/maize cobs	172
Figure 4.19: CH consumption of control, calcined clay and calcined clay/ sawdust	173
Figure 4.20 ²⁷ Al MAS NMR spectra of hydrated cement and cement/ calcined clay paste; A-3 days, B- 7days, C- 28 days.	175
Figure 4.21 ²⁷ Al MAS NMR spectra of hydrated cement and cement/ calcined clay and palm kernel shells paste; A-3 days, B- 7days, C- 28 days.	176
Figure 4.22 ²⁷ Al MAS NMR spectra of hydrated cement and cement/ calcined clay and rice husk paste; A-3 days, B- 7days, C- 28 days.	177
Figure 4.23 ²⁷ Al MAS NMR spectra of hydrated cement and cement/ calcined clay and maize cob paste; A-3 days, B- 7days, C- 28 days.	178
Figure 4.24 ²⁷ Al MAS NMR spectra of hydrated cement and cement/ calcined clay and sawdust paste; A-3 days, B- 7days, C- 28 days.	179
Figure 4.25: ²⁹ Si MAS NMR spectra of hydrated cement and cement/ calcined clay paste; A-3 days, B- 7days, C- 28 days.	182
Figure 4.26: Average measured total and autogenous shrinkages of CON, 20P800 and 20PK2 mortars.....	183
Figure 4.27: Average measured total and autogenous shrinkages of CON, 20P800 and 30RH1 mortars	183
Figure 4.28: Average measured total and autogenous shrinkages of CON, 20P800 and 20MC1 mortar prisms	184

Figure 4.29: Average measured total and autogenous shrinkages of CON, 20P800 and 20SD2 mortar prisms	185
Figure 4.30: Sorptivity of control, calcined clay and calcined clay/palm kernel shells pozzolan mortars	186
Figure 4.31: Sorptivity of control, calcined clay and calcined clay/rice husk pozzolan mortars	187
Figure 4.32: Sorptivity of control, calcined clay and calcined clay/maize cob pozzolan mortars	188
Figure 4.33: Sorptivity of control, calcined clay and calcined clay/sawdust pozzolan mortars	189
List of Tables	

Table 2.1: Sources and different definitions of sustainability	23
Table 2.2: Classification of biomass (Vassilev et al (2012)	33
Table 2.3: Carbohydrates and lignin components of different biomass (Vassilev et al (2002)	34
Table 2.4: Occurrence of significant inorganic constituents in biomass (Oberberger et al, 1997).	34
Table 2.5: Some biomass feedstocks and their usage around the World.....	35
Table 2.6: Production of some principal food crops in Ghana (FAOSTAT 2011/2012)	37
Table 2.7: Estimated biomass production and residues generation in 2012(FAOSTAT, 2013; Duku et al 2011)	38
Table 2.8: Main characteristics of palm kernel shells	42
Table 2.9: Main characteristics of corn waste residues	45
Table 2.10: Main characteristics of raw rice husk.....	47
Table 2.11: Main characteristics of sawdust	48
Table 2.12: Chemical composition of biomass ashes	51
Table 2.13: Summary of chemical data for a selection of Portland cement (Lea, 1970)	57
Table 2.14 Main mineral compounds in Portland cement (Neville, 2003).....	58
Table 2.15: Clay deposit in Ghana (Kesse, 1985)	78
Table 2.16: Indian standards classification based on strength activity index (Day, 1990)	92
Table 2.17: ASTM classification based on strength activity index (Day, 1990)	92

Table 3.1 Properties of portlland cement, clay, PK, RH, MC and SD	125
Figure 3.3: Flow chart for the experimental approach	128
Table 3.2: Clay and biomass mix proportions	130
Table 3.3: Mortar mixture name and proportions for strength activity determination	134
Table 4.1: Chemical composition of biomass ashes at 800°C	143
Table 4.2 Mortar mix proportion for strength activity index of calcined clays	155
Table 4.3: Mortar mixture proportion containing Portland cement and calcined clay	157
Table 4.4: Mortar mix proportions of Portland cement and calcined clay based biomasses	158
Table 4.5: Setting times of binder paste	168
Table 4.6: Calcium hydroxide content of control and hydrated paste samples	169
Table 4.7: Estimated annual Portland cement and SCM consumption	191
Table 4.8: Estimated cost of cement and SCM consumption	191
Table 4.9: Estimated annual consumption of calcined clay and biomass.....	191
Table 4.10: Estimated annual carbon emissions	192



List of Appendices

Appendix 3.1: Chemical composition of Ashgrove and Ghacem cements	228
Appendix 3.2: t-Test on Portland cements	228
Two-Sample Assuming Unequal Variances	228
Appendix 4.1(a): Compressive strength values of blended cement and clay pozzolana mortars	229
Appendix 4.1(b): Mean, standard deviation and coefficient of variance of strength values in a	229
Appendix 4.3: Student t-test analysis between 20RH1 and 30RH1	230
Appendix 4.4: Student t-test analysis between 10MC2 and 20MC2.....	230
Appendix 4.5: Comparison of strength performance of control and mortar mixes	231
Appendix 4.6: Anova outcome of control and optimum mortar mixes	231
Appendix 4.7: Anova test for shrinkage of CON, 20P800 and 20PK2 at 7, 11, and 18 days	231



CHAPTER ONE

1.0 Introduction

1.1 Background

Sustainable development and resiliency are of enormous interest globally and require us to meet the needs of the present while allowing future generations the ability to adapt to meet their needs. Human development activities on the earth, while improving living conditions, do irrevocable damage to the planet. Globally, it is now accepted that sustainable development and resilient design are the models for shaping our future. The world's scientific community has a plethora of definitions regarding sustainable development; however, the definition according to the United Nations sponsored committee, the Brundtland Committee remains the most accepted. The report produced by the Brundtland committee in 1987 continues to be the main tool for championing sustainability. Sustainability concepts are underpinned by the following: environmental conservation, economic development, social justice and the elimination of poverty especially in developing countries. Environmental conservation refers to waste and pollution reduction, and energy efficiency. Economic development also refers to better distribution and management of resources, affordability and greater efficiency whilst the social dimension involves alternative growth, alternative vision of society, etc.

The agricultural industry is arguably the most important industry sector since it provides food security for a sustained survival of humanity. Ghana is no exception to this;

Ghanaian agriculture provides over 90% of the country's food needs (Duku et al. 2011).

Major food crops grown are starchy staples (cassava, plantain, cocoyam, and yam), cereals (maize, rice, millet, and sorghum), industrial or energy crops (cocoa, coffee, coconut, sugarcane and oil palm), and legumes (groundnut, cowpea and soybeans). Data from FAOSTAT has shown yearly increases in agricultural activities (Anon, 2013). The annual growth in agriculture production means an increase in industrial agricultural biomass waste from the additional food production. Biomass residues obtained from agricultural activities has now become an interesting area for many researchers because of their renewability and as a cleaner energy source. Currently many programs have been put in place by the United Nations and European Union to foster biomass use by promoting research, technology dissemination and piloting of projects. In most of these sponsored programs, biomass has been utilized to produce biodiesel, biofuel, and heat and power (Bergmann et al, 2013).

As biomass becomes better utilized for fuel, the construction industry has begun paying a great deal of attention to the possibility of beneficially using agricultural waste products. Many countries have successfully used lignocellulosic biomass feedstock to obtain sustainable construction materials. Examples of such construction materials are pozzolans from rice husk, corn husk, palm kernel shells, vetiver grass, etc; partition boards from sawdust, wood chippings, grasses, etc. Burning these agricultural waste products creates energy and also converts the elemental silica contained within the plant cells into an amorphous form which can be used in cement-based materials (Demis et al, 2014). Ghana, an agricultural nation abounds in biomass resources; however, biomass is not beneficially utilized. Results from this research project will allow biomass residue to be converted into value-added construction products of great necessity to the nation. Among the principal

biomass produced in Ghana, the cereal industry and the energy crop industry could potentially be suitable for the production of construction building materials such as bricks and pozzolans. The abundance of clay minerals in Ghana is a good source of such raw material. Around the globe, many researchers have reported on the enormous benefits of pozzolanic materials which include cost reduction in concrete formation, reduction of anthropogenic harmful gases (carbon dioxide) from the cement industries, concrete and mortar strength improvement, and formation of durable concretes. This research is unique because it utilizes the feedstock energy in the waste agricultural biomass to thermally activate the local clay materials, producing a low-cost, regional building material.

Creation of a material which allows low cost infrastructure development while supporting and benefiting food production, could be the future model for developing nations. The use of supplementary materials that could be produced locally could save the country from the burden of foreign exchange. Pozzolans produced from natural occurring minerals such as clays, shales, diatomaceous earth and zeolitic materials have very wideranging overall chemical and mineralogical compositions. For this reason, clay pozzolans can tolerate the presence of different types of biomass in considerable percentages which may not necessarily compromise their usage in construction. Using biomass residue as both the heating fuel and as an elemental silica and aluminate components with the clay could be an added advantage to the reactive nature of calcined clay.

1.2 Statement of Problem

The problems identified for the research can broadly be placed into two dimensions; namely the construction industry and the biomass industry.

1.2.1 The construction industry dimension

The problems the construction industry poses on planet earth could be viewed from three different angles which include environmental, economic and technical issues. The environmental concerns are basically centered on pollution and resource extractions. Economic growth through infrastructural developments has largely been dependent on Portland cement. As the industrialized countries continue to grow coupled with a boom in massive infrastructural developments in many emerging and other large economic countries such as China, India and Brazil, the trend of world cement production will continue to increase. However, the increased production and demand for Portland cement means an increase in environmental pollution. Figure 1.1 shows the world trend of cement production between 2004 and 2013. In the year 2004, cement consumption rose from 2.1 billion tonnes to 2.83 billion tonnes and further to approximately 3.77 billion tonnes and 4.0 billion tonnes by 2012 and 2013 respectively (Global Cement Report, 2013).

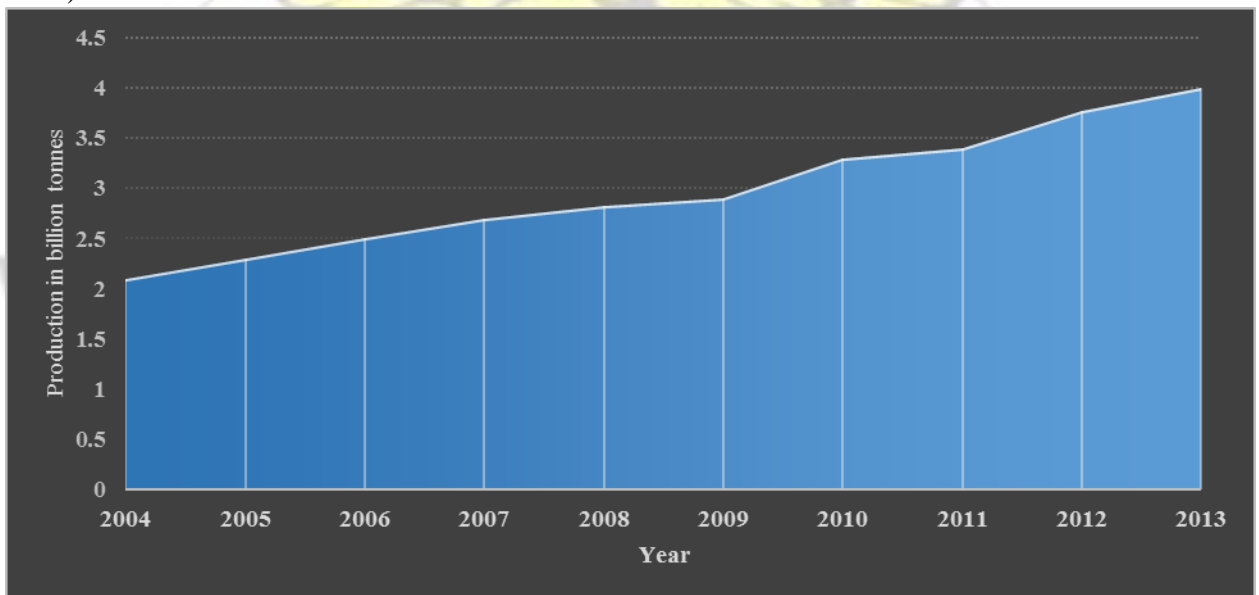


Figure 1.1: World production of cement from 2004-2013 (Source: Global cement production)

For a tonne of cement produced approximately one tonne of carbon dioxide and other greenhouse gases are released into the atmosphere (Gartner and Macphee, 2011). With cement production, CO₂ emissions are obtained through the combustion and calcination processes of the calcareous and argillaceous materials that lead to clinker formation. The cement industry contributes between 5-10% of global CO₂ emissions and other greenhouse gases, the main causes of global warming (Alwood et al, 2010; Faludi, 2004). The consequences of global warming is associated with the melting of glaciers, occurrence of cyclones (hurricanes, tsunamis and other intense rotating storms), drought which is prevalent in some Asia and African countries.

With the increasing demand of Portland cement for infrastructural developments in the industrialized countries, the booming infrastructure development in the large economic nations, the cement production is projected to reach 4.3 billion tonnes and 5 billion tonnes worldwide by 2015 and 2030 respectively (Potgieter, 2012; OECD/IEA, 2003). This trend will have a significant impact on the worldwide level of harmful anthropogenic greenhouse gases (GHG) emission. The trend of cement consumption looks very unpleasant for the future of global environment and therefore has prompted the cement industries to approach this matter with all seriousness in minimizing cement plants emissions.

The cement industry in Ghana also plays a significant role in global greenhouse gas emissions due to the progressively increasing demand for Portland cement. Though clinker is not produced in Ghana and therefore direct CO₂ emissions are very minimal, however

our dependence on foreign clinker-producing factories indirectly contributes to greenhouse gas levels worldwide. Figure 1.2 shows the cement consumption trends in Ghana from 1999 to 2012. The Figure indicates that the consumption of cement increased from 1.8 million tonnes in 1999 to 2.6 million tonnes in 2005 and then to approximately 3.5 million tonnes in 2012 (Global Cement report, 2013). It is projected to reach over 5 million tonnes of consumption by the year 2020. By this, it could be inferred that Ghana would be contributing approximately 5 million tonnes of carbon emissions by the year 2020.

The progressive increase of cement use in the country is attributed to demand for shelter due to population increase and other infrastructural developments for a nation that has attained a lower middle income status. Similar to the world's trend on cement production, the Ghanaian consumption trend cannot insulate herself as a contributor to carbon dioxide and other greenhouse gas emissions. Global harmful anthropogenic gas emissions could best be dealt with through local or country interventions. Supplementary cementitious materials utilization is known to reduce CO₂ emissions and consequently a significant reduction on the threats of global warming. The United Nations sponsored program, the Kyoto Protocol instituted a carbon credit program. The program is implemented through a mechanism called Clean Development Mechanism (CDM) which has a great incentive for projects that reduce CO₂ emissions in developing countries (Fairbairn et al, 2010). CDM allows emission-reduction or removal to earn Certified Emission Reduction (CER) credits, each equivalent to one tonne of CO₂. A replacement of about 50% of cement worldwide among cement consuming countries with cementitious materials will reduce CO₂ emissions by more than one million tonnes (Codeiro et al, 2011).

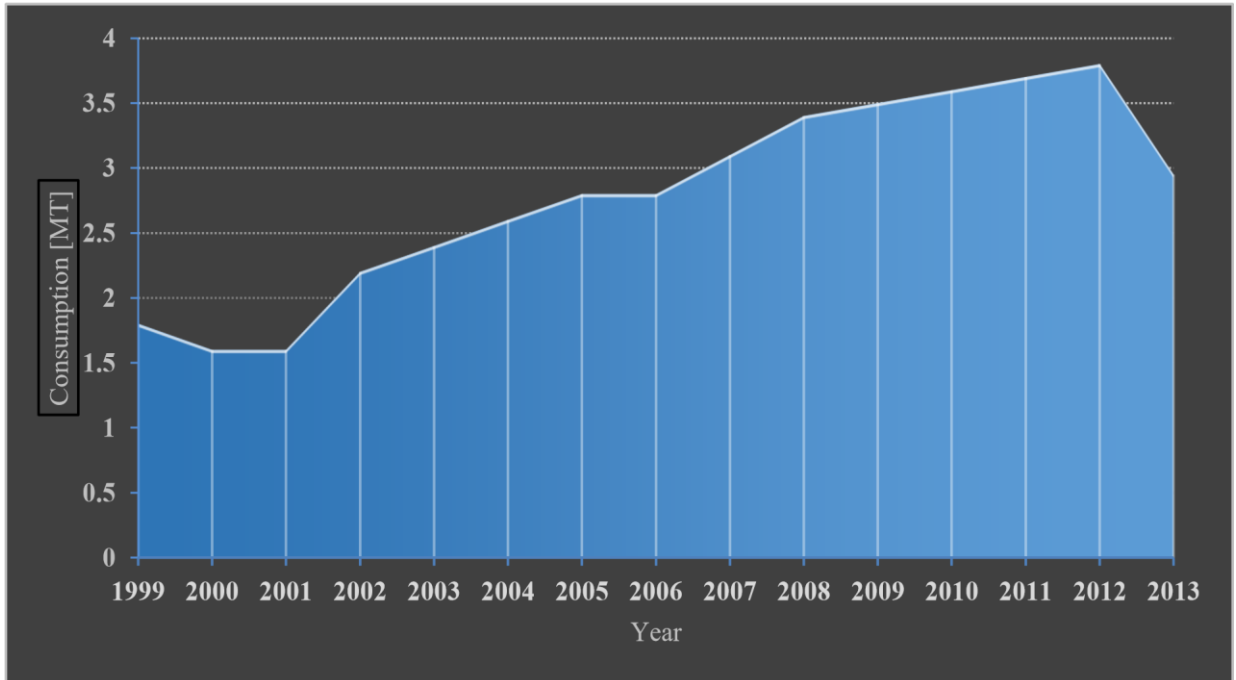


Figure 1.2: Portland cement consumption trends in Ghana (Global cement report, 2013)

The second problem is viewed from the angle of economics. Portland cement remains a highly-demanded commodity in the Ghanaian construction industry. It is the main binding ingredient available to almost every builder in the country. As has been indicated earlier the main ingredients for Portland cement production, clinker and gypsum are imported. Cement producers in Ghana operate as grinding companies. Due to the importation of cement ingredients to the country huge amount of funds is used as foreign exchange for its importation. It is reported that over US\$270 million is used annually for clinker importation (Kudiabor, 2013). In the worse scenario of extreme depreciation of the Ghanaian cedi (GHc) against major currencies such as the United States dollar (\$), the Schengen nations Euros (€), and other trading currencies, foreign exchange demand for cement ingredients (clinker and gypsum) surges up.

The consequence of foreign exchange demand for clinker and gypsum importation coupled with unreliability of the Ghanaian Cedi against major currencies has been the major cause of annual cement price increases in the country. This usually causes the increase in cost of housing and other construction delivery in Ghana, a major hindrance for low income earners in building decent accommodation, creating an increase in indecent structures, makeshift houses and slums in our cities and villages. Meanwhile, the country has over 70% of income earners within the middle and low income groups (Ghana statistical service, 2012). Indeed, the case of indecent houses which is very prone to weather attack like rainfall is very common in the villages of Ghana where over 70% of the farming activities are found.

Moreover, the unstable nature of cement prices is also a major constraint for most private and government project execution (Bediako et al, 2012). The Ghana government social intervention program such as the affordable housing project has been stalled till date and among the reasons given to it is the high cost of cement. Figure 1.3 shows the trend in prices of 50kg of cement gathered in Ashanti region between 2000 and 2014. The figure shows that the price of a 50kg bag of cement has risen by approximately 12 folds since 2000 till now. The prices of cement differ from region to region due to the proximity to cement manufacturing companies located in the port cities of the country at Tema and Takoradi in the Greater Accra and Western region respectively. Keeping in mind the main problem of shelter, low cost housing is the right solution. In low cost housing, the major component that affects the economy is ordinary Portland cement.

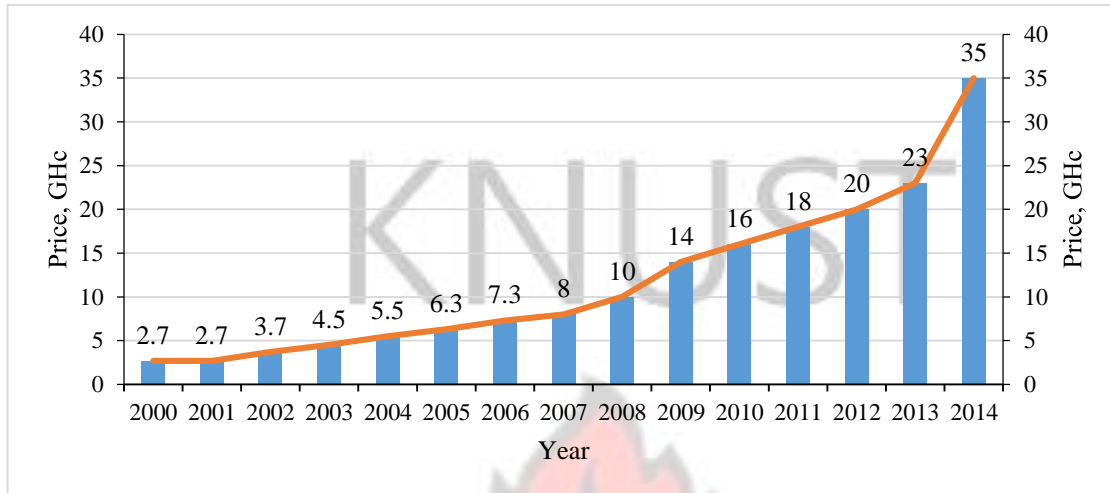


Figure 1.3: Average retail price of Portland cement in Ashanti region from 2000-2014

Cement manufacturing companies have made some interventions to minimize the importation of clinker and gypsum and to decrease housing cost. However, their form of intervention is creating environmental threats which perhaps are unknown to the society.

The intervention has been the production of blended cements using limestone. Almost all Ghanaian limestone resources have been grabbed by these cements manufacturers and mined for composite cement production (Anon, 2010). The Ghana government as well as the society has been made to accept the good part of this intervention which is minimization of foreign exchange demand; however, the hard fact is that Ghana in no time will be left impoverished due to dwindling nature of our limestone resources through the activities of cement manufacturers. As limestone will soon become a limited resource, renewable biomass and clay mixes, very abundant in Ghana could be considered and processed as alternative pozzolanic materials for non-renewable natural resource like limestone. Poor communities could also benefit from using less costly blended cement for infrastructure development such as homes, schools, community

centers, etc.

The third problem under this dimension is a technical-based issue. The use of Portland cement for mortar and concrete formation is associated with diverse problems which include concrete cracking due to thermal and shrinkage effect, and rise of ions through the pores of concrete and mortars which leads to sulphate, chloride and acid attacks (Bediako and Frimpong, 2013). All these that happen in cement concretes point out that cement alone is not very durable. These problems threaten cement buildings service life which has a direct impact on sustainability. The principle of sustainability is controlled by the durability of materials. Structural failure could be facilitated because of shrinkage effect and rise of ions within available pores in a cement matrix. The use of pozzolanic materials with the help of chemical admixtures could provide better remedies to such problems when used as a component of the cement concrete matrix.

1.2.2 The Biomass industry dimension

Under this dimension, the problems of the biomass industry are considered from three different perspectives; environmental, economic and technological. The environmental dimension is center on pollution and disposal of biomass residues. In Ghana most farmers dispose biomass residues in two ways: 1) via open burning either in the farmland or by the roadside and 2) leaving residues on farmlands to decay. The former generates carbon dioxide through open burning activities which poses environmental and health threats while the latter are usually taken away by driving rains choking storm drainages resulting in flooding and creation of unsightly cities after serious downpour. It has been reported that flooded areas and communities breed plenty of mosquitoes which lead to malaria, a major disease in Ghana which puts much pressure on government expenditure. All these are

serious disincentives to environmental sustainability especially in the farming communities.

Waste generated from biomass forms part of the organic components in the area of solid waste. The nation generates approximately 3.6 million tonnes of solid waste and an average amount of \$9.91 is spent to collect a ton of solid waste (Ofori-Boateng et al, 2013; Anon, 2010). It is estimated that about \$36 million is spent annually on solid waste collection. The lack of technological advancement to convert biomass residues into useful resources make them to be perceived as waste materials. The Ghanaian biomass industry holds many prospects for the construction industry, producing abundance of biomass feedstock. The ability to produce construction materials using biomass as a major constituent could ensure sustainability by minimizing the amount spent on solid waste collection by metropolitan, municipal, district assemblies, provision of additional revenue and employment opportunities for farming communities in Ghana.

1.3 Objectives of the study

The main objective of the work is to produce supplementary cementitious materials using clay and biomass mixtures termed as biomass clay pozzolan (BCP). Clay cannot be used as a cementitious material without first heating (partial calcination). Using biomass residue as both the heating fuel and as an elemental component with the clay is novel and has a great potential to create a high quality building material. In achieving this objective, the following specific objectives were outlined:

1. Characterization of the selected biomasses in terms of their calorific values, chemical and mineralogical properties of their ashes.

2. Determination of the optimum calcination temperature and optimum dosage of the calcined clay pozzolan
3. Determination of optimum mixture proportions and optimum dosage of calcined clay and biomass mixtures
4. Evaluation the durability of calcined clay and biomass mixtures
5. Analysis on the sustainability of using supplementary cementitious materials containing biomass.

1.4 Research hypothesis

Clay can be processed into a cementitious material called clay pozzolana. In the same vein, some biomass could also be produced and processed as pozzolanic materials similar to clay pozzolan. On that basis, there could be an enhanced pozzolanic property which could be very suitable for construction when the two, clay and potential pozzolanic biomass, are mixed together and processed as such.

The study therefore seeks to address the following questions:

1. Does the inclusion of biomass affect the mechanical and non-mechanical properties of these calcined clays?
2. What influence does biomass inclusion in clay has on the phase composition of biomass clay pozzolan?
3. Does the addition of biomass in calcined clay influence the hydration products?
4. Why should biomass and clay be considered as a more sustainable construction material in the cement industry?
5. How can biomass and clay be optimized to produce reactive pozzolana?

1.5 Research significance

The following contributions will be made from the project:

1. Reduction in the environmental footprint caused as a results of global anthropogenic gas emissions from cement production and consumption as well as mineral extraction through local interventions.
2. There will be an expansion in the available alternative cementitious materials for construction
3. Provide cost effectiveness in housing delivery especially for low-income earners.
4. Provide a window in the the treatment and disposal of solid waste management
5. Create additional revenue for farmers by converting an agricultural waste into a demand-driven commodity.
6. Create jobs in the farming communities.
7. Capacity building of people to progress towards sustainable development This project has the potential to provide economic value to a current waste product while increasing the ability of Ghanaian people especially the rural folks to obtain quality infrastructure. Moreover, the successful development of biomass clay pozzolana will be beneficial to other West African countries whose economies are driven by agriculture. This could be executed within African states through technology export and policy transfer among the West African states.

1.6 Justification of the study

The following reasons justify the study:

1. Scientific evidence has proven that global warming is a threat to human survival on earth. The path to success for low carbon emitting cement industry requires a

collaborative and integrated approach from all members. Cement industries are targeting emissions reductions through local mediation approaches. The statement that says “Think Globally, Act locally” applies to the approach.

2. There is limited information on biomass clay pozzolana. In this case the technological principle for producing pozzolana from biomass and clay mixtures is not well developed and documented in our research institutions.
3. Biomass and clay that can be used for the production of pozzolana are readily available in Ghana

1.7 Scope of the study

The experimental approach for this study was segmented into six different phases and they included biomass characterization, optimum temperature of clay calcination and dosage determination, maximum clay/biomass mixture and optimum dosage determination, influence of calcined clay and clay/biomass mixture on Portland cement hydration and pozzolanic reaction, durability studies and sustainability analysis. In this study two major cereal crops constituting about 90% of cereal production, maize and rice husk residues, sawdust and an energy crop, oil palm, which constitute about 65% of energy crops grown in the country were selected and used as part of raw feed in clay to produce biomass clay pozzolana (BCP). The clay sample that was used for the study was sourced from Nyamebkyere, a farming community that is very rich in clay in the Atwima Nwabiagya district located at the Western part of Ashanti region.

CHAPTER TWO

2.0 Literature Review

2.1 Sustainability and Sustainable Development: the use of the term from literature

The term sustainability and sustainable development are used interchangeably within the research fraternity by many researchers from different field of studies. In most cases both terms are used in a manner to connote the same meaning. Examples of such could be traced in the studies of Bond & Morrisons-Saunders (2011), some sustainability reports produced by the United Nations Stockholm conference on environment in 1970, the World Commission on Environment also known as the Brundtland Commission report in 1987 set up by the United Nation, the 1992 Rio Earth Summit and the 2002 World Summit on sustainable development. The two terms, sustainability and sustainable development have already with time become a popular term especially in ecological or environmental economics (Mori & Christodoulou, 2012). However, these two terms have sometimes been used distinctively by either the government and private sector or the academics and non-governmental organizations (NGOs). Whilst the government and private sector organizations have tended to adopt the term sustainable development, the academicians and NGOs use the term sustainability in similar context (Robinson, 2004).

2.2 Sustainable Development: History and Emergence

2.2.1 History

Sustainability concepts have a historical antecedent emanating from the teachings and ethics of religious beliefs and traditions. Old Religions such as Judaism and Christianity are more environmentally minded and therefore have been agents in preserving our

environment (Gottlieb, 1996). The Hawaiian traditional belief view the entire world as being alive in the same way that humans are alive whilst in the African tradition, man is considered as a friend and a beneficiary, hence must obey the laws of natural, moral and mystical order (Mbiti, 1996). If these are unduly disturbed, it is man who suffers (Mebratu, 1998).

In 1713, an idea of sustainable development i.e. “sustainable yield” first appeared in a forest science literature “*Sylvicultura Oeconomica*”. The book was edited by a German metallurgist called Hans Carl Von Carlowitz. In this book he argued that timber would be as important as our daily bread and that it should be used with caution in a way, that there is a balance between timber growth and lumbering thus promoting a continuous and a steady use of timber (Jalkanen and Nygren, 2005).

Other theories which were developed after Carlowitz have also laid a platform for understanding sustainability. Example is the Malthus’s economics and the theory of limits which came into the limelight when the industrial revolution of the world surfaced. The surfacing of the industrial revolution brought some problems like unemployment, poverty and disease to humanity. According to the ideas of William Goldwins and Marquis de Condorcet, evil human institutions contributed to the problems associated with the industrial transformation (Mebratu, 1998). However, the Malthus theory disagreed with the ideas of the two gentlemen and rather stated that the main vices and misery that plagued society was due to the fecundity of the human race. His reason was that the fixed amount of land available meant that as the population grew, diminishing return would minimise

per capita food supply. The invention of technical innovations such as the use of fertilizers revealed the theory's short-falls by increasing food production output on fixed lands but didn't eliminate the problem of diminishing returns entirely. These entire culminations can be considered a precursor to sustainability concepts.

2.2.2 Emergence

The world's industrial revolution which transitioned into the second wave of post industrial revolution resulted in near scarcity of earth's natural resources and global environmental crisis such as pollution and destruction of natural resources (Elzen and Wieczorek, 2005).

The awareness of all these problems made the United Nations organized its first international conference on Human Environment in 1972 in Stockholm, Sweden (Seyfang, 2003). The conference represented a major step forward in the development of sustainability concepts.

Around the same time of the Stockholm conference was also the meeting of some eminent scientists in Rome discussing the global environmental crisis. The meeting in Rome was later referred to as the Club of Rome. A report which was issued after the Rome gathering emphasized that the industrial society was going to exceed most of the ecological limits within matter of decades, if it continued to promote the kind of economic growth witnessed in 1960s and 1970s (Mebratu, 1998). This particular economic growth was more of over-exploitation of natural resources which supported life on earth hence harming humanity.

The subsequent years after the Stockholm conference and the Rome gathering saw series of meetings internationally with a main focus on a marriage between the environment and development which was absent in the Stockholm meeting (Seyfang, 2003). Years following

the Stockholm conference witnessed all kinds of terminologies emerging such as “environment & development,” “development without destruction,” and “environmentally sound development” (Mebratu, 1998). In 1978, a United Nation Environment Program (UNEP) review program finally emerged with the term ecodevelopment. The term became internationally recognized creating the mindset that environmental and developmental ideas needed to be considered concurrently.

In 1980, a conceptual insight of bringing the environmental and developmental ideas under one umbrella was well established by three organizations namely the International Union for the Conservation of Nature (IUCN), United Nation Environment Program (UNEP) and the World Wildlife Fund (WWF). The concept was launched in the same year entitled “World Conservation Strategy”. Though the strategy remained diffuse due to the absence of time, however the introduction of the element of time directly into the environment and development debate, the strategy discovered a truly synthesizing and a definite factor in sustainability studies (Khosla, 1995).

Public concerns over poorly planned resource use, exploitation of finite resources, pollution and failure among countries to advance the concept of sustainability were popularized by reports such as that produced after the Stockholm conference, Club of Rome, etc. Batterham (2003) termed these failures the tragedy of the commons. These factors led to a UN-sponsored program known as the World Commission on Environment and Development (WCED) chaired by the then Prime Minister of Norway, Gro Herlem Brundtland in 1987 (Sneddon et al, 2008). The commission produced a report also known

as the Brundtland commission's report which led to the emergence of the term "sustainable development" now used in many scientific literature (Bond & Morrisons-Saunders, 2011). The commission's report "Our common future" marked a watershed in the thinking on environment, development, and governance.

2.3 What is Sustainability?

According to Hanson (2010), the definition of sustainability can be divided into two major classes namely the strong and the weak concepts of sustainability. Strong sustainability is whereby some natural capital provides functions which are not substitutable by human-made capital (Hansson, 2010). This means that natural capital stock handed over to future generations must not be smaller than that enjoyed by the current generation (Bond & Morrison- Saunders, 2011). The reasons for the preservation of natural capital are shown in the work of Howarth (2007) and they are to (1) provide raw materials for production and direct consumption such as food, timber and fossil fuels, (2) assimilate the waste products of production and consumption, (3) provide amenity services, such as visual amenity of landscape and (4) provide basic life-support function on which human life and other living organisms depend on.

Weak sustainability on the other hand is whereby natural and human-made capital is considered to be substitutable (Bond & Morrison- Saunders, 2011). Ayres et al (2001) argued that with the concept of weak sustainability the present generation can pass on less environmental resources to coming generations as long as we pass on more humanmade capital instead. According to this view, we can deplete more natural resources and yet

comply with the precepts of sustainability if the present generation develops new technologies that reduce the future generation needs of natural capital (Hansson, 2010).

The 1987 Brundtland commission's report that paved the way for the concept of sustainable development thrives on the back of the definition of weak sustainability. The report defines sustainable development as *development which meets the needs of the present without compromising the ability of future generations to meet their own needs* (WCED, 1987). The commission's work brought together and popularized the concept of time alongside environment and development. Though the commission's work was seen as a major break-through in popularizing sustainability concept internationally, the scientific community has viewed this definition as non-converging and very ambiguous (Mori & Christodoulou, 2012).

Down the line from the time that the Brundtland's definition emerged, all sorts of definitions have arisen. For example, we have those that advocate for environmental sustainability, while others advocate for social and economic sustainability (Burger & Christen, 2011). The non-convergence nature of sustainability definition indicated by Burger & Christen (2011) has given way to a plethora of definitions. The definition of sustainability is inevitably vague, yet not necessarily meaningless (Guest, 2010). Table 2.1 enumerates some definitions of the term sustainability or sustainable development based on the Brundtland definition. The concept of strong sustainability is seen by some researchers of sustainability science as impracticable as compared to that of weak sustainability (Hansson, 2010). However, some authors also argue that both strong and

weak sustainability can be pursued on different levels depending on the nature of sustenance.

KNUST



Table 2.1: Sources and different definitions of sustainability

Source	Definition
Oliveira de Paula & Cavalcanti (2000)	The constant process of obtaining the same or better living conditions for a group of people and their successors in a given ecosystem.
Batterham (2003)	The advance of human prosperity in a way that does not compromise the potential prosperity and quality of life of future generation.
Heal (1999)	Doing things that can be continued indefinitely: doing things that can be continued over long periods without unacceptable consequences.
Garcia-Serna et al. (2007)	Continues ensuring dignified living conditions with regard to human rights by creating, expanding, enlarging, redefining and maintaining the wildest possible range of options for freely defining life spans.
Wackernagel & Rees (1996)	Living within the regenerative capacity of biosphere or maintaining natural capital.
Cohen (1995)	Human carrying ability
Dasgupta, 2001	Non declining utility over long term hence intergenerational equity is considered.
Seyfang (2003)	Human development which protects the earth's environment and makes a better, fairer future for everyone.

2.3.1 The commonalities between the definitions of sustainability

Voinov & Farley (2007) has stated that whatever the focus of the different definitions may be it strong or weak sustainability; there is a common component in all of them which is a goal of avoiding decline. Among the sustainability concepts, weak sustainability appears to be the most pursued concept which happens to be contained in the Brundtland commission's report. The definition by Brundtland has been the most widely used sustainability definition in the field of sustainability developments and science. This definition is also seen by many authors as having many diverging issues and problematic in its pursuance.

2.3.2 The Brundtland Commission's Definition: Ambiguities versus Commonalities

The commission's definition of sustainability is embodied with deep conceptual ambiguities. One aspect of the confusion is that the future generation is an entity we do not know, non existing beings. Solow (2000) posed the question that "Can the present generation have an obligation or duty to beings that do not exist"? In the midst of the ambiguities, at least two principles indicated by Anderson et al. (2012) generate broad support from the definition. First is the issue of intergenerational equity i.e. fairness across generations. Intergenerational equity brings to mind the future generation of which sustainability is about, our concerns toward it and our acceptance of responsibility for our actions that affect them, the next generation (Oliveira de Paula & Cavalcanti, 2000). Ness et al. (2007) have identified three areas to be sustained namely nature, life support systems and community. Through the principle of "Fair-sharing" the next generation would not be stripped-of their due. The Fair- sharing principle in effect holds that natural resource stocks are the joint property or patrimony of the present and future generation. In view of this, the

present society has no legitimate right to degrade the environment unless it takes steps to ensure that its successors receive their proportionate share of the ensuing benefits (Howarth, 2007). Norton (2011) and Kates & Parris (2003) have explained that the patterns of resource use, savings, investment and conservation in a particular generation clearly affect the opportunities available to the future generation.

Secondly, according to Anderson et al. (2012), sustainability is anthropocentric meaning it considers the needs of human beings as the most significant entity in the universe. The development of the human capital has been the central focus of human needs and this include better education, good health and a quality life. Meeting the needs of human beings have in- turn led to economic and social growth of great nations. A typical example is what is termed the “East Asian” miracle (Anand and Sen, 2000). This miracle of economic prosperity arrived when the human capital was developed. Anand and Sen (2000) have mentioned that the development of human capital and skill would be important not just in raising productivity, but also in devising ways and means of dealing with environmental and other challenges.

2.4 Principles and pillars of sustainable development

2.4.1 Principles

It has been mentioned earlier that the Brundtland commission paved the way for the term sustainability; however, the UN sponsored 1992 Rio Earth summit in Brazil set out 18 principles of sustainable development which is referred to as Agenda 21.

Notwithstanding these principles, Drexhage and Murphy (2010) tend to emphasise what they have termed as “a few common principles” of which some were earlier highlighted in

the Brundtland report. The first is commitment to equity and fairness i.e. giving priority to the improving conditions of the world's poorest and making decisions to account for the future. The second issue is that the international body believes in scientific solutions to sustainable development, however, where there are threats of serious or irreversible damage, lack of full scientific certainty shall not be used as a reason for postponing cost effective measures to prevent environmental degradation. The third emphasis is integrating, understanding and acting on the complex interconnectivity between the environment, economy and society.

2.4.2 Pillars

Economic and social developments as well as environmental protection are the three main independent and mutually reinforcing pillars of sustainable development (Hosseini and Kaneko, 2011; Gimenez et al. 2012). The United Nations Environmental and Development program refers to these three pillars as “the triple bottom line” (TBL), a concept developed by Elkington (1998) whilst some authors like Harris (2000) also see the three as systems having varying internal logics. The economist might tend to give much weight to economic issues, the ecologist to environmental responsibilities whilst the social theorist to the social issues. Harris argues that the human society forms part of the total system and that development which considers a balance between the three will make the earth utopian. TBL has been the main tool used to address sustainable development by a wide range of including businessmen, policy makers, educators, architects, engineers, property developers, investors and many more (Cam, 2013).

The economic perspective of sustainability focuses more on fairness in resource allocation across time and equity which refers to intra and intergenerational equity of capital i.e natural, human and created capital (Elliot, 1999). The social aspect of sustainability is bipolar, addressing problems at the individual and at the collective level (Lehtonen, 2004). At the individual level social sustainability focuses on capacity building through the provision of quality life to people such as better education, food security, shelter and improved health facilities (Anon, 1990). At the collective level, Hedger (2005) has stated that the society should be capable of dealing with social, economic and environmental problems whilst actively shaping the development of the overall ecosystem.

The components of social sustainability have been stretched to include cultural and institutional values. According to Hedger (2011), cultural sustainability deals with a balance between externally imposed changes with cultural continuity and development from within society. Institutions have been described as essential to sustainable development because of their indispensable role in implementing social, economic and environmental objectives (Hossein & Kaneko, 2011). The environmental dimension of sustainability addresses environmental burdens such as global warming potentials, deterioration of ecological systems, energy consumption, pollution, waste management, natural resource exploitation, etc (Li, 2006; Chen et al, 2005).

2.5 The construction industry and sustainability

The construction industry is one of the top consumers of natural resources which pose a great environmental threat, significantly impacting on the sustainability of earth natural resources (Morbi et al, 2010). Most of these natural resources are classified as

nonrenewable (Senadheera, 2010). Moriconi (2010) has mentioned that enormous amount of water and some non-renewable natural resources such as soil, stones and sand are consumed annually for the production of concrete. The increase in global population is expected to cause a higher consumption rate of these natural resources use. According to Moriconi (2010), it has become clear in this century that the world is running out of natural resources for construction.

The cement industry that supports the construction industry for infrastructure development continues to contribute to the unsustainable woes of the planet. Dwindling amount of limestone and emission of CO₂, a greenhouse gas which contributes to global warming are all attributed to the cement industry (Naik, 2010). The global carbon emissions are reported to have increased from 33 billion tonnes in 2010 to 34 billion tonnes in 2011 and then to 35.6 billion tonnes in 2012. These are all due to human activities. The cement industry is found to contribute between 5-10% of the total anthropogenic CO₂ emissions (Alwood et al, 2010, Faludi, 2004). This places the cement industry as the third biggest greenhouse gas culprit after the transportation and energy generation sectors (Faludi, 2004).

Mehta (2009) has indicated that in this finite planet earth, the model of unlimited growth, unrestricted use of natural resources and uncontrolled pollution of the environment is a recipe for self-destruction. Sobolev et al (2007) argue that for the construction industry, sustainability means progress that meets the needs of the society, economic development, environmental preservation and efficient use of resources. In this 21st century, many researchers are making efforts to produce cements that ensure a sustainable future (Zhang et al, 2012).

2.6 Sustainable development practices in the global construction industry

Sustainable development practices provide a wide range of alternative solutions to economic, social and environmental issues globally and functions as the leading role model for shaping our future. Sustainable development mechanisms in the industry around the world is underpinned by projects that reduce greenhouse gas emission (GHG) as well as projects that provide positive economic, social and environmental benefits, not just GHG (Parnphumeup and Kerr, 2011).

Under the 1992 Kyoto Protocol organized by the United Nations, projects which have a central focus on sustainable development mechanisms such as carbon emission reductions are referred to as Clean Development Mechanism (CDM). In modern times, several researchers are pursuing the agenda of sustainable development or cleaner production technologies through the utilization of biomass and pozzolanic materials. This has given the chance for new challenges both in research and policy areas with respect to the biomass, pozzolana and the cement industry.

2.7 The Biomass industry

2.7.1 What is Biomass?

Twidell and Weir (2005) define biomass as the biological materials derived from plants and animals as well as their waste and residues. Biomass formation happens when carbon dioxide from the atmosphere combines with water from earth through the process of photosynthesis resulting in carbohydrates production, the main building blocks of biomass. The energy derived from the sun in biomass is stored in the structural components of plants and some animal waste (cattle and poultry manure).

2.7.2 Classification of Biomass

Biomass can generally be classified as the woody and non-woody biomass. Woody biomass involves mainly products and by-products derived from forest, woodland and tree sector. Non woody biomass comprises of agricultural crops, agro-forestry residue, herbaceous products, animal waste as well as tertiary waste (Chew and Doshi, 2011).

Table 2.2 presents the various classifications of biomass groups.

2.7.3 Composition of Biomass

The composition of biomass varies among species, but with plants the major components are carbohydrates or sugars (~75%) and lignin (~25%), accompanied by some fractions of extractives (protein, triglycerides, lipids, colour) and ash-forming elements (Eom et al, 2012). The carbohydrate content comprises of many sugar molecules interconnected together in long chains or polymers. Cellulose and hemicelluloses as well as lignin are the respective carbohydrate and non-carbohydrate compounds with significant value in plants. The structural component of these chemical compositions comprise of carbon, oxygen and hydrogen.

Cellulose is the fibrous substance that gives strength to plants. It is a linear polysaccharide β -D glucopyranose unit linked with (1-4) glycosidic bonds with a generic formula of $(C_6H_{10}O_5)_n$. Hemicellulose is polysaccharide of variable compositions including five or six carbon monosacharride units (Jenkins et al, 1998). It has a generic formula of $(C_5H_8O_4)_n$. It occurs in association with cellulose in the cell walls. The lignin is an irregular polymer of phenylpropane units (Sudo et al, 1989). The lignin component serves as glue that holds

the cellulose fibers together. It has very high energy content, and also resists biochemical conversion (Roewell, 1984).

Table 2.3 illustrates the carbohydrates and lignin fractions in different species of biomass. Several authors have reported on the order of the structural components for biomass and is given as Cel > Hem > Li (McKendry, 2002; Robinson et al, 2002). Biomass composition presents a complex heterogeneous mixture of organic matter mostly from the structural component (cel, hem, lig), and to a lesser extent, inorganic matter containing various solid and liquid intimately associated phases (Vassilev, 2012). The liquid fractions in biomass are mostly inorganic elements. The formation of both organic and inorganic components could be through the following process: syngenetic (during plant growing), epigenetic (after plant dies), pre-syngenetic and post-epigenetic (before and after plant collection).

The inorganic fractions are the ash forming compounds in biomass. Different species of biomass show significant differences in the ash-forming compounds. The ash-forming compounds include these metallic elements: Si, Ca, Mg, K, Na, P, S, Cl, Al, Fe, Mn and some fractions of heavy metals such as Cu, Zn, Co, Mo, As, Ni, Cr, Pb, Cd, V, Hg (Oberberger et al, 1997). These elements are deposited in the plants from the soil. Table 2.4 presents the occurrence of five main ash constituents which have significant impact on biomass conversion system.

Table 2.2: Classification of biomass (Vassilev et al (2012))

Biomass groups	Biomass sub-groups, species and varieties
Wood and woody biomass	Coniferous or deciduous, angiospermous or gymnospermous and soft or hard such as stems, barks, branches (twigs), leaves (foliage), bushes (shrubs), chips, lumps, pellets, briquettes, sawdust, sawmill and others from various wood species
Herbaceous and agricultural biomass	Annual or perennial, arable or non-arable and field-based or processed-based biomass from various species such as: a. Grasses and flowers (alfalfa, arundo, bamboo, bana, cane, miscanthus, reed canary, ryegrass, switchgrass, timothy, others) b. Straws (barley, bean, corn, flax, mint, oat, paddy, rape, rice, rye, sesame, sunflower, triticale, wheat, others) c. Stalks (alfalfa, arhar, arundo, bean, corn, cotton, kenaf, mustard, oreganum, sesame, sunflower, thistle, tobacco, others) d. Fibers (coconut coir, flax, jute bast, kenaf bast, palm, others) e. Shells and husks (almond, cashewnut, coconut, coffee, cotton, hazelnut, millet, olive, peanut, rice, sunflower, walnut, others) f. Pits (apricot, cherry, olive, peach, plum, others) g. Other residues (fruits, pips, grains, seeds, coir, cobs, bagasse, food, fodder, marc, pulps, cakes, others) from various species
Aquatic biomass	Marine or freshwater, macroalgae or microalgae and multicellular or unicellular species (blue, blue-green, brown, golden, green and red algae; diatoms, duckweed, giant brown kelp, kelp, salvinia, seaweed, sweet-water weeds,

	water hyacinth, others)
Animal and human biomass wastes	Bones, chicken litter, meat-bone meal, sponges, various manures, others
Contaminated biomass and industrial biomass	Municipal solid waste, demolition wood, refuse-derived fuel, sewage sludge, hospital waste, paper-pulp sludge,
wastes (semi-biomass)	waste papers, paperboard waste, chipboard, fibreboard, plywood, wood pallets and boxes, railway sleepers, tannery
	waste, others
Biomass mixtures	Blends from the above varieties

□



Table 2.3: Carbohydrates and lignin components of different biomass (Vassilev et al (2002))

Biomass	Cellulose	Hemicellulose	Lignin
Wood	42	22	36
Pine Sawdust	45.9	26.4	27.7
Woody biomass	50.6	24.7	24.7
Corn stalk	49	37.9	13.1
Corn cob	48.1	37.2	14.7
Rice husk	43.8	31.6	24.6
Millet husk	44.9	36.2	18.9
Cattle manure	32.7	28.8	22.9

Table 2.4: Occurrence of significant inorganic constituents in biomass (Oberberger et al, 1997)

Ash element	Range
Silica	0.5-15%
Potassium	1-2%
Calcium	0.1-5%
Sulfur	0.1-0.5%
Chlorine	0.2-2%

2.7.4 Some examples of biomass feedstock and their usage around the globe

Major products obtained from the processing of biomass include heat and power, ethanol and biodiesel. These products are sourced from biomass feedstocks such as agricultural waste, animal manure, forestry waste, industrial and municipal waste, sewage sludge, crops and lignocellulosic feedstocks (Maghanaki et al, 2013). Biomass feedstock could be either solid or wet in state.

The conversion process of biomass feedstock into useful products could be done through thermo-chemical or biochemical process depending on the state of the feedstock. Solid state feed stocks conversion is done through combustion, gasification and pyrolysis. Oil crops are converted through extraction means, sugar crops through fermentation whilst other wet biomass undergoes anaerobic digestion for their conversion process (Mohammed et al, 2013). Table 2.5 presents some biomass feedstock around the world and their uses.

Table 2.5: Some biomass feedstocks and their usage around the World

Biomass feedstock	Usage	Source
Wheat beet	Bioenergy	Simionato et al (2013)
Oil palm residue	Power generation	Umar et al (2014)
Corn waste beet	Ethanol production use as biofuel	Demibras (2011)
Peanut oil	Biodiesel	
Sunflower oil	Biodiesel	Mofijur et al (2013)
Rapeseed oil	Biodiesel	Mofijur et al (2013)
Palm oil	Biodiesel	Sharon et al (2012)
Sewage sludge	Biogas for heat generation	Maghanaki et al (2013)
Cow manure	Biogas for heat generation	Maghanaki et al (2013)

2.8 The Ghanaian biomass

The Ghanaian biomass industry is obtained from agriculture, animal waste, forestry residues, urban waste and others. The principal agricultural produce in the country are grouped as industrial crops or energy crops, cereals, starchy staples, legumes, and fruits and vegetables. The industrial/energy crops comprise of cocoa, oil palm, coconut, coffee,

cotton, kola, rubber, sugarcane and jatropha. Major cereals grown largely in Ghana are maize, millet, rice and sorghum. The starchy staples commonly found in the country include cassava, yam, plaintain and cocoyam. The legumes also involve groundnuts, cowpea and soyabeans whilst the fruit and vegetables commonly available includes pineapple, citrus, banana, cashew, pawpaw, mangoes, tomato, pepper, okro, eggplant, onion, Asian vegetables (Anon, 2010). In Ghana, the main crop residues potentially good for bioenergy is the cereals such as maize, rice, millet and sorghum and some energy crops including sugarcane, oil palm fruit, coffee, cocoa and jatropha (Mohammed et al, 2013).

The country generates significant amount of waste in the form of manure from livestock farmers. The most common livestock animals in the country are cattle, sheep, goat and pig. Forest biomass is mainly in the form of wood fuels and is prepared in the form of firewood and charcoal. It has been used in Ghana to meet about 60% of final energy demand in the country (Mohammed et al, 2013). Forest biomass generates significant amount of biomass from logging and wood-processing. The Ghanaian wood-processing industry according to Duku et al (2011) generates about 21% of sawdust from solid wood and this residue is seen as a promising energy feedstock. Other sources of biomass could be obtained from the urban waste and other wastes which include municipal waste, food industry wastes, industrial wastewater, sewage sludge, bio-solids (Duku et al, 2011). Table 2.6 shows the production of some principal biomass agricultural crops produced in Ghana.

2.9 Potential biomass feedstock considered for pozzolan production in Ghana

The biomass resource in Ghana is very enormous; however its use as renewable energy is very low. As an agriculture nation, the industry leaves behind huge amounts of biomass residues from different crops. Principal among them are solid biomass generated by the oil palm industry, rice mill, corn and the wood processing industry.

Table 2.7 shows the estimated production and residues of some potential biomass feedstock which can serve as raw meal for artificial pozzolana production. The production of rice and maize which belong to cereals group constitute about 85% of that group whilst oil palm that belongs to energy crops constitute about 62% of that crop group.

Table 2.6: Production of some principal food crops in Ghana (FAOSTAT 2011/2012)

Crop	Area Harvested (Ha)	Production (10³T)	Yield (Hg/ha)
<i>Starchy staples</i>			
Cassava	868,550.00	1457	167489.25
Yam	426,343.00	6639	155716.57
Plantain	336,497.00	3620	107,574.03
Cocoyam	196,328.00	1271	64701.21
<i>Cereals</i>			
Maize	1,042,083.00	1945	18711.53
Rice	189,529.00	481	25385.77
Millet	172,470.00	180	10418.28
Sorghum	230,841.00	280	12128.82
<i>Industrial and energy crops</i>			
Oil, palm fruit	350,000.00	1900	54285.71
Cocoa	1,600,300.00	700	4374.3
Coconut	60,000.00	305	50833.33
Coffee	7,800.00	1.25	1602.5
Sugarcane <i>Legumes</i>	6,000.00	148	246666.67

Groundnut	345,186.00	475	13762.32
Cowpea	n.a	n.a	n.a
Soyabean	n.a	n.a	n.a

n.a: not applicable

Biomass residue from these industries has the potential to be utilized as energy source for the production of pozzolanic materials. However, the potential of the biomass utilization is very much dependent on the reaction kinetics and ash properties of the biomass residue. Biomass residue to product ratio (RPR) indicated in Table 2.7 is extracted from the studies of Duku et al (2011).

Table 2.7: Estimated biomass production and residues generation in 2012(FAOSTAT, 2013; Duku et al 2011)

Biomass	Production (10 ³ Tonnes)	Residue to Pro- duct ratio (RPR)	Residue	
			(wet, 10 ³ Tonnes)	Residue (Dry, 10 ³ Tonnes)
Oil palm fruit	1900	0.25	475	190
Rice	481	1.5	721.5	613.28
Maize	1945	1.5	2915.5	2478.25
Sawlogs and Veneer- logs	644.5	0.21	135.35	121.82

2.10 Thermal decomposition of solid biomass

2.10.1 General mechanism

Solid biomass covers a wide range of materials such as wood, straw, agricultural residue, algae and seaweeds. Solid biomass may exclude materials such as manures, meat byproducts, partially decaying plants and other waste food (Williams et al, 2012). The energy in solid biomass can be rejuvenated through a decomposition process of the

biomass. One main process for thermo-chemical conversion is combustion. LopezGonzalez (2013) defines combustion as the conversion of biomass fuels to several forms of useful energy in the presence of air or oxygen. A good understanding of biomass decomposition during the conversion process is important for developing efficient processing technology (Lopez-Gonzalez, 2013).

The general mechanism of solid biomass combustion consists of these steps: heating-up, devolatilization and char combustion. The heating-up process takes off moisture content in the biomass. This occurs at temperatures below 300°C and this process could be described as torrefaction. Torrefaction is a thermal treatment process where biomass is heated within a temperature range of 200-300°C under an inert atmospheric condition (Sabil et al, 2013). Newly cut biomass may contain about 50% wt moisture whilst ambient dried treated biomass contains between 15-20% moisture content (Williams et al, 2012). Moisture treatment by the torrefaction process before combustion is very expensive. The expensive nature of the torrefaction process creates great attention to it and therefore sometimes carried out separately from the combustion process.

Biomass devolatilization occurs at different combustion temperatures because of biomass composition. Cellulose degrades between 315 and 400°C, hemicelluloses between 220 and 315°C whilst lignin decomposes between 500 and 900°C (Shadangi and Mohanty, 2014). The devolatilization stage produces chars and volatiles consisting of tars and gases. Volatile gases produced at this stage includes CO, CO₂, H₂O, CH₄, H₂ and some trace inorganic products and light hydrocarbons (Williams et al, 2012; Korobeinichev et al,

2013). Williams et al (2012) again indicated that the volatile contents contribute about 70% of the heat of biomass combustion. Combustion of the biomass char can contribute about a third of energy content of the biomass. However, in energy contributing terms, the volatile contents far outweigh that of char. Char combustion is influenced by the size of the biomass particle. Char combustion occurs after devolatilization in thin particles however with thick particles the combustion starts from the particle surface and passes to the center of the particle as volatile products escape from inside the biomass particle.

2.11 Biomass characterization and ash properties

The characterization of raw biomass is usually based on the proximate, ultimate and sometimes the chemical composition (Sabil et al, 2013; Ninduangee and Kuprianov, 2013). In proximate analysis the following are determined: moisture (M), volatile matter (VM), fixed carbon (FC) and ash content. Moisture content influences the amount of heat required for pyrolysis whilst the ash forming properties are of great concern to the power generating industries. For them lower ash content is preferred for their work however the pozzolanic industry would prefer higher ash content.

In the ultimate analysis, the following are of much importance: carbon (C), hydrogen (H), oxygen (O), nitrogen (N) and sulphur (S) contents. Ultimate analysis of biomass could be determined easily with mass spectrometer. Both carbon and hydrogen are oxidized during combustion and contribute effectively to the calorific values. Oxygen content however contributes negatively to the calorific value of biomass (Ghani et al. 2013). The calorific values are determined either by the bomb calorimeter or proposed equations given by some

authors including Ninduangdee & Kuprianov (2013) and Mansaray & Ghaly (1998). These proposed equations are given as follows:

$$HHV \left(\frac{MJ}{kg} \right) = 0.3491C + 1.1783H + 0.01005S - 0.1034O - 0.0151N - 0.0211Ash$$

Equation 2.1

$$HHV \left(\frac{KJ}{kg} \right) = 354.3FC + 170.8VM$$

Equation 2.2

Equations 2.1 and 2.2 are the given equations by Ninduangdee & Kuprianov (2013) and Mansaray & Ghaly (1998) respectively. The extent of gaseous pollutants is determined by the presence of nitrogen and sulphur. Under combustion nitrogen and sulphur are converted to gaseous nitrogen and nitric oxides (NO, NO₂) and SO₂. The calorific or heating values are most of the time recorded as part of ultimate analysis and it is an important parameter for measuring the energy content of the biomass sample (Okoroigwe and Shaffron, 2012). The content of chemical composition could be a way of determining the nature of pyrolysis product as well as the extent of syngas yield. Lower lignin content (< 30%) produces lighter pyrolysis products whereas higher hemicellulose and cellulose contents produce relatively hydrogen rich gas yield than that composed of higher lignin (Ninduangdee & Kuprianov 2013; Ioannidoua et al, 2009)

2.11.1 Palm kernel shells

The processing of oil palm generates the following solid wastes: palm kernel shells, palm fiber and empty fruit bunch. For a ton of oil palm produced, 0.07 tons of Palm kernel shells, 0.146 tons of palm fiber and 0.2 tons of empty fruit bunch are produced as solid waste (Ghani et al, 2010). Table 2.8 presents the main characteristics of raw palm kernel shell

samples given by different authors. The labels 1, 2 and 3 shown in the table correspond to the authors indicated under the reference column. The thermal behavior of palm kernel shells shows that the first weight loss occurs at 100°C due to moisture evaporation. Between 200 and 400°C is the second weight loss due to hemicelluloses and cellulose decomposition whilst above 400°C, the third weight loss occurs due to lignin decomposition (Kim et al, 2010). Okoreigwe and Shaffron (2012) presented the thermal decomposition in a combined plot of TG and DTA in Figure 2.1. The figure indicates three different peaks at 187.94°C, 254.68°C and 312.20°C which represent hemicellulose and cellulose decomposition. Lignin decomposition occurs at a peak around 411.93°C much higher than hemicellulose and cellulose.

Table 2.8: Main characteristics of palm kernel shells

Biomass composition	wt%			Reference
	1	2	3	
Cellulose	20.8	33.04	8	Sabil et al (2013); Kim et al (2010);
Hemicellulose	22.3	23.82	26	Okoroigwe and Shaffron (2012)
Lignin	50.7	45.59	52	
Proximate analysis				
Moisture	9.79	9.4	5.4	Sabil et al (2013); Kim et al (2010);
Volatile matter	68.35	82.5	71.1	Ninduangee and Kuprianov (2013)
Fixed carbon	19.28	1.4	18.8	
Ash content	2.58	6.7	4.7	
Ultimate analysis				
Carbon	48.06	51.6	45.1	Ninduangee and Kuprianov (2013);
Hydrogen	6.38	5.52	5.1	Wab Ab Karim Ghani et al (2010)
Oxygen	34.1	40.91	49.2	
Nitrogen	1.27	1.89	0.56	
Sulphur	0.09	0.05	0.04	
HHV(MJ/kg)	19.03	22.97	20	Sabil et al (2013); Wab Ab Karim-

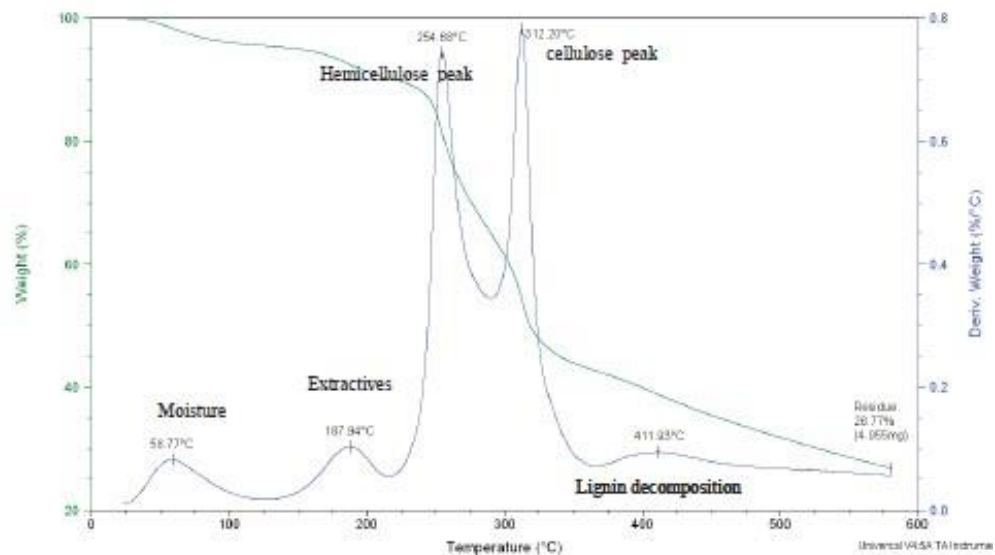


Figure 2.1: Thermal decomposition of palm kernel shells (Okoreigwe and Shaffron, 2012)

2.11.2 Maize residues

Corn cob, stalks and straws are the main residues generated after corn harvesting. In most cases corn waste is a mixture of the residues. The main characteristics of corn residues are presented in Table 2.9. The thermal degradation of corn residuum is of three steps: moisture evaporation, devolatilization and char combustion (Demiral et al, 2012).

Moisture evaporation occurs between 100 and 200°C. Devolatilization occurs between 200 and 400°C and peaks at 324°C. This range represents decomposition of cellulose and hemicelluloses which gives out organic volatiles. The last decomposition which also starts from 200°C and ends at 700°C represents lignin decomposition.

The peak temperature of lignin decomposition is 545°C. Figures 2.2 and 2.3 present the decomposition process on the thermographic graph. The thermal decomposition processes give weight loss. The moisture evaporation causes weight loss in the range of 8.07%, devolatilization around 54.92% whilst a further 74.65% of the total weight is lost during the char fast pyrolysis (Uzan and Sarioglu, 2009).

2.11.3 Rice Husk

Rice husk accounts for 22% of the weight of the paddy and 78% obtained as rice with the remaining 1% broken down during processing (Wab Ab Karim Ghani et al, 2010). Main characteristics of rice husk are shown in Table 2.10. The figure names 1, 2 and 3 shown in the table corresponds to the references indicated besides the biomass composition. The decomposition processes of rice husk involve moisture elimination, active and passive zone pyrolysis. Moisture elimination occurs around 100°C, active pyrolysis zone which characterizes the main degradation occurs between 184°C and 380°C. At this zonal temperature range evolution of volatile compounds are attributed to hemicelluloses and cellulose decomposition. After 380°C, a change in the decomposition slope is seen which indicates the initiation of the second reaction zone known as the passive zone. The passive zone is seen between 470 and 500°C. The decomposition reaction continues slowly until somewhere around 700°C which shows char reaction (Mansaray and Ghaly, 1998). A similar thermochemical graph is outlined by the studies of Ramadhansyah et al (2012). Further and better particulars of the thermochemical reaction are also supported by the DTG graphs presented by Mansaray and Ghaly (1998) and indicated in Figure 2.4. The figure shows that the active zone may occur in two steps: hemicelluloses and cellulose decomposition that occurs at the range of 300-325°C and 344-364°C

respectively

Table 2.9: Main characteristics of corn waste residues

	wt%			Reference
	1*	2**	3***	
Biomass composition				
Cellulose	41.04	34.3	32.4	Ninduangee and Kuprianov (2013);
Hemicellulose	35.49	40.53	40.8	Ioannidou et al (2009)
Lignin	8.11	18.8	2.5	
Proximate analysis				
Moisture	8.94	7.36	6.44	
Volatile matter	77.87	79.58	91.26	Ninduangee and Kuprianov (2013);
Fixed carbon	8.65	11.57		Ioannidou et al (2009); Demiral et-
Ash content	4.55	1.49	2.3	al (2012)
Ultimate analysis				
Carbon	42.99	49.32	43.8	Ninduangee and Kuprianov (2013);
Hydrogen	5.8	5.32	6.42	Ioannidou et al (2009); Demiral et-
Oxygen	49.27	44.7	49.78	al (2012)
Nitrogen	1.21	0.63	-	
Sulphur	<0.1	-	-	
HHV(MJ/kg)	17.01	16.66	18.25	Ninduangee and Kuprianov (2013);
				Ioannidou et al (2009); Demiral et-
				al (2012)

Note: 1*-cob, stalk and straw residues, 2**-corn cob, 3***- corn stalk

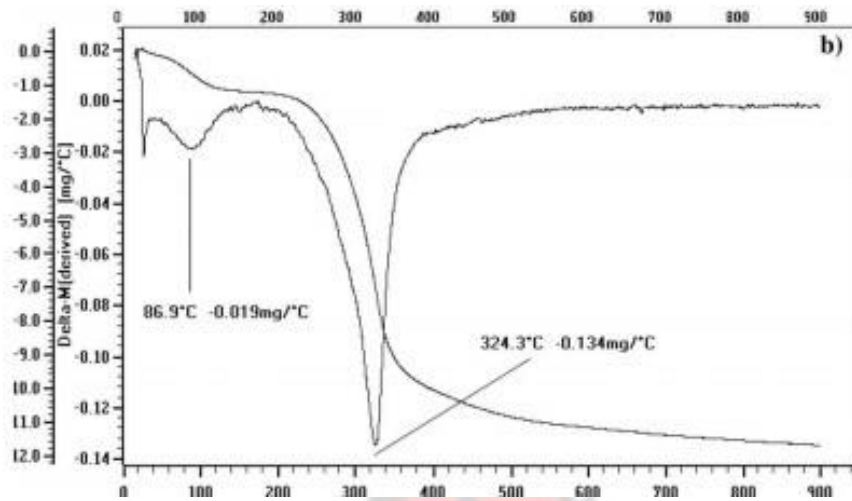


Figure 2.2: TG/DTG graph of corn residuum

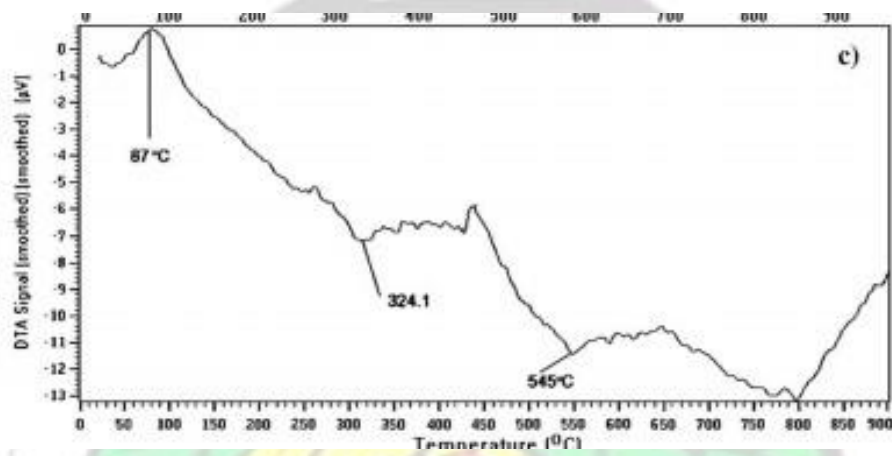
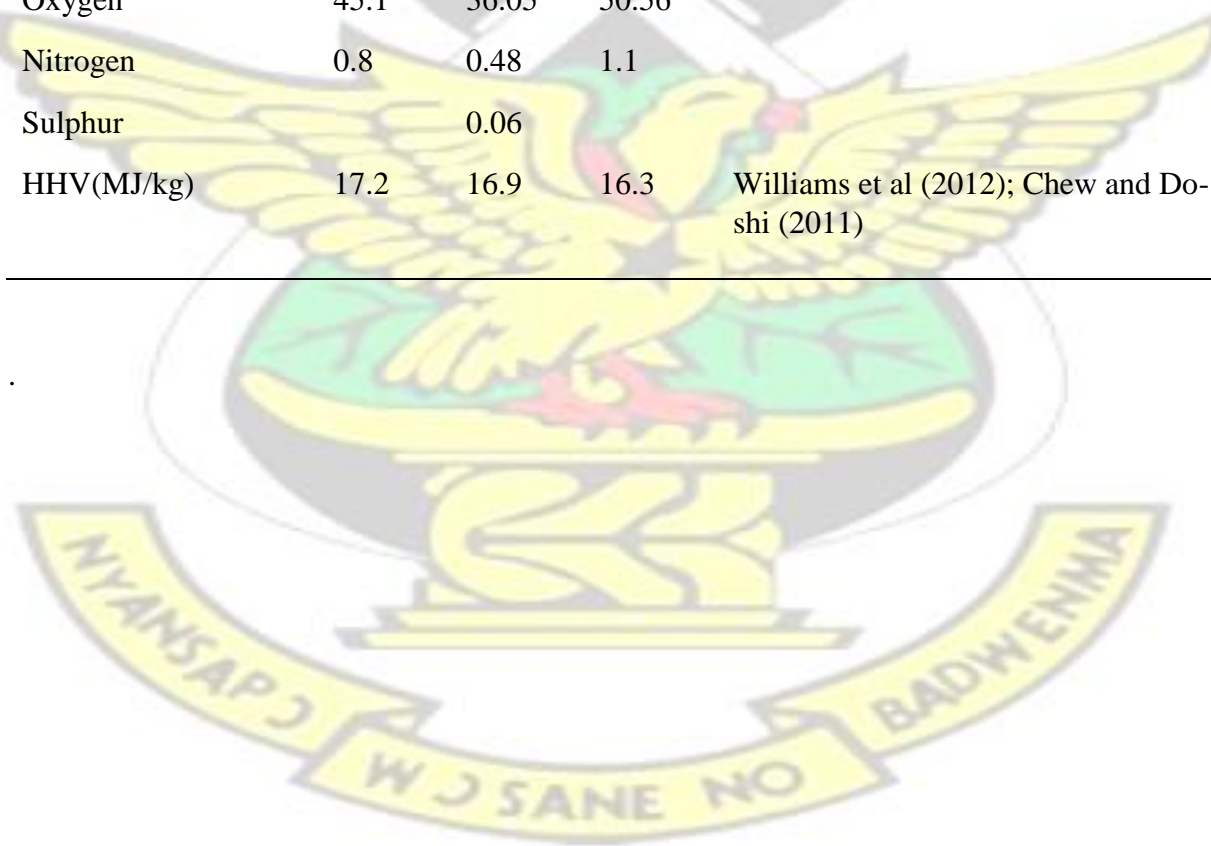


Figure 2.3: DTA graph of corn residuum

Table 2.10: Main characteristics of raw rice husk

	wt%			Reference
	1	2	3	
Biomass composition				
Cellulose	37.15	35.5	43.8	Xiujuan et al (2011); Mansaray and-Ghaly (1997); Vassilev et al (2012)
Hemicellulose	23.87	21.35	31.6	
Lignin	12.84	24.95	24.6	
Proximate analysis				
Moisture	6.73	12.08	9.4	Fu et al (2012); Gu et al (2013); Vassilev et al (2012)
Volatile matter	61.23	60.55	74	
Fixed carbon	14.95	15.02	13.2	
Ash content	17.09	12.35	12.8	
Ultimate analysis				
Carbon	47.4	45.48	42.3	Worasuwannarak et al (2007); Gu et al (2013); Williams et al (2012)
Hydrogen	6.7	4.5	6.1	
Oxygen	45.1	36.05	50.56	
Nitrogen	0.8	0.48	1.1	
Sulphur		0.06		
HHV(MJ/kg)	17.2	16.9	16.3	Williams et al (2012); Chew and Doshi (2011)



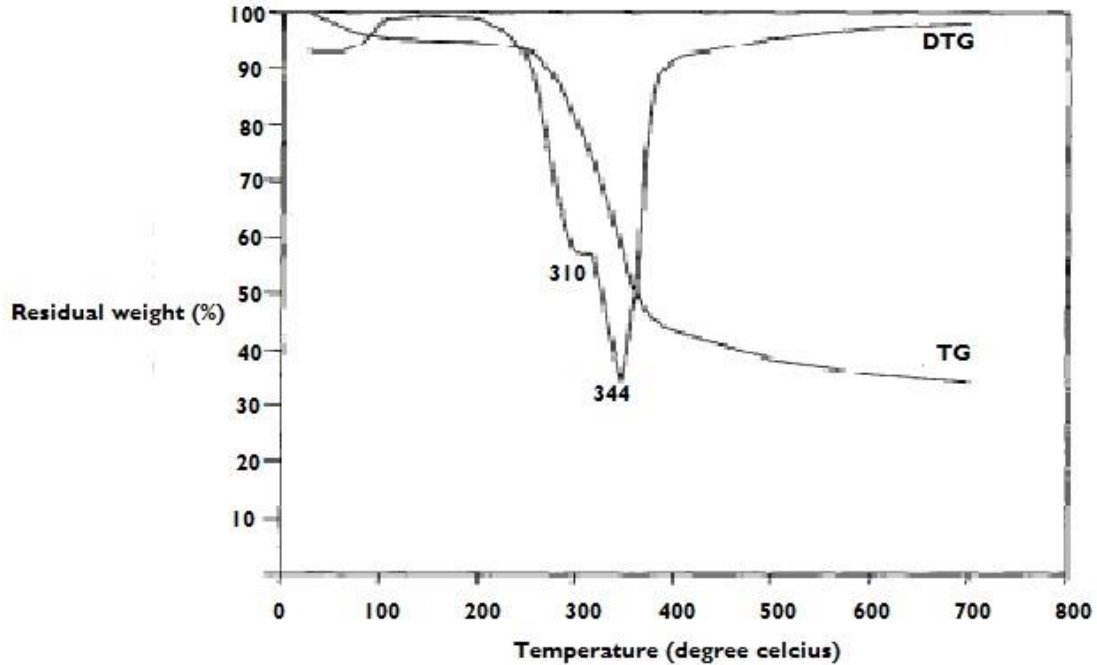


Figure 2.4: Thermochemical conversion of rice husk (Mansaray and Ghaly, 1998)

2.11.4 Saw dust

Sawdust obtained from processing of woody biomass is mainly lignocellulosic, a very good energy source. Table 2.11 presents the main characteristics of some sawdust waste. The figure names 1, 2 and 3 shown in the table corresponds to the references indicated besides the biomass composition. The thermochemical processes of sawdust pyrolysis consist of three stages. The studies of Gao et al (2013) indicate that the first stage of the process is moisture evaporation which occurs at about 120°C followed by the active pyrolysis zone which occurs in the range from 200-405°C. Approximately 73.25% of the total weight is lost at this stage. The third stage is lignin decomposition which slowly starts at about 200°C and ends at about 700°C. At this stage the total weight loss was approximately 87.5%. Figure 2.5 presents the thermochemical process of sawdust pyrolysis.

Table 2.11: Main characteristics of sawdust

	wt%			Reference
	1	2	3	
Biomass composition				
Cellulose	44.75	19.64	33.8	Gu et al (2013); Li et al (2012);
Hemicellulose	16.73	27.2	22.6	Sinag et al (2011)
Lignin	30.72	51.48	33.7	
Proximate analysis				
Moisture	9.6		3.8	Gu et al (2013); Li et al (2012);
Volatile matter	75.54	80.49	81.5	Dong et al (2007)
Fixed carbon	11.15	19.42	12.3	
Ash content	3.7	0.24	2.4	
Ultimate analysis				
Carbon	45.5	53.4	46.51	Gu et al (2013); Ghani et al (2013)
Hydrogen	6.26	6.7	5.64	
Oxygen	47.2	36.8	45.74	
Nitrogen	1.04	3.1	2.07	
Sulphur		0	0.04	
HHV(MJ/kg)	18.3	18.3	19.9	Ghani et al (2013); Ghani et al (2013) Park et al (2010)

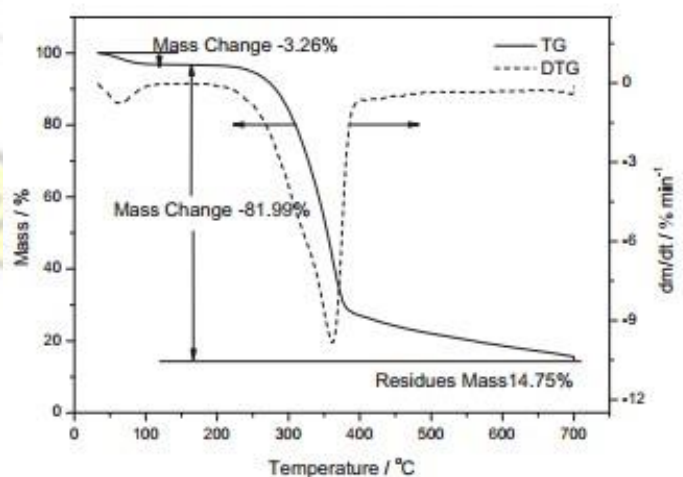


Figure 2.5: Thermochemical process of sawdust pyrolysis (Gao et al, 2013)

2.11.5 Chemical composition of biomass ashes

The chemical composition of biomass ashes can be a means of characterizing them. The ash characterization helps to predict its behavior in cement applications. The ash can be characterized based on its filler, pozzolanic or latent hydraulic properties. Filler materials means the ash is chemically inert however it affects cement hydration by introducing a catalytic effect. Pozzolanic effect also contributes late strength development to cement concrete and mortars. Latent hydraulic means the ash may undergo hydration on its own in the presence of water and contribute to the strength of concrete and mortar (Neville, 2003). Table 2.12 shows the chemical compositions of some selected biomass ashes.

2.12 Introduction to pozzolana

Pozzolanic materials have been known to builders since the ancient Greek and Roman Empires. It dates back more than two millennia (Rowland and Howe, 2001). Scientists have proven that many historical buildings in Greece and Italy were built with pozzolanalime mortars and concrete (ACI C232, 1994). Examples are the Pantheon, the Bath of Caracalla and the Colessuem (2nd century AD) (Wilson and Ding, 2007). Many other water-bearing structures such as tanks, aqueducts and dams in the developed countries (Europe and US) were made from mortars containing pozzolana (Velosa et al, 2010).

Table 2.12: Chemical composition of biomass ashes

Biomass ash-	Chemical composition									Reference	
Source	SiO ₂	Al ₂ O ₃	Fe ₂ O ₃	CaO	MgO	Na ₂ O	K ₂ O	SO ₃	LOI		
Palm kernel											
shell	59.62	2.54	5.02	4.92	4.52	0.76	7.52	1.28	8.25		Awal and Shehu (2013); Olu-
Palm kernel shell	54.81	11.4	0.36	8.79	6.11	-	0.52	-	-		toge et al (2012); Awal and-
Palm kernel shell	49.2	5.45	5.73	7.5	3.93	0.9	5.3	1.73	-		Nguong (2010)
Corn residue	66.38	7.48	4.44	11.57	2.06	0.41	5.64	1.07	-		Adeseenya and Raheem (2009)
Corn residue	38.33	0.22	0.47	8.99	5.01		27.58	1.72	11.4		Kevern and Wang (2010)
Rice husk	93.2	0.4	0.1	1.1	0.1	0.1	1.3	-	3.7		Chindaprasirt et al (2009)
Rice husk	90.9	0.83	0.6	0.8	1.2	0.4	0.4	-	-		Mandandoust et l (2011)
Rice husk	82.6	0.4	0.5	0.8	0.7	0.1	1.8		11.9		Cordeiro et al (2011)
Saw dust ash	66.4	6.07	3.49	4.21	3.39	1	11.09	2.89	-		Nimyat and Tok (2013)
Saw dust ash	48.95	13.65	13.34	5.4	4.6	-	9.01	1.00	-		Raheem and Sulaiman (2013)
Saw dust ash	19.9	5.6	2.9	63.7	1.5	0.2	0.7	2.3	-		Elinwa and Mahmood (2002)



KNUST

51

□



2.12.1 What is Pozzolana?

Pozzolanas are defined as a siliceous or alumino-siliceous material, which in itself possesses little or no cementitious value but will, in finely divided form and in the presence of moisture, chemically react with calcium hydroxide at ordinary temperatures to form compounds possessing cementitious properties (ASTM C618-03). The term pozzolana originated from the United States implication of “pozzolana” which evolves from the location “Puzzouli, Italy”. At this location the Romans, who were also the then superpower of the world discovered this reactive silica-based material of volcanic origin.

The Roman era saw a widespread utilization of pozzolana in other parts of Europe, Asia, Northern America and Africa in most of their useful ancient structures (Velosa et al, 2010; Lea, 1998).

2.12.2 Types of pozzolana

Lea (1998) mentions two types of pozzolana and they are the natural and the artificial pozzolana. Natural pozzolana can occur in three different forms. These are: (1) those from the volcanic origins, (2) sedimentary origins and (3) the mixed origins. The volcanic origins involve incoherent materials such as glassy volcanic pozzolanas very common in Campania area, Italy and Rhenish trass found in Germany, Russia, Romania as well as compact materials or tuffs such as zeolitic materials. The sedimentary origins involve some clays and diatomaceous earth also known as Moler. Examples are montmorillonite clay and amorphous opal. The mixed origins could involve diatomaceous earth and volcanic ash, etc. In modern times most natural pozzolanas are calcined before use.

Artificial pozzolanas are produced by the heat treatment of potential pozzolanic materials from their raw state (Al-Rawas and Hago, 2006). Examples of artificial pozzolanas are calcined clays and shales, metakaolins, industrial by-products which include fly ash (from burning coal in power plants), silica fume (from silicon industries), blast furnace slag (from iron and steel production) and some ashes of agricultural waste materials such as ashes from rice husk, sugarcane bagasse, palm oil, etc (Tironi et al 2013; Montakarntiwong, 2013). Modern construction trends have shown that around the globe many projects have successfully utilized huge tonnages of both natural and artificial pozzolana as cement replacement material or blended cements (Sabir et al, 2001).

2.12.3 The benefits of using pozzolanic materials

The benefit of using pozzolana in the construction industry is better understood by its influence on the properties of mortar and concrete. Many authors have viewed these benefits from three different angles: technical, ecological or environmental and economic benefits (Tirono et al, 2013; Bediako et al, 2012; Cordeiro et al, 2009; Setina et al, 2012). The technical benefits show that pozzolana utilization in mortars and concretes improves workability, reduces permeability and voids, minimizes micro cracking and early cement shrinkage, increases compressive strength, increases resistance to chloride and sulphate attack thus preventing steel corrosion in reinforcement concrete, and finally reduces heat of hydration (Kumar et al, 2012). These technicalities are attributed to the nature of pozzolanic reaction with cement.

From the environmental perspective, it has already been mentioned that Portland cement production is environmentally unsustainable due to damage it causes as a results of raw

materials extraction (limestone and clay) and global warming problems due to CO₂ emissions during cement production (Quyng et al, 2011). Cordeiro et al (2012) have indicated in their studies that using pozzolanic materials causes significant reductions in natural raw materials consumption, energy consumption and greenhouse gas emissions. Moreover, waste generated from industries including fly ash, slag, silica fume, etc when used in concrete helps to reduce the burden of disposal into landfills which helps the environment.

In the economic sense, it is mentioned in several studies that the intense energy used for Portland cement production coupled with raw material extraction as well as transportation make the product very expensive. Bediako et al (2012) in their studies on Ghanaian mineral admixtures showed that the use of pozzolana reduced the cost per area of mortar formation between 15-20% when compared with only using Portland cement. Many construction works in United States have shown a significant cost reduction in the use of industrial waste pozzolans (Komatska and Wilson, 2011).

2.12.4 Pozzolan utilization in Ghana

In Ghana, the Building and Road Research Institute (BRI) of the Council for Scientific and Industrial Research (CSIR) has performed extensive research on certain artificial pozzolans obtained from suitable clays and bauxite waste. Atiemo (2009) investigated into the production of clay pozzolan from some suitable clay deposits in Ghana. His work indicated that 800°C was suitable to produce clay pozzolan which can substitute up to 40% of cement without compromising Portland cement properties.

Nwoko and Hammond (1978) produced pozzolan from bauxite waste and found that 40% of the waste was suitable for construction in Ghana. In most of the studies on pozzolans developed from clays and bauxite waste in Ghana, the focus centered more on the physical properties including compressive strength and durability with respect to sulphate attacks. Hammond (1987) stretched his study on bauxite waste pozzolan a little bit by investigating into the hydration products formed using thermogravimetric analysis and the scanning electron microscope. In all these studies, there were certain common gaps identified and they were:

1. The lack of studies on the determination of the structural transformation of the calcined materials intended to be used as supplementary cementitious materials
2. The lack of studies on the degree of pozzolanic reaction of calcined clay and bauxite waste pozzolans
3. Lack of information regarding the structural transformation involving aluminates and silicates environment of the hydrated products between cement and a pozzolan.
4. Little information on incorporating potential pozzolanic biomass as a component in clay.

These gaps created a platform for the need for further investigations especially on the creation of supplementary cementitious materials with a mind set of pursuing sustainable agenda. Studies regarding the incorporation of biomass into clay for the production of clay pozzolana could present a unique and a novel approach for clay pozzolan production. Whilst solving environmental problems, waste biomass could also serve as an elemental silica and energy source for calcining suitable clay.

2.13 The cement industry

Portland cement is the most common cement utilized in almost every part of the world. The understanding of the embodiment of Portland cement can lead to a more sustainable concrete and mortar design especially with the introduction of secondary materials such as natural and artificial pozzolana. Portland cement is instant glue that bonds aggregates (fine and coarse) together to make Portland cement concrete or mortar. It chemically reacts with water to attain setting and hardening properties used in the construction of buildings, roads, bridges and other structures. Portland cement was patented by Joseph Aspdin in 1824 and was named after the cliffs on the Isle of Portland in England (Kosmatka et al, 2002).

2.13.1 Production of Portland cement

Cement is made by heating a mixture of calcareous and argillaceous materials to a temperature of about 1450°C (Svinning and Høskuldsson, 2006). The calcareous material is a calcium oxide (CaO), such as limestone, chalk, or oyster shells. Argillaceous materials are combination of silica (SiO₂) and alumina (Al₂O₃) that can be obtained from clay, shale, and slag (Mamlouk & Zaniewski, 2006). The calcareous and the argillaceous material are mixed together in a grinding mill in an appropriate proportion using either a wet or dry process. The process to be chosen depends on the nature of the raw materials used.

The predefined mix of the raw materials is feed into a rotary kiln at a clinkering temperature (1450°C-1650°C). In the kiln, partial fusion or calcination takes place and nodules of clinker is formed (Svinning, 2006). The clinker is cooled and stored. The final stage of the production involves pulverizing the cooled clinker with a ball mill. During milling, a small

amount of gypsum ($\text{CaSO}_4 \cdot 2\text{H}_2\text{O}$), between 3% and 5%, is added together with some other additives such as limestone.

2.13.2 Properties of Portland cement: Chemical, mineralogical and physical

The raw materials used to produce Portland cement as already indicated are normally rich in the following oxide components: CaO , SiO_2 , Al_2O_3 and Fe_2O_3 . In addition, small amounts of other compounds are also present and they include MgO , SO_3 and some alkalis (K and Na) (Neville, 2003). Table 2.13 shows the chemical composition of a raw feed for cement production.

Table 2.13: Summary of chemical data for a selection of Portland cement (Lea, 1970)

Component	Minimum	Average	Maximum
SiO_2	18.40	21.02	24.50
Fe_2O_3	0.16	2.85	5.78
Al_2O_3	3.10	5.04	7.56
CaO	58.10	64.18	68.00
MgO	0.02	1.67	7.10
SO_3	0.00	2.58	5.35
Na_2O	0.00	0.24	0.78
K_2O	0.04	0.70	1.66
Equivalent alkalis	0.03	0.68	1.24
Free lime	0.03	1.24	3.68

During calcinations, the component oxides in the raw feed interact with each other to form a complex mixture of inorganic phases to form cement clinker (Neville, 2003). Four compounds are regarded as the major mineralogical constituent of cement. These are shown in Table 2.14.

The Portland cement clinker grain is typically composed of 50-75% of alite, 10-20% of belite, 5-10% of celite and about 10% of felite (Hong et al, 2001). Direct analysis cannot be used to determine the mineralogy; however, knowing the composition of the oxides, the Bogue equation given in Equations 2.3 to 2.6 could be used.

Table 2.14 Main mineral compounds in Portland cement (Neville, 2003).

Name of Compound	Oxide Composition	Abbreviation	Scientific name
Tricalcium Silicate	3CaO. SiO ₂	C ₃ S	Alite
Dicalcium silicate	2CaO. SiO ₂	C ₂ S	Belite
Tricalcium aluminate	3CaO. Al ₂ O ₃	C ₃ A	Celite
Tetracalcium aluminoferrate	4CaO.Al ₂ O ₃ .Fe ₂ O ₃	C ₄ AF	Felite

Table 2.14 shows the chemical composition of cement powder. Neville (2004) gives the Bogue's equation as follows:

$$C_3S = 4.07 (C) - 7.60 (S) - 6.72 (A) - 1.43 (F) - 2.85(S^i) \quad \text{Equation 2.3}$$

$$C_2S = 2.87 ((S^i) - 0.754 (C_3S)) \quad \text{Equation 2.4}$$

$$C_3A = 2.65 (A) - 1.69 (F) \quad \text{Equation 2.5}$$

$$C_4AF = 3.04 (F) \quad \text{Equation 2.6}$$

The notations C, S, F and Sⁱ represent the percentage weights of CaO, SiO₂, Fe₂O₃ and SO₃.

Other methods such as the use of the X-ray diffractometer, wet chemistry, and the differential scanning calorimeter are methods used in identifying the proportions of mineral phases in the clinker (Ferret & Feret, 1999). A recent study by Jain (2012) identified the various minerals present in unhydrated cement using X-ray diffractometer and is shown in Figure 2.6. In recent times, softwares have come as alternatives to the traditional methods of analysis. Example is the C^{em}QUANT software developed by Feret and Feret (1999).

The physical properties of Portland cement include colour, fineness and specific gravity. Portland cement has a grayish color with fineness between 3.0 m²/kg and 3.5m²/kg, and a specific gravity from 2.8 - 3.2.

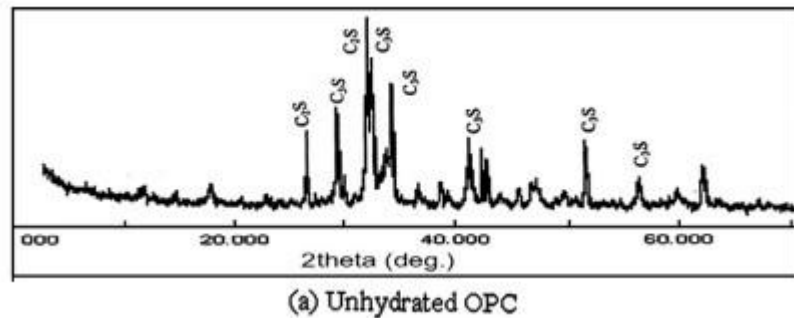


Figure 2.6: X-ray diffraction analysis of unhydrated cement (Jain, 2012)

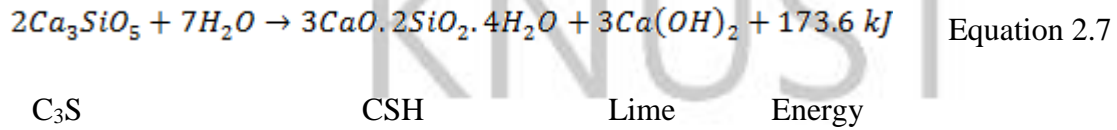
2.13.3 Reaction of cement compounds

Upon wetting with an aqueous solution, cement compounds undergo individual reactions with water. Whilst some of the reactions are very quick and rapid others are slow.

2.13.3.1 Tri-calcium silicate

The tricalcium silicate (C₃S) compound as reported by Peterson et al, (2006) constitutes about 50-70% by weight of Portland cement and remains the most important and abundant constituent of normal cement. It is important because the products after reaction contribute enormously to setting and hardening of cement. A study by Stark (2011) indicates that the initial reaction of C₃S after making contact with water is terminated within a few minutes, followed by a period of very low chemical activity lasting between one and six hours. The seemingly inactive period is designated as the dormant or induction period. Many authors have found that the end of the dormant period marks the onset of the main hydration period (Lothenbach et al. 2008; Bullard, 2008; Korpa et al. 2008). The hydrated phases of C₃S

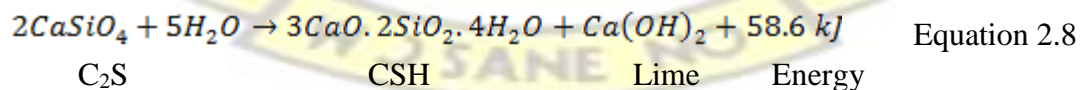
comprise of massive amount of calcium silicate hydrate (C-S-H), lime (Ca(OH)₂) and the release of thermal energy (Gallucci & Scrivener, 2007). In the study of Peterson et al (2006), the chemical reaction of C₃S with water is given as:



2.13.3.2 Di-calcium silicate

Lea (1998) established that dicalcium silicate (C₂S) is known to have different forms which include α-C₂S, β-C₂S and γ-C₂S. Taylor (1998) has explained that the structures of the belite (C₂S) belongs to one big family, the glaserite (K₃Na(SO₄)₂). At high temperature α-C₂S exist and at a reduced temperature around 1450°C, β-form is found. It converts into γ-C₂S at a lower temperature at about 500°C (Taylor, 1997). In Portland cement production both the β and γ form are preserved. The less dense nature of the γC₂S causes the amorphous nature of β-C₂S to crack and fall to a more voluminous powder on cooling. The γ-C₂S scarcely reacts with water at ordinary temperature.

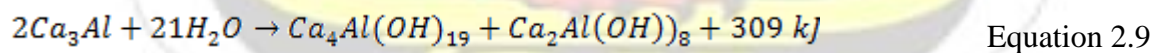
Peterson et al (2006) and Taylor (1997) have indicated that the β-form of dicalcium silicate is the second most abundant constituent of clinker, and falls between 15% and 30% by weight of clinker. The reaction of C₂S is considerably slower than C₃S, produces less amount of Ca(OH)₂ and energy than C₃S, however the CSH gel produced is similar to that of C₃S CSH gel. The reaction of C₂S given by Peterson et al (2006) is:



2.13.3.3 Tri-calcium aluminate

Tricalcium aluminate (C₃A) constitutes 5-10% of most normal Portland cement clinker (Mohammed and Sharp, 2002). C₃A reacts very quickly with water to form poorly crystalline calcium hydroaluminites or AFt phases generally described with the chemical formulae C₂AH₈ and C₄AH₁₉ and releases a high heat of hydration (Thomas et al, 2011). Since the reaction is very fast, if is left unchecked a mechanism called flash set will occur (Quennoz and Scrivener, 2012). The AFt phases formed belong to a group having a general formula, [Ca₂(Al,Fe)(OH)₆]X.xH₂O where X represents half or doubly charges of different anions present during Portland cement hydration or exchangeable single charge (e.g. chloride) (Lea, 1970, Matschei et al, 2007; Taylor, 1998). The most common anions present in cement hydration are OH⁻, SO₄²⁻ and CO₃²⁻.

After about 25 minutes of C₃A reaction with water and in ambient temperature, the AFt phases are then converted into a more thermodynamically stable hydrogarnet, C₃AH₆ (Ca₃[Al(OH)₆]₂) (Leach, 2001). From the studies of Quennoz and Scrivener (2012), the reaction equation is given as:



C₃A Water C₄AH₁₉ C₂AH₈ Energy

The metastable nature of the products formed finally converts to a more stable product, C₃AH₆ at ordinary temperature.

2.13.3.4 Tetracalcium alumino-ferrate

Felite also known as calcium aluminoferrite (C₄AF) constitute 8-14% by weight of cement clinker. It was discovered as cement constituent some years after C₃S, C₂S and C₃A have

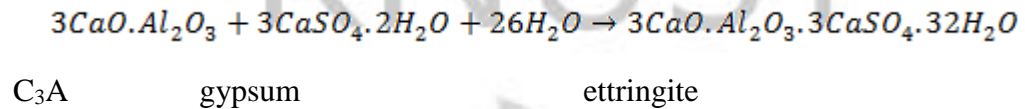
been known (Brouwers, 2005). Many authors have reported that the hydration products of C_4AF are similar to those of C_3A (Csizmidia et al, 2000; Taylor, 1998). In the presence of water C_4AF and absence of gypsum, unstable hexagonal hydrate is formed which later transforms to a more stable cubic hydrogarnet containing Fe^{3+} and Al^{3+} (Taylor, 1998; Csizmidia et al, 2000). The hydrogarnet formed is $Ca_3AlFe(OH)_6$ (C_3AFH_6). The hydration of C_4AF is strongly exothermal.

2.13.4 Mechanism of Portland cement hydration

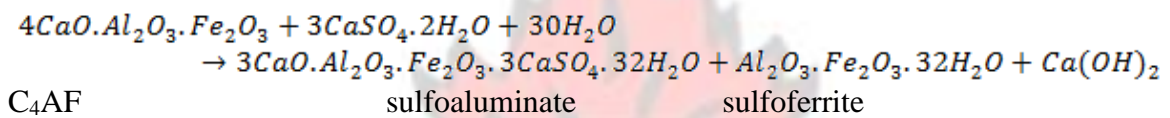
Cement compounds are anhydrous in nature; however, decompose after wetting, forming hydrated compounds in a temporal form of supersaturated and unstable solutions (Lea, 1998). The chemical reaction between anhydrous cement compounds and water is known as hydration of cement. In a cement grain, both the cement compounds and gypsum (13%) constitutes its composition. Cement hydration is in the first instance a reaction of the individual constituents and the calcium sulphate ($CaSO_4 \cdot 2H_2O$) also known as gypsum present in it.

The studies of Jansen et al (2012) have shown that cement hydration is subdivided into about four periods which are as follows: the initial, induction (dormant), the acceleration and retardation periods. At the initial period (up to 20hrs), the belite and the aluminate (C_3A and C_4AF) phases dominate the reaction with a high thermal energy. The presence of gypsum in cement is known to affect the reaction pattern of the aluminate phase dramatically (Thomas et al, 2011). Quick setting of the aluminate phase is very undesirable in concrete hence controlled by the addition of gypsum (Neville, 2002). The consumption of gypsum happens during the dissolution of the aluminate phases. For C_3A , it reacts with

gypsum to give an initial formation of calcium aluminosulphate and later to calcium monosulphoaluminate when all the gypsum is consumed. C₄AF also combines with the gypsum to form a solid solution of sulphoaluminate and sulfoferrite (Lea, 1998). The chemical equations of C₃A and C₄AF and are shown in respective terms as



Equation 2.10



Equation 2.11

Taylor (1998) has indicated that the hydration products of felite accelerate the silicates hydration because it provides nucleation site for portlandite growth. At the induction period the reaction rate behaves inactive for some few hours (about 6 hours), a typical characteristic of C₃S. C₃S at an initial contact with water terminates the reaction rate shortly. This period sees much of dissolution of the main compound, C₃S and crystal growth from solution. The end of the induction period marks the onset of the main hydration period associated with massive amount of calcium silicate hydrate (CSH) and lime formation (Lothenbach et al, 2007; Lothenbach et al, 2008; Korpa et al, 2008). This period is denoted as the acceleration period. The acceleration and the deceleration periods can combine to denote the main period (Stark, 2011). At this point, CSH grows transiting Portland cement crystals into the hardening stage. The heat of hydration reaches a peak level during this main period. The cement compound, C₂S is slowly attacked by water. The chemical reaction as shown previously generates CSH and lime similar to C₃S. The

difference between C_3S and C_2S is in the generation of lime. C_3S generates more lime than C_2S during hydrolysis. Strength development of Portland cement is dependent on the CSH hydrating products contributed by the two, C_3S and C_2S compounds. New research works have embraced the incorporation of secondary products which consists of natural and artificial pozzolanas as additions to Portland cement for strength enhancement and many other parameters. Artificial pozzolana produced from clay minerals is new in the pozzolana industry and has in recent times attracted interest from numerous researchers.

2.13.5 Microstructure of the hydrated phases of cement

The hydration of major compounds present in Portland cement is explained by Scrivener (1984) with schematic illustrations shown in Figure 2.7. Richardson (1999) reported that an understanding of Portland cement-based material requires knowledge at its microstructure level. The microstructure determination is quite complex due to multiphase nature of cement clinker phases and the numerous hydration products such as C-SH, CH, AFt and AFm. However, research into their microstructure analysis has made it to be well understood.

From Figure 2.7, 'A' shows the unreacted cement grain which comprises of C_3S , C_3A and C_4AF . Under the influence of water also known as hydration shown in 'B', approximately 10 mins after that, some portions of C_3A reacts with gypsum ($CaSO_4 \cdot 2H_2O$) in solution forming aluminosulfates on the grain surface and short nods of ettringite (AFt) which nucleate at the edge and in solution. In 'C', the reaction may have attained between 6 and 10 hrs and some portion of C_3S reacts to produce "outer hydration product C-S-H" on AFt nods network. The outer C-S-H product starts the formation of shells leaving about $1\mu m$ between cement grain surface and hydrated shell. These shells formed start connecting with

other parts of the hydrating matrix through outer C-S-H (Gallucci et al, 2010). Gallucci et al (2010) also stated that the outer C-S-H act as a support for the deposition of both inner and outer C-S-H on either side. The formation of C-S-H is well explained by Taylor (1997) who stated that C-S-H is considered to be made of two varieties; inner product C-S-H developed as hydration shells within the original boundaries of the cement grains and the outer product C-S-H formed by throughsolution deposition in the originally water-filled space.

At 'D', the reaction is assumed to attain approximately 18 hrs of which the remaining C_3A hydrates to produce long rods of AFt. At this stage too, inner product of C-S-H starts to form producing inner shell from continued hydration of C_3S . The sketch in E shows a strength gain between 1-3 days where C_3A reacts with any ettringite inside the shell forming hexagonal plates of monosulfates (AFm). An obvious separation occurs between the grain surface and hydrated shell. Hollow shells are also formed as dissolving cement grain continues to progress (Kjellsen and Justnes, 2004). Smaller cement grains may undergo rapid and complete hollow shell hydration, and leave empty hydration shells.

At 'F' the process was estimated to attain a hydration period of approximately 14 days. At this time sufficient inner C-S-H is formed to fill in the space between grain and shells. Inner C-S-H product formed becomes more stable whilst the outer C-S-H attains fibrillar morphology. The microstructure in 'G' shows cement grain hydrated for a long period, approximately one year. At this age the remaining anhydrous materials react by a slow solid state mechanism to form additional inner products C-S-H. Gallucci et al (2010) mentioned that whatever the age of the specimen the shells are formed mostly around the

neighbourhood of silicate parts of the grains. The ferrite phase appears to remain unreacted as appeared in G.

A vital microstructure development of Portland cement apart from sulphate and aluminate phase is crystallization and precipitation of portlandite. Portlandite grows with a variable shape and deposits everywhere in the cement matrix. The presence of gypsum acts as nucleation site favoring the formation of portlandite crystals (Gallucci and Scrivener, 2007).

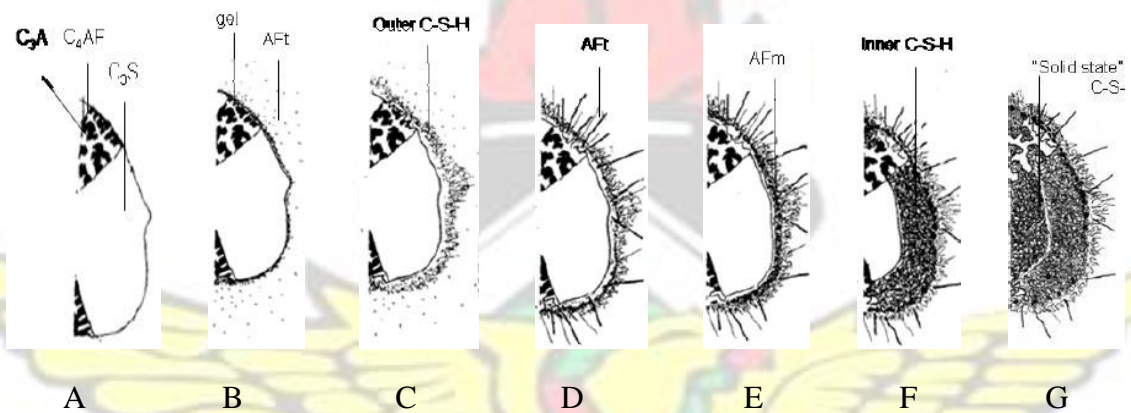


Figure 2.7: Schematic illustration of the microstructure development of OPC (Scrivener, 1984)

Scanning electron microscope back scattered electron (SEM-BSE) imaging is reported by many authors (Costoya Fernandez, 2008; Kjellsen and Justnes, 2004; Diamond, 2004; Scrivener and Pratt, 1984) as one of the most versatile technique for studying microstructure of cementitious materials which evolve quantitatively and qualitatively during hydration. Image analysis used to detect the morphology of hydrated cement components is based on gray level nature under BSE-SEM. According to Diamond (2004) between black and white is a customary division of 256 gray levels or shades of darkness. In Costoya Fernandez (2008) work, water-filled space appears black, unhydrated grains appear bright, portlandite as light gray and C-S-H as a darker gray. The work of Scrivener (2004) states that with

brightness ferrite solid solution remains the brightest, followed by alite and then both belite and aluminate having almost similar gray level scale. Diamond (2004) mentions that unhydrated crystals in cement have much higher electron backscatter coefficients than hydrated products hence appear brighter in BSE-SEM in sea of darker areas. The level of gray according to Scrivener (1984 & 2004) is also dependent on the atomic number of the hydrate. From Figure 2.8 (a), C and B shown inside the microstructure represent unreacted cement grain (C_3S) and portlandite growth (CH) whilst the darker regions show pores. A rim of hydrated C-S-H gel is formed surrounding C indicating a slightly dark gray level.

The microstructure analysis of cement grain at early and late age of hydration differs in terms of water-filled spaces, C-S-H, CH and other hydrated components formation. Costoya Fernandez (2008) reports on the microstructure behavior of alite at 4hrs, 8hrs, 1day, 7 days and 28 days. Between the end of the induction period and about 24hrs of cement hydration time, some cement grains deposit only a thin shell of C-S-H and then 'hollow out' internally, partly or completely (Diamond, 2004). These hollow hydrated shells are also known as Hadley grains which is presented in Figure 2.8 (a) as A. Kjellsen and Justnes (2004) also illustrate Hadley grains well in the visible rectangular mark shown in the right side of figure 2.8 (b). As hydration proceeds between 7 and 14 days (see Figure 2.9) the Hadley grains close-up because larger grains hydrate to form denser C-S-H gel to fill the pores. The morphology of a matured cement paste is presented in Figure 2.10. The figure indicates that at 100 days, some cement grains become hydrated forming more and dense inner product C-S-H whilst unhydrated core of cement grain also remains unhydrated in the matrix.

(a)

(b)

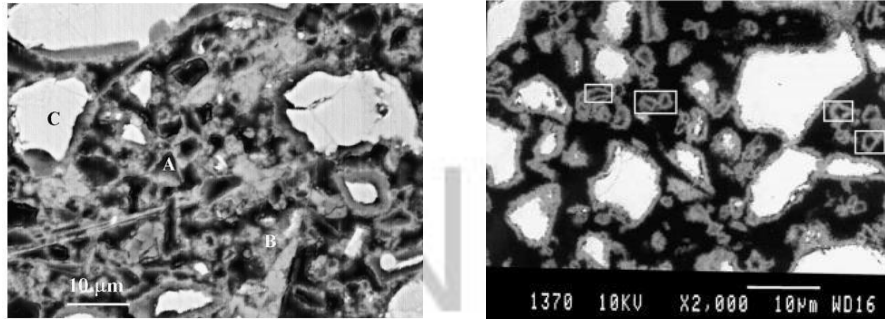


Figure 2.8: 1-day old cement grain (Diamond, 2004 and Kjellsen and Justnes, 2004)

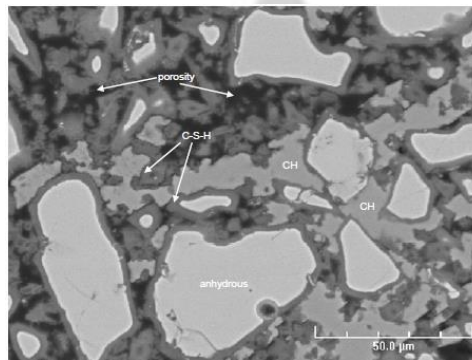


Figure 2.9: Microstructure of alite cured for 14 days at room temperature (Costoya Fernandez, 2008)

Furthermore, in Figure 2.10 (a) microstructure bright shards of ferrite left unhydrated remain as remnants. The microstructure shown at Figure 2.10 (b) differentiates an alite from a belite. With alite rim of C-S-H is formed around the core labeled as A whilst the belite shows almost no evident inner product hydration shell labeled as B. The crosshatched appearance it displays is characteristic of partially hydrated belite, a significant component of Portland cement (Diamond, 2004). The labeled C indicates a fully hydrated core with no cement grain. Bright gray shard shown below C indicates ferrite containing reacted aluminate.

(a)

(b)

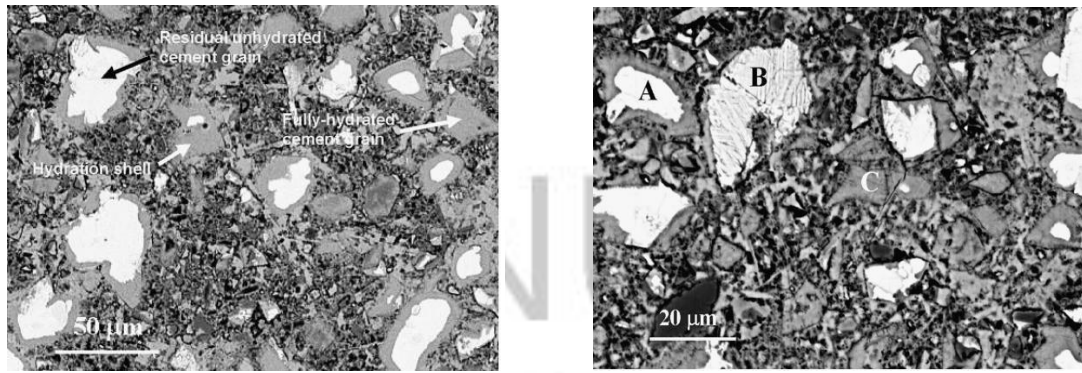


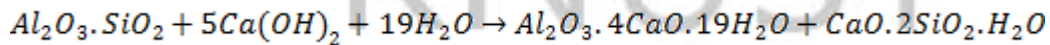
Figure 2.10: Microstructure of a 100-day old cement paste (Diamond, 2004)

2.14 Pozzolanic reaction

Earlier it has been shown from Portland cement hydration that calcium hydroxide is released from the reaction. In fully hydrated cement, between 25% and 30% of Ca(OH)_2 remains as surplus (Kosmatka, 2002; Sabir et al, 2001; Rao, 2003). According to Rao (2003), the morphology of Ca(OH)_2 is relatively weak, brittle and not cementitious which doesn't favor concrete and mortar. Edwin and Dunstan Jr. (2011) reported that the amount of lime generated in hydrated cement varies due to the variance in the amount of C_3S and C_2S .

In many studies, it is indicated that surplus lime could be made cementitious when pozzolanic materials are blended with cement (Sabir et al, 2001; Parande et al, 2011). With blended cement containing pozzolana, two different reactions happen and these are cement hydration and pozzolanic reaction. Cement reaction is known to be faster whilst pozzolanic reaction is very slow. Principally the reaction of pozzolana that happens between surplus lime and aluminosiliceous pozzolanic material leads to the formation of siliceous and aluminum hydrates. Both hydrates are additional secondary hydrates formed out of

pozzolanic reaction which contribute to strength of mortar and concrete. Pozzolanic reaction can still be active even after one year. The investigations of Singh and Garg (2006) on reactive pozzolana from India clays produced the pozzolanic reaction equation which shows aluminate and silicate hydrates formation.



Pozzolana lime water aluminate hydrate silicate hydrate

Equation 2.12

2.15 Clays and clay pozzolana production

2.15.1 Clay

The definitions of clay exist in different ways and are dependent on a particular scientific discipline. However, many of the disciplines define clay by using their particle size. For instance, the geologist and sedimentologist describe it as a geological material of <4µm particle size, the soil scientist <2µm and the colloidal scientist <1µm. For the mineralogist clay is defined as naturally occurring material composed of fine-grained mineral, which is generally plastic at appropriate water content and will harden upon drying and firing (Guggenheim and Martin, 1995). This definition which tries to link particle size with minerals raises the vital issue of clay compositions and implicitly the definition of clay mineral. Clay minerals are basically minerals which occur in clay. These clay minerals mostly referred to are phyllosilicate minerals as well as minerals which impart to clay and harden upon drying or firing also known as the associated phases in clay. Phyllosilicates are a large family of minerals that commonly show layered structures and form component sheets.

2.15.2 Types of clay minerals

Clay minerals can be segmented into three main types depending on the layered structure.

They are

1. Kaolin group (kaolinite, Nacrite, Dickite)
2. Smectite group (Montmorillonite, Nontronite, Biedelollite)
3. Illite group (Illite, Glauconite)

Clay may possess associated phases in a form of interlayer materials and it separates layered structures. The interlayered materials may consist of quartz, calcite, dolomite, feldspars, cations, hydrated cations, organic phases, etc or non-crystalline phases such as colloidal silica, iron hydroxide gels, organic gels, etc (Guggenheim and Martin, 1995). A unit clay structure is a total assembly and consists of both the layered and interlayered materials (Guggenheim et al, 2006).

Clay minerals fundamentally have different structures and compositions; however the basic building blocks are all the same (Zhou and Keeling, 2013). The building blocks form sheets of tetrahedral and octahedral layer which defines the atomic structure of every clay mineral. Tetrahedral sheets do not exist by themselves; however it is linked at apical oxygen to form sheets. A common example of a tetrahedral sheet is silicon tetrahedron shown in Figure 2.11 (i). Grim (1962) and Erberl (1984) have indicated that the octahedral sheet is a cation (Al^{3+} , Mg^{2+} , Fe^{2+} , but not Ca^{2+} or K^{+}) surrounded by six oxygen or hydroxyls (see Figure 2.11 (ii)). Examples of octahedral sheets are brucite ($\text{Mg}(\text{OH})_6$) and gibbsite ($\text{Al}_2(\text{OH})_6$).

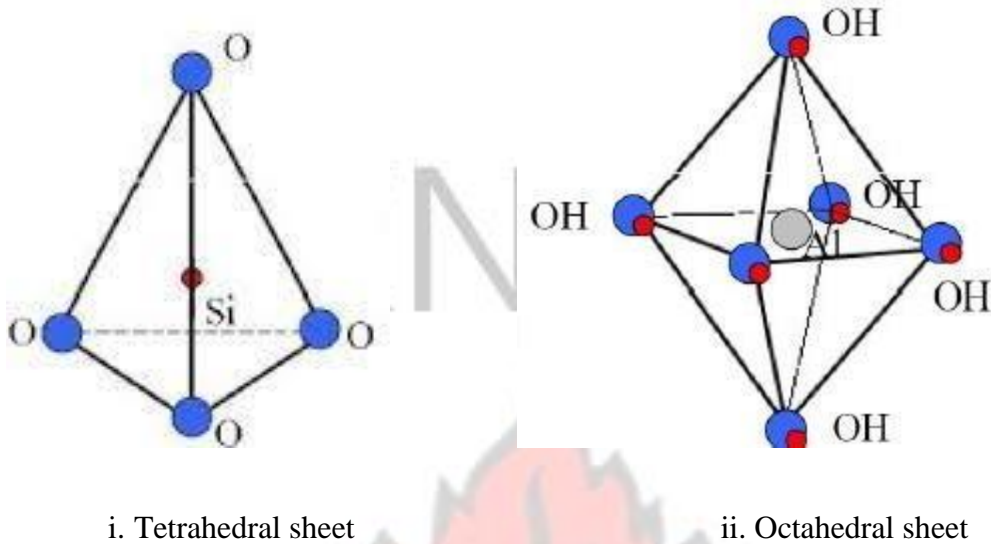


Figure 2.11 Sheet components of clay mineral (Erberl, 1984)

2.15.3 Clay layer

There are two types of layers depending on the ratios of the component sheet: a 1:1 layer has one tetrahedral sheet and octahedral sheet and a 2:1 layer has an octahedral sheet in between two opposing tetrahedral sheets (Guggenheim, 2006). Figures 2.12 and 2.13 present the structures of a 1:1 and 2:1 component sheet. In a clay mineral, tetrahedral sheet is always combined with octahedral sheet. In clay structure shared oxygen bind sheets into layers whilst hydrogen ions surrounding octahedral layers hold sheets tightly together (Zhang et al 2010). Different layers involving silica and aluminium sheets combine together to form different clays. Clay structure can also consist of varying mixed layers of different clay minerals that forms interstratified layers (Murray, 1999). An example of a 1:1 layer is the kaolinite group which includes di-octahedral mineral sheets such as kaolinite, dickite, nacrite, hallosite and tri-octahedral mineral sheets such as antigorite, chamosite, chrysotile, and cronstedite (Grim, 1962).

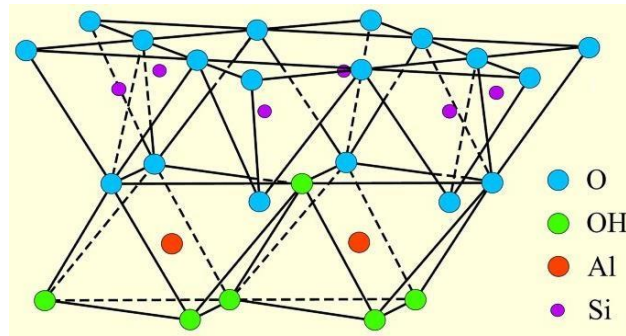


Figure 2.12: Structure of 1:1 layer (Anon, 2001)

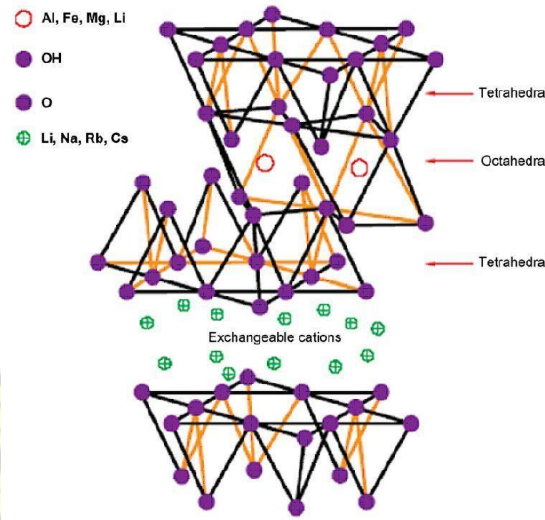


Figure 2.13: A structure of 2:1 clay mineral (Kurecic and Smole, 2012)

Di-octahedral mineral is when two sites of the three valent aluminium present in octahedral sheet are occupied by cations whereas tri-octahedral is when all three sites are occupied with cations in a di-valent atom (Mg^{2+} and Fe^{2+}) to fulfill charge balance. Kaolinite is found predominantly in metamorphic or magmatic rocks rich in aluminosilicates like feldspar.

Major types of 2:1 clay minerals are smectite, vermiculite, illite and chlorite. In dealing with 2:1 clay types, it is important to know the charge of a clay mineral which is mostly a negative charge. The negative charge of clay arises because of isomorphous substitution,

very typical with 2:1 component sheets. Isomorphous substitution is substituting an ion of similar size and generally of lesser charges (Grim, 1962; Murray, 1999). For instance, Mg^{2+} substituted for Al^{3+} leaves a net negative charge of oxygen unattached.

Smectite clay type has large interlayer space attributed to the lack of H-bonding that holds layers together. The cation exchange phenomena allow it to lose water at the surface and also absorb more water to fill the interlayer space. This makes smectite clays shrink and swells hence can be called expansive clays. Typical substitutions are Al^{3+} for Si^{4+} , Mg^{2+} for Al^{3+} . A typical example of smectite clay is montmorillonite (Murray, 1999). Bentonite is predominantly made of montmorillonite clay mineral formed through weathering of alkaline, magmatic rocks or volcanic ashes (Danner, 2013). The swelling behavior of bentonite is the substitutions of mainly magnesium, iron, or aluminum, with hydrated sodium or calcium cations occurring in the interlayer positions (Murray, 1999; Mirza et al., 2009; Alver and Alver, 2012). The predominant cation is used in the classification of high-swelling (sodium) bentonite or low-swelling (calcium) bentonite (Mirza et al., 2009).

Vermiculite clay type has thinner interlayer space as compared to smectite. Cation substitution in the tetrahedral sheet involves Al^{3+} for Si^{4+} whilst Fe^{3+} , Fe^{2+} , Mg^{2+} may substitute Al^{3+} in octahedral layer. The nature of the substitution results in a high net negative charge of vermiculite clay.

The illite clay type has K^+ ions filling the interlayer space. The hydrogen bonding in the octahedral sheet holds the layers tightly together therefore this type of clay is nonexpansive.

Possible cation substitution is Al^{3+} going for Si^{4+} in the tetrahedral layer. This therefore leaves this clay type a high net negative charge. With chlorite type of clay, interlayer basically brucite ($\text{Mg}_6(\text{OH})_{12}$). The H-bonds between layers are very strong therefore non expansive. The possible substitution is Al^{3+} , Fe^{3+} or Fe^{2+} for Mg^{2+} .

Example of this clay type is shales.

2.15.3.1 Clay formation

Clay formation occurs across a wide range of geological environment and throughout geological time (Zhou and Keeling, 2013). They are found as major components of soil, continental and marine sediments, weathered rocks and sediments, altered volcanic deposits, hydrothermal alteration systems and fault gouge (Zhou and Keeling, 2013). The mechanisms of clay formation are broadly explained by three mechanisms: inheritance, neoformation and transformation (Eberl, 1984).

Inheritance is when a clay mineral present in a natural deposit originated from reactions that occurred in another area during a previous stage in the rock cycle, and that the clay is stable enough to remain inactive in the current environment. Inheritance clay formation has a slow reaction rate coupled with the attainment of chemical equilibrium therefore makes the clay formed gain stability (Eberl, 1984).

Neoformation is when the clay formation is as a result of precipitation from solution or has formed from reaction of amorphous materials. The transformation mechanism is when already formed clay keeps some of its inherited structure intact while undergoing chemical reaction. The chemical reaction may take a form of ion exchange or layer transformation. Ion exchange is when loosely bound ions are exchanged with those of the environment

whilst with layer transformation, the arrangements of tightly bound octahedral, tetrahedral or fixed cations are modified (Eberl, 1984).

All these mechanisms occur within the jurisdiction of the geological environment which consists of the weathering, sedimentary and diagenetic hydrothermal environment. The weathering environment is the upper part of the earth crust very near the atmospheric interface with varying temperature and pressure over a relatively narrow range of earth surface conditions. The upper layers of soil on the earth crust undergo continuous erosion with varying solution composition resulting from the parent rock, rainfall, evaporation and drainage. The continuous erosion tends to reduce the reaction time between the earth crust and the atmosphere, which is usually of the order of thousands of years.

The sedimentary environment is located near or below sea or lake level, in depressed areas of the earth crust sometimes downhills. This zone is known as the sedimentary water interface. The ocean floor is an example of this zone. Clay formed in this zone has a longer reaction, millions of years because the rate of sedimentation and subsidence, rate of sea floor subduction is a slow process (Eberl, 1984). Clays that originate in the diagenetic hydrothermal environment are those that come in contact with hot water.

The geological environmental condition that leads to clay formation is a cyclical process. Figure 2.14 presents the process cycle. Clay's neofomed from crystalline rocks in the weathering environment are washed away into the sedimentary environment. In this zone the weathered rock fragments are buried and heated in the diagenetic-hydrothermal zone. In this environment they are recrystallised through a metamorphic action and with uplift and erosion, the cycle restarts again

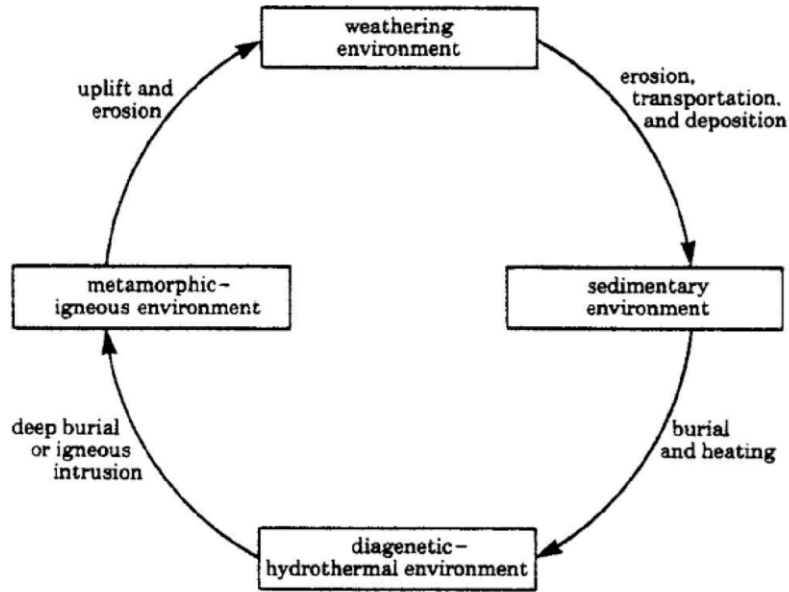


Figure 2.14: Process cycle for clay formation (Eberl, 1984)

2.15.3.2 Availability of clays in Ghana

Large deposits of clay exist in higher quantities all over Ghana (Kesse, 1985). The total estimated clay deposited is over 1500 million tonnes. Table 2.15 presents the estimated deposits in the ten regions of the country.

2.15.4 Clay pozzolana production

The production of clay pozzolana from different clay minerals consisting of 1:1 (kaolinite) and 2:1 (smectite, illite, chlorite) component sheets have been well investigated by many authors (Momade and Atiemo, 2004; Singh and Garg, 2006; AlRawas and Hago, 2006; Buchwald et al, 2009). In almost all these studies, clay pozzolana production has been done through thermal activation or calcinations in furnaces or calcination kilns.

Table 2.15: Clay deposit in Ghana (Kesse, 1985)

Region	Tonnage(million)
Central	106
Greater Accra	200
Eastern	90

Western	742
Ashanti	39
Brong Ahafo	17
Volta	165
Northern	11
Upper East and West	22

2.15.5 Degree of dehydroxylation based on calcination temperatures

Tironi et al (2013) reported that calcination temperatures from 500-900°C produce suitable pozzolanic product from clay. In the general sense, during thermal activation of clay within the temperature range, three stages happen: dehydroxylation, calcinations and crystallization (Al-Rawas, 1998; Heller-Kallai, 2006). The dehydroxylation of clay mineral is preceded by mass loss between the temperature range of 30 and 200°C attributed to drying of physically absorbed water (Fernandez et al, 2011). With the process of dehydroxylation, two hydroxyl groups, from the hydroxyl surface, join to form a water molecule leaving the once bonded oxygen as a superoxide anion. The instabilities caused by the anion imbalance result in crystal structure collapse forming metastable, anhydrous aluminium silicates (Taylor-Lange et al, 2015). Mendelovici (1997) has reported that the octahedral sheet loses water and decomposes into disordered meta-state in the situation of collapsing clay mineral. Many authors have shown that reactive pozzolana is obtained at the meta-stable state because of the formation of amorphous silica (Sabir et al, 2001; Kakali et al, 2001; Singh and Garg, 2006). The extent of disorderliness influences the extent of reactivity of clay pozzolana.

Dehydroxylation of clay mineral can be observed at a temperature ranging between 400 and 800°C depending on the clay type. Studies by Fernandez et al (2011) have shown that dehydroxylation of 1:1 clay mineral like kaolinite is completed at 600°C whereas the 2:1

clay mineral such as illite, montmorillonite are observed above 600°C. Their studies further confirmed that kaolinitic clays among other clay minerals had a higher potential for pozzolana activation due to the easiness of hydroxyl group removal than the other 2:1 clay types.

The metastable state at higher temperature (above 1000°C) is transformed from the amorphous state into crystalline units. Reactivity of pozzolana becomes inhibited with the presence of crystalline matters. The calcination temperature occurs just above the completion of the dehydroxylation peak and below the onset of the crystallization peak (Al-Rawas, 1998). The investigations of Buchwald et al (2009) have shown that the firing temperatures and conditions to obtain amorphous silica are functions of clay minerals, dehydroxylation and recrystallization behavior. The differential thermal analysis is useful to provide dehydroxylation, calcinations and crystallization temperatures. Figure 2.15 shows the dehydroxylation thermograms of three clayey structures, kaolinite, illite and montmorillonite. Kaolinite and illite showed small mass loss between 30 and 250°C through the drying of absorbed water. The high amount of water released at the initial stage of drying is usually typical of montmorillonite clays which have much water in between layers. In the dehydroxylation process, kaolinite peaked between 400 and 650°C, illite between 400 and 750°C whereas montmorillonite peaked between 600 and 800°C.

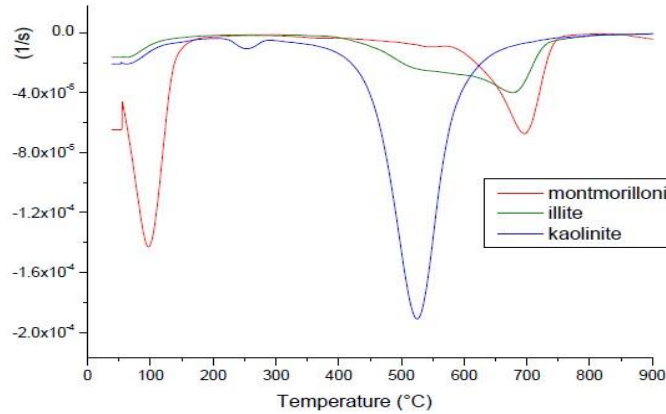


Figure 2.15: Differential thermal analysis of kaolinite, illite and montmorillonite clay structures (Fernandez et al, 2011)

2.15.6 Degree of dehydroxylation based on calcination time

The time factor in the dehydroxylation process of clay during calcination is important when economics is of great essence. The work of Ilic et al (2010) showed that calcining kaolinitic clays above 60 and 90 mins has little or no effect on the clay materials. Figure 2.16 presents the results obtained when kaolinitic clay were calcined at temperatures between 550 and 700°C for different times at 30, 60, 90, 120, 150 and 180 mins.

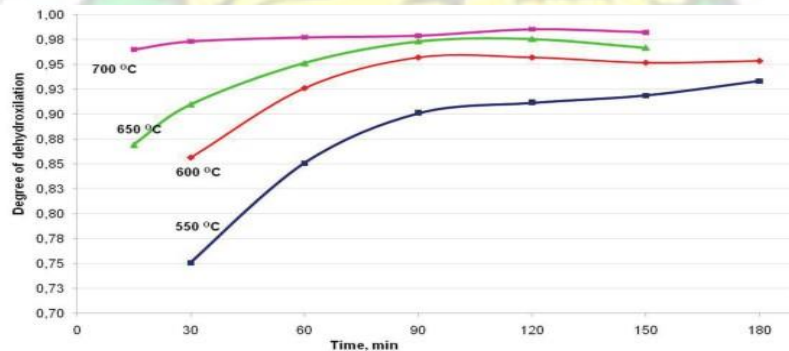


Figure 2.16: Dehydroxylation of calcined clays at different temperatures and time (Ilic et al, 2010)

2.16 Characterization of pozzolana

The characterization of pozzolanic materials gives indications of the material reactivity and suitability for various cement-based applications. The pozzolanic reactivity is the ability of a pozzolanic material to produce components of binding properties as a result of reaction with lime and other cement constituents (Uzal et al, 2010; Fernandez et al, 2011). Day (1990) has characterized pozzolana, both natural and artificial in two broad classifications. These classifications involve 1) systems based upon the chemistry or mineralogy of the material and 2) systems based upon the reactivity and performance characteristics of the pozzolan.

2.16.1 Classification based on chemistry or mineralogy

Muhmood et al (2009) have provided the information that both the chemistry and mineralogy of pozzolanic materials are related therefore the type of minerals present in the material can also explain the chemistry or chemical composition of the particular pozzolana. The mineralogy and chemistry of pozzolanic materials vary depending on the composition and source of clay material (Lea, 1998; Taylor, 1998) thus forms a complex and many different minerals after pozzolana production. The produced pozzolana depending on the mineral present could be characterized as a kaolinitic, mica (illite, montmorillonite) clay type, etc. Many different procedures exist from literature in the determination of mineralogy or chemistry of pozzolanic materials. Examples of such methods include X-ray diffraction analysis, morphological analysis using SEM-EDX, TG-DTA analysis, etc (Lea, 1998; Taylor, 1998).

The ASTM C618 classifies pozzolana based on the active mineral of silica, alumina and iron oxide. The summation of the three; silica, alumina and ferrate should not be less than 70%. The greater the amount of silica, alumina and ferrate put together, the greater its assumed pozzolanic activity. Malvar and Lenke (2006) have reported that higher contents of SiO_2 in the mix of appropriate content of both alumina and iron oxide contribute effectively to pozzolanic effect of the material. Silica alone when considered cannot be much effective as aluminosilicates (Shvarzman et al, 2003). For high reactivity, the silica should be greater than 40%, alumina greater than 30%, iron oxide 20% (Al-Rawas et al, 1998). The chemical composition of most pozzolanic materials including clay pozzolana contains many different elements in a form of oxides. However, in cement science two main oxides classified as major and the minor oxides as well as loss of ignition (LOI) are of much interest. The major oxides include SiO_2 , Al_2O_3 and Fe_2O_3 whilst the minor components include CaO , MgO , Na_2O , K_2O , SO_3 . These oxides and the LOI values have significant effect on the pozzolanic reaction in unique and distinct manner.

Cement and pozzolana mixture during interaction forms CSH and CAH (containing Al and Fe), therefore a good proportion of the active phases in a pozzolan may be considered as an indication of the Portlandite binding potentials. Helmuth (1987) has shown that for a pozzolana to reach complete reaction with cement in a cement pozzolana mixture, the equation 2.13 below could be specified. Assuming a pozzolana in a total mix is α , cement portion will be $1-\alpha$. Following the active compounds present in pozzolana and cement, the amount of α could be deduced. However, this theory may entirely not be the case when results are not corroborated with other parameters. In most instances natural and artificial pozzolanas consist of heterogeneous mixture of phases therefore it becomes very difficult

to establish a direct relationship between the active chemical compounds and pozzolanic activity.

$$\frac{\%SiO_2 + \%Al_2O_3 + \%Fe_2O_3}{\%CaO} = 1 \quad \text{Equation 2.13}$$

Considering the minor compounds, an increased presence of MgO (greater than 2%) may be detrimental to the soundness of cement, especially at late ages. Beyond that limit it appears in clinker as free MgO called periclase. Periclase reacts with water to form $Mg(OH)_2$, and this is the slowest reaction among all other hardening reactions. Since $Mg(OH)_2$ occupies a larger volume than the MgO and is formed on the same spot where the periclase particle is located, it can split apart the binding of the hardened cement paste, resulting in expansion cracks commonly known as magnesia expansion (Ali *et al*, 2008). In Lea (1999), between 0.1% and 4% is appreciable in a cement matrix. High percentage of SO_3 tends to cause unsoundness of cement. The Americans in their standard, ASTM C618 limits SO_3 to 4% and 5% whilst the Indian standard is less or equal 2.75%. The cement technology identifies K_2O and Na_2O as the most important alkalis. The reason is that these alkalis at higher levels and in the presence of moisture give rise to reactions with certain types of aggregates to produce gel which expands and give rise to cracking in mortars and concretes. In ASTM C618, the maximum value for combined alkali content is 1.5%.

LOI indicates the amount of unburnt carbon in the material. However, with natural pozzolans like clay and shales, LOI values may not necessarily be a measure or indication of carbon content. It may be burning away of residual calcite, bound water molecules and clay materials (Kosmatka and Wilson, 2011). High LOI content may be detrimental to concrete and mortar. It is also known that a high value of LOI results in increased water

requirement and dosage of super plasticizer usage in mortar and concrete (Sata et al., 2007). Maximum LOI values for both American and Indian standards for common pozzolanic material are 10% and 12% respectively.

2.16.1.1 Analysis of calcined clays using XRD

Xu et al (2012) state that highly reactive pozzolana should possess maximum amount of amorphous silica and the presence of many silanol groups. The amorphous nature of pozzolana and its associated silanol groups are highly influenced by the combustion temperature and sometimes duration of calcination. At appropriate calcination temperature and time, clay pozzolana can exhibit low crystalline or amorphous silica and other vitreous materials. The amorphousness of pozzolanic materials could be studied on the XRD pattern as a “hump” (Heikal et al, 2013). An example is shown in Figure 2.17 where a halo/ hump appear between 15 and 30° of 2θ axis. However, high crystalline structures such as mullite, haematite, α-quartz, etc emerge when clays are calcined at high temperatures. Sometimes crystalline matters are found in clays as associated minerals and they grow with heating. Fraix et al (2007) argue that the crystalline phase at an increased temperature is related to the recrystallization process from amorphous silica at the dehydroxylation and calcinations temperature. Both the crystalline and noncrystalline phases present in clay pozzolana are identified by analyzing the mineralogical composition.

Samet et al (2007) and Escalera et al (2012) present examples of thermally activated clay minerals of kaolin and illite/montmorillonite type shown in Figure 2.18 (a and b). Figure

2.18a indicates the presence of kaolinite and non-clay mineral (quartz) whilst Figure 2.18b showed the presence of crystalline matters (mullite, haematite), an indication of higher temperature burning of clay mineral.

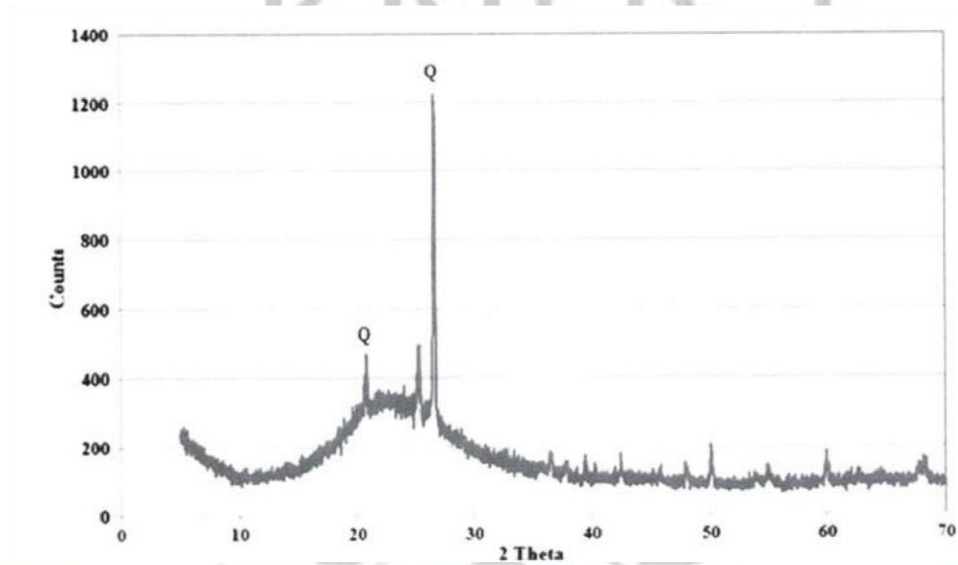
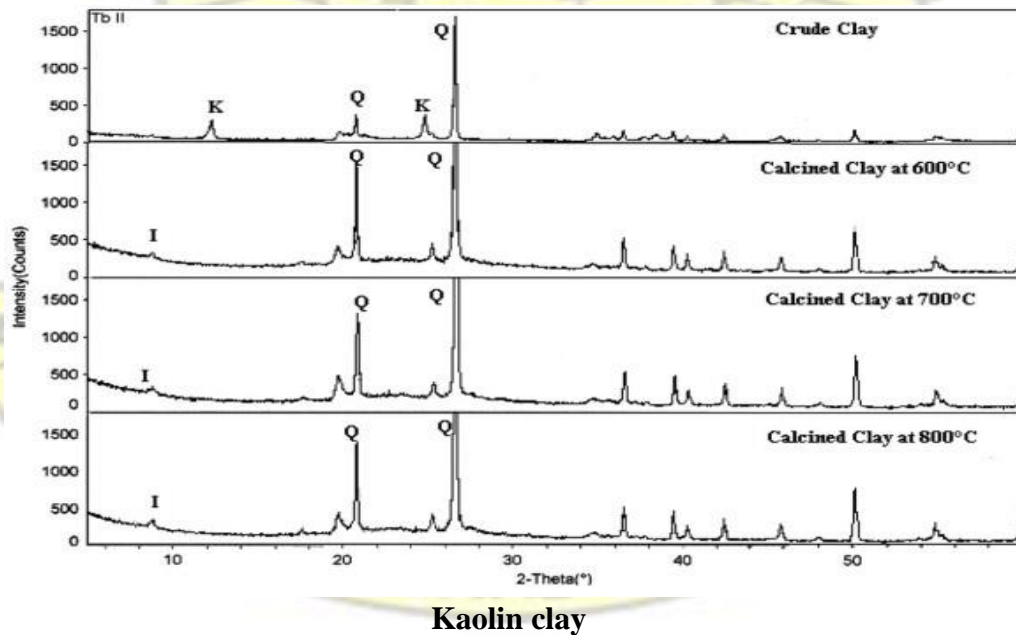
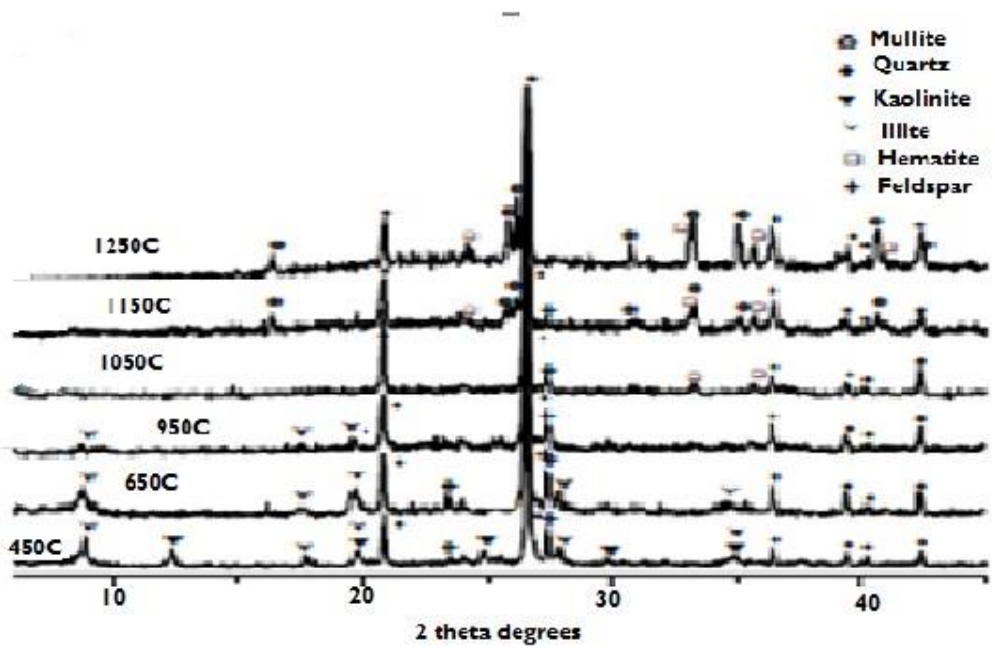


Figure 2.17: Hump structure between 2 theta= 15-35 of metakaolin (750°C) (ALSalami et al, 2013)

(a)

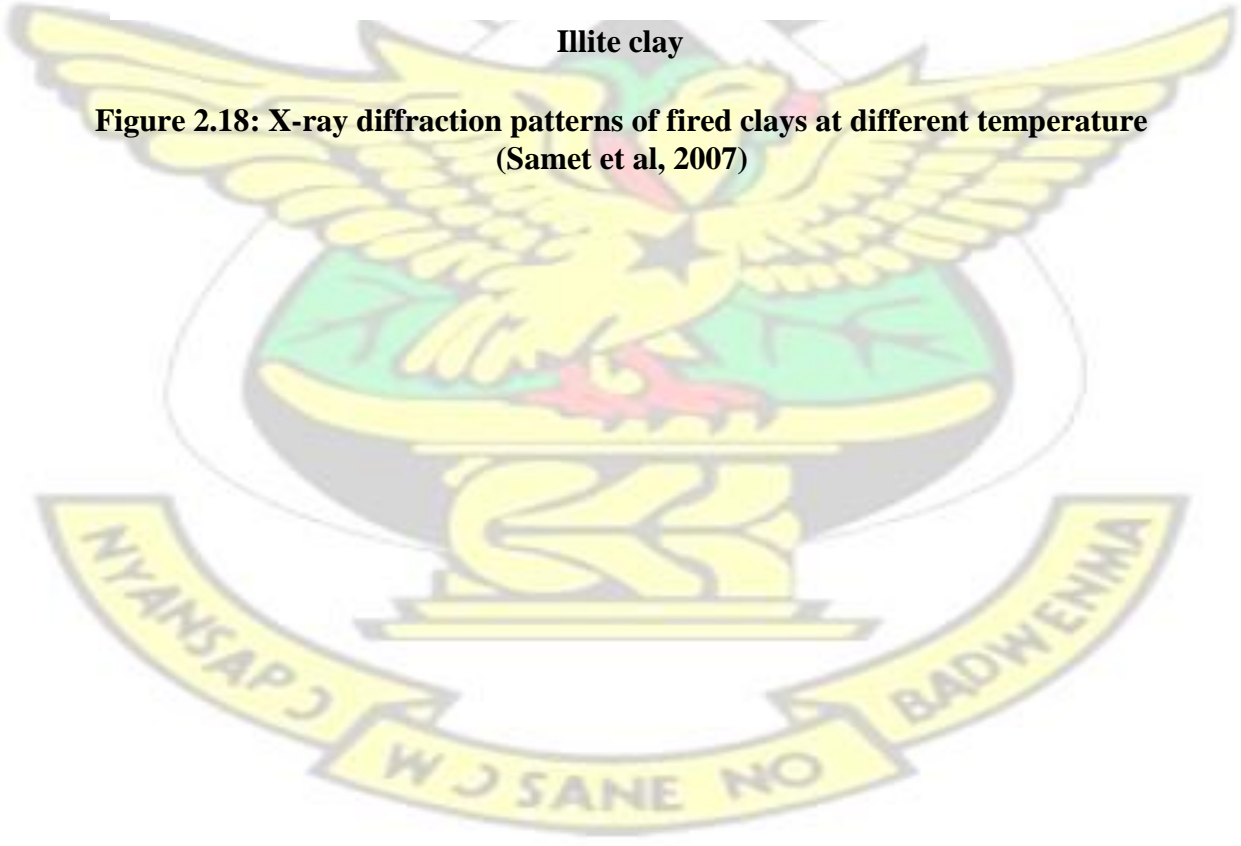


(b)



Illite clay

Figure 2.18: X-ray diffraction patterns of fired clays at different temperature (Samet et al, 2007)



2.16

.1.2 Analyses of calcined clayey structures using MAS NMR

The calcination process discussed earlier showed that clay attains a disordered structure after pyro processing. The Magic Angle Spinning Nuclear Magnetic Resonance (MAS NMR) is the appropriate tool used to determine the chemical environment of aluminium or silicon atoms whilst quantifying the different atomic coordination. Sometimes the mineralogical analysis using the XRD may not be enough to determine the effect of dehydroxylation of clay. XRD is limited to crystalline and sometimes amorphous phases however MAS NMR is not limited to that rather nuclei and its surrounding environment except paramagnetic nuclei such as Fe and Mn.

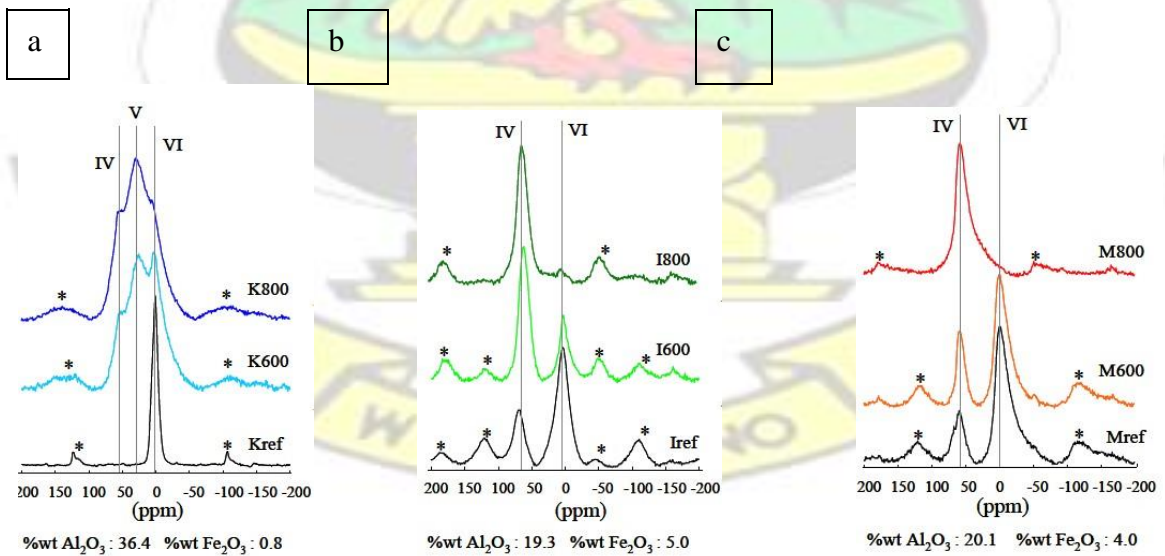
2.16.1.2.1 ^{27}Al NMR on clay

^{27}Al NMR probes into the aluminate phases of aluminosilicate materials. ^{27}Al NMR distinguishes between the tetrahedrally (Al^{iv}) and octahedrally (Al^{vi}) coordinated aluminium (Mendes et al, 2011). It is generally known from literature that the tetrahedral coordinated Aluminium resonates between 50 and 80 ppm whereas the octahedral coordinated aluminium also resonates between -20 and 20 ppm (Hanna et al, 1995). Calcined clays could be identified by four and six coordinated aluminium, however with metakaolinites there could be the presence of five coordinated Al around the chemical shift of -23 ppm, and sometimes 26.1 ppm (Fernandez et al, 2011; Fraiss et al, 2013). The transition from six to four coordinated aluminium could be a criterion to determine reactivity of calcined clays. This could be determined through the analysis of the intensities and the nature of shielding relating a particular resonance peak at the Al^{iv} . In the studies of Klimesch et al (1998) and Pena et al (2008), they indicated that reactivity of calcined

clays are greater when the population of six-fold coordination Al is minimal whilst the five and four-fold coordination is high.

Figure 2.19 indicates Al NMR spectras of kaolinite, illite and montmorillonite clays respectively. The sharp peak observed at Al^[vi] in the uncalcined clay indicate a well ordered octahedral structure. The studies of Murgier et al (2004) and Massaza (1993) confirmed this trend. Calcining kaolinite at 600°C showed the appearance of Al^[v] and Al^[vi] peaks at 28 and 56 ppm respectively. A further calcination at 800°C shifted Al^[vi] to Al^[v] to reach a peak level indicating a disordering of the original crystalline structure. This shows a vivid sign of dehydroxylation as OH groups in clayey soils are originally bound to aluminium.

The behavior of montmorillonite clays under heat treatment is similar to that of illite clay structures. The clear difference between the two is that the transition of Al^[vi] to Al^[iv] is a gradual process as shown in Figures 2.19b and 2.19c.



2.16

Figure 2.19: NMR spectras of kaolinite (a), illite (b) and montmorillonite (c) (Fernandez et al, 2013)

.1.2.2 ^{29}Si NMR of clay

Si NMR probing could also be used to determine the environment of layered silicates and as an indicator of the reactivity of calcined clays. Usually the local silicate tetrahedral is designated as Q^n , where Q is the silicon tetrahedron bonded by four oxygen atoms and n is the number of other Si atoms via oxygen (Mendes et al, 2011). MacLeren and White (2003) stated that an increase in the Si atom bonded to the central Si tetrahedron produces an increase in the average electron density. This results in a more negative chemical shift. The studies of Hjorth et al (1988) indicate that between -68 to -76ppm is Q^0 , -76 to 82ppm is Q^1 , -82 to -88ppm is Q^2 whereas -110 ppm is Q^4 . The work of Skibsted and Hall (2008) showed that Q^3 resonates around -93ppm. Higher coordination numbers which include Q^5 and Q^6 also show a chemical shift at ~ -150 ppm and from -180 to -190 ppm respectively (Stebbin and Kanzaki, 1991). They stated that the $\text{Si}^{[vi]}$ coordination usually is the most common silicate on earth formed as a results of high pressure.

Studies of Si MAS NMR show little or no difference in the breath of Si resonances for highly ordered and disordered aluminosilicates like clays. Behavior of peaks in Si MAS NMR could give an indication of the extent of amorphousness of a disordered aluminosilicate material. Figure 2.16 presents Si MAS NMR of uncalcined and calcined kaolinitic clay between 600 and 800°C. The figures show a chemical shift showing differences in resonances. The figures from Figure 2.20 (A-D) indicate that clay calcined

at 700°C and resonating at a highest point of 103 ppm may be more reactive than the rest even though the local silicate tetrahedral designated is Q⁴ for all of the calcined clays.

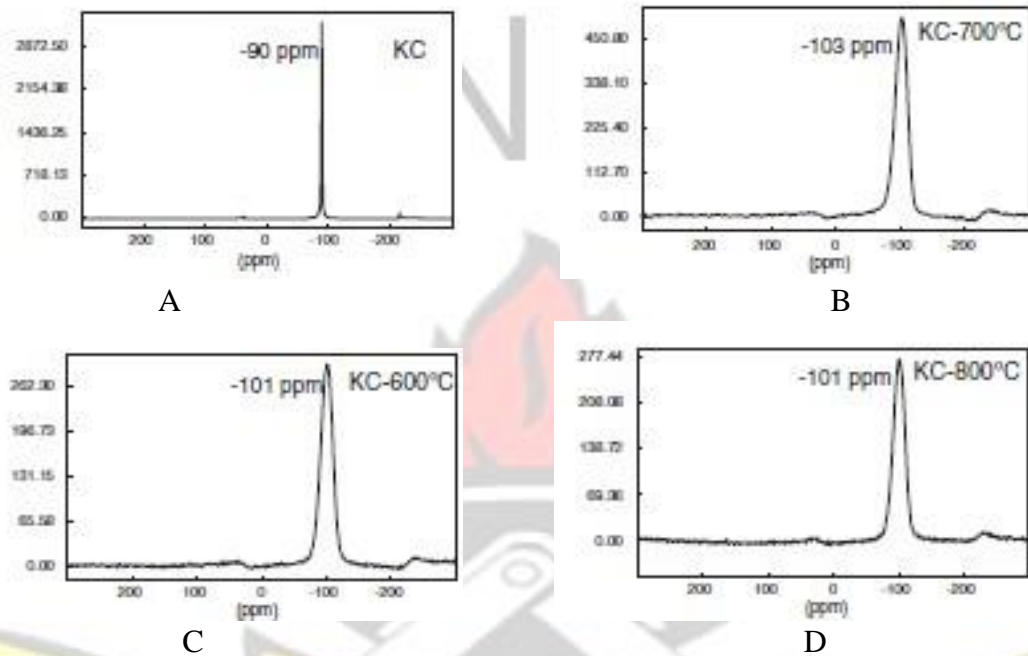


Figure 2.20: Si MAS NMR spectra for calcined kaolinitic clay between 600 and 800°C (Maia et al, 2014)

2.16.1.3 Analysis of calcined clayey structures using TGA/DTA analysis

The TGA can also indicate the effectiveness a given thermal treatment could be on clay dehydroxylation. As shown in Figure 2.21a, at 600°C, the amount of hydroxyl that remains in kaolinite is negligible. Illite clay structures showed a partial completion at 600°C but totally disappeared at 800°C showing a complete dehydroxylation in Figure 2.21b. With montmorillonite clay, at 600°C, dehydroxylation remained incomplete however at 800°C there was a complete dehydroxylation as shown in Figure 2.21c.

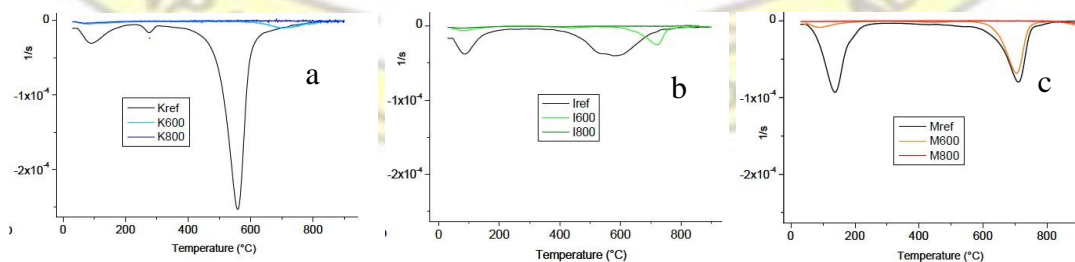


Figure 2.21: DTG curves for raw and calcined kaolinite, illite and montmorillonite clay structures

.2 Classification based on performance

The performance based form of pozzolanic material classification is sometimes more reliable than the chemistry/mineralogical classifications (Day, 1990). Literature presents a wide range of performance based test to determine the pozzolanic activity. This could broadly be classified as either direct or indirect methods of test (Donatello et al, 2010). According to Donatello et al (2010) the direct method monitors the presence of $\text{Ca}(\text{OH})_2$ and its subsequent reduction in abundance with time as pozzolanic reaction proceeds whilst the indirect method measures a physical property of a test sample that indicates the extent of pozzolanic activity. The direct method uses analytical methods such as X-ray diffraction (XRD), thermogravimetric analysis (TGA) or classical chemical titration which involves the Frattini and saturated lime test (Frais et al, 2007; Rahhal and Talero, 2004). In recent times, MAS NMR is used to quantify aluminosilicate phases in a hydrated material. The indirect test methods may involve measurement of properties such as compressive strength, electrical conductivity and heat evolution by conduction calorimetry (Shi et al, 2005; McCarter & Tran, 1996; Paya et al, 2001). The American Society for the Testing of Materials (ASTM) overall performance of pozzolana is based on strength (pozzolanicity), workability (water requirement), serviceability (shrinkage) and durability (alkali aggregate reactivity) (Day, 1990). Some available standards have straight forward values which gives indication of its pozzolanic activity based on the strength index. The strength activity index is influenced by factors such as nature of hydration reaction, packing effect and pozzolanic reaction (Mehta, 2009). Tables 2.16 and 2.17 present classifications based on strength activity index by the Indian and the American standards respectively. Other performance

based classifications have been studied by different authors. An example is the investigations by Mehta (2009) given in Table 2.18. His classification is based on whether a material is cementitious or pozzolanic which could be highly reactive, normal or weak in reactivity. It has been reported by Donatello et al (2010) that results from indirect pozzolana reactivity test are often corroborated with results from the direct test to confirm that pozzolanic reaction is occurring.

Table 2.16: Indian standards classification based on strength activity index (Day, 1990)

Activity	Strength (MPa)
Very inactive	<1.4
Inactive	1.4- 2.8
poor activity	2.8-4.1
intermediate	4.1- 5.5
Active	5.5- 6.9
Very active	>6.9

Table 2.17: ASTM classification based on strength activity index (Day, 1990)

Activity	Strength (MPa)
Poor or inactive	<2.6
Intermediate	2.6-5.6
Active	>6.9

2.17 Pozzolanic activity of clay pozzolana

It has been indicated already that pozzolanic activity of clay pozzolan is determined using the direct (X-ray diffraction and thermogravimetric analysis, chemical titration) or indirect method (strength activity index, electrical conductivity, titration and heat evolution determination). For the direct methods, Talero (2005) and Fraiss et al (2007) stated that the titration method is the commonest in literature.

Table 2.18: Mehta classification of performance based pozzolanic materials (Mehta, 2009)

Class	Description	Example
I	Cementitious	granulated blast furnace slag
II	Cementitious: Pozzolanic	High calcium fly ash
III	Highly reactive pozzolana	Silica fume, Rice husk ash
IV	Normal pozzolans	Low Calcium fly ash
V	Weak pozzolans	slow- cooled blast furnace slag, Open pit rice husk ash

The direct method is a reaction between pure phases, i.e between CaO or Ca(OH)_2 and a pozzolana excluding other constituents of cement. This therefore provides little or no information with regards to realistic reactions which take place between clay pozzolana and cement. In general, the direct method of analysis characterizes lime activity.

The strength activity index (SAI) is also a popular and preferred method for the indirect test methods compared to the electrical and heat evolution method. Though Luxan et al

(1989) report that the electrical conductivity method under the indirect method of test is not time consuming as strength activity index, it differs from SAI. The reason is that the electrical conductivity is sensitive to only the pozzolanic effect of powder materials, however excludes the filler effect whereas SAI test method is sensitive to both pozzolanic effect and packing effect. Sinthaworn and Nimityongskul (2009) have indicated that both the pozzolanic and the packing effects combine to give an improvement in the compressive strength of concrete and mortar containing a good pozzolana.

Among the two popular methods i.e the titration and the strength activity index methods, several authors concluded that strength activity index gives a realistic presentation of pozzolanic activity of a powdered pozzolanic material. The reason is that the process to achieve strength combines almost the characteristics including lime reactivity and filler effect to give a real reaction between a pozzolan and cement. Several authors such as Donatello et al (2010), Tironi et al (2013) have used strength activity index to explain pozzolanic activity of pozzolonas.

2.17.1 Pozzolana strength activity index

This method is determined based upon a comparison of the compressive strength of mortars containing a pozzolan as a partial replacement for Portland cement to reference mortar containing only Portland cement as binder. In many research works on pozzolanas, a great reliance has been on ASTM C 311 which states that the pozzolanic activity index of a pozzolan incorporated concrete or mortar after 7 and 28 days of curing should at least be greater than 75% of the reference mortar or (Agarwal, 2006; Shi et al,

2005). Cheriaf et al (1999) also give 85% of strength at 90 days. Moreover, the description and details of SAI values are well explained in Tables 2.16 and 2.17 shown above.

2.17.2 Optimum temperature determination of calcined clays using strength activity index

Pozzolanic strength activity index covers all reactions happening among the active phases of pozzolan, calcium hydroxide from cement and water. The quality and quantity of the active phases are influenced by calcination temperature (Tironi et al, 2013). Pozzolanic activity of clay at different calcination temperature has varying capacities in reacting with lime from cement. Amin et al (2012) used the strength activity method to determine the optimum temperature of clay calcined between 400 and 800°C. His optimum temperature of the clay upon many considerations such as economics and time was at 600°C.

Cheng (2012) also determined the optimum temperature of a natural pozzolana with the strength activity index. At 800°C, their results showed a superior hydration and pozzolanic reactivity than other temperatures. Optimal thermal activation of clay could lead to a high reactive pozzolana and at a high optimal replacement level of cement improves the strength of mortar (Quyang, 2011).

2.18 Influence of clay pozzolana in cement matrix

2.18.1 Physical properties of cement paste and mortar

The physical properties regarding paste and mortar containing clay pozzolana could be categorized into mechanical and non-mechanical properties. The mechanical properties of mortar are behavior under the effect of load whereas the non-mechanical properties are

characteristics of cement paste and mortar other than load response, which affect selection, use, and performance (Mamlouk and Zamiewski, 2006). There are so many characteristics of cement paste, mortars and concretes that are very necessary; however, the materials engineer would prefer some important characteristics including mechanical and some non-mechanical properties especially with respect to cement and pozzolanic studies. In this regard, the mechanical properties mostly preferred include compressive, tensile, and flexural strengths whilst non-mechanical properties include normal consistency, setting times, workability, shrinkage and soundness.

2.18.1.1 Compressive strength

For pozzolanic material development, the most important strength considered is compressive and tensile strengths. Several studies have shown the strength characteristics of mortar and concretes containing both natural and artificial pozzolanas (Chindaprasirt *et al* 2005; Ezziane *et al*, 2007; Rukzon and Chindaprasirt, 2012). An intelligent use of pozzolanic materials considerably enhances strength. Many research works regarding cement replacement with pozzolana have been in the range of between 20 and 30% and beyond this replacement value, strength decreases (Oriol and Pera, 1995; Peckmeszci and Akyuz, 2004; Samet *et al*, 2007 and Toledo Filho *et al*, 2007). The study of strength properties of mortar and concrete is observed from two different dimensions, the early and late strength development. In standard practice, early days are between 1, 3 and 7 days where about 10-20% of strength is achieved whilst the late ages are days after 28 days where about 80% of strength is achieved (ASTM C109; EN 197; Siddique and Klaus, 2009). Other reactive pozzolanas require 28 to 90 days to exceed control strength, depending on the curing conditions and mixing proportions.

At early ages most pozzolanic materials retard strength however their trends are usually different at the late ages. It is usually marked with a significant increase in strength values either higher or similar to Portland cement. An example of a recent work on calcined clay utilization is the studies of Tironi et al (2013). They replaced cement with clay pozzolana and at 7 days attained a lower strength than the controlled mortar whilst at 28 days attained about 30% more than the control mortar. This study is supported by investigations from different authors such as Badogiannis et al (2005), Curcio et al (1998) and Khatib and Hibbert (2005). Strength properties are influenced by hydration reaction, pozzolanic reaction and the cement matrix densification or packing effect (Mehta, 2009).

Hydration reaction occurs between Portland cement and water whereas pozzolanic reaction is also between the silico-aluminous component of a pozzolana and portlandite which is released during Portland cement hydration. Portland cement at any quantity in a matrix undergoes hydration; however, with a partial replacement with pozzolanic materials, Agarwal and Gulati (2006) argue that there is the occurrence of cement dilution within the given matrix. The dilution effect limits the rate of Ca(OH)_2 production thus reducing cement hydration and this is seen at the early age strength reduction of cement with pozzolana. The dilution effect also creates avenue for more space to accommodate new hydration products. Besides the dilution effect, others have attributed the early age strength reduction to the slow nature of pozzolanic reaction which occurs after 7 or 14 days (Kadri et al, 2012; Indrawati and Manaf, 2008). This slow process inhibits cement hydration hence reduces the early strength. Strength gain of pozzolanic materials at later ages which sometimes surpasses or is similar to the control mix could be attributed to these factors;

cement matrix densification or packing effect and pozzolanic reaction. The mention of packing effect brings to the fore material fineness. Isaia et al (2003) define packing effect as the proper arrangement of small particles which fill voids or pores during cement hydration and contribute to the increment of compressive strength. Some observations have been made by Indrawati and Manaf (2008) and these observations indicate that pozzolanic reaction takes up lime and creates pore size refinement of the hydrated cement matrix. This lime consuming process and the associated pore refinement process leads to increased strength as well as other important properties such as pozzolana cement matrix impermeability, durability and chemical resistance.

2.18.1.2 Optimal replacement level of cement with pozzolana

The reason for achieving optimum pozzolana dosage in cement mortar or concrete is usually influenced by the following factors: (1) reduction of portlandite in cured pozzolana and cement system (2) degree of pozzolanic reaction (3) the mechanical strength of mortars or concrete (Malquiro, 1960; Lothenbach et al, 2011). Portlandite reacts with silica and alumina phases in pozzolana which leads to surface etching and a redissolution of both components. During cement and pozzolana hydration, sufficient amount of pozzolana reacts with portlandite to enhance strength development.

Inadequate pozzolana would render portlandite redundant in cement hydration products.

On the other hand, more pozzolanas also generates low concentrations of portlandite ions (Ca^{2+}). In cases like this the ratio of Ca/Si ratio becomes less than 1 which make hydrates very unstable and therefore decomposes. Low concentrations of Ca^{2+} especially at early hydration stage produces low pozzolanic reactivity hence decreases compressive strength.

Helmuth (1987) proposed an equation based on the ratio of the active components (Silica, alumina and Ferrate) to calcium oxide in both cement and pozzolana. The formula is shown in 2.14 below. He suggested that if the pozzolana fraction is α , then that of cement will be $(1-\alpha)$. Therefore, the summation of the active component in cement and pozzolana using Equation 2.15 could produce an estimated value of the optimum pozzolana needed to react with portlandite given in Equation 2.2.

$$\frac{\%SiO_2 + \%Al_2O_3 + \%Fe_2O_3}{\%CaO} = 1 \quad \text{Equation 2.14}$$

$$\frac{\sum(SiO_2 + Al_2O_3 + Fe_2O_3)(1 - x) + \sum(SiO_2 + Al_2O_3 + Fe_2O_3)(x)}{\sum CaO(1 - x) + \sum CaO(x)} = 1 \quad \text{Equation 2.15}$$

In other studies, the ratio of gel/space ratio has been used to obtain optimum replacement dosages. The determination of gel to space ratio is determined from the use of the thermogravimetric analyser (Lin et al, 2010). They explained the gel/space ratio as the ratio of the volume of hydrated cement to the sum of the volumes of hydrated cement and capillary pores. The analyzer helps to estimate the degree of hydration from empirical formula leading to the determination of the gel-to-space ratio. The studies of Lin et al (2010) showed that compressive strength is dependent on the gel/space ratio. An increase in the ratio increases the formation of cement hydration products which fills available pores of cement pastes to improve strength properties.

2.18.1.3 Effect of water-to-cement ratio on compressive strength

Water to cement or binder ratio (w/c) is an important parameter worth considering since it affects strength of cement based materials. High strength is achievable in mortar and concrete with minimum cement content and an appropriate w/c ratio. Wassermann et al (2009) stated that high cement content in mortar or concrete does not necessarily mean high strength. Mindess et al (2003) and Kosmatka et al (2002) found out that increasing w/c ratio decreases strength. The strength decrease is attributed to an increase in capillary porosity (Kosmatka and Wilson, 2011). About 0.4 water-to-cement ratio is required for a complete hydration of cement (Kosmatka and Wilson, 2011). To further increase strength would require a further reduction of the w/c ratio.

Cement based products prepared below 0.4 water-to-cement ratio will require the use of water reducing admixtures. Water reducing admixtures disperse cement through electrostatic and stearic repulsive forces. According to Collepardi and Valente (2006), the acidic group in this admixture binds the positive ion on cement particle surface giving the cement a negative charge as well as cement layered surface. This phenomenon creates the electrostatic and stearic repulsion forces between individual cement grains, releasing the water tied up in agglomeration reducing viscosity of cement paste. This water by action of stearic hindrance is allowed to totally surround the cement grain for complete hydration. The repulsive forces break down immediately when the hydrating cement releases more ions into the matrix. Some water reducers have dual action; acting as an accelerator as well as water reducer.

2.18.1.2 Consistency and setting times

The ability of a freshly mixed cement paste or mortar to achieve relative mobility is known as consistency. Consistency in mortar and concrete can be related to workability. For cement paste Vicat apparatus is used whilst the flow table is usually used for mortar. The consistency of cement is influenced normally by the water-to-cement ratio. A high water to cement ratio increases the relative mobility of cement paste or mortars.

Likewise, other chemical admixtures can increase the relative mobility of cement paste. These include super plasticizers, air entrainment, etc (Komsatka and Wilson, 2011).

Literature indicates that most natural pozzolans like calcined clay, shales normally produce binder paste with a high normal consistency value than the normal cement (Uzal and Turani, 2003; Naceri and Chikouche, 2009, Bediako et al, 2012, Bediako and Osei Frimpong, 2013). Few exceptions have been recorded from literature especially with fly ash which by nature is glassy and very spherical. The glassy and spherical nature of this pozzolana renders it less porous and a relatively smaller surface area (Chindaprasirt et al, 2004). Most natural pozzolana calcined between 600-800°C usually shows a high absorptive nature which makes them require more water. Many different reasons have been used to explain the high demand of water when non-glassy pozzolanic materials are used. Sinthaworn and Nimityongskul (2009) attribute this trend to the high porous nature whilst Ganesan et al (2007) and Singh et al (2000) explain the trend using the high surface area of such pozzolanic materials. In some occasions the content of LOI in a particular pozzolana gives an indication of the water demand. Higher LOI values results in higher water demand (Sata et al, 2007).

Setting times characterize the transformation of cement paste into a hardened state. It also determines whether the cement is undergoing hydration. Usually two sets are defined with binders and they are the initial and the final setting times. The initial setting time is the time from mixing dry cement with water till the starting of binder gel interlocking with each other. At this time the cement or binder paste stiffens considerably. The final setting time is the time from mixing the binder with water till the end of interlocking of cement gel. At this time, binder paste hardens to a point where minimum load could be sustained the setting time is reported to guide transportation, placing, compaction and shaping of cement paste. In most of the studies of Portland cement containing calcined clay pozzolan, both the initial and the final set progressively increased with increasing pozzolan content (Morsy et al, 1997; Bediako et al, 2012; Brooks and Johari, 2001). The delay in the setting times of cement containing pozzolana has been attributed to the nature of pozzolanic reaction which is a slow process (Fu et al 2002). Brook et al (2000) also attribute this trend to lower cement content which causes slower stiffening of mortars.

2.18.2 Analysis of the hydrated phases of cement and blended pozzolana cement

It has earlier been indicated that cement and pozzolanic materials mixture undergo both hydration and pozzolanic reaction with the addition of moisture. Both hydration and pozzolanic reaction results in the formation of hydrated phases. The hydrated products formed as a result of pozzolanic reaction are similar to cement hydration which basically includes hydrates of calcium-silicates and calcium aluminates, ettringite (Aft), monosulphates (AFm) and other minor components (Wilinska and Pacewska, 2014; Taylor, 1997). The identification of cement and pozzolan hydration products are traditionally determined with thermal gravimetric analysis (TG-DTA), XRD/ Rietveld analysis and the back

scattered electron image analysis (BSE/IM) (Bentz et al, 2012; Zhang et al, 2000). TG-DTA is helpful to determine and quantify portlandite consumption and combined bounded water in a cement-pozzolana system. The XRD is a bulk technique which provides information on crystalline hydrated products including highly and poorly crystalline components and amorphous phases (Mendes et al, 2011).

Many researchers have found the use of TG-DTA and XRD to have major limitation. Both are not able to quantify hydrated products formed as well as hydration and pozzolanic reaction dynamics. Modern cement science study utilizes the Magic Angle Spinning Nuclear Magnetic Resonance (MAS NMR) for enhanced analysis of cement and pozzolana hydrated products. All these analytical tools corroborate with each other to reduce the uncertainties in the complex system formed between cement and cementpozzolana mixes.

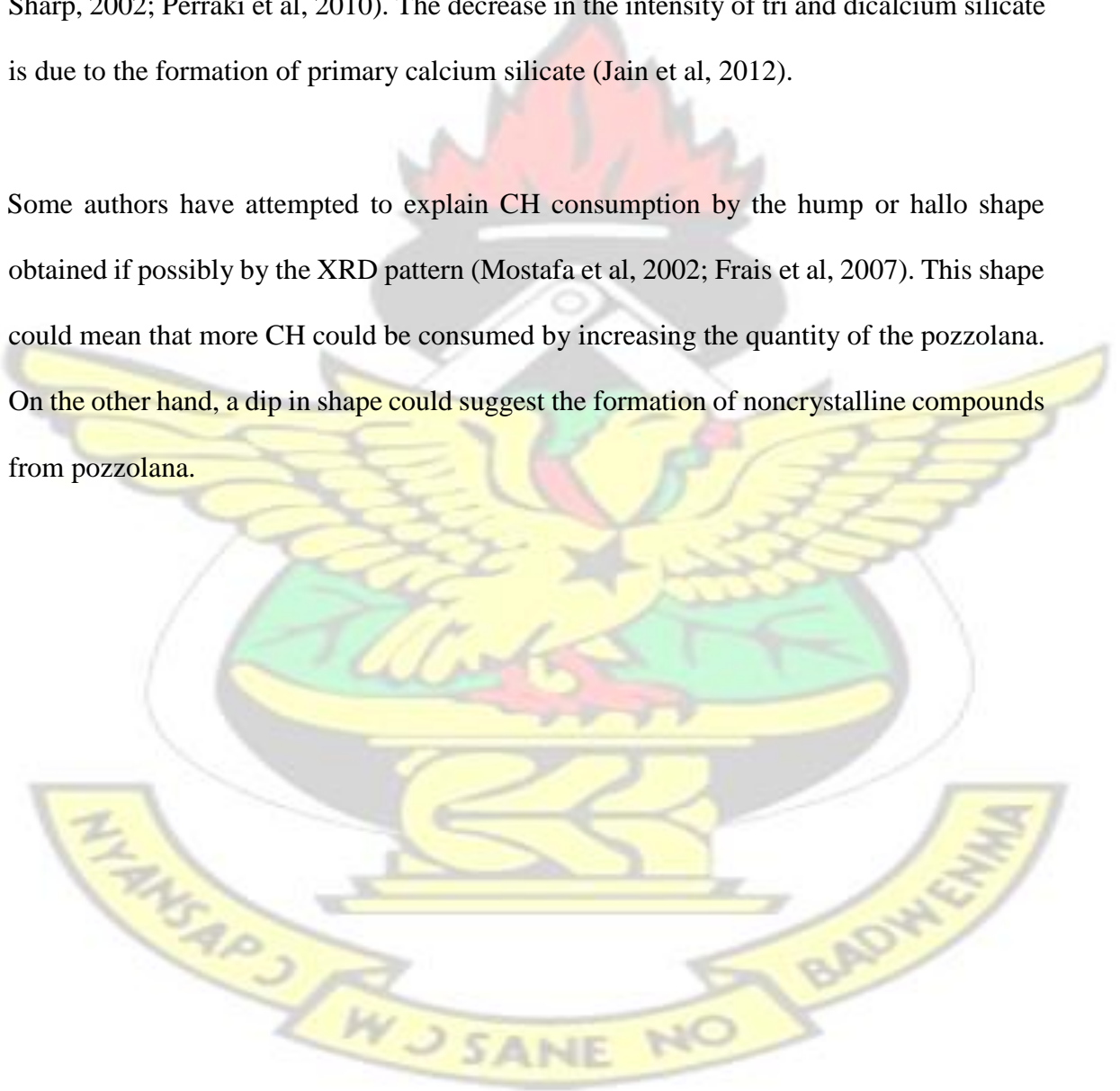
2.18.2.1 Analysis using XRD

The progress of pozzolanic reaction can be followed by monitoring portlandite consumption with hydration time. Many mineralogical studies determined by XRD have shown that the principal hydration products of pozzolana and Portland cement combination are essentially similar to those given by pure cement. At early ages XRD patterns show high presence of calcium hydroxide together with other crystalline components such as calcium carbonate, ettringite, tri and dicalcium silicates (Hill and Sharp, 2002; Jain et al, 2012). The intensity of the major crystalline components: CH, CaCO_3 , C_2S and C_3S disappear at late ages.

The uptake of lime in both situations brings about the clear differences (Taylor, 1997). Figure 2.22 presents the studies of AL-Salami (2013) which gives a good explanation of

the various diffractions shown by hydrated phases between white cement and calcined kaolin at 750°C used to replace cement between 0 and 14 percent. The figure indicated that as the pozzolana content increased CH content also reduced whilst major crystalline products such as CSH increased. The diminishing trend of CH could be as a result of pozzolanic action, however this effect is dependent on the reactivity of pozzolana (Hill and Sharp, 2002; Perraki et al, 2010). The decrease in the intensity of tri and dicalcium silicate is due to the formation of primary calcium silicate (Jain et al, 2012).

Some authors have attempted to explain CH consumption by the hump or halo shape obtained if possibly by the XRD pattern (Mostafa et al, 2002; Fraix et al, 2007). This shape could mean that more CH could be consumed by increasing the quantity of the pozzolana. On the other hand, a dip in shape could suggest the formation of noncrystalline compounds from pozzolana.



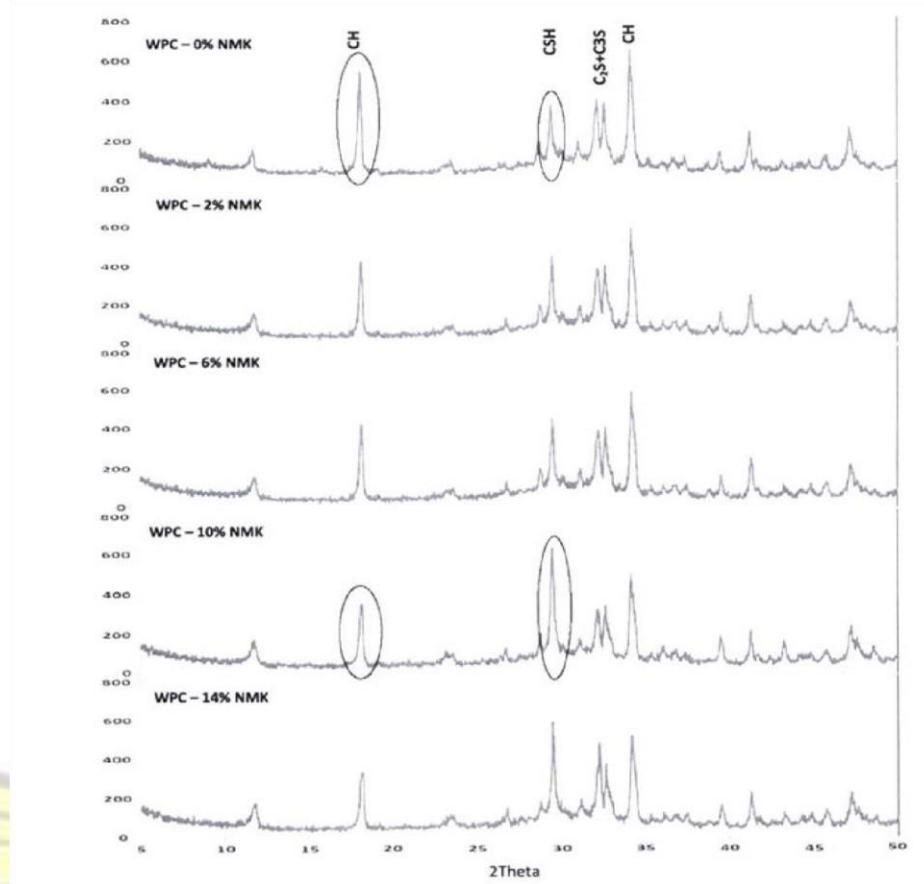


Figure 2.22: XRD patterns of white cement and calcined kaolin hydrated pastes at 28 days (AL-Salami et al, 2013)

2.18.2.2 Analysis using TGA

Calcium hydroxide (CH) fixation is a major function of pozzolanic materials in cement/pozzolana system which in turn refines particle sizes of hydrated products or cement/pozzolana matrix densification. The uptake of lime as already indicated is performed using the thermogravimetric analyser (TGA). TGA could also be used to estimate the content of chemically bounded water in cement/ pozzolana system. With bonded/ non evaporable water in a pozzolana/cement system, optimum pozzolana in cement will increase bonded water. This is because of the acceleration of CH to react with

silicate and aluminate phases. At a point where the siliceous material content is high, chemically bonded water decreases which is attributed to little or no water to continue hydration of excess silica content (Gomez-Zamorano and Escalante-Garcia, 2010).

Differential Thermal Analyzer (DTA) functions by locating the ranges corresponding to thermal dehydration and decomposition/dehydroxylation, whilst TGA measure the weight loss due to decomposition (Esteves, 2011). On a TGA, the curves relate to the effect of dehydration and decomposition of hydrated phases. These curves could be either endothermic or exothermic. Dehydration and decomposition occur as endotherm whilst crystallization of new products occurs as exotherms. On the DTA graph, endotherms below 200°C are known to be dehydration of hydrated gels (CSH, CAH, CASH), ettringite and possibly unreacted gypsum; above 400°C is the decomposition of CH whilst above 550°C is the decomposition of carbonates induced with solid components (Wilinska and Pacewska, 2014). Figure 2.23 presents an example of a combined TG/DTA graph. The graphs show cement and pozzolana (silica fume) hydrated at 24hrs and 28 days by Esteves (2014). The first endotherm peak is related to dehydration, the second to CH decomposition whilst the exotherm peak refers to crystal growth probably CSH formation. The dehydration decreased with time from 24 hrs to 28 days just as the CH content. However, the CSH development grew from 24 hrs to 7 and 28 days. Other studies such as Cabrera and Rojas (2001), Gomez-Zamorano & Escalante-Garcia (2010), Morpoulou et al (2004) have all pointed out the extent of lime fixation in a cement and pozzolana interaction.

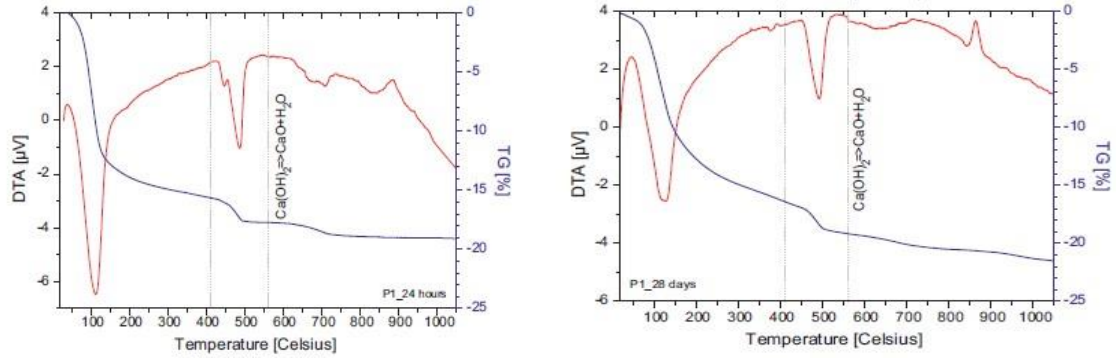


Figure 2.23: TG/DTA of cement and 15% silica paste cured at 24 hrs and 28 days (Esteves, 2014)

Lime fixation is obtained through estimation from the results of the TG/DTA graph.

From the studies of Mendoza and Tobon (2013), the lime content can be expressed as

$$Ca(OH)_2 = \frac{H}{MW_{H_2O}} \times MW_{Ca(OH)_2} \quad \text{Equation 2.16}$$

where H is the mass loss due to the dehydroxylation around 500°C and registered on the mass loss curve, MW the molecular mass of either the water (MW_{H_2O}) or the calcium hydroxide ($MW_{Ca(OH)_2}$). The above given equation 2.16 is good for a mixture between pure lime and a pozzolana. However, if the mixture is between cement and a pozzolana, there is an expectation of the decomposition of other components like carbide, ettringite, and CSH. In this case, Yu et al (2015) in his studies provided equations 2.17 and 2.18 for the estimation of bonded or non-evaporable water and CH content. T_a denotes the amount CSH resulting from dehydration, ettringite and carbide amount of decomposition occurring between 50-400°C, T_b is the amount of matter decomposition occurring between 400-550°C, and T_c similarly is the amount of material decomposition above 550°C. The weight loss is expressed as a percentage by weight of the ignited sample and a percentage by weight of the cement in the sample. From experimental studies Yu et al (2015) stated that

two-thirds in T_c that decompose is from carbide whilst the remaining one-third decomposes as water in CSH gel and ettringite.

$$\text{Content of Bond water} = T_a + T_b + \frac{T_c}{3} + \frac{2}{3} \times \frac{T_c}{44} \times 18 \quad \text{Equation 2.17}$$

$$\text{Content of CH} = \left(\frac{T_b}{18} + \frac{2}{3} \times \frac{T_c}{44} \right) \times 74 \quad \text{Equation 2.18}$$

Lam et al (2000) and Poon et al (1999) have shown that the CH content in a Portland cement paste indicates the degree of hydration. On the other hand, CH consumption in blended cement paste also shows the degree of pozzolanic reaction. It has been suggested by Malquori (1960) that evaluation of pozzolanic material must be based on the reduction of free CH in the hardened pozzolanic cement. The degree of pozzolanic reaction could be calculated from the fixated CH using Equation 2.19 taken from the studies of Mendoza and Tobon (2013). The degree of pozzolanic reaction is related to the CH fixation or consumption (Poon et al, 1999). A positive CH reduction meant that pozzolanic reaction occurred and was consuming more CH than that produced by the hydration between cement and water.

$$\% \text{ Fixation } Ca(OH)_2 = \frac{Ca(OH)_{2i} - Ca(OH)_{2t}}{Ca(OH)_{2i}} \times 100 \quad \text{Equation 2.19}$$

Where $Ca(OH)_{2i}$ is the initial amount of calcium hydroxide in the sample, and $Ca(OH)_{2t}$ is the amount of calcium hydroxide consumed by cement/pozzolan at a determined curing time (t).

2.18.2.3 Analysis using MAS NMR

MAS NMR presents a good opportunity to analyze the complex transformation reaction of hydration phases. Si NMR provides valuable information relating CSH gel, the main

hydrated phases of cement whilst Al NMR is useful to probe calcium aluminate hydrates (CAH) and aluminate hydrates such as ettringite and monosulphate hydrates (Mendes et al, 2011). The NMR indicates chemical shifts within ranges and this is a function of bond length and bond valence all related to polymerization or crystal growth (Mendes et al, 2011).

2.18.2.3.1 ^{27}Al MAS NMR

Probing of ^{27}Al phases in a hydrated cement sample can be followed from the resolution of tetrahedral and octahedral coordinated Al species. Their ratio i.e. $\text{Al}^{(\text{vi})}/\text{Al}^{(\text{iv})}$ provides a good estimation of the progress of hydration of the aluminate. In a hydrated state the aluminate phase shift from $\text{Al}^{(\text{iv})}$ to $\text{Al}^{(\text{vi})}$ (Brunet et al, 2010), opposite to anhydrous phase of cement or calcined clays. Many authors have indicated the chemical shift range that identifies Al species. $\text{Al}^{(\text{iv})}$ is generally observed between 50 ppm and 80 ppm whilst $\text{Al}^{(\text{vi})}$ usually resonates between -20 and 20 ppm (Hanna et al, 1995; Skibsted et al, 1993).

The aluminate phases produced in cement or cement/pozzolana system involves calcium aluminate hydrate (CAH), ettringite (Aft) formed from an initial hydration of C_3A and later converts into a thermodynamically stable monosulphate (AFm). Chemical shift that occurs around 13ppm is attributed to ettringite, between 8 and 11.8 ppm is monosulphate whereas at 5ppm is attributed to minor amounts of monosulphates or poorly disordered CAH (Skibsted et al, 1993; Anderson et al, 2006). Resonance peaks that occur between 66 and 72ppm are attributed to Al substitution in CSH (Andersen et al, 2003). Fernandez et al (2011) pointed out that peaks around 60ppm are usually assigned to $\text{Al}^{(\text{iv})}$ in an aluminosilicate anion in the interlayer stratlingite (C_2AH_8), an AFm phase. For anhydrous samples, a broad centered

resonance occurs between 80 and 40 ppm which is related to unhydrated materials like C_3A . Between 81 and 86 ppm are attributed to alite and belite respectively originating in the tetrahedral coordinated Aluminium environment (Anderson et al, 2006; Dai et al, 2014). An example of an Al MAS NMR showing hydrates from aluminate phases is shown in Figure 2.24. The figure depicts Al NMR spectra of cement and clay pozzolana (kaolin, illite and montmorillonite) mixtures of both anhydrous and hydrated pastes at 28 days. Calcined clay addition affects the overall

signal which is shown in the anhydrous phases of the mixes such $Al^{(iv)}$, $Al^{(v)}$ and $Al^{(vi)}$ from calcined clays. At 28 days of hydration, four peaks resonated at 9, 11, 60 and 70 ppm. The first two 9 and 11 ppm are assigned to ettringite and monosulphates respectively occurring in the octahedral Al environment. The last two peaks at 60 and 70 ppm are assigned to the aluminate replacing silicate in CSH in the tetrahedral environment of Al. At the 60 ppm resonance peak, it overlaps which shows $Al^{(iv)}$ in aluminosilicate anion in the interlayer stratlingite (C_2AH_8), a monosulphate phase (Fernandez et al, 2011). The figure clearly shows the formation of stratlingite containing

AFm phases. The reason is that more Al passes into the alkaline solution of cement paste. In the metakaolin paste mix, the presence of stratlingite explains the lower intensity of ettringite (Aft).

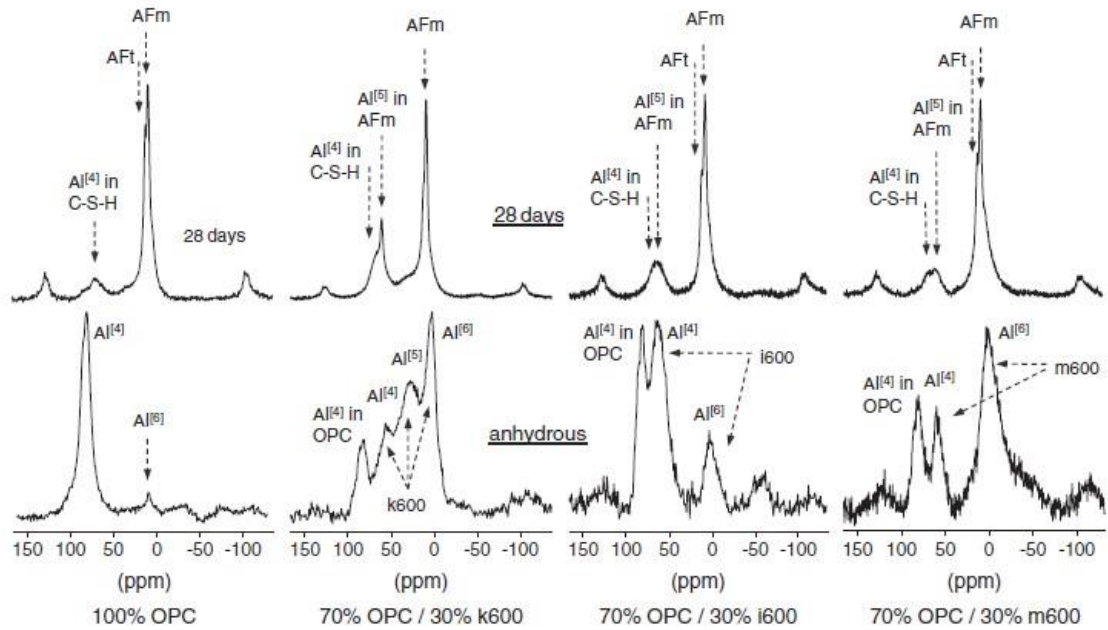


Figure 2.24: Al NMR spectra of anhydrous blends and pastes at 28 days (Fernandez et al, 2011)

2.18.2.3.2 Si MAS NMR

The Si-NMR chemical shift provides a strong indication of the degree of polymerization and hydration of silicate phases, since silicon has tetrahedral coordination almost everywhere in cement or cement/pozzolana paste (Mendes et al, 2011). The analysis of Si NMR spectra gives an idea of local silicate tetrahedral environment and usually denoted as Q^n , where Q represents the silicon tetrahedron bonded to four oxygen atoms, and n denotes the number of SiO_4 (Q units) connected or attached to the central Q tetrahedron under consideration. Si NMR peaks usually have a more negative chemical shift (i.e electron rich field) when there is an increase of Q units connected to the central Si atom (MacLaren and White, 2003). The Q^0 represents monomeric orthosilicate anion (SiO_4^{4-}), Q^1 represents an end group chain of CSH, Q^2 represents the middle group chain of CSH whereas Q^3 and Q^4 represent points where branching in silicate structure may occur

(Alonso and Fernandez, 2004). Several studies have indicated on the Si NMR spectras relating to Q^0 - Q^4 . Hjorth et al (1998) pointed out that Q^0 resonates between -68 and -76 ppm, Q^1 between -76 and -82 ppm, Q^2 between -82 and -88 ppm. The investigations of Xiamong et al (2011) showed that chemical shift from -88 ppm to -92 ppm corresponds to Q^3 . However, at -88 ppm, Al^{3+} was incorporated in the calcium silicate phase. The hydrated phase that corresponded to a chemical shift between -88 ppm and -92 ppm represented a highly polymerized structure of gehlenite, an aluminum rich hydrate (Xiamong et al, 2011). Skibsted and Hall also indicated that Q^3 resonates around 91.5 ppm. Q^4 resonates from -100 ppm to -125 ppm representing an amorphous nature of the material (Poulsen, 2009). Si NMR could be used to interpret the extent of Al incorporation in CSH. According to Schneider et al (2001) and Richardson (1999), Al substitutions in the tetrahedral sites are found only in Q^2 groupings usually at the peak around -81.1 ppm, and -81.5 ppm. For unreacted species alite (C_3S) and belite (C_2S) occur around -74.6 ppm and -71.3 all located in the Q^0 environment (Alonso and Fernandez, 2004; Castellote et al, 2009). Figure 2.25 shows the spectrum of chemical shift regions indicating the different types of condensation of Si tetrahedral.

The measurement of relative intensities of Q^0 to Q^4 can be used to monitor the progress of hydration (Mendes et al, 2011). The study of Hjorth et al (1998) revealed that the Q units i.e. Q^2 and Q^1 can be used to correlate compressive strength. They stated that a high Q^2/Q^1 ratio gives high compressive strength and vice versa. Figure 2.25 present an example of Si NMR of hydrated cement paste. Resonance peaks assigned to Q^0 , Q^1 , Q^2 , and Q^3 are shown in the figure. From the Figure 2.26 (A-D), the proportion of Q^1 and Q^2 silicon species

increases in relation to Q^0 silicon species as the hydration proceeds. The increased formation of Q^1 and Q^2 are as a result of a pozzolanic reaction (Brough et al, 1996). In some cases, Q^4 centered around -101 ppm depolymerizes through Q^3 ranges into Q^2 and Q^1 regions of the spectra (Coleman, 2000). Depolymerization occurs when siloxane linkages between silicate species are cleaved in highly alkaline condition created by a cementitious system (Coleman, 2000). Figure 2.26 (A-D) showed that the Q^2/Q^1 ratio increased with hydration time which could be computed and related to the compressive strength.

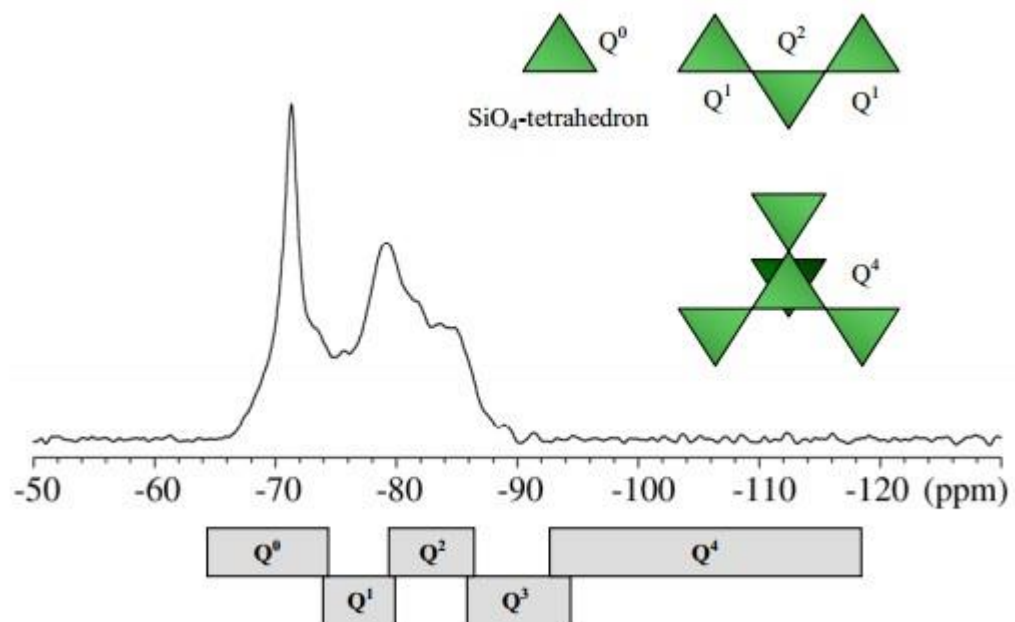


Figure 2.25: Spectrum of chemical shift regions of different Si tetrahedral, Q^n showing the number of Si atoms connected to the central Si atom (Maclaren and White, 2003).

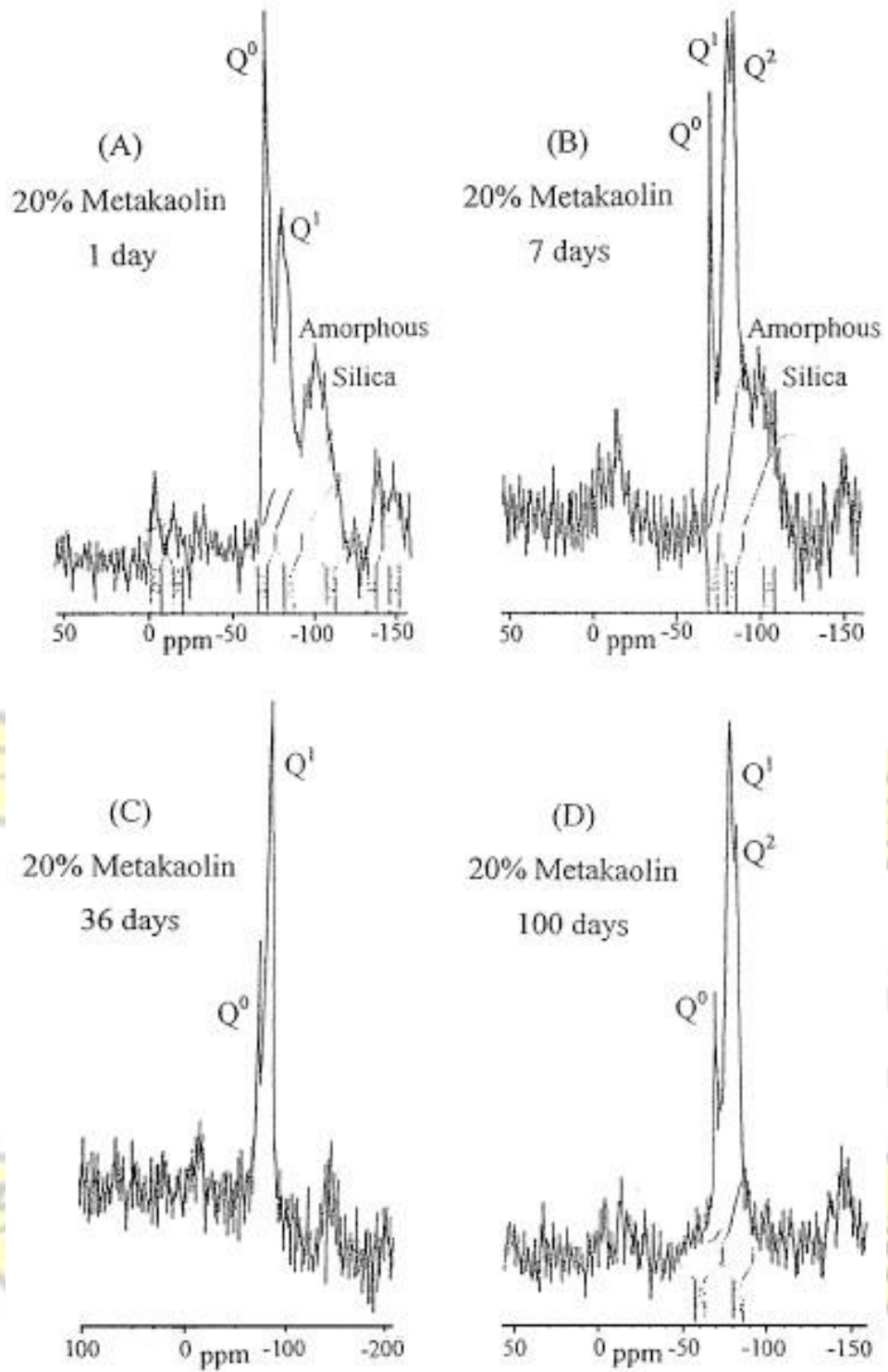


Figure 2:26: Si MAS NMR spectra of the hydration products of a blend of 80%OPC/20%MK ordinary 1, 7, 36 and 100days (Brough et al, 1996).

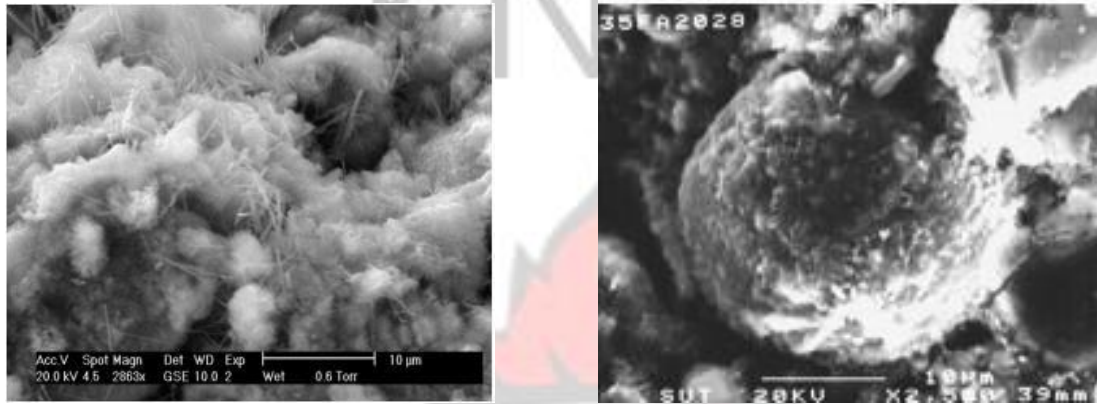
2.18.3 Microstructure of hydrated phases

Lea (1998) reported that the microstructure of Portland cement paste is basically similar to cement paste incorporated with either natural or artificial pozzolana. The only difference is that at early hydration time (2-24hrs), the presence of pozzolana in Portland cement is seen unreacted. Furthermore, Portlandite content, degree of hydration of alite, degree of reaction of pozzolana and the combined water differentiate it from the parent cement.

In the cement compounds, unlike C_3A and C_4AF , the end products of alite and celite formed during and after hydration undergoes pozzolanic reaction with materials with pozzolanic origin which could easily be identified microstructurally. At early age of hydration (3 and 7 days), unreacted grains of pozzolana are seen serving as nucleation site for calcium hydroxide formation (Chindaprasirt et al, 2007). At this time the calcium-to-silica ratio (C/S) near pozzolana grain rises up indicating a high basic solution content or increased portlandite generation. As the period proceeds, pozzolana grains are attacked by H_3O^+ proton contained in the basic solution and this result in calcium silicate and aluminates attack (Lea, 1998). The hydrolysis later produces amorphous layer rich in Si and Al on the surface of the pozzolana grain. The release of Al and Si from pozzolans into the pore solution form additional CAH and CASH hydrates and lowers the Ca/Si ratio (Deschner et al, 2012). At this stage the ratio between Al and Si surges up signaling the effect of pozzolanic reaction.

Antiohos et al (2006) and Chindaprasirt et al (2007) present the microstructures of cement and pozzolana (fly ash) hydrated at 7 and 28 days respectively in Figure 2.27.

Figure 2.27a shows nucleation of portlandite around the surface of fly ash and ettringite rods formation whilst Figure 2.27b shows the surface of fly ash has etched indicating attack from high intensity H_3O^+ .



a) Cement and fly ash paste at 7days

b) Cement and fly ash paste at 28days

Figure 2.27: Hydrated cement paste containing pozzolanic fly ash (Antiohos et al, 2006)

Jain et al (2012) investigated a paste mixture between cement and 20% pozzolanic rice husk ash and indicated that at 7 days of curing microstructure of cement becomes much denser with pronounce formation of needlelike crystals like Figure 2.27a and circular features. At 28 days, they showed that the hydrated grains became interconnected through the fibrillar outer C-S-H forming a continuous structure shown in Figure 2.27b. Figure 2.28 shows the presence of calcium hydroxide (CH), ettringite (E) and tobermorite (T) or C-S-H.

During the hydration period, the electron diffraction X-ray analysis (EDX) attached to the SEM could be used to identify the amount and morphology of C-S-H since different pozzolanic materials gives different amount. An example is the illustration given in

Figure 2.29 by Antiohos et al (2008). Their EDX results conducted on the hydrate shows that crystals of gehlenite hydrate (CAS_2H_4) are formed which then intercepts the production of C-S-H.

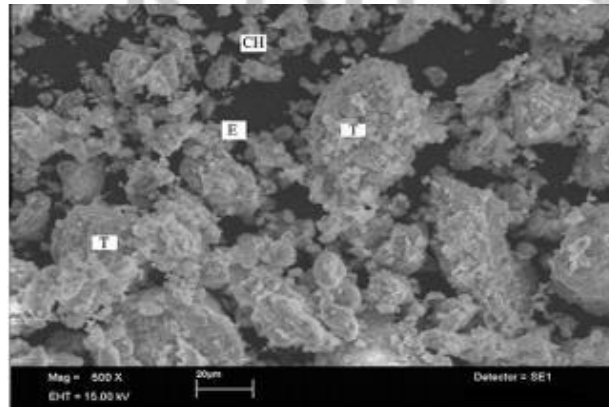


Figure 2.28: SEM of 28 days hydrated 20% pozzolana (RHA) blended cement (Jain, 2012)

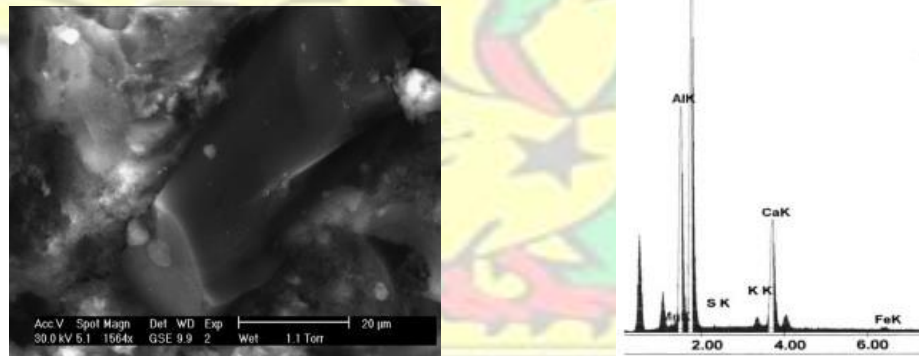


Figure 2.29: Crystals of hydrated cement-pozzolana (fly ash) system at 90 days and EDX analysis (Antiohos et al, 2006)

2.19 Durability studies of cement and pozzolana based system

Durability is an important engineering property of mortar and concrete which could be used to compliment the results of mechanical and other properties of Portland cement and composite cement. It determines the life span of mortar and concrete very significantly.

Due to the interactions of mortar and concretes with external influences, their durability may be threatened and lost. The threatening factors to mortar and concretes are many. Among the threatening factors reported in past studies are freezing and thawing, abrasion, corrosion of steel and chemical attacks resulting from structural pores, and shrinkage (Zivica and Bajza, 2001; Itim et al, 2011). Durable materials benefits environment by conserving earth's meager resources, decrease waste and commutative impact related to repair and replacement. This section of durability is focused more on shrinkage and water sorptivity.

2.19.1 Shrinkage of cementitious mortars

Itim et al (2011) mentioned that shrinkage prediction is of very great essence for durability study and the inclination for long term functioning of concrete structures. Structural deformation due to shrinkage is well known to be the origin of cracks and even more rarely failure of concrete structures (Tam et al. 2012). Cracks generation in concrete is solely because they undergo volume changes for various reasons coupled with their weakness in tensile forces. Therefore, shrinkage could be defined as volumetric change of concrete induced by moisture loss. Kosmatka and Wilson (2011) stated that volume changes in concrete is related to linear expansion and contraction which occur due to hydration reaction, temperature change and moisture loss. Tam et al (2012) stated that shrinkage of concrete is believed to take place in the cement paste matrix. Most aggregates show little response to change in moisture content.

Many authors have pointed out different types of shrinkage that leads to length change in cement paste which includes plastic, drying, chemical, autogeneous, creep, carbonation, etc. However, laboratory conditions of shrinkage consider usually drying (total or free) and

autogeneous shrinkage. Total shrinkage occurs as a result of loss of evaporable water in a cement mortar mix to the environment having a specific relative humidity and ambient temperature. Autogeneous shrinkage is caused by a reduction in the pore relative humidity as a result of hydration products formation (Jensen and Hansen, 1996). This shrinkage shows evidence of hydration progress and self desiccation due to water consumption by the chemical process of hydration. Shrinkages, total and autogeneous generate stresses that cause cracks within product matrices. With autogeneous shrinkage the formation of new hydration products is where the problem is and that leads to the formation of tensile stresses (Li et al, 2010). The works of Itim et al (2011), Cheah and Ramli (2012) observed drying shrinkage as the result of the difference between the free and the autogeneous shrinkage. However, many other authors' calculation of drying shrinkage is a result of the total shrinkage without a consideration of the autogeneous length change (Kara et al, 2014; Guneyisi et al, 2008; Bao-guo et al, 2007).

Shrinkage values have been given out by Kosmatka and Wilson (2011) and they state that a high strength concrete with a lower w/c ratio of 0.30 can experience autogeneous shrinkage of between 200millionth (0.02%) and 400millionth (0.04%). Autogeneous shrinkage is usually a half of the drying shrinkage therefore reduces the volume of the sealed specimen to about 15millionth (0.015%). Drying shrinkage of small, plain, concrete specimens (without reinforcement) ranges between 400millionth (0.04%) to 800millionth (0.08%) when exposed to air and at 50% relative humidity.

Drying and autogeneous shrinkage have been controlled significantly with pozzolanic cementitious materials including fly ash, calcined kaolin, silica fume, slags (Bao-guo et al,

2007; Itim et al, 2011). Though the use of various forms of pozzolanic materials controls shrinkage, Komatska and Wilson (2011) have warned about the use of cementitious materials that demand much water. This implies that fineness of cementitious materials must be within a tolerable range. A typical example is the use of silica fume which has very fine particles thus demanding much water and consequently causes a higher shrinkage effect unless that is compensated for in the mix design.

The ability of pozzolanic materials to reduce shrinkage effect in a cement matrix is attributed to dilution effect and the formation of additional hydrates (Itim et al, 2011; Gleize et al, 2007). With dilution effect, decrease of the cement dosage limits shrinkage from the binder whilst with the formation of hydrates, it makes cement matrix less porous, rigid and less deformable hence restraining shrinkage especially with autogeneous. Massaza (1993) has already pointed out that shrinkage depends on cement content and water-to-cement ratio. Concrete or mortar with lower shrinkage strain has lower w/c ratio thus a lower capillary absorption coefficient. A lower coefficient implies a lesser moisture movement within the specimen.

2.19.2 Water Sorptivity

Water sorptivity is a form of transport property of water or ions in an unsaturated porous surface. It characterizes the material's ability to absorb and transmit water or ions through it by capillary suction (Sabir et al, 1998). Lockington et al (1999) have demonstrated that sorptivity experiment is a simple experiment used as a measure of concrete resistance to exposure in aggressive environments. Many other researchers support this argument and

have further pointed out that the use of sorptivity is an important parameter in measuring concrete durability (Hall, 1989; McCarter et al, 1996).

The pore size distribution in concrete or mortar influences the rate of transport or sorptivity. Sabir et al (1998) mentioned that the pore system of the cement paste in a matrix is the principal feature that relates to transport of water or sorptivity. They again stated that aggregates contribute less significantly to sorptivity because of their disjointed pores. The hardened cement paste is the only continuous phase in a mortar or concrete matrix that controls water or ions movement. The theory behind sorptivity states that if a mortar or concrete surface is exposed to wetting by water, then the commulative water absorption, i is proportional, during the initial absorption period, to the square root of elapsed wetting time t :

$$i = S\sqrt{t}$$

Equation 2.20

S is the sorptivity measured in g per mm² (of wetted area) per sec^{1/2}. It is easily determined from the slope of the linear part of i versus $t^{1/2}$ curve (Sabir et al, 1998).

The work of Siddique (2009) stated that reducing sorptivity is important to decrease ingress of chemical compounds including chloride and sulphate which can cause serious damage. Several researchers have achieved minimal sorptivity with the optimal use of pozzolanic materials (Chan and Ji, 1998; Khatib, 2004; McCarter et al, 1992). The reduction in sorptivity in the application of pozzolanic materials could be attributed to the pore refinement at the interface which is highly enhanced (Razack et al, 2004).

CHAPTER THREE

3.0 Materials and Methods

3.1 Materials

The materials used for the study were Portland cement, clay, biomass, silica sand, high range water reducer and potable water.

3.1.1. Portland cements

Portland cement conforming to ASTM C150 Type I/II was used. The cement was manufactured by Ashgrove from Chanute, Kansas City, Missouri in the United States. Table 3.1 contains the physical properties, cement mineralogy and chemical compositions. ASTM C150 type cement used in this study was statistically not different from Ghacem class 42.5N commonly used in Ghana. Appendix 3.1 presents the chemical composition of Ashgrove and Ghacem Portland cement. The t-test results between Ashgrove and Ghacem cements are shown in Appendix 3.2.

3.1.2 Clay

The clay used was obtained from a farming community called Nyamebikyere in the Atwima Nwabiagya district located at the Western part of Ashanti region. This location was selected because of the availability of the material. Clay lumps obtained were milled into smaller particles between 150 μ m and 2mm. The milling of the clay was performed using a hammer mill machine for 15 minutes.

3.1.2.1 Geophysical characteristics of clay source

The village, Nyamebkyere is categorized as upland sub-catchments of the Ofin River Basin, within the south western river system of Ghana. Nyamebkyere is classified as low land-use intensity catchment and covers an area of 5.74 km². The village is small and isolated and is not well connected to other villages and towns. There are three first-order streams that are located in the Forest Reserve: The Nyasi, the Anikokoo and the Aseka, with the latter two flowing very briefly after storms. The stream, Nyasi stretches approximately 80.66 km long to join the Ofin River. Figure 3.1 shows the map of Nyamebkyere village. The chemical properties of the clay are shown in Table 3.1.

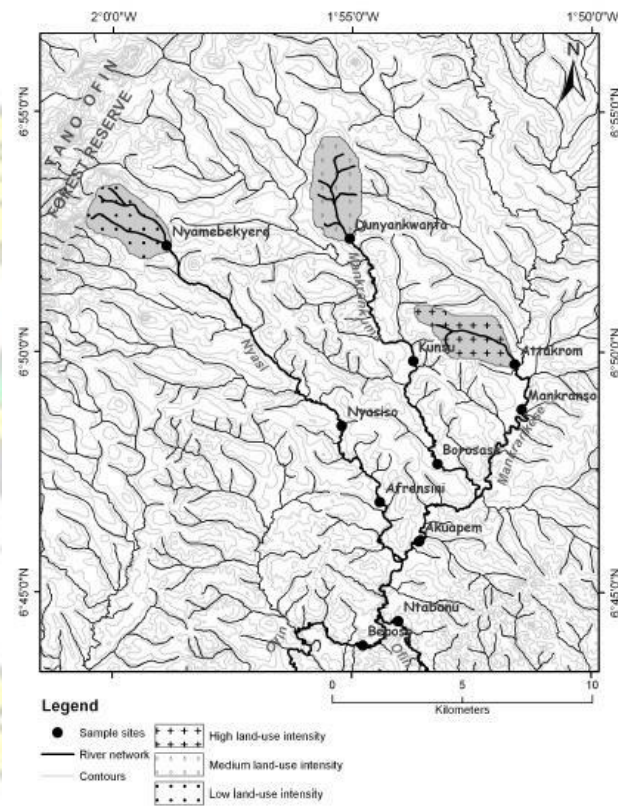


Figure 3.1. Map showing the location of Nyamebkyere in Ashanti region

3.1.3 Biomass

The biomass waste materials used were palm kernel shells (PK), rice husk (RH), maize cob (MC) and sawdust (SD) which is shown in Figure 3.2. PK and RH were obtained from palm kernel oil producers and a rice milling plant respectively located in the Konongo area of Ashanti region whilst MC obtained from CSIR- Crop Research Institute and the SD from a wood processing industry at Fumesua, Ashanti region. The location where the biomass materials were sourced from was as a result of the materials availability and proximity from CSIR-BRRI where the preconditioning of the materials was performed. The physical properties of the biomasses are shown in Table 3.1. The properties of the Portland cement where obtained from Ashgrove whereas the relative densities of the biomass materials where determined using a cylindrical bottle having a known volume of 953 cubic centimeters.



Figure 3.2: Biomass waste, a. Palm kernel shells, b. rice husk, c. maize cob, d. sawdust

3.1.4 Sand

Graded standard silica sand obtained from Ashgrove in Kansas was used. The sand conformed to the requirements of ASTM C778.

3.1.5 High range water reducer

High range water reducer (HRWR) possessing a polycarboxylated technology obtained from BASF Chemical Company, United States conforming to ASTM C595 specifications was used.

Table 3.1 Properties of portland cement, clay, PK, RH, MC and SD

	PC	Clay	PK	RH	MC	SD
Property Physical						
Bulk density	-	1.32	0.9	0.16	0.26	0.21
Fineness	401.7					
Specific gravity	3.13					
Chemical						
SiO ₂ (%)	20.49					
Al ₂ O ₃ (%)	4.26					
Fe ₂ O ₃	3.14					
CaO (%)	63.48					
MgO (%)	2.11					
SO ₃ (%)	2.9					
Na ₂ O+K ₂ O (%)	0.49					
LOI (%)	2.2					
Mineralogy						
C ₃ S (%)	56					
C ₂ S (%)	15					
C ₃ A (%)	6					
C ₄ AF (%)	9					

3.2 Experimental approach

The approach to this work was a multi-phase experimental procedure. The study was segmented into six phases. Figure 3.3 presents a detailed flow diagram of the phases. Phase 1 characterized the biomasses in terms of their chemical composition, mineralogy and

heating values in terms of calorific properties. The data obtained helped to understand the participation of biomass in clay in terms of ash properties being pozzolanic.

Phase 2 determined the optimum temperature and replacement dosage of the calcined clay. Raw clay was pulverized and calcined at different temperatures ranging between

600 and 1000°C for three hours. Loss on Ignition was determined on the clay powder at the respective temperatures. The calcined powder materials were tested based on ASTM

C618 recommendations on strength activity index (SAI) and supported by ASTM C311.

The replacement of cement with clay pozzolan was carried out according to ACI 212 standard practice. The standard recommends a 20% dosage value for natural pozzolans.

After obtaining the optimum calcination temperature using SAI, the optimum dosage was determined by replacing cement between 10 and 40%. At this stage, the results of the calcined clay were investigated using the TGA and MAS NMR. The results obtained were corroborated with each other and the SAI results in confirming the optimum calcination temperature.

Under Phase 3, the aim was to determine the maximum proportions and dosages of each of the four different groups of clay/biomass mixes which included clay-palm kernel shells (CP-PK), Clay-Rice Husk (CP-RH), Clay-Maize Cobs (CP-MC) and Clay-Sawdust (CPSD). All the clay/biomass mixtures were calcined at the optimum temperature obtained under Phase 2. Prior to calcination, the clay/biomass mixes were pelletized with sizes ranging between 2-5mm. After calcination, the calcined pellets were pulverized and used in conjunction with cement and sand to form mortars. The ASTM recommended practice for strength activity index explained in ASTM C311 and the dosage recommended in ACI

212 were used. The performance of SAI of the clay/biomass mixture proportions were evaluated and used to arrive at the choice of maximum clay/biomass mixtures and the maximum dosage increasing effect. The determination of the maximum clay/biomasses mixture proportions were performed at a replacement level of cement between 10% and 40% of the calcined products.

In phase 4 of the work, the main aim was to investigate the influence of the calcined products on Portland cement. In essence the effect of biomass on calcined clays was analyzed. The calcined products used for the investigation involved the optimum and maximum values obtained in Phases 2 and 3, respectively. Samples used as hydrated specimen for the analysis were obtained from the proportioned binder paste used for the determination of normal consistency and setting times. Specimens obtained after the setting times determination were reconditioned and cured in saturated lime water for 3, 7 and 28 days. Hydrated binder pastes were analyzed with quantitative tools. These tools included TGA and MAS-NMR studies. The TGA determined the calcium hydroxide content as well as the degree of hydration whilst the MAS-NMR probed into the polymerized properties as a result of hydration and pozzolanic reaction in terms of ^{29}Si and ^{27}Al environments.

The analysis under Phase 5 focused on the determination of the durability properties of the various optimum values. Under this phase, two methods of durability analysis were performed. These were shrinkage and sorptivity analysis.

In Phase 6, the aim was to determine the sustainability of the study. Sustainability analysis was mainly based on the optimum mixture proportions obtained under the

Phases 4 and 5 of the study.

KNUST



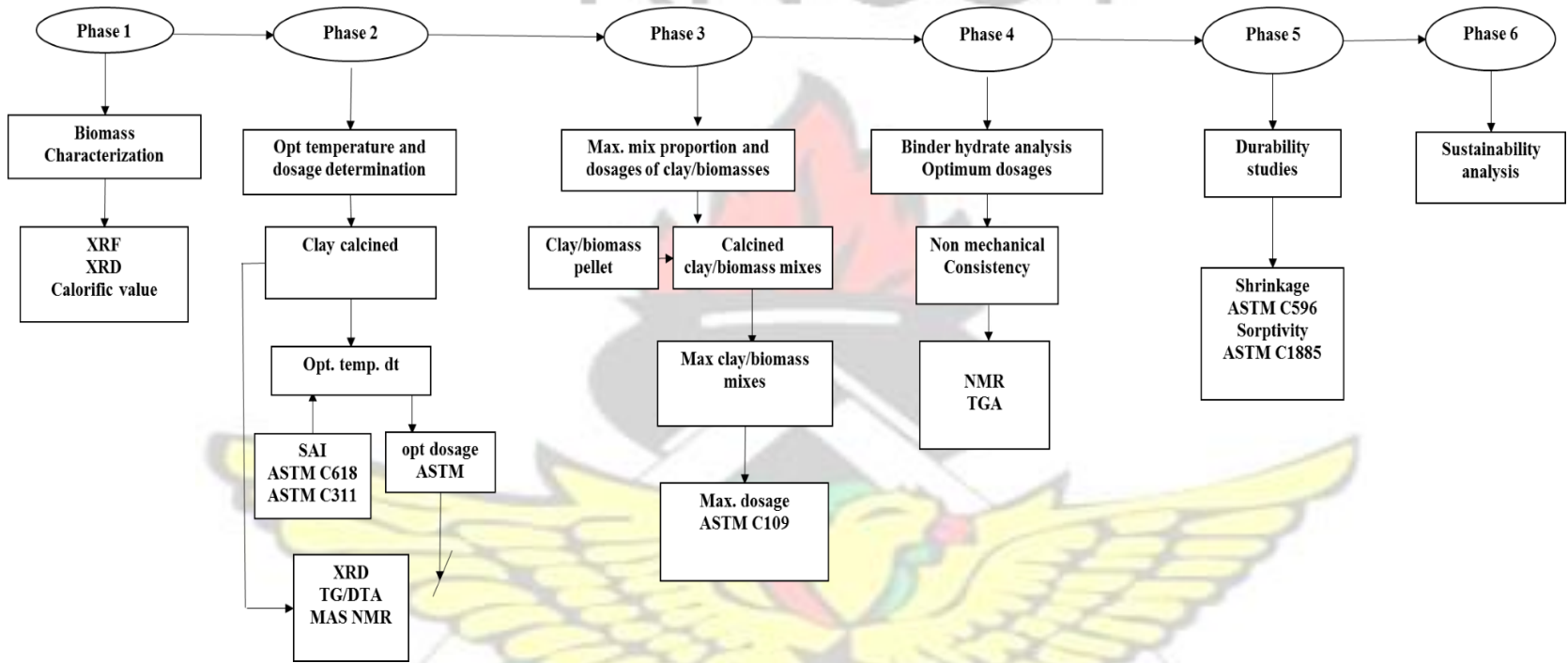


Figure 3.3: Flow chart for the experimental approach



128

KNUST



3.3 Test methods

3.3.1 Formation of clay/biomass pellets

Pelletized materials comprising of clay and the biomasses were formed. Prior to the formation, clay lumps were milled into powder (45- 150 microns) using a hammer mill. The biomasses which included palm kernel shells (PK), maize cob (MC), rice husk (RH) and sawdust (SD) were all milled into reduced sizes ranging between 150 microns and 2 mm. Milled biomasses were used to replace milled clay at different proportions. For palm kernel shell, replacement values of 10%, 20% and 30% were used whilst for maize cob, rice husk and sawdust, the replacement values were 1%, 1.5% and 2%. Table 3.2 presents the mixture names and the content of clay and biomass in the pellets. The replacement of clay powder with milled biomass was done on a mass to mass basis using the relative densities/specific gravity of the material shown in Table 3.1. The high specific gravity of PK as compared to the rest of the biomasses accounted for the huge disparity in the percentage replacement levels. For Clay/PK mixes, above 30% PK replacement provided a poor cohesion of the clay and palm kernel shells. This was similar with the other biomasses above 2% replacement.

The formation of clay and the biomass were performed in a rotating cylindrical bucket operated by a low speed motor. During rotation, potable water was sprayed on the mixture leading to the formation of pellets or nodules which were further dried in an open space.

Table 3.2: Clay and biomass mix proportions

Mix Name	Content (%)	
	Clay powder	Biomass
PK1	70	30
PK2	80	20
PK3	90	10
RH1	98	2
RH2	98.5	1.5
RH3	99	1
MC1	98	2
MC2	98.5	1.5
MC3	99	1
SD1	98	2
SD2	98.5	1.5
SD3	99	1

3.3.2 Test on biomass samples

3.3.2.1 Heating Values

The bomb calorimeter (Model 6200 EA 115V) located in the laboratory of Ashgrove cement plant in Kansas was used.

3.3.2.2 Chemical composition

XRF analysis was performed on a pressed powder pill of the powdered ash samples using “Omnia” semi-quant software on a PANalytical Axios wavelength dispersive spectrometer.

3.3.2.3 Mineralogical composition

Powder X-ray diffraction data was obtained on a PANalytical X'Pert Pro utilizing copper K-Alpha (wavelength= 1.54056) radiation and operating at 45 kV and 40 mA.

3.3.3. Calcination of samples and pulverization

Calcination of clay samples was performed in a laboratory furnace (Barnstead Thermolyne 6000 furnace). A known mass of the samples put into a ceramic bowl was placed in the furnace and heated at the optimum temperature for three hours after which the furnace was switched off. The samples were allowed to cool in the furnace to room temperature before dislodging from the furnace. Calcined clay pellets obtained at room temperature after calcination were crushed into powder using a mortar and pestle. The calcined powder samples, clay and clay/biomass were sieved through a 75 μ m sieve size using a sieve shaker.

3.3.4 Test on raw and calcined powder materials

The powdered materials analyzed were the clay, calcined clays and calcined clay/biomass mixes. The tests determined included specific gravity, chemical composition, mineralogical composition, thermal analysis of the powder materials and MAS NMR.

3.3.4.1 Specific gravity

The specific gravity test was performed in accordance with the ASTM C188 test methods.

3.3.4.2 Mineralogical composition

Powder X-Ray diffraction data was obtained on a PANalytical X'Pert Pro utilizing copper K-Alpha (wavelength= 1.54056) radiation and operating at 45kV and 40mA.

3.3.4.3 Thermogravimetric analysis (TGA)

TGA results were obtained using a Mettler Toledo TGA/ SDTA 851 e analyzer heated to 1200°C, ramping at 15°C per minute in N₂ gas.

3.3.4.4 Magic Angle Spinning Nuclear Magnetic Resonance (MAS NMR)

Tecmag Apollo Console (Houston, TX) with 8.45 T magnet and homebuilt, single channel, 4 mm wide-bore NMR probe was used to determine ²⁷Al and ²⁹Si spectra. About 90mg of sample was taken for each analysis and signal represented as chemical shift value; δ: ppm. The ²⁷Al and ²⁹Si Larmor frequencies were 93.074 MHz and 70.958 MHz respectively. ²⁷Al spectra were acquired with MAS spinning frequency, last delay and 90° pulse length of 8 KHz, 1s and 2.5 μs, respectively. ²⁹Si spectra were acquired with MAS spinning frequency, last delay and 60° pulse length of 8kHz, 20s and 5.5 μs, respectively. Aluminum nitrate [Al(NO₃)] and Tetramethyl silane (TMS) were used as reference compounds for ²⁷Al and ²⁹Si spectra respectively. All experiments were performed at ambient temperature without any corrections for sample heating.

3.3.5 Strength test on mortars

3.3.5.1 Mortar preparation, casting, curing and testing

The mechanical property determined on mortar was compressive strength test. The mortar compressive strength test was determined in accordance with ASTM C109. A ratio of cementitious material (Portland cement plus calcined clay or clay/biomass) to sand was set at a constant of 1 to 2.75 and water-cementitious material kept at 0.485. Mixing of material was performed in a Hobart mixer in accordance with ASTM C305. To achieve the flow as specified in the ASTM C109 (105-115%), a small dosage of high range water reducer (HRWR) was added through an iterative means.

The addition of HRWR also ensured maximum hydration of cement powder particles and the prevention of cement paste agglomeration. Flow measurements were performed using a digital caliper in accordance with ASTM C1437. Once the desired spread flow was achieved, the batch of mortar was used to prepare mortar cubes for strength testing.

The specimens were cast in a three-gang 50 mm cubic mold and covered with a white plastic sheet and moist burlap to prevent water evaporation from the specimen. After 24 hrs the specimens were demoulded and placed under saturated lime water and cured at room temperature (24°C). For specimens prepared purposely for strength activity analysis, testing was performed at 7 and 28 days on an average of three samples. However, specimens that were prepared purposely to study effect of increasing dosage of calcined clay material were tested at 3, 7 and 28 days of lime water curing. Mix proportions for strength activity index and dosage increasing effect were prepared in batches of six and nine specimens respectively in accordance with ASTM C109 standard specifications. Table 3.3 provides the names for the mortar mixture proportions.

3.3.6 Test on cementitious binder paste

Generally, the test performed on the cementitious paste formulations included normal consistency, setting times, TGA and MAS-NMR analysis. Samples of hydrated materials obtained after the setting time test were reconditioned by curing them in saturated lime water solution for 3, 7 and 28 days. For the identification and investigations on the influence of the calcined products on Portland cement, TGA and MAS-NMR were used to study the degree of pozzolanic reaction and the extent of polymerization respectively.

Table 3.3: Mortar mixture name and proportions for strength activity determination

Mix name	Content (%)	
	Cement	Pozzolan
CON	100	0
CP/OPC		
20P600	80	20
20P700	80	20
20P800	80	20
20P900	80	20
20P1000	80	20
CP-PKS/OPC		
PK1	80	20
PK2	80	20
PK3	80	20
CP-RH/OPC		
RH1	80	20
RH2	80	20
RH3	80	20
CP-MC/OPC		
MC1	80	20
MC2	80	20
MC3	80	20
CP-SD/OPC		
SD1	80	20
SD2	80	20
SD3	80	20

CP: Clay pozzolan, OPC: Ordinary Portland cement, PK(S): Palm kernel shells, RH: Rice husk, MC: Maize cob, SD: Saw dust

3.3.6.1 Normal consistency and setting times

The normal consistency of the cementitious paste was performed using the prescribed method according to ASTM C187. The standard prescribes the use of a Vicat apparatus. 650 g of cement was mixed with water on an iterative basis until the plunger rod settled to

a point 10 ± 1 mm below the original surface in 30 s after being released. For the cementitious binders (cement + pozzolana), dosage of water reducers was added to the paste on an iterative trial basis to achieve normal consistency.

The tests for the setting times (initial and final) were determined in accordance with ASTM C191. Initial setting time was performed by a 1 mm needle on a paste that started to set after achieving normal consistency. The Vicat initial time of setting is the time elapsed between the initial contact of cement and water and the time when the penetration is measured or calculated to be 25 mm (ASTM C191). The final setting time is determined by the needle with a ring. The Vicat final time of setting is the time elapsed between initial contact of cement and water and the time when the needle with a ring fails to make an impression in the paste surface.

3.3.6.2 Sample preparation for TGA and MAS-NMR

The samples used for TGA and MAS-NMR testing were obtained from cured paste specimens for 3, 7 and 28 days. The cured samples were dried in an oven at a temperature of 80°C for six hours. The oven dried samples were removed, and left to cool for 10 mins and then ground into powder using mortar and pestle. The ground samples were then sieved through the $75\mu\text{m}$ sieve size. 10 g of the ground samples was transferred into sealed centrifuge bottles where methanol was added to the samples in the bottle to cease or stop further hydration. The methanol in the sealed bottles were left to dry out when the bottles were placed back in the oven operated at 80°C .

3.3.6.3 TGA test on hydrated samples

Approximately 35 mg of the hydrated samples were used in a Mettler Toledo TGA/ SDTA 851 e analyzer heated to 750°C, ramping at 10°C per minute in N₂ gas.

3.3.6.3 MAS NMR test on hydrated samples

The MAS NMR analyses performed on the hydrated samples were similar to the description given above for the NMR test performed on calcined clay materials.

3.3.6 Durability test

3.3.6.1 Shrinkage

The shrinkage tests were determined in accordance with the ASTM C596 standard test on mortar specimen. Mortar samples were prepared to achieve a flow of 110±5%. For the cement blended mortars, the desired flow was achieved with the aid of HRWR (Glenium 7500). Six mortar samples were cast in 25 by 25 by 285mm prismatic moulds. The specimens were covered with a transparent plastic sheet and moist burlap to prevent evaporation. After 24 hrs of moist curing, samples were demoulded and divided into two halves. A total of three specimens each were designated for total and autogenous shrinkage respectively.

Initial lengths of the specimens were taken after 24 hrs of curing with a length comparator in accordance with ASTM C490. Specimens designated for total shrinkage test were placed under curing water for 72 hrs after which their lengths recorded whilst specimens designated for autogenous shrinkage were sealed with wax and exposed in an environmental chamber at 23°C

and 50% relative humidity. The unsealed samples after lime water curing were also exposed to the conditions in the environmental chamber.

Length measurements were recorded at 4, 7, 11, 18 and 25 days of exposure.

3.3.6.1.1 Strain calculation

The length changes or strain calculated for both total and autogeneous shrinkages were determined according to equation 3.1 given as

$$\Delta L(\%) = \frac{L_f - L_i}{L_r} \times 100\% \quad \text{Equations 3.1}$$

Where ΔL = strain or length change

L_f = length recorded at a particular exposure period

L_i = Length recorded after 24 hrs of moist curing

L_r = Length comparator rod at a constant value of 295.26mm

3.3.6.2 Water Sorptivity

Water sorptivity determination was performed in accordance with the ASTM C1585. 25 mm cube mortar samples cured after 1 and 7 days were conditioned. For the conditioning process, samples were placed in a desiccator containing saturated solution of potassium bromide (KBr) placed at the bottom part inside the desiccator without making any contact with the specimen. KBr was used to maintain a high humidity environment (about 98%). The desiccator and content were placed in an oven at a temperature of 50°C for 3 days. After the three days, the desiccator and content were removed from the oven. Mortar samples were placed in sealable transparent plastic containers and placed in an environmental chamber maintained at 50% humidity and 23°C for at least 15 days. The sealed plastic bags were removed from the chamber after the conditioned period and

samples taken out from the sealed plastic bags for their weight measurement. The sides and the top part of the specimens were covered with a black duct tape leaving the side opposite to the top part uncovered. This was done to allow water to flow in one direction. The mass of the covered specimen was recorded as the initial mass of water absorption. A support device was placed at the bottom of a rubber container (shoe box) and filled with tap water up to the height of the of the support device. The uncovered portion of the mortar specimen was placed on the support device while the water level was increased to about 2mm above the specimen from the bottom. Figure 3.4 shows a schematic diagram of the apparatus. A stop watch was started at the time water made contact with the specimen. Mass of the specimen was taken at different times as shown in Table 3.4.

Table 3.4 Times and tolerance for mass recording

Time	60 s	50 min	20 min	30 min	60 min	Every hour up to 6 h	Once a day up to 3 days	Day 4 to 7	Day 7 to 9
								3 measurements 24 h apart	1 (one) measurement
Tolerance	2 s	10 s	2 min	2 min	2 min	5 min	2 h	2 h	2 h

The absorption of the specimen denoted as I was determined as the change in mass divided by the results of the exposed area divided by density of water.,

$$I = \frac{m_t}{a/d} \quad \text{Equation 3.2}$$

where:

I = the absorption, m_t = the change in specimen mass in grams, at the time t , a = the exposed area of the specimen, in mm^2 , and d = the density of the water in g/mm^3 .

An average of three mortar specimens was used for the absorption calculations. The gain in mass per unit area over the density of water was plotted versus the square root of the elapsed time. The slope of the line of best fit of these points was taken as the sorptivity value. The rate of water absorption obtained between 60 secs and 6 hrs from the graph determined the initial sorptivity coefficient (S_i) whereas between 1 and 7 days determined the secondary sorptivity coefficient (S_s).

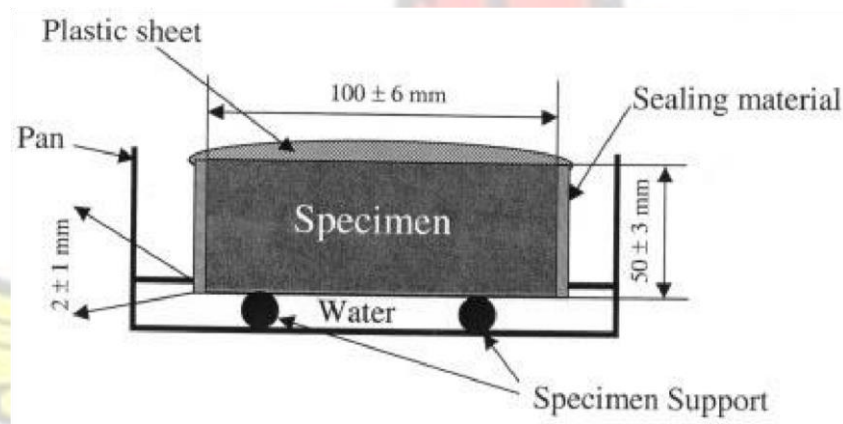


Figure 3.4: Schematic diagram of sorptivity experiment (After ASTM C1885) CHAPTER FOUR

4.0 RESULTS AND DISCUSSIONS

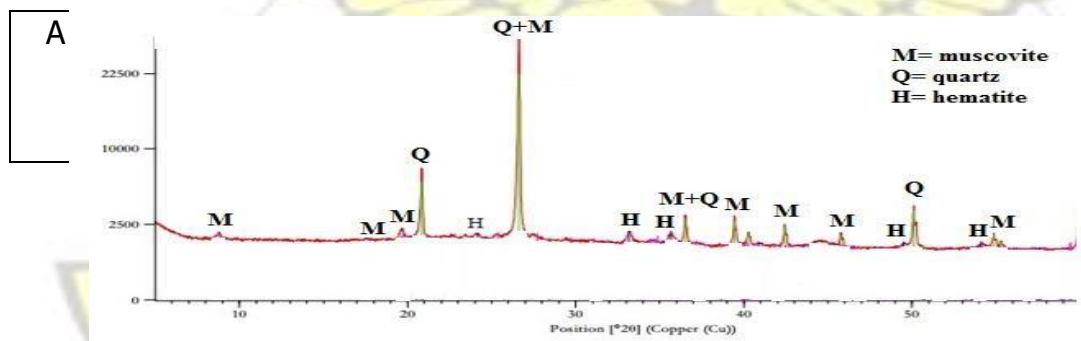
4.1 Properties of selected biomass

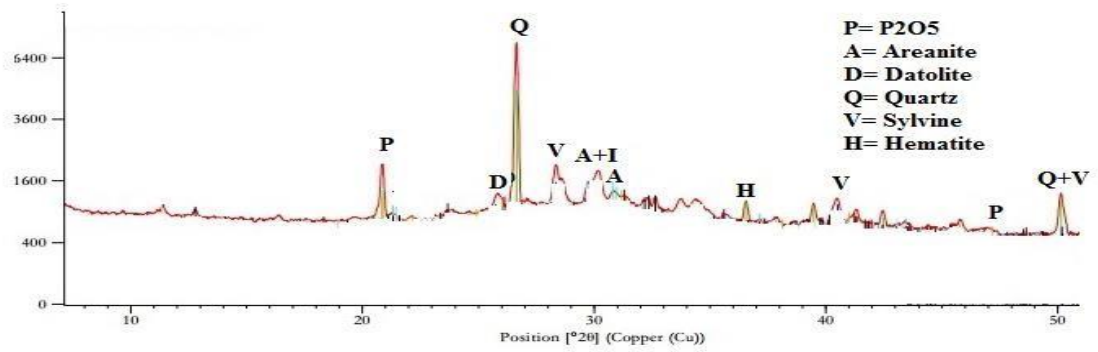
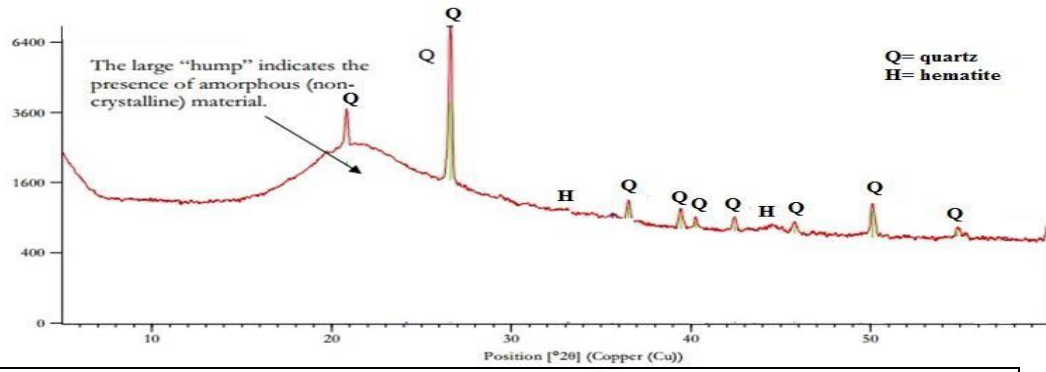
4.1.1. Mineralogical composition

Figure 4.1 (A-D) presents the X-ray diffraction patterns of the ashes of the biomasses: palm kernel shells, rice husk, maize cobs and sawdust. Figure 4.1A shows the diffraction patterns of palm kernel shell ashes. The crystal structure found was composed of muscovite (M), quartz (Q), hematite (H). Quartz showed a higher intensity together with muscovite

while hematite showed lower intensities. The presence of the crystalline quartz and muscovite could probably be from the high temperature of calcination or handling of the material which may introduce soil or clay particles forming a portion of the shells.

Figure 4.1B presents the diffraction patterns of rice husk ash. The pattern shows both intense and broad diffused peak. The broad peak shown between 16° and 25° 2θ indicates the amorphous nature of the ash. Quartz is the main crystalline shown in the pattern. Smaller peaks that correspond to hematite were also seen. The quartz present may be a disordered form of silica. The occurrence of the crystalline peaks may be attributed to the calcination temperature (800°C). Patel et al (1987) have pointed out that to prevent the transformation of amorphousness to crystalline form, the calcination temperature should be below 700°C .





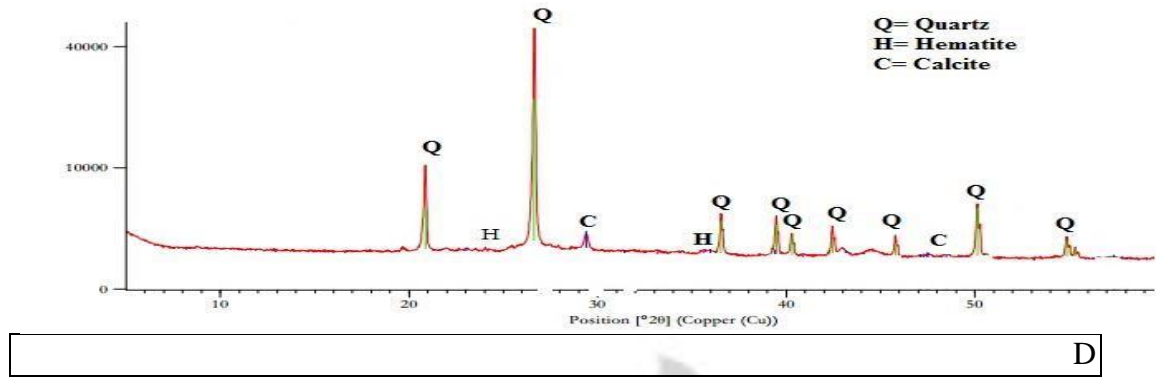


Figure 4.1: X ray diffraction analysis of biomass ashes: A-palm kernel; B-rice husk; C-miaze cob; D-sawdust

Figure 4.1C shows the diffraction patterns of maize cob ash. Reflective peak that corresponded to quartz was identified together with other minor reflective peaks which included a metastable mineral of phosphate origin ($P=P_2O_5$), sylvine (V), areanite (A), and hematite (H). Figure 4.1D presents the XRD analysis results of sawdust ash. The diffraction pattern shows quartz (Q) as the main peak. In addition to quartz, the XRD detected additional minor peaks corresponding to hematite (H) and calcite (C).

4.1.2 Chemical composition

The chemical compositions of the biomass ashes are presented in Table 4.1. The summation of the major oxides of rice husk ash (RHA), saw dust ash (SDA) and palm kernel ash (PKA) where higher than 70%. The results of the summation of the major oxide satisfied ASTM C618 which states that the summation of SiO_2 , Al_2O_3 , Fe_2O_3 shouldn't be less than 70%

when the material is considered as a pozzolan. Higher content of the active ingredient ($\text{SiO}_2 + \text{Al}_2\text{O}_3 + \text{Fe}_2\text{O}_3$) makes it possible to achieve a higher compressive strength. Maize cob ash (MCA) had a summed value of 46.14% which was less than the prescribed value by ASTM C618 which indicates that MCA may probably be a less reactive supplementary material as compared to RHA, SDA and PKA. The content of SiO_2 of RHA in the midst of its associated Al_2O_3 and Fe_2O_3 may probably contribute very well to pozzolanic effect, followed by SDA and then PKS. Malvar and Lanke (2006) stated that a higher content of SiO_2 in the midst of appropriate content of aluminate and ferrate contributes effectively to pozzolanic effect.

Al_2O_3 in the PKA had the highest value, followed by SDA. This chemical content may have the potential to cause accelerated setting which is a characteristics of cement when used as a component in a supplementary material (Cheng, 2012). MCA had a higher content of equivalent alkalis which makes it less favorable as a material to be considered especially where alkali-silica reaction is of paramount interest. Moreover, the high content of K_2O showed that the material was rich in K^+ . The XRF and XRD results of the MCA show that the ash properties may be very poor in pozzolanic properties i.e less reactive phases.

Table 4.1: Chemical composition of biomass ashes at 800°C

Compound	Ashes			
	RH	SD	PK	MC
SiO_2	93.01	79.33	71.79	40.11
Al_2O_3	1.86	6.04	14.47	2.92
Fe_2O_3	1.12	4.53	8.72	3.11
CaO	0.97	5.19	0.67	1.87
MgO	0.45	ND	0.7	2.68
SO_3	0.2	0.35	0.11	0.99
Na_2O	0.09	0.3	0.16	0.5

K ₂ O	1.53	2.71	1.77	38.68	
TiO ₂	0.14	0.61	0.51	0.37	
P ₂ O ₅	0.32	0.39	0.34	5.8	
Mn ₂ O ₃	0.18	0.06	0.04	0.07	
SrO	0.01	0.03	0.01	0.01	
Cr ₂ O ₃	0.06	0.34	0.37	0.11	
Cl	0.02	0.02	0.02	1.72	
F	ND	ND	0.23	0.81	
Br	ND	ND	ND	0.02	
NiO	ND	0.01	0.01	0.01	
CuO	0.01	0.01	0.01	0.01	
ZnO	0.01				
Total	99.98				
Eq Al	1.1				
SiO ₂ +Al ₂ O ₃ +Fe ₂ O ₃	95.99				
Calorific values	16.80	16.70	17.51	17.00	
		0.01	0.01	0.14	
		99.91	99.93	99.92	4.2
		2.08	1.32	25.95	
		89.9	94.98	46.14	

Properties of raw and calcined clay

4.2.1 Thermal gravimetric analysis of powder clay

Figures 4.2(a) and (b) present thermal gravimetric and differential thermal analysis of the powdered clay, respectively. The thermal treatment of the clay yielded basically three processes namely dehydroxylation, calcination and recrystallization. Usually the dehydroxylation is preceded by mass loss as a result of loss of physically adsorbed water and residual matters found in clay (Fernandez et al, 2011). From Figure 4.2(a), the mass loss due to moisture and residual matters was approximately 1.4%. The two, adsorbed water and residuals matter decomposition were shown in the initial two endothermic peaks in Figure 4.2 (b). The third endothermic peak (C) shown in Figure 4.2 (b) characterizes the dehydroxylation process which occurred between 325°C and 731°C. In Figure 4.2(a),

approximately 11% mass loss was estimated due to dehydroxylation of the clay. The completion of the dehydroxylation peak marks the calcination temperature.

Figure 4.2(b) indicated that the effective calcination temperature was approximately 731°C. The figure also showed that between 731°C and 904°C, there was a complete dehydroxylation. This indicates that calcined clay between 731°C and 904°C may possess similar characteristics. The small exothermic peak (D) shown in Figure 4.1 (b) between 905°C and 1036°C indicates crystal formation.

Complete dehydroxylation of clay mineral which is indicated between 731°C and 904°C shows that octahedral aluminium sheets dehydroxylizes into a metastable disordered state, collapsing a higher quantity of crystalline clay minerals to produce a more reactive calcined clay (Mendelovici, 1997). Fernandez et al (2011) have shown that the extent of reactivity is influenced by the extent of disorderliness which cannot be determined easily by thermogravimetric analysis (TGA). The growth of crystals between 905°C and 1036°C supports the argument of Fernandez et al (2011) that at higher temperatures a metastable state transforms from amorphous condition into crystalline units which inhibits reactivity of calcined clays. The TGA results gave additional information to support other XRD analysis especially with the emergence of mullite.

The findings from Heller-Kallai (2006), Tironi et al (2013), and Fernandez et al (2011) pointed out that 1:1 kaolinitic clays completely dehydroxylise mostly at approximately 600°C whereas the 2:1 clay minerals which includes illite and montmorillonite completely

dehydroxylizes above 600°C. The trend of the results from Figures 4.2 (a) and (b) may probably characterize the clay as a 2:1 clay mineral.

KNUST



KNIL ICT

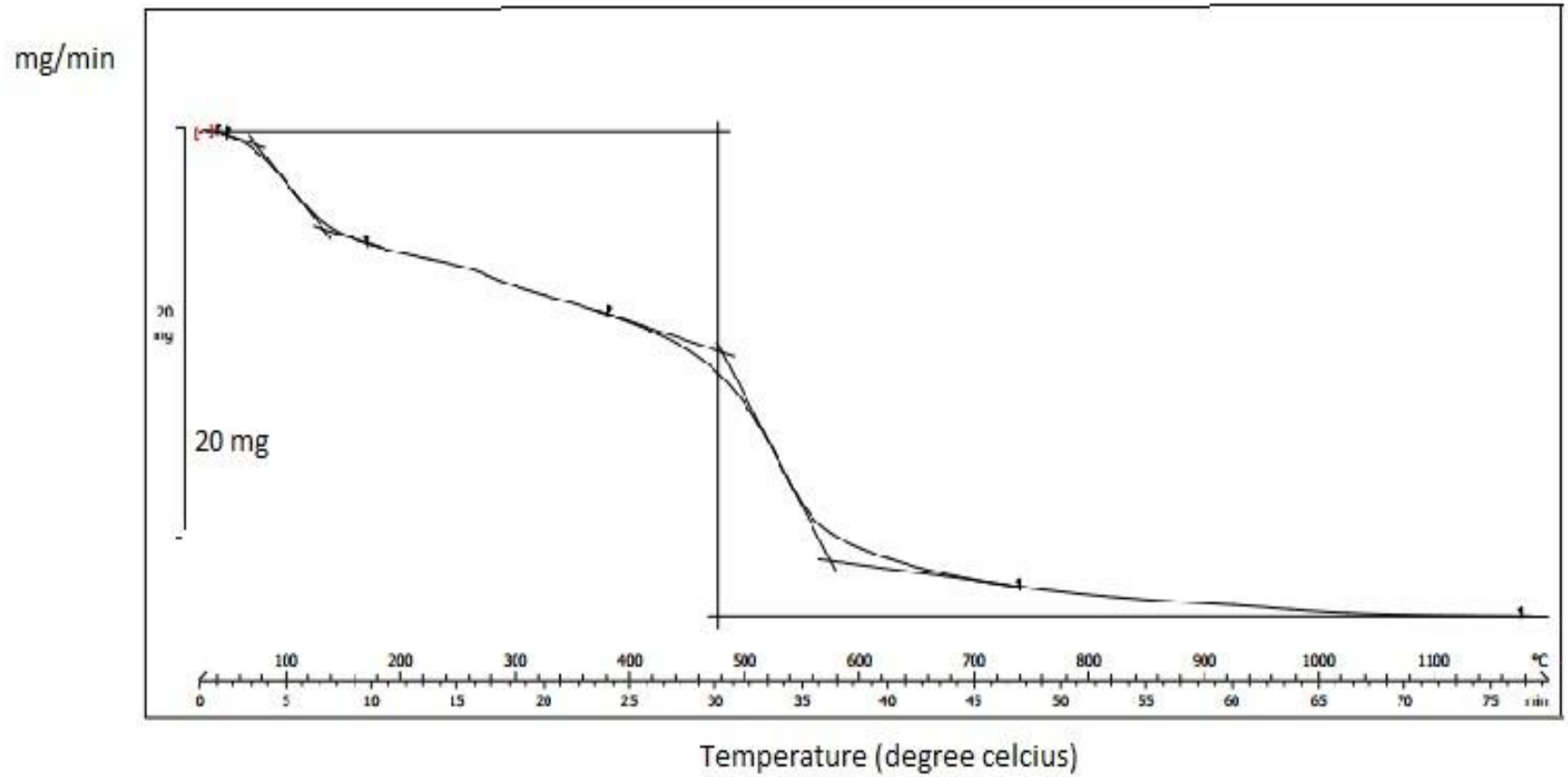


Figure 4.2(a): TGA analysis of powdered clay

146

□



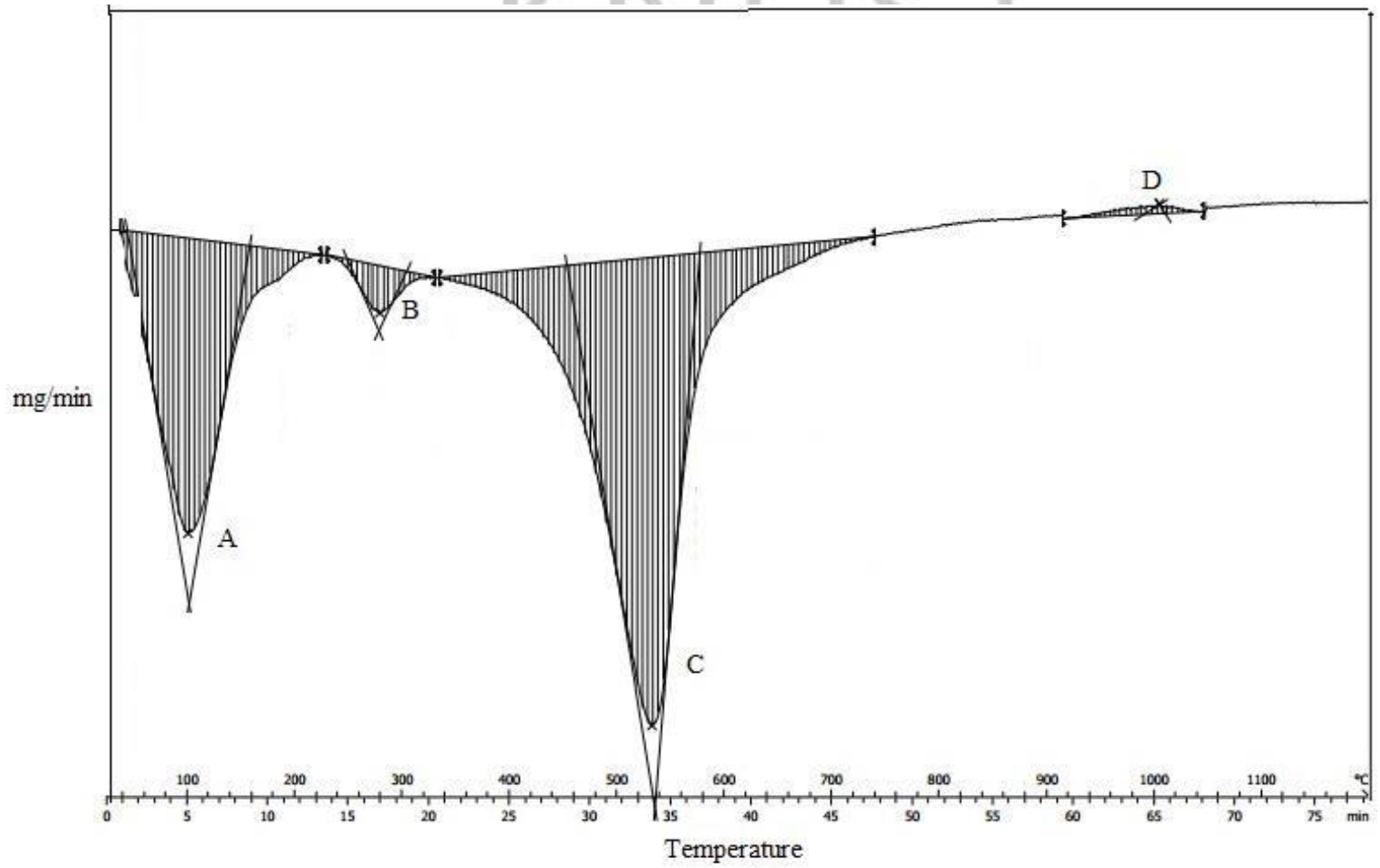
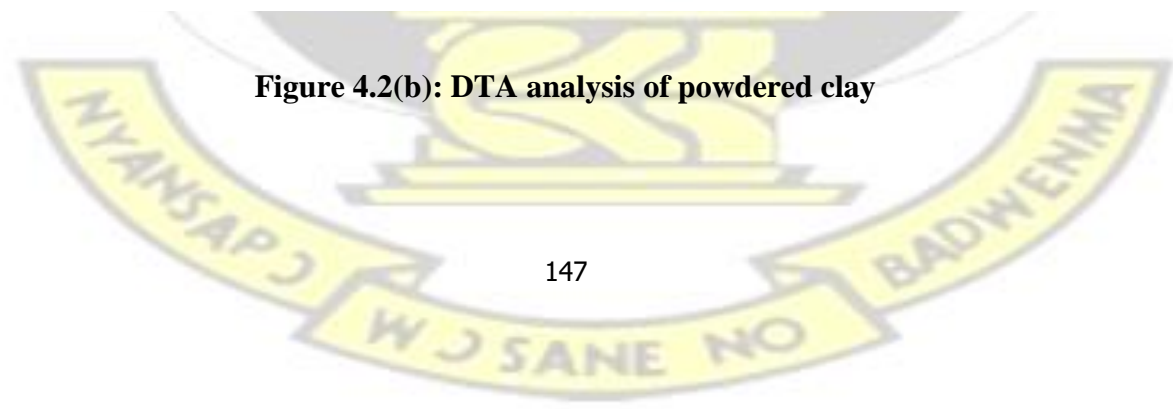


Figure 4.2(b): DTA analysis of powdered clay



KNUST



4.2.2 Mineralogical composition

Figure 4.3 presents the X-ray diffraction patterns of raw and calcined clay at temperatures of 600°C, 800°C and 1000°C. The calcined materials at 700°C and 900°C were not considered since their results would be most likely similar to 600°C and 800°C which is shown in the TGA graph (see Figure 4.2 (b)). Calcinations of the raw clay at 600°C, 800°C and 1000°C had little influence on quartz (Q). However, crystalline products including kaolinite (K) and montmorillonite (S) diminished significantly as the temperature increased. At 1000°C, there was the appearance of the highly crystalline product, mullite (U).

Quartz which was present throughout the calcination temperatures may be an associated mineral of the raw clay. The temperatures, 600°C, 800°C and 1000°C which caused a reduction in the crystallinity of clay could be appropriate calcination temperatures (Heikal et al, 2013) to produce reactive calcined clay pozzolan. However, the presence of crystalline mullite at 1000°C showed recrystallization of amorphous silica therefore affecting the choice of temperature selection. The presence of high crystalline products which include mullite renders calcined clay less reactive (Xu et al, 2012). Therefore, calcined clay at 1000°C could probably be less reactive as compared to 600°C and 800°C.

KNUST



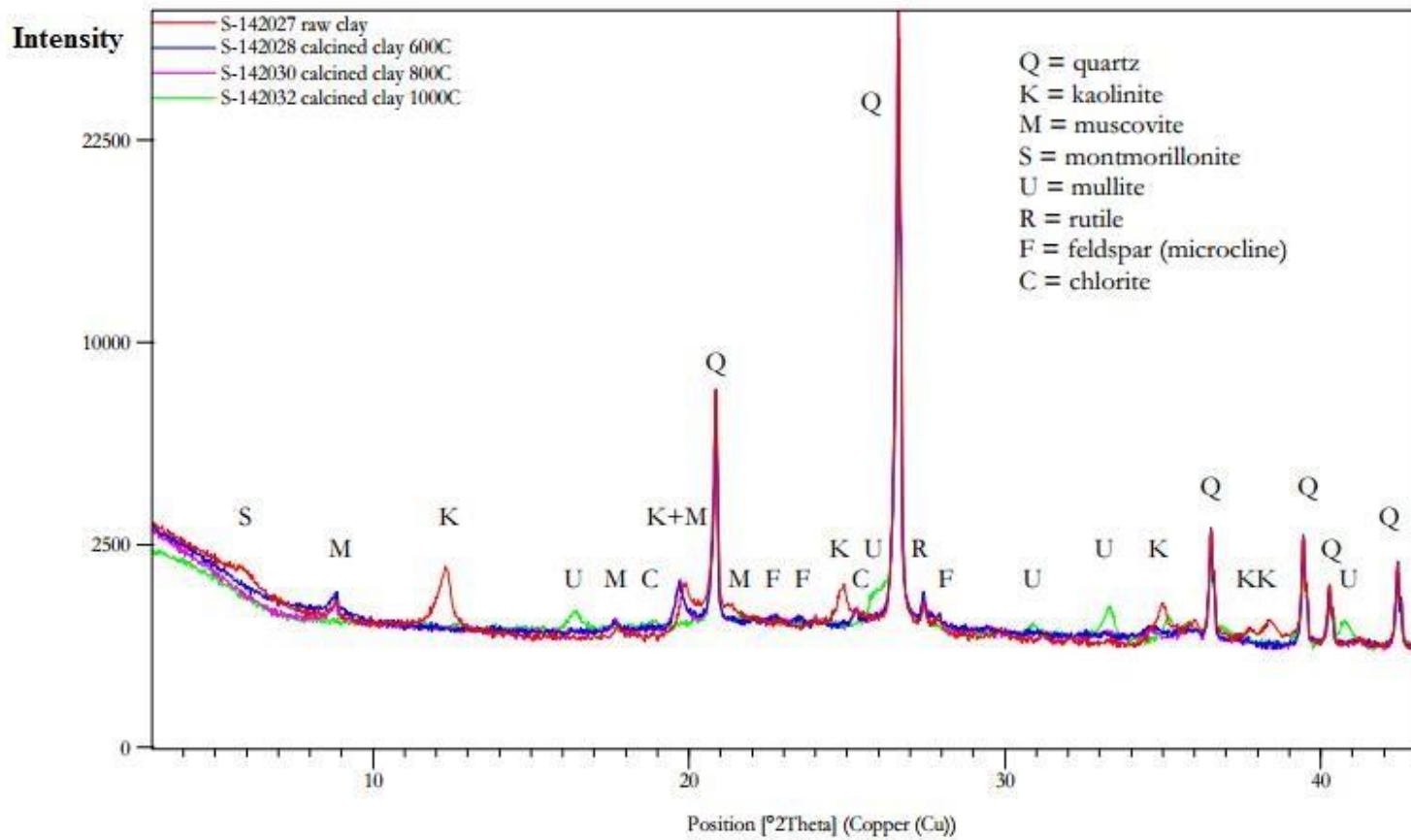


Figure 4.3: XRD overlay of raw clay and calcined clay at 600°C, 800°C and 1000°C

149

□



4.2.3 MAS NMR analysis

4.2.3.1 ^{27}Al and ^{29}Si NMR of calcined clays

Figure 4.4 presents the solid state magic angle spinning (MAS) nuclear magnetic resonance (NMR) of raw and calcined clay from 600°C-1000°C. The raw clay showed two distinct peaks which resonated at 68.30 ppm and -0.76 ppm respectively. This indicated a 1:1 kaolinite group of clay. The use of MAS NMR instrument has usually been a useful tool in confirming clay much better than the TGA. As it has already been explained from literature, a 1:1 group represents octahedral and tetrahedral sheets. Hanna et al (1995) confirmed that tetrahedral sheets resonate from 50 ppm to 80 ppm whereas the octahedral sheets also resonate from -20 ppm to 20 ppm. A particular chemical shift could also be dependent upon to assess the crystallinity of a calcined materials. A more negative chemical shift shows a higher electron density which is indicative of the presence of a more crystalline pattern (Liu et al, 2011).

Calcined clays exhibited a decrease in their intensities of $\text{Al}^{(\text{vi})}$ and increased intensities at the $\text{Al}^{(\text{iv})}$ environment with reference to the raw clay. An increased intensity at $\text{Al}^{(\text{iv})}$ than $\text{Al}^{(\text{vi})}$ indicates a greater reactivity of calcined clays (Klimesch et al, 1998; Pena et al, 2008). From Figure 4.3, calcined clays although showed a decreased population at the octahedral Al population, there were specific shifts for each calcined temperature. The

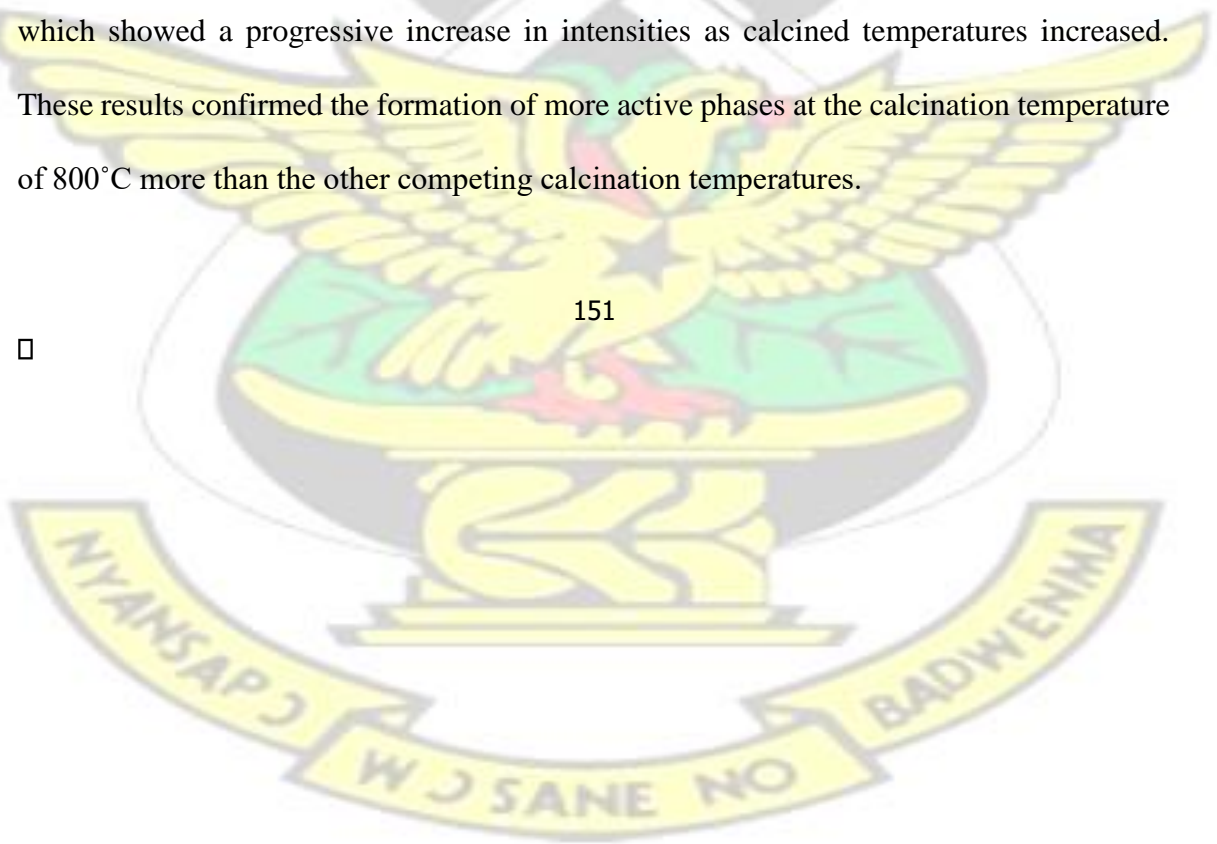
figure indicates that calcined clays at 600 and 800 had similar chemical shifts to -0.25 ppm which is lower than that for the raw clay at -0.76 ppm. Calcined materials at 700, 900 and 1000°C showed chemical shifts to -1.76 ppm, -2.77 ppm and -6.30 ppm which are much higher than that for the raw clay. This shows the development of more

150

□ crystalline matters at the octahedral environment. The high negative chemical shift at 900 and 1000°C confirmed the presence of mullite, a crystalline material as shown from the XRD and TGA graphs. The NMR results gave a better confirmation with regards to the presence of crystalline and nature of metastable materials in calcined clay at 900°C even though it wasn't so clear from the TGA results. Figure 4.3 indicated that calcined clay at 600°C and 800°C may be more reactive with cement than those at the other temperatures. Since the intensity at the octahedral Al environment of calcined material at 800°C was lower than that of the intensity of calcined clay at 600°C, it is an indication of more reactivity. The intensities of the results at the four coordinated ($\text{Al}^{(\text{iv})}$) environment of ^{27}Al were very difficult to ascertain because of the nature of the reference clay peak. The nature of the peak shown at 68.30 ppm on the spectra of the reference clay was not suitable to give an accurate intensity as a baseline. However, it could be that the $\text{Al}^{(\text{iv})}$ population of

clay calcined at 800°C could possess a higher intensity than the clay calcined at different temperatures.

Figure 4.5 presents the ^{29}Si MAS NMR of the raw clay as well as calcined clay materials. Raw clay showed a chemical shift at -110 ppm and -126 ppm. These shifts correspond to Q^4 silicon coordinated environment formed usually at the earth crust under environmental temperature and pressure (Hjorth et al, 1988; Stebbins and Kanzaki, 1991). The calcination process collapsed one of the Q^4 around -110 ppm populations leaving the Q^4 at -126 ppm which showed a progressive increase in intensities as calcined temperatures increased. These results confirmed the formation of more active phases at the calcination temperature of 800°C more than the other competing calcination temperatures.



IRNII ICT

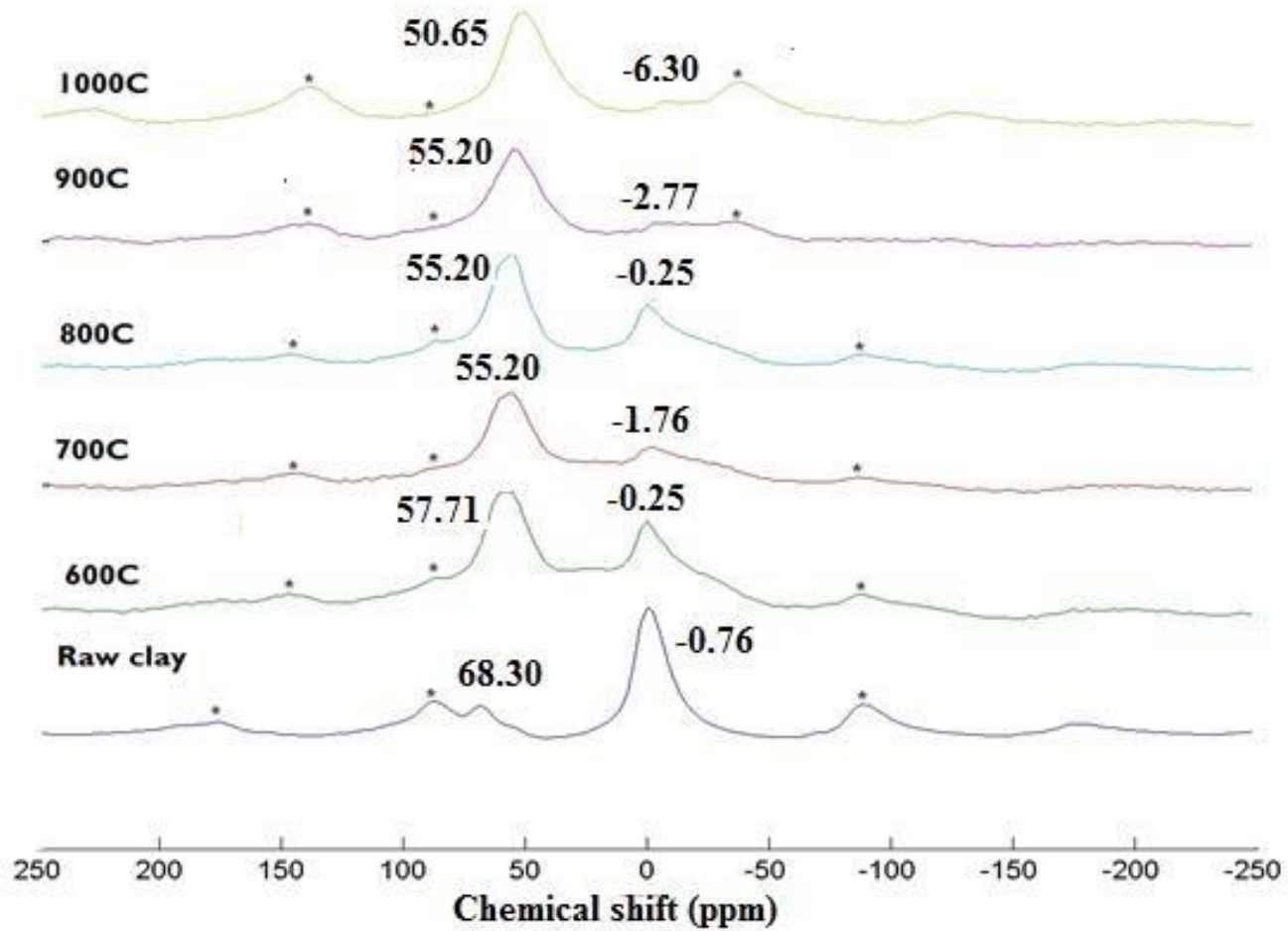


Figure 4.4: ^{27}Al solid state MAS NMR of raw and calcined clays

□



UNIICT

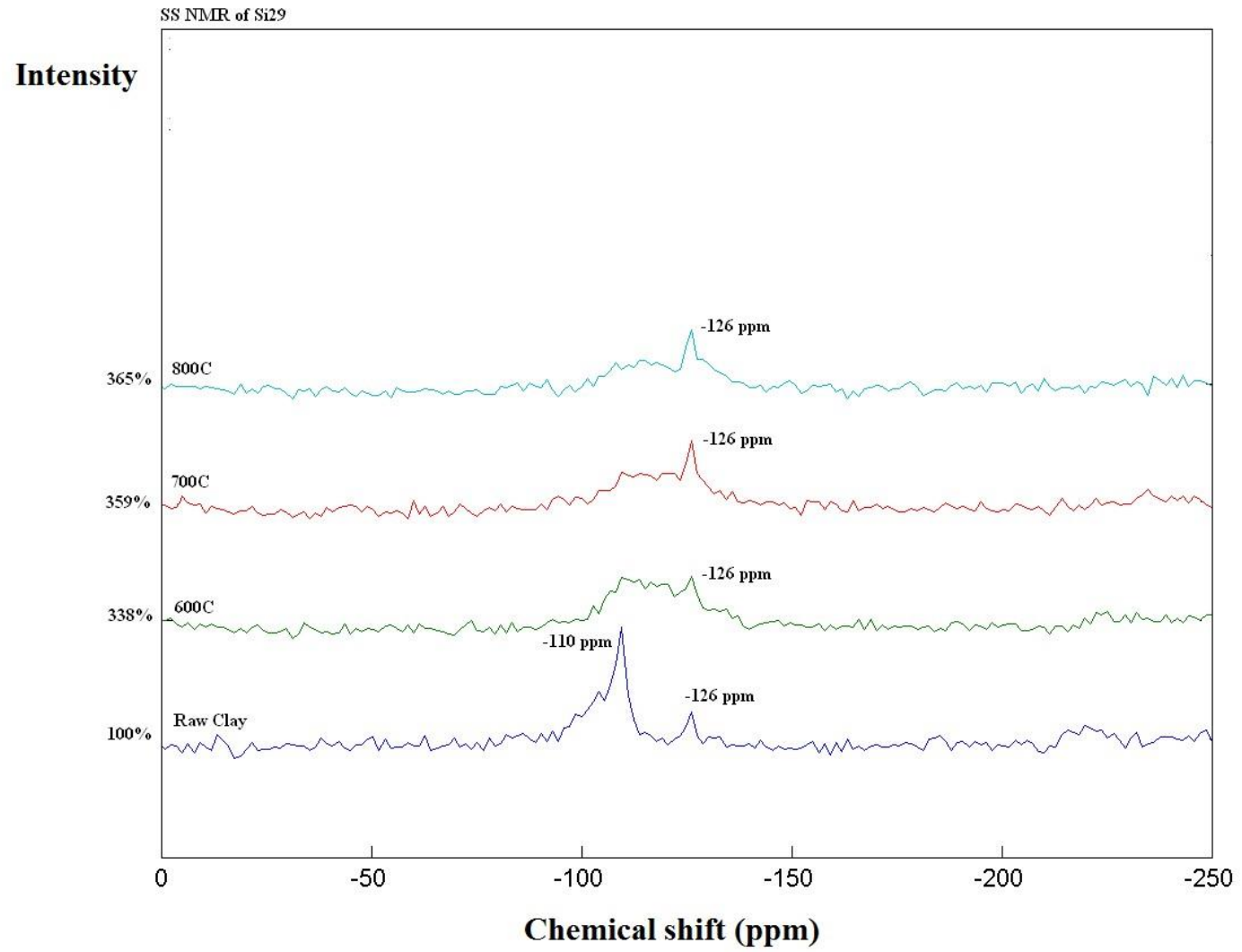


Figure 4.5: ^{29}Si solid state MAS NMR of raw and calcined clays

□



4.3 Optimum calcination temperature and replacement level of calcined clay

4.3.1 Optimal temperature determination

The mortar mixture proportion used for the batch mixes for strength activity test is shown in Table 4.2. The table shows that water-to-binder (w/b) ratio of the mortar mixes were maintained at 0.485, sand-to-cement ratio at 2.75 and a superplasticizer in a form of high range water reducer (HRWR) added to achieve the required flow according to ASTM C1437. The dosage of HRWR which was used to achieve the desired flow for clay calcined between 600°C and 800°C was 0.4%. However, at temperatures of 900°C and 1000°C, HRWR dosage was reduced to 0.3% and 0.2%, respectively after series of iterative runs. The reduction in the amount of HRWR at temperatures 900°C and 1000°C is most likely due to reduction in particle size and absorption caused by recrystallization of clay at higher temperatures (Kartina, 2011; Moodi et al, 2011). This is confirmed in the TGA and XRD results shown in Figures 4.2 and 4.3 respectively. Less absorptive crystalline phases in calcined clays improve workability or flowability, hence a reduction in water quantity.

Figure 4.6 presents the pozzolan strength activity results of thermally activated or calcined clay from 600°C-1000°C together with the control mortar mix. ASTM C618 indicates that the pozzolanic activity at 7 and 28 days of any acceptable pozzolan should be greater than 75% of the control mortar mix. From Figure 4.6, clay thermally activated between 600°C and 1000°C met that requirement. The results of the strength activity of clay calcined at 800°C attained maximum strength among all the temperatures at 7 and 28 days. The pozzolanic activity of clay calcined at 800°C showed that the clay mineral was sufficiently calcined (see TGA results from Figure 4.2 (b)), produced quality pozzolanic active phases

as indicated from the ^{27}Al and ^{29}Si solid state MAS NMR results shown in Figures 4.4 and 4.5 respectively. Tironi et al (2013) indicated that at optimum calcination temperature, strength improves due to the pozzolanic active phases (amorphous phases) formed. Appendix 4.1a gives detailed information of the compressive strength results of the calcined clay at 800°C.

Table 4.2 Mortar mix proportion for strength activity index of calcined clays

Temp (°C)	Mix name	Mass (g)					HRWR (%)	Flow (%)
		Cement	Clay	Sand	Water	w/b		
Control	Control	500	0	1375	242	0.485	0.0	106
600	20P600	400	100	1375	242	0.485	0.4	111
700	20P700	400	100	1375	242	0.485	0.4	110
800	20P800	400	100	1375	242	0.485	0.4	110
900	20P900	400	100	1375	242	0.485	0.3	115
1000	20P1000	400	100	1375	242	0.485	0.2	116

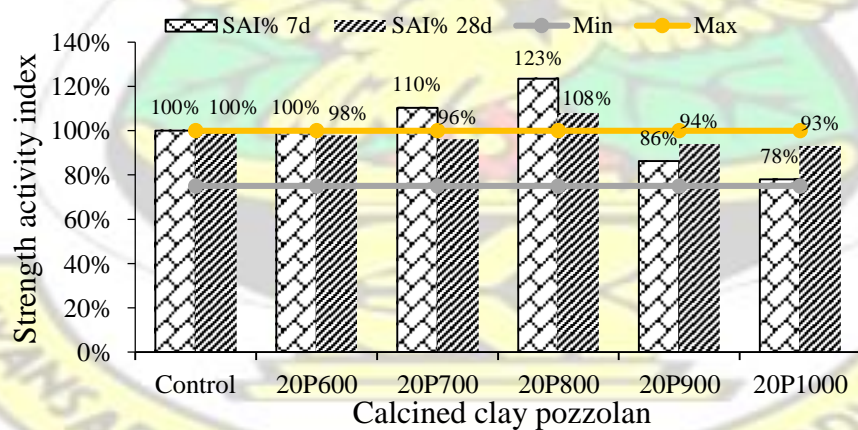


Figure 4.6 Optimum temperature for thermally activated clay

4.3.2 Obtaining the optimal replacement level

Table 4.3 presents the mortar mixture proportion of blended Portland cement and calcined clay. The water-to-cement ratio and the sand quantity were maintained constant at values of 0.485 and 2035g respectively. HRWR was added to mortar mixes to achieve the desired flow between 105 and 114%. The table shows that the amount of HRWR increased with increasing quantity of the calcined clay. This trend indicates that as the amount of calcined clay increases, the surface area also increases within the blended cement and pozzolana system making the system demand more water.

The compressive strength of Portland cement partially replaced with clay calcined at 800°C from 10-40% is shown in Figure 4.7. Details of the strength values including the mean, standard deviation, coefficient of variance are presented in Appendix 4.1b. The control mortar strength at 3, 7 and 28 days were 29, 33 and 44 MPa respectively. The strength values for 10% cement replacement (10P800) and 20% replacement (20P800) at 3, 7 and 28 days were 29, 33, 40 MPa and 31, 40, 48 MPa, respectively whereas that for 30% (30P800) and 40% (40P800) cement replacements were 21, 28, 35 MPa and 18, 24 and 30 MPa respectively. The results show that compressive strength improved steadily up to 20% cement replacement. Beyond 20% replacement, strength decreased substantially. Cement replacement with calcined clay at 20% gave the best results and thus considered to be the optimum in terms of increase in compressive strength at different ages. The optimal replacement level which improved the strength of mortar much better than the control mortar could be attributed to the degree of pozzolanic reaction (Malquiro, 1960). The 20% cement replacement showed that the pozzolan quantity was enough to take up almost all

the portlandite content. The decrease in strength beyond 20% of cement replacement meant that the calcined materials behaved as inert fillers with little contribution to strength enhancement.

Table 4.3: Mortar mixture proportion containing Portland cement and calcined clay

<u>Mix</u>	<u>Content (%)</u>			<u>Mass (g)</u>				<u>HRWR (%)</u>	<u>Flow</u>
	<u>Cement</u>	<u>Clay</u>	<u>w/b</u>	<u>Cement</u>	<u>Clay Pozzo</u>	<u>Sand</u>	<u>Water</u>		
control	100	0	0.485	740	0	2035	359	0.00	107
10P800	90	10	0.485	666	74	2035	359	0.14	107
20P800	80	20	0.485	592	148	2035	359	0.32	114
30P800	70	30	0.485	518	222	2035	359	0.34	105
40P800	60	40	0.485	444	296	2035	359	0.45	107

w/b: water-to-binder ratio

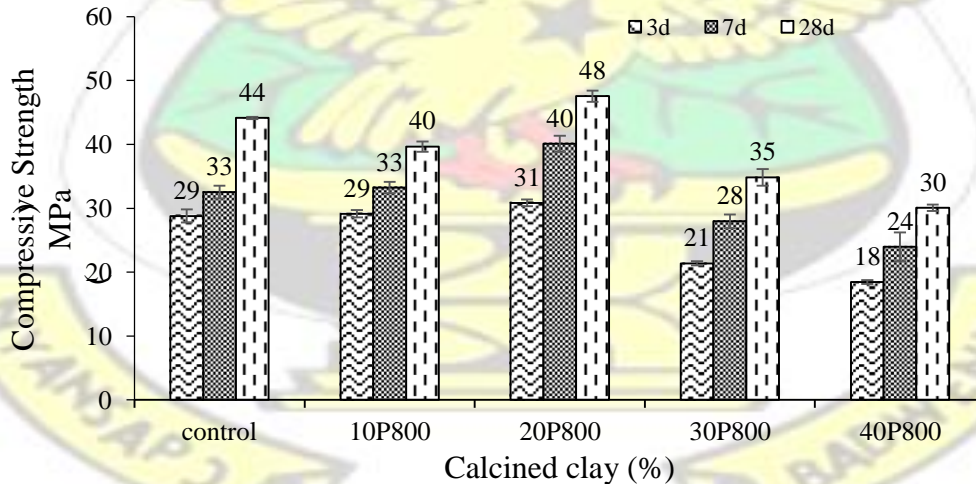


Figure 4.7: Compressive strength test of mortars containing calcined clay pozzolana (800°C)

4.4 Determination of maximum clay/biomass proportions based on strength activity index

Table 4.4 shows the mortar mixture proportions used to determine the strength activity indices of cement and calcined clay/biomass pozzolanas. The w/b ratio for all the mortar mixes was maintained at 0.485. HRWR was added to mortar mixes containing the pozzolan to achieve the desired flow in accordance with ASTM C618. With cement and calcined clay/palm kernel shell mixtures (PK1, PK2, PK3), HRWR dosage was between 0.2 and 0.3%. Cement and calcined clay/rice husk mortar mixes (RH1, RH2, RH3) were the same at 0.3%. HRWR dosage for cement and calcined clay/maize cob mortar mixture proportions (MC1, MC2, and MC3) ranged from 0.24-0.36% whilst cement and calcined clay/sawdust pozzolan (SD1, SD2, SD3) were between 0.26 and 0.3%. The flow values shown in the table for all the mortar mixture proportions were between 105 and 115 which satisfied the flow requirement of ASTM 311.

Table 4.4: Mortar mix proportions of Portland cement and calcined clay based biomasses

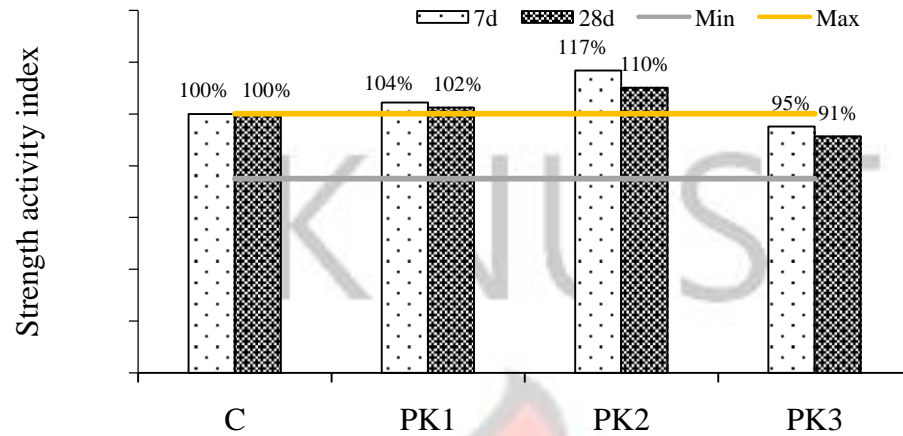
Mix Name	Mass (g)			w/b	HRWR (%)	Flow (%)
	OPC	Pozzolana	Water			
C	500	0	242	0.485	0	107
PK1	400	100	242	0.485	0.2	107
PK2	400	100	242	0.485	0.3	111
PK3	400	100	242	0.485	0.3	107
	400					
RH1		100	242	0.485	0.3	109
RH2	400	100	242	0.485	0.3	110
RH3	400	100	242	0.485	0.3	109
	400					
MC1		100	242	0.485	0.3	111
MC2	400	100	242	0.485	0.26	107

MC3	$\frac{400}{400}$	100	242	0.485	0.24	110
SD1		100	242	0.485	0.3	111
SD2	400	100	242	0.485	0.3	115
SD3	400	100	242	0.485	0.26	106

NB- OPC: Ordinary Portland cement, C/B: Clay and biomass pozzolana

Figures 4.8-4.11 present the strength activity index of Portland cement and clay/biomass mortar mixes. The figures show that co-fired clay and biomass mixture proportions had effect on the strength indices of the mortars compared to the control mortar. This effect yielded maximum strength results at specific biomass inclusiveness in calcined clay. From the figures the light grey and yellow solid lines represent strength activity index of Portland cement only at 75% and 100% respectively. As already stated, the ASTM C618 indicates that at 7 and 28 days, the pozzolanic activity index must not be less than 75% of the cement mortar mix.

Figure 4.8 shows the strength activity index of mortars containing cement and calcined clay/palm kernel shell mixes. All the mixes, PK1, PK2 and PK3 met the requirement of ASTM C618. The strength activity index at 7 and 28 days for PK1 were 104 and 102%. For PK2 and PK3, strength activity indices were 117% and 110%, and 95% and 91% respectively. Among the mortar mixture proportions within this series, PK2 had the maximum strength activity index. The results show that the combination of 20% palm kernel shells and clay (PK2) after calcination produced higher pozzolanic active components. Strength activity indices of PK3 (30% PKS) at the 7 and 28 days decreased because of the introduction of more crystalline phases associated with calcined palm kernel shells.



140%
120%
100% 80%
60%
40%
20%
0%

Calcined clay and palm kernel shells mixture

Figure 4.8: Pozzolan strength activity index of cement and clay/palm kernel shell pozzolana

Figure 4.9 shows the strength activity index of mortar containing cement and calcined clay/rice husk ash mixture proportions. All the mortar mixture proportions, RH1, RH2 and RH3 met the ASTM C618 strength requirements and were all higher than the control mortar. The 7 and 28 days' strength activity indices for RH1 and RH2 were 116% and 119%, and 118% and 116% respectively whilst that for RH3 was 105% and 106%. Strength activity indices at 7 and 28 days for both RH1 and RH2 showed close values noted to be the maximum index within this mortar series. A further analysis between the two mortar mixes using student t-test indicated an insignificant effect (see Appendix 4.2). Therefore,

basing the optimum activity index on maximum strength, biomass residues which impart negatively on environmental sustainability and economic gains discussed before, RH1 proved to be the optimum.

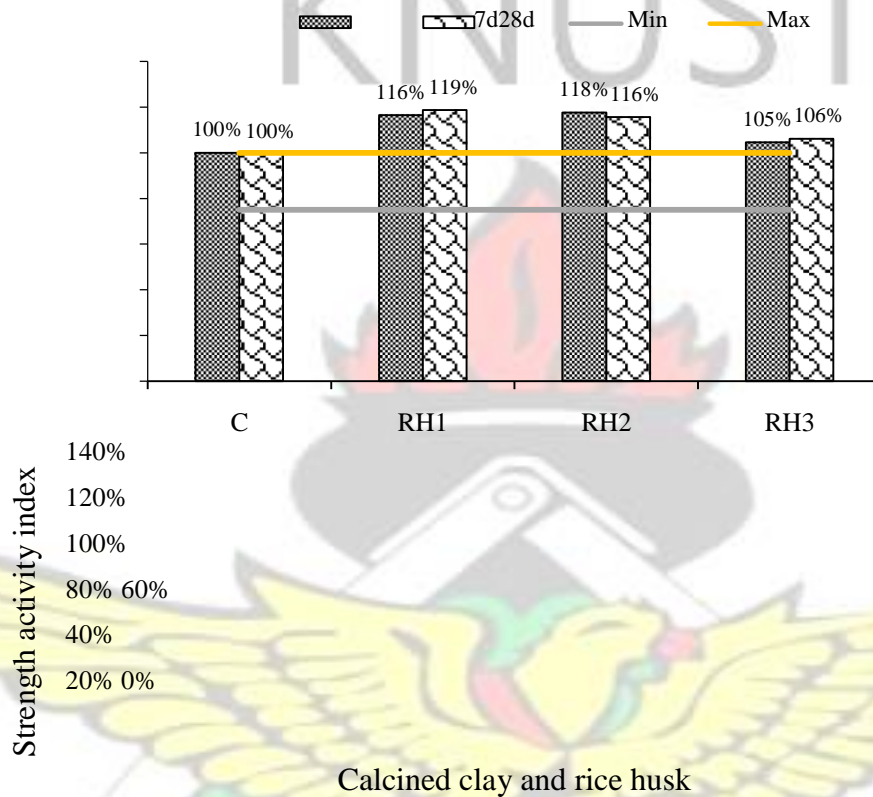


Figure 4.9: Pozzolana strength activity index of cement and rice husk pozzolana

Figure 4.10 presents the activity index of mortars containing cement and calcined clay/maize cob mortar mixture proportions. Within this series of mortar, the ASTM C618 requirement at 7 and 28 days were met by all the mortar mixes. Strength activity indices of MC1, MC2 and MC3 at 7 and 28 days were 114% and 101%, 99% and 92%, and 103% and 97% respectively. MC1 attained the maximum strength activity index at 7 and 28 days compared to the control mortar within this mortar series hence considered as the optimum proportion. Strength activities at MC2 and MC3 which showed reduction

compared to the control could be attributed to the presence of less amorphous products and low content of SiO₂ contribution to the clay within the clay-maize cob matrix.

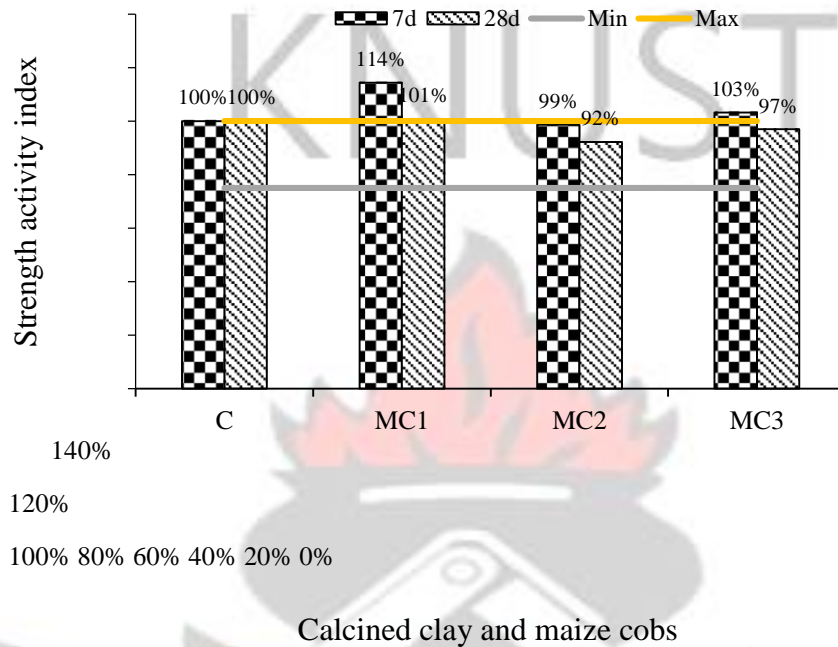


Figure 4.10: Pozzolana strength activity index of cement and maize cobs

Figure 4.11 provides the strength activity index of mortars containing cement and calcined clay/sawdust mortar mixture proportions. All the mortar mixes in this series met the ASTM C618 prescriptions for strength activity index at 7 and 28 days. The strength activity indices of SD1, SD2, and SD3 were 116% and 103%, 120% and 111%, and 107% and 94% respectively. SD2 obtained maximum strength activity values within this mortar series compared to the control mortar therefore selected as the optimum mixture proportion. The reason for their maximum values could be attributed to the contribution of amorphousness from that content of sawdust and limited content of crystalline materials present within the clay-sawdust matrix of SD2.

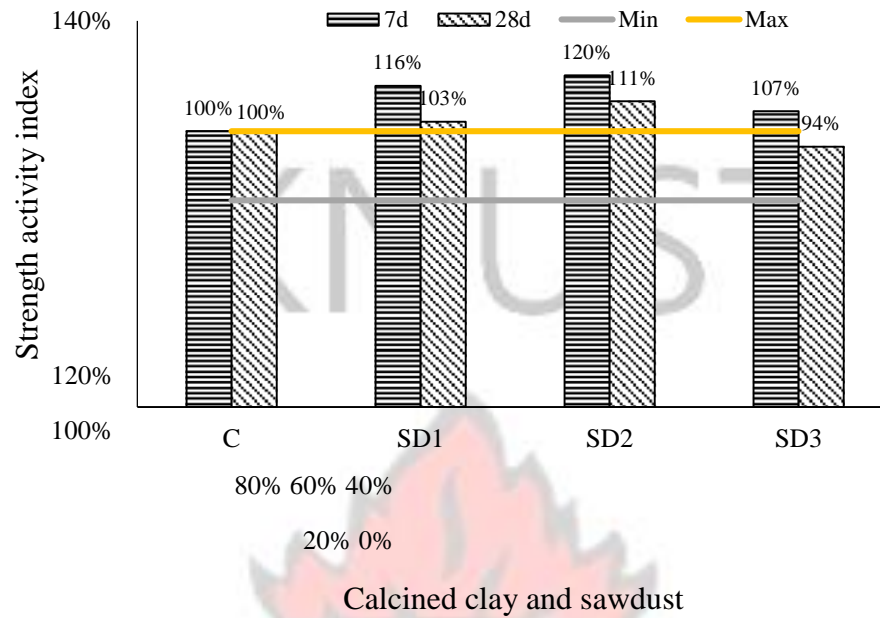


Figure 4.11: Pozzolana strength activity index of cement and sawdust

4.5 Optimum replacement of Calcined clay/biomass mixes

Figures 4.12-15 present the effect of increasing dosage of calcined clay/biomass mixtures obtained from formulated mortar mixtures. Figure 4.12 shows the strength results of mortar prepared from cement and calcined clay/palm kernels shell mixtures. The early 3day strength of 10PK2 (10% calcined clay containing 20% palm kernel shells) was 34MPa, the highest; followed by 20PK2 (20% calcined clay containing 20% palm kernel shells) which was 28MPa. At 7 days and 28 days, 20PK2 attained compressive strength values of 38MPa and 49MPa, representing the maximum compressive strength values among this series of mortar mixture proportions. The trend of the results indicated that 20PK2 had maximum strength values compared to the other mortar mixture proportions particularly the control. The results indicate that the dosage of 20% replacement of cement with calcined clay/palm kernel shell mixture was enough for conversion of excess portlandite (Lea, 1998; Malquiroy, 1960)

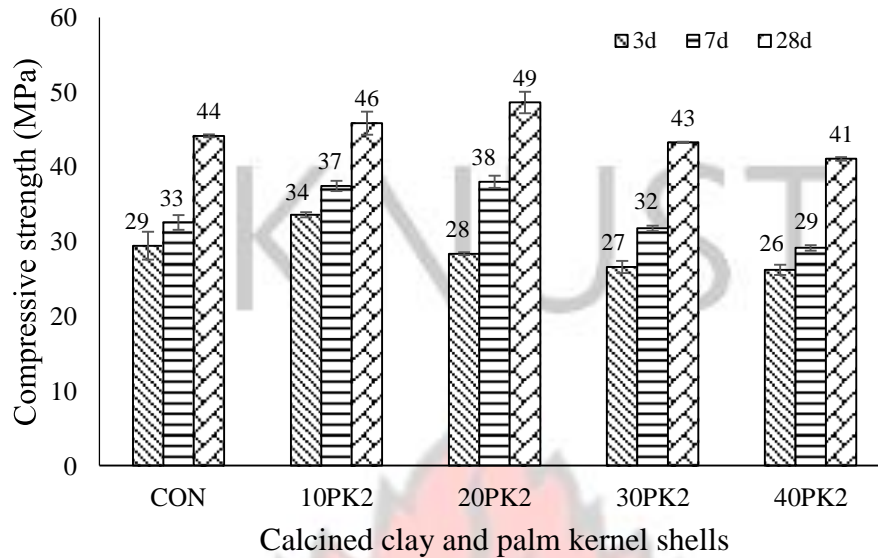


Figure 4.12: Compressive strength of mortar with varying calcined clay/palm kernel shells

Figure 4.13 presents the compressive strength results of mortar prepared from cement and calcined clay/rice husk mixture proportions. The early age strength at 3 and 7 days of 10RH1, 20RH1 and 30RH1 were all higher than the control mortar except 40RH1. However, at 28 days, all the mortar mixture proportions attained compressive strengths which were higher than the control mortar. The maximum strength value was found to be either 20RH1 or 30RH1. Furtherance to the strength results, a t-test analysis (see appendix 4.2) were performed between the two. The t-test results showed that there was no effect. Since higher quantity of the calcined material application indicates reduction in cost and environmental benignity, the maximum choice was 30RH1.

Figure 4.14 shows the compressive strength results of mortar prepared from cement and calcined clay/maize cob mixtures. The early age strength at 3 days of 10MC1 and 20MC1 were 31MPa and 30MPa, higher than the control mortar which had strength value of

approximately 29MPa whereas that of 30MC1 was also 29MPa similar to the control mortar.

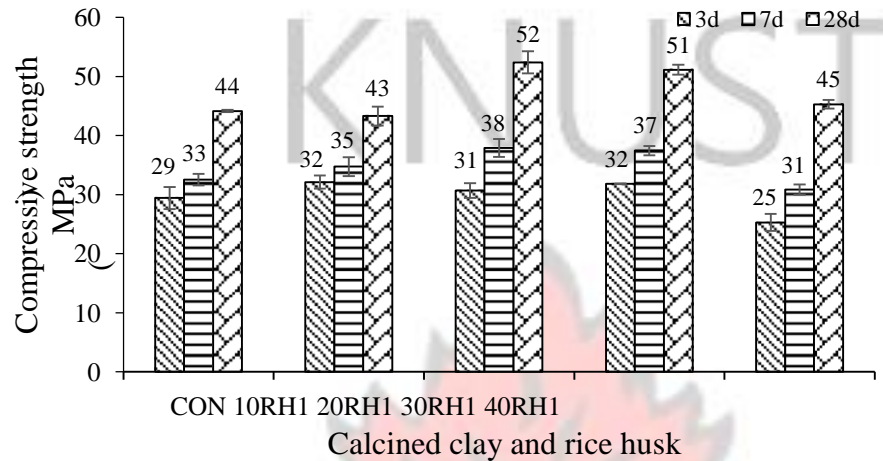


Figure 4.13: Compressive strength of mortar with varying calcined clay/rice husk pozzolan

At 7 days, 10MC1, 20MC1 and 30MC1 attained strength values of 36MPa, 37MPa and 36MPa, respectively, higher than the control mortar. At the 28 days' late age strength, both 10MC1 and 20MC1 had similar strength of 44MPa comparable to the compressive strength value of the control mortar. Compressive strength results of 10MC1 and 20MC1 competed for the choice of maximum strength selection because of the similarities of their strength values. Furtherance to the strength values, a student t-test performed between the two, 10MC1 and 20MC1 had no effect (see appendix 4.3). As already indicated, higher volumes of the calcined materials application for mortar formulation means lower mortar cost and environmental benignity. From this result, the preferred mixture proportion was 20MC1.

Figure 4.15 provides the compressive strengths of mortar prepared from cement and calcined clay/sawdust mixture proportions.

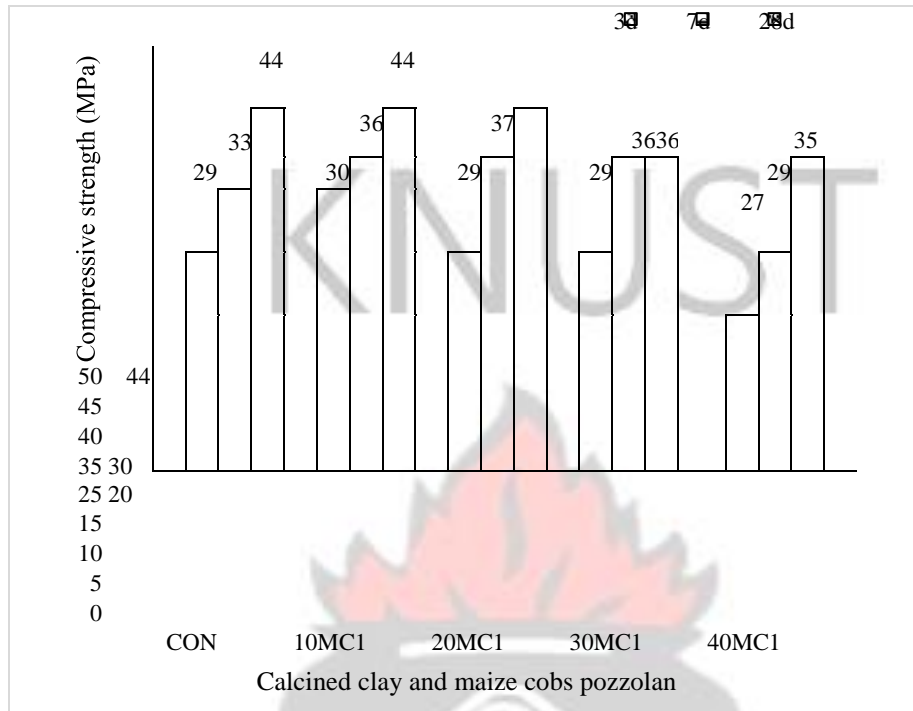


Figure 4.14: Compressive strength of mortar with varying calcined clay/maize cobs pozzolan

The early age strength at 3 and 7 days as well as the late age strength at 28 days of 10SD2, 20SD2 and 30SD2 was higher than the control mortar mix. 20SD2 had the maximum compressive strength at both the early (7 days) and late ages. Based on the results, the preferred maximum strength in this series of mortar was 20SD2.

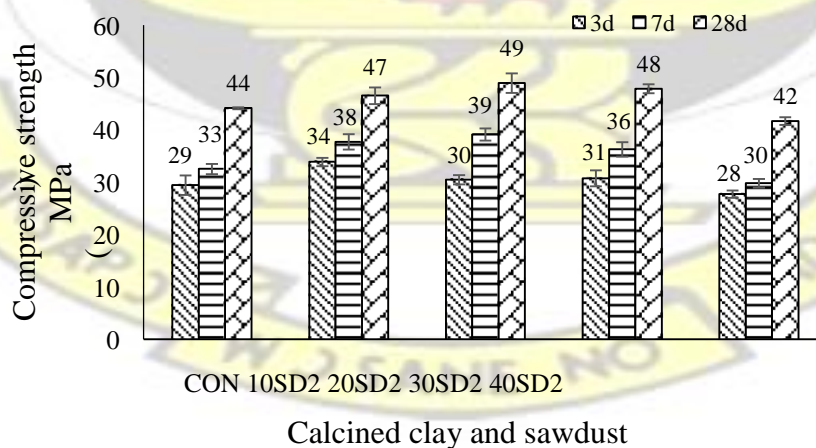


Figure 4.15: Compressive strength of mortars with varying calcined clay/sawdust pozzolan

4.5.1 Comparison of compressive strength of control and optimum mixes

Appendix 4.5 presents a comparative analysis of the compressive strength performance of the various optimum mortar mixes. The figure shows that all optimum mixes attained higher strength at all ages than the control. Analysis of variance (ANOVA) was performed on the strength results and the outcome is shown in Appendix 4.6. The predictive (p) values were approximately 0.08 and 0.000012 for rows (mortar mixes) and columns (curing ages) respectively. The inference that could be drawn from the ANOVA results is that the type of binder does not really matter that much because any of the mortar mixes of any binder type when used give strength values. However, when it comes to strength values or performance with respect to curing ages, the type of mortar used matters i.e very significant. The differences among the various mortar mixes became clearer at 28 days of curing. In this case, mortar mixes were ranked in order of strength performance as curing proceeded. The best performing mix was 30RH1, followed by 20SD2, and then 20PK2 and 20MC1 in that order.

4.6 Consistency and setting times of optimum mixtures

Table 4.5 provides the setting times results of the binders. Each binder paste represents the optimum dosage obtained from the different series of mortars formulated from the combination of cement and calcined clay as well as the various calcined clay/biomass mixture proportions. Water-binder-ratio (w/b) was maintained at 0.305 while an admixture

in a form of polycarboxylate high range water reducer (HRWR) was used to achieve the desired consistency.

The results show that the addition of calcined clay or calcined clay/biomass mixtures to Portland cement increases the amount of HRWR significantly relative to the control. Another observation was that, relative to cement and calcined clay binder paste (20P800), calcined clay/biomass mixture proportions further increased their quantity of HRWR. Calcined clays at temperatures between 600 and 800°C incorporated in cements have been found to increase the surface area in the matrix (Ganesan et al, 2007). The further increase in the quantity of HRWR with calcined clay/biomass mixture proportions relative to 20P800 was most likely as a result of further increase in the porosity of the whole cement matrix system (Sinthaworm & Nimityongskul, 2009). The setting times (initial and final) showed that relative to the control, binder paste incorporated with calcined clay or clay/biomass caused a delay in both setting times. Comparing calcined clay/biomass mixture proportions to calcined clay mixture, the observations were that 30RH1 experienced the most delayed setting times whereas 20SD2, 20PK2 and 20MC1 had faster setting times compared to the control. The delay in setting times of calcined clay pozzolanas as compared to the control paste could be due to the slow nature of the pozzolanic process and the decrease in cement content, the main stiffening agent (Brooks et al, 2000; Fu et al, 2012).

Table 4.5: Setting times of binder paste

Mix Name	w/b	Ad/b (%)	Setting times (mins)	
			Initial	Final
Control	0.305	0	175	215
20P800	0.305	0.32	244	305
30RH1	0.305	0.6	275	309
20SD2	0.305	0.5	220	300

20PK2	0.305	0.467	223	285
20MC1	0.305	0.467	227	277

NB: w/b- water-to-binder ratio; Ad/b- Admixture-to-binder ratio

4.7 Test on hydrated phases

4.7.1 Calcium hydroxide content and degree of pozzolanic reaction

As already mentioned thermogravimetric analyser (TGA) was used to determine the calcium hydroxide (CH) content as well as the degree of pozzolanic reaction which occurred between Portland cement and the calcined products. Table 4.6 presents the CH content of the hydrated paste samples at 3, 7 and 28 days. The CH content in the blended cement paste indicates the degree of cement hydration. From the table, both 20P800 and 20SD2 attained a higher CH content than the control at 3 and 7 days. This indicates that the two materials behaved like fillers and for that matter created nucleation sites for the formation of CH crystals. However, all the mixture proportions had their CH content dropping when compared with the hydrated cement samples (control) at 28 days. This confirmed the work of Malquiro (1960) that stated that at the hardened state of the material (pozzolanic cement), there must be a reduction in CH. The reduction of CH is as a result of the interaction between CH and reactive silicates and aluminates forming calcium aluminosilicates hydrates.

Table 4.6: Calcium hydroxide content of control and hydrated paste samples

Mix name	CH content (%)		
	3d	7d	28d
Con	16	19	20
20P800	23	24	16
20PK2	17	15	16
30RH1	14	15	15

20MC1	18	18	15
20SD2	20	21	17

The degree of pozzolanic reaction involving Portland cement and the calcined products are presented in Figures 4.16-19. The figures indicate the influence of calcined clay/biomass mixtures on cement and clay calcined at 800°C. Generally, the figures showed both negative and positive values on the y-axis. Negative values denoted consumption of CH below the control paste whereas the positive values denoted consumptions above the control paste. Figure 4.16 shows the CH consumption pattern of the control, calcined clay (20P800) and calcined clay/palm kernel shells (20PK2). The CH consumption of 20PK2 peaked at 7 days and remained almost constant to the maximum age of 28 days whereas the calcined clay peaked at the maximum 28 days. This indicated that pozzolanic reaction of 20PK2 occurred earlier than the control and the calcined clay mix (20P800). The pozzolanic reaction was also very high with the inclusion of palm kernel shells to clay than calcined clay. At 28 days, the consumption content of the calcined products was almost the same. This showed that the active phases introduced by PKS ashes were virtually used-up earlier with little remaining at the late age at 28 days. Both calcined products showed a higher consumption of CH content than the control paste at 28 days, a sign of the occurrence of pozzolanic reaction (Lam et al, 2000; Poon et al, 2001).

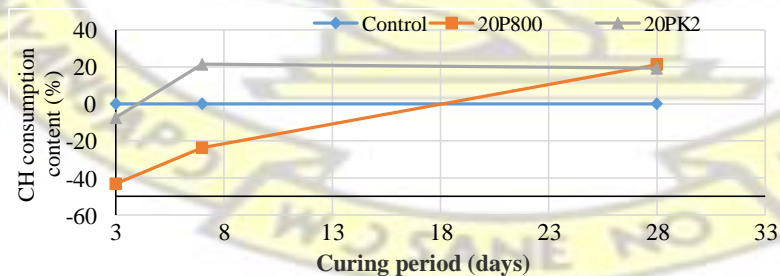


Figure 4.16: CH consumption of control, calcined clay and calcined clay/palm kernel shells

Figure 4.17 shows the CH consumption pattern of the control, calcined clay and calcined clay/rice husk (30RH1). The figure showed that CH consumption by 30RH1 peaked at an early age of 7 days than the calcined clay. The CH consumption of 30RH1 was very high at all ages than the control and the calcined clay. This indicated that pozzolanic reaction was higher with 30RH1. The pozzolanic activity of calcined clay/ rice husk (30RH1) also indicated that the calcined product (30RH1) contained more active pozzolanic phases than the calcined clay therefore making 30RH1 more reactive with Portland cement.

Figure 4.18 shows the CH consumption content of the control, calcined clay (20P800) and calcined clay/maize cob (20MC1). The CH consumed at the early age of 3 days by 20P800 and 20MC1 were lower than the control paste. This meant that the two materials introduced a filler effect to the cement matrix.

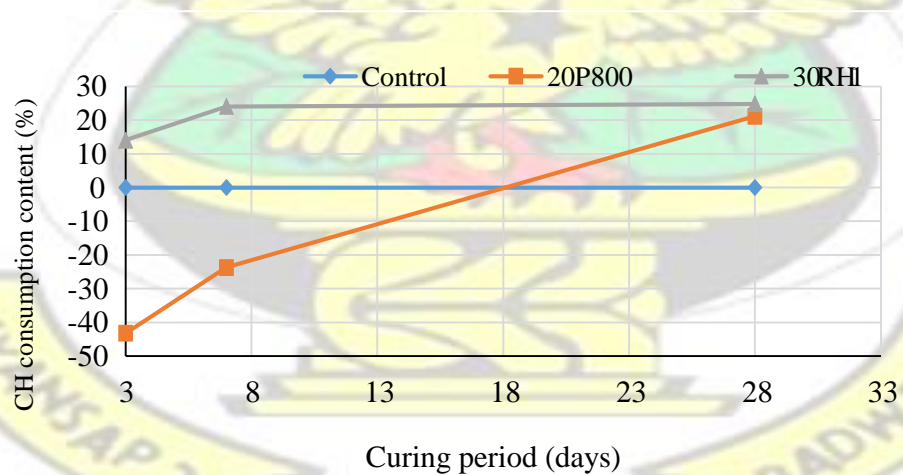


Figure 4.17: CH consumption of control, calcined clay and calcined clay/rice husk.

The filler effect improves strength, a more reason why the 20MC2 attained higher strength at the early 3 than the control. However, 20MC2 showed a high degree of pozzolanic reaction than 20P800 at the 3 days. At 7 days, there was a higher degree of pozzolanic reaction of 20MC1 than the control and 20P800. The figure shows that calcined products, 20P800 and 20MC1 attained a higher degree of pozzolanic reaction at the maximum 28 days than the control. However, the degree of pozzolanic reaction still remained higher for 20MC1 as compared to 20P800 and the control paste. This indicated that the amorphous silicate phases from the maize cob ashes were reactive and therefore increased the degree of pozzolanic reaction.

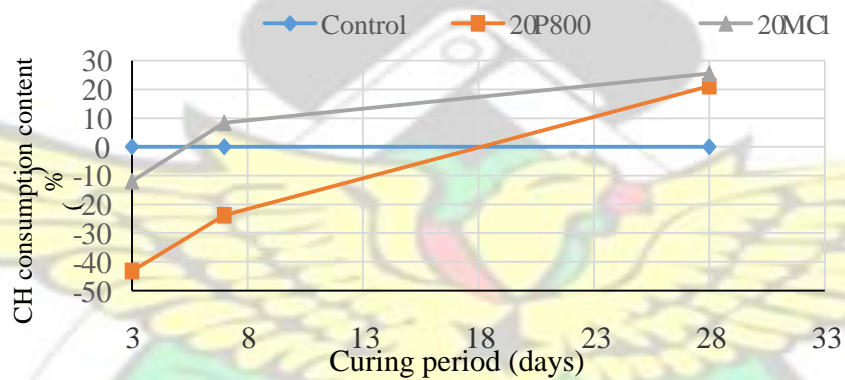


Figure 4.18: CH consumption of control, calcined clay and calcined clay/maize cobs

Figure 4.19 presents the CH consumption content of the control, calcined clay (20P800) and calcined clay/sawdust (20SD2). The figure showed that the trend of CH consumption between 20P800 and 20MC1 were very similar. At 3 and 7 days, the amount of CH consumed by the calcined products was lower than the control paste. This is very typical of pozzolana due to the introduction of filler effect which facilitates early hydration of Portland cement. However, the degree of pozzolanic reaction by 20SD2 was relatively higher than 20P800 at 3 and 7 days. It was seen from the figure that both the calcined

products attained higher degree of fixated CH at the maximum 28 days, an indication of the occurrence of pozzolanic reaction which was shown by the higher CH consumed as compared to the control paste

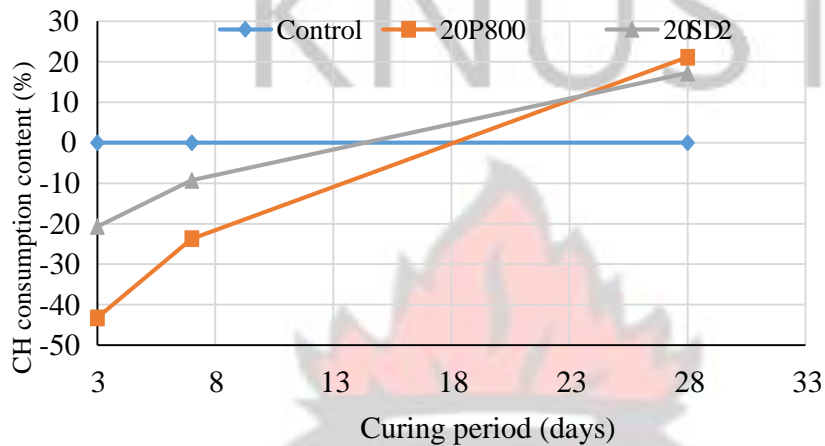


Figure 4.19: CH consumption of control, calcined clay and calcined clay/ sawdust

4.7.2 MAS NMR analysis

4.7.2.1 ^{27}Al and ^{29}Si of cement and calcined products

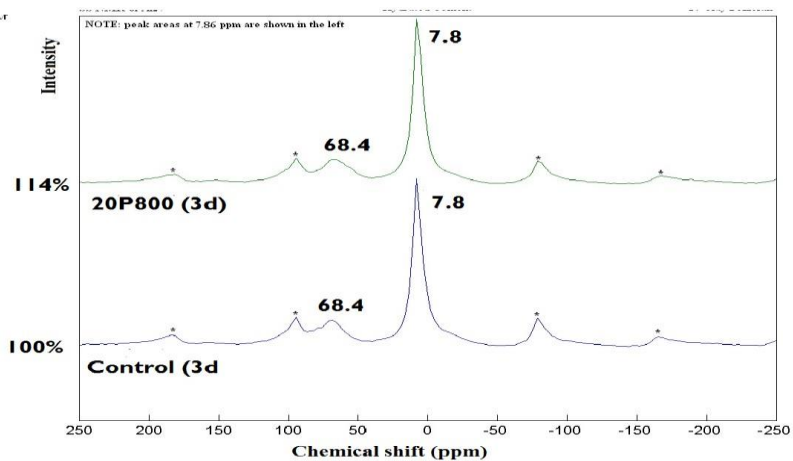
Figure 4.20 (A, B and C) presents the ^{27}Al MAS NMR spectra analysis of cement and calcined clay binders i.e. 20P800 hydrated for 3, 7 and 28 days. Generally, the figures showed two distinct chemical shifts which occurred around 68 ppm and 7.8 ppm. This explained that the aluminate phase shifted from $\text{Al}^{(\text{iv})}$ to $\text{Al}^{(\text{vi})}$ environment which is typical of hydrated binder paste (Brunet et al, 2010). Chemical shift around 68 ppm showed Al substitution in the calcium silicate hydrate (CSH) in the tetrahedral environment of Al, a metastable form of hydrogarnet or calcium aluminosilicate hydrate (CASH) (Anderson et al, 2003; Chenguang et al, 2014). The chemical shift around 7.8 ppm corresponds to thermodynamically stable monosulphates (AFm) which occurred in the $\text{Al}^{(\text{vi})}$ environment (Skibsted et al, 1993; Anderson et al, 2006). As hydration progressed from 3 days to 28

days, the intensities of both the tetrahedral and octahedral Al environment increased progressively. This indicated that the inclusion of calcined clay provided more aluminium phase in the tetrahedral environment that dissolved in the alkaline environment to form a stratlingite (C_2AH_8), a stable monosulphate phase (AFm) containing Si substitution with Al (Skibsted et al, 1993; Anderson et al, 2006). The dissolution process shows the occurrence of pozzolanic reaction. The AFm phase in the tetrahedral Al environment, a metastable state shown in the figure transformed into a well crystalline cubic AFm phase as monosulphates in the octahedral Al environment. The well crystalline cubic AFm phases also increased in intensities with hydration period in the Al octahedral environment. This shows the substitution of Al^{3+} for Si^{4+} to form calcium aluminosilicate hydrates. Chenguang et al (2014) mentioned that Al^{3+} substitution for Si^{4+} promotes the stability of calcium silicate hydrates. The increase in stable compound in the aluminate phases in the CSH structure explained the reason for the high strength of 20P800 more than the control (CON). Similar trends were seen with the mixtures between cement and calcined clay/biomass mixtures shown in Figures 4.21 to 4.24. Figure 4.21 (A-C) presents the ^{29}Si MAS NMR spectroscopy of Portland cement and calcined clay (20P800) hydrated for 3, 7 and 28 days. At 3 days (Figure 4.21A), both spectra shown represented hydrated samples of the control (CON) and Portland cement and calcined clay (20P800). Both spectra showed a chemical shift at -89.7 ppm and 109.1 ppm. The shift at -89.7 ppm could indicate partly a Q^2 and Q^3 (1Al) unit confirming the studies of Xiaoming et al (2011). At this chemical shift Al entered the CSH structure forming an aluminium rich compound called gehlenite (Poulsen, 2009). The incorporation of calcined clay in Portland cement partially responded to pozzolanic

reaction after 3 days which is indicated as a slightly intensified peak on the 20P800 spectra.

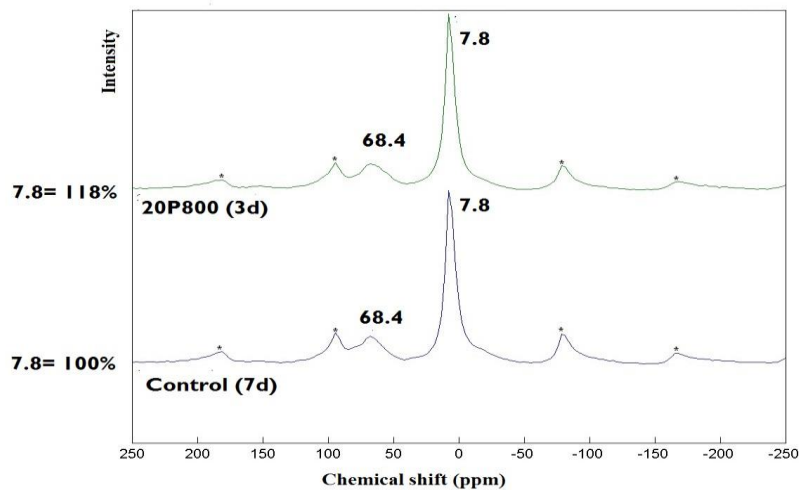
At 7 days (Figure 4.21B), the two spectra of CON and 20P800 showed a chemical shift at

-90.7 ppm
ppm.



and -109.1

A



B

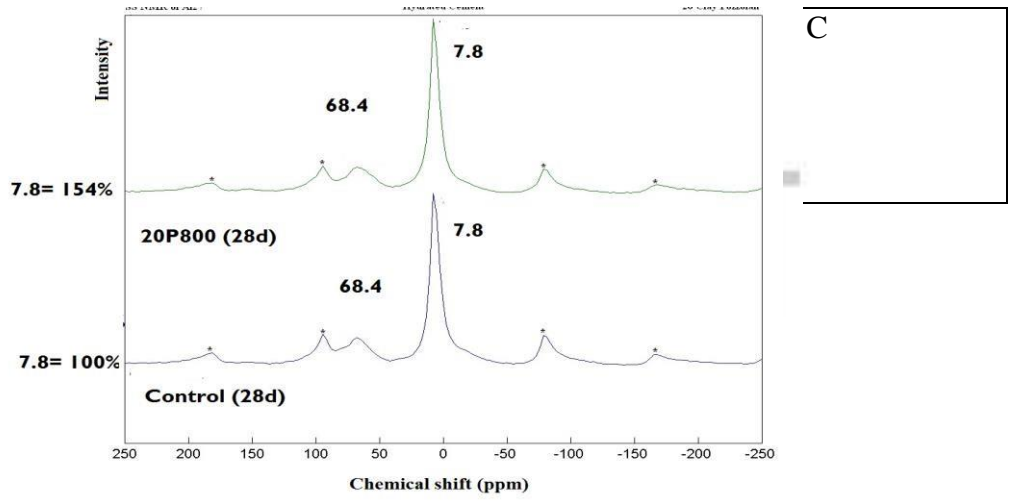
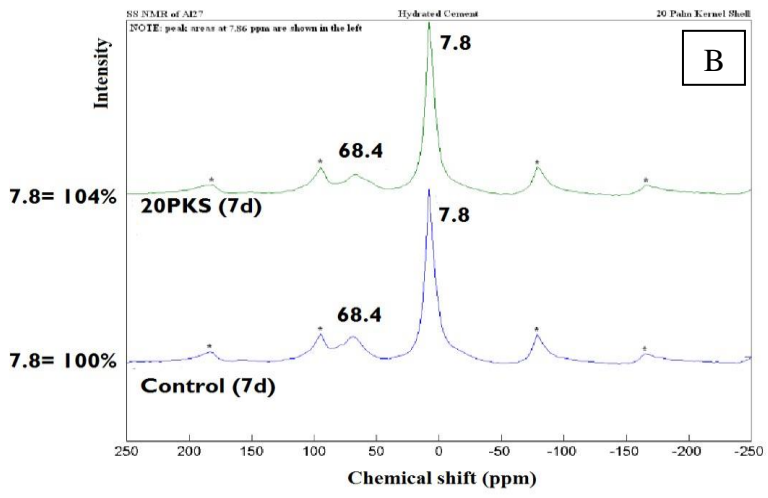
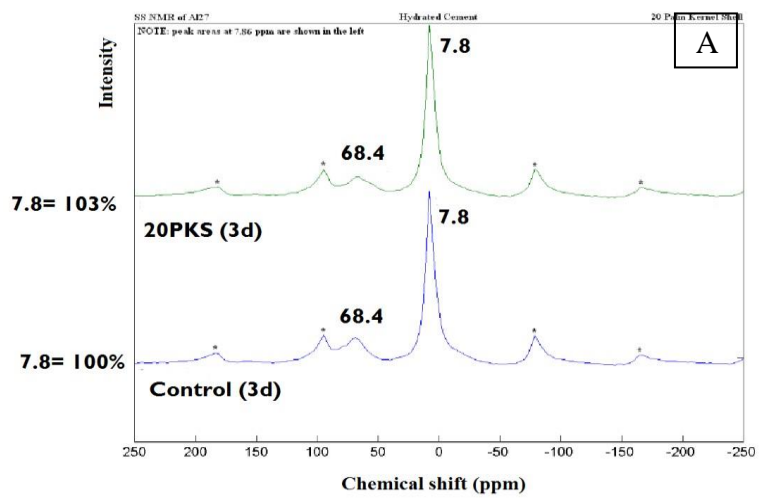


Figure 4.20 ^{27}Al MAS NMR spectra of hydrated cement and cement/ calcined clay paste; A-3 days, B- 7days, C- 28 days.



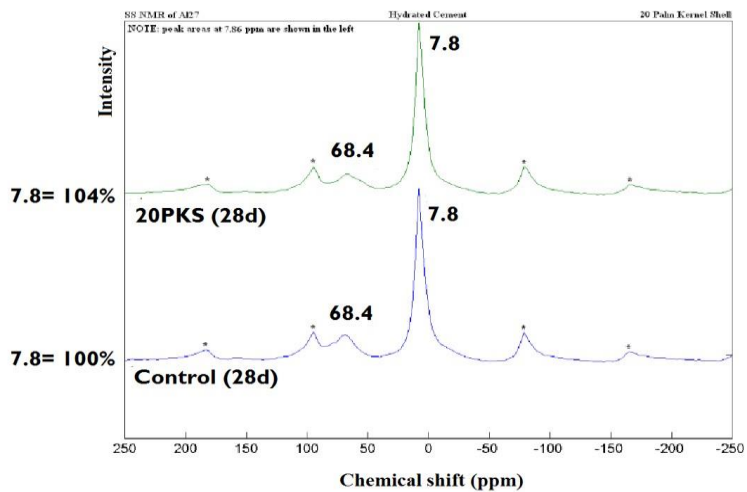


Figure 4.21 ^{27}Al MAS NMR spectra of hydrated cement and cement/ calcined clay and palm kernel shells paste; A-3 days, B- 7days, C- 28 days.



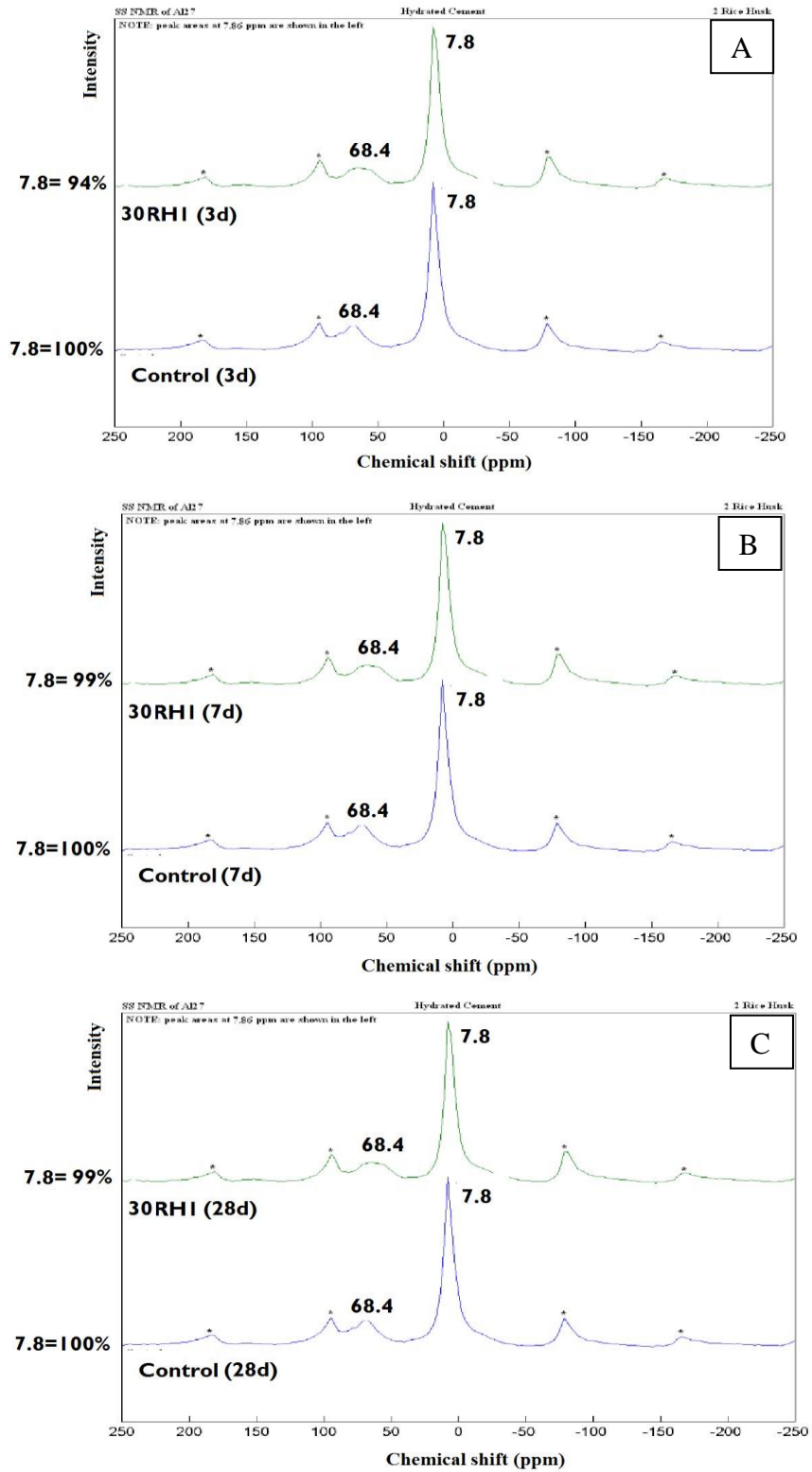


Figure 4.22 ^{27}Al MAS NMR spectra of hydrated cement and cement/ calcined clay and rice husk paste; A-3 days, B- 7days, C- 28 days.

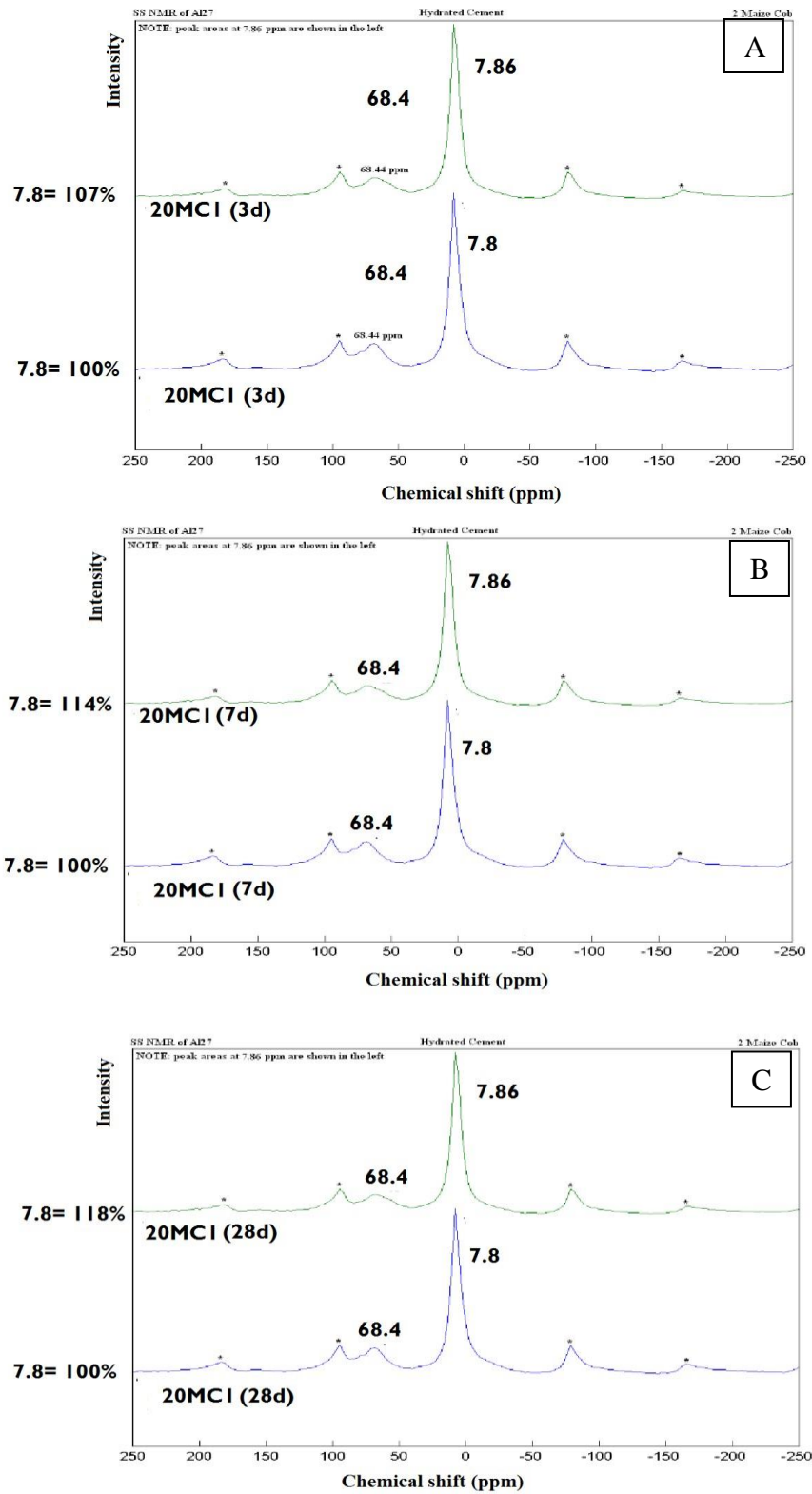


Figure 4.23 ^{27}Al MAS NMR spectra of hydrated cement and cement/ calcined clay and maize cob paste; A-3 days, B- 7days, C- 28 days.

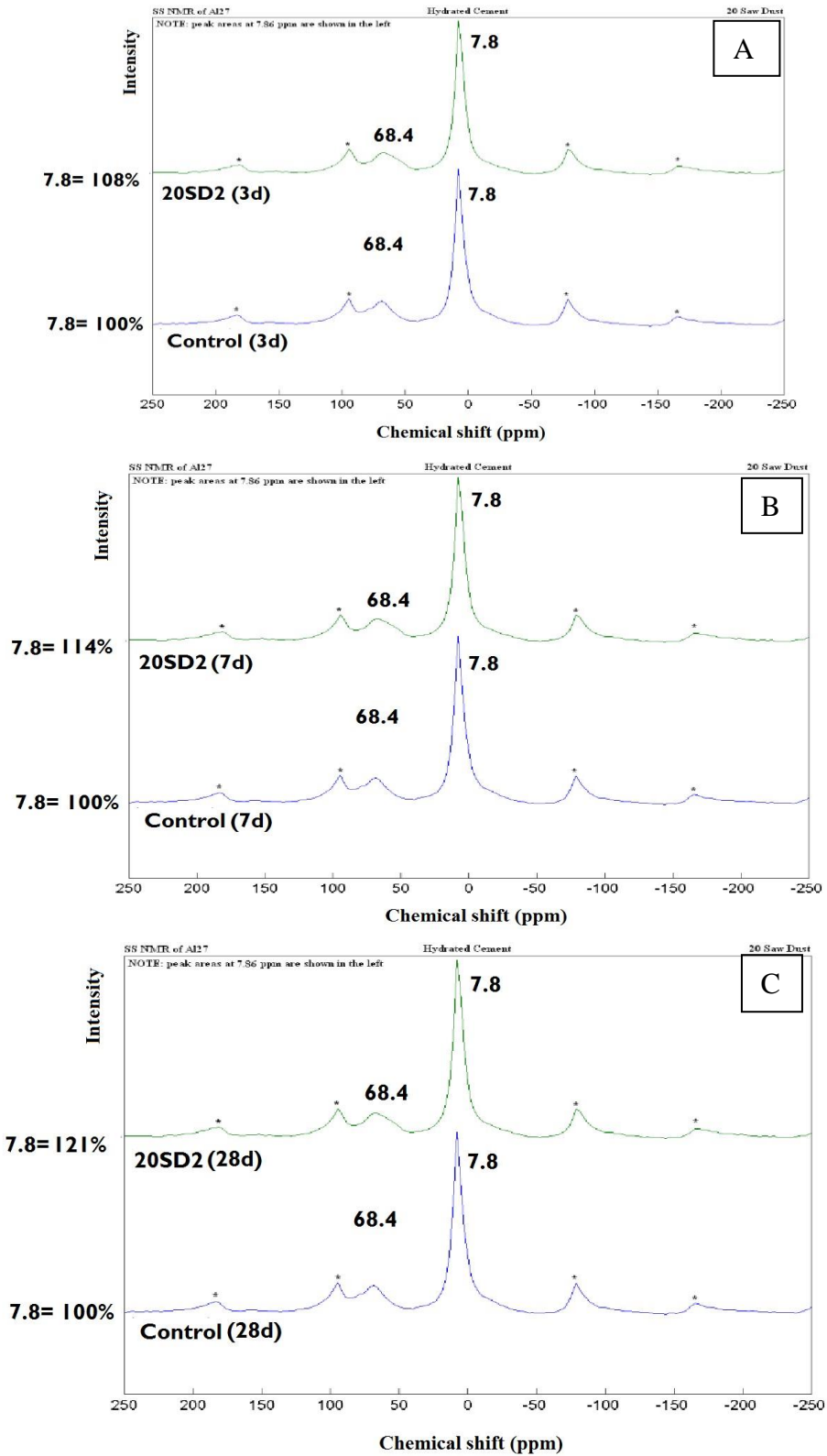


Figure 4.24 ^{27}Al MAS NMR spectra of hydrated cement and cement/ calcined clay and sawdust paste; A-3 days, B- 7days, C- 28 days.

The figure showed a slight chemical shift from -89.7 ppm at 3 days to -90.1 ppm at 7 days which is indicative of an increase polymerization with time. 20P800 spectrum showed the formation of an additional peak at -109.1 ppm which could be attributed to the effect of pozzolanic action.

After 28 days' hydration, there was a slight shift from -90.1 ppm at 7 days to -89.7 ppm (see Figure 4.21C). This indicates a decrease in the crystallinity of CSH content in the Q2 and Q3 units. The increase in polymerization was confirmed with the slight shift from 109.1 ppm at 7 days to -109.5 ppm at 28 days on the CON spectrum. The chemical shift from -109.1 ppm at 7 days to -112.3 ppm at 28 days as well as the formation of an additional chemical shift at -122.8 (Q4(01Al) unit confirmed that the addition of calcined clay to cement caused a significantly enhanced polymerized material. This also shows that pozzolanic reaction occurred and caused an increased strength of 20P800 more than the control. The formation of polymerized substance that impacted on the strength and durability properties of 20P800 could be used to explain the hydrated products formed from Portland cement and calcined clay/ palm kernel shells (20PK2), calcined clay/ rice husk (30RH1), calcined clay/ maize cob (20MC1), calcined clay/ sawdust (20SD2). The results of their MAS NMR are shown in appendix 4.6-9.

4.8 Durability studies

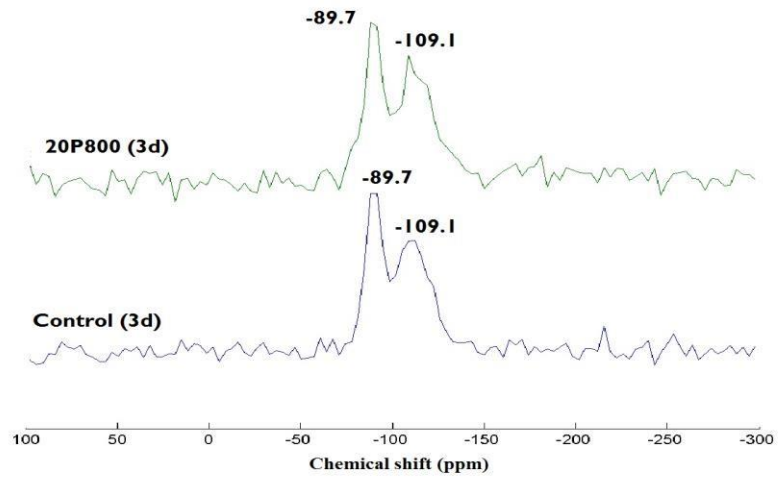
4.8.1 Shrinkage

Figures 4.26-29 present the shrinkage results for both total and autogeneous shrinkage of unblended and blended cement mortar mixtures. The figures show a comparison of the calcined clay/biomass mortar mixtures with the control and calcined clay mortar mixtures.

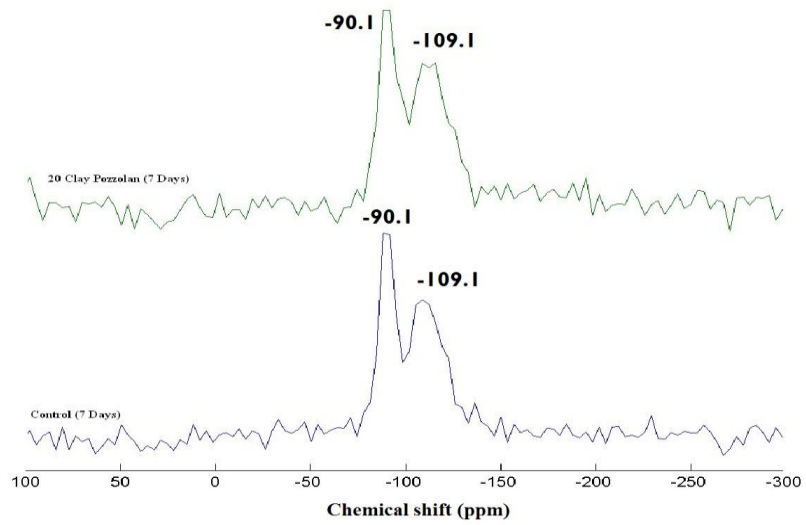
The general trend as indicated from the results show that total shrinkages had higher strain values than that of autogenous shrinkage.

Figure 4.26 presents the shrinkage results of calcined clay/palm kernel shells mortar mixtures compared with the control and calcined clay mortars. The autogenous shrinkage indicated similar trends at the 1 day and 3 days. However, at 4 days, 20P800 showed a more restrained autogenous shrinkage results than CON and 20PK2 mortars.

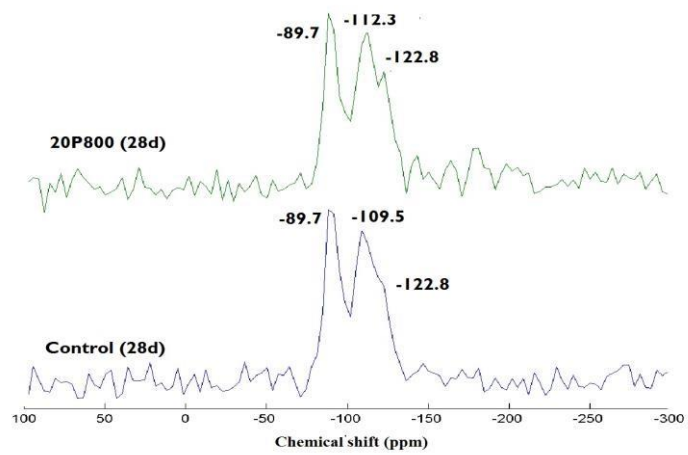
After 4 days, the trend was not significantly different among the three mortars, CON, 20P800 and 20PK2 (see appendix 4.7). The autogenous shrinkage performance of 20P800 at 4 days could probably be attributed to the formation of extra hydrates more than CON and 20PK2. Gleize et al (2007) and Itim et al (2011) have pointed out that formation of hydrates makes the product less porous, rigid and less deformable. The total shrinkages of the mortar mixtures, CON, 20P800 and 20PK2 remained almost the same between 1 and 7 days. After 7 days, the total shrinkage of 20PK2 was again not statistically significant from that of CON and 20P800 mortar specimens (see Appendix 4.5). The results indicated that palm kernel shells inclusion in calcined clays after 4 days behaved the same as the unblended cement and calcined clay/cement mortars. Figure 4.27 presents the shrinkage results of calcined clay/rice husk (30RH1) mortar mixture and that of the control (CON) and the calcined clay (20P800) mortars. At the fourth day of exposure, both 30RH1 and 20P800 exhibited significantly more restrained autogenous shrinkage than the control (CON). This behavior of the mortars at the fourth day probably indicated formation of additional hydrating compounds which increased the pore relative humidity (Gleize et al, 2007; Itim et al, 2011).



A



B



C

Figure 4.25: ^{29}Si MAS NMR spectra of hydrated cement and cement/ calcined clay paste; A-3 days, B- 7days, C- 28 days.

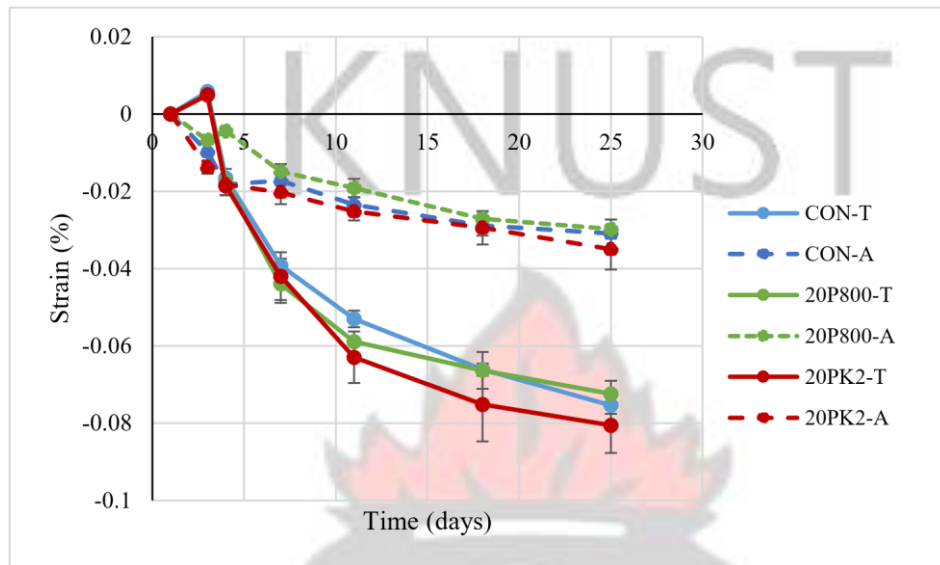


Figure 4.26: Average measured total and autogenous shrinkages of CON, 20P800 and 20PK2 mortars

Autogeneous shrinkages regarding the three mortar mixtures after the fourth day weren't significantly different from each mortar mixture with respect to the period of exposure.

The trend for total shrinkage as shown in Figure 4.27 showed that there wasn't any significant effect with respect to the type of mortar mixture.

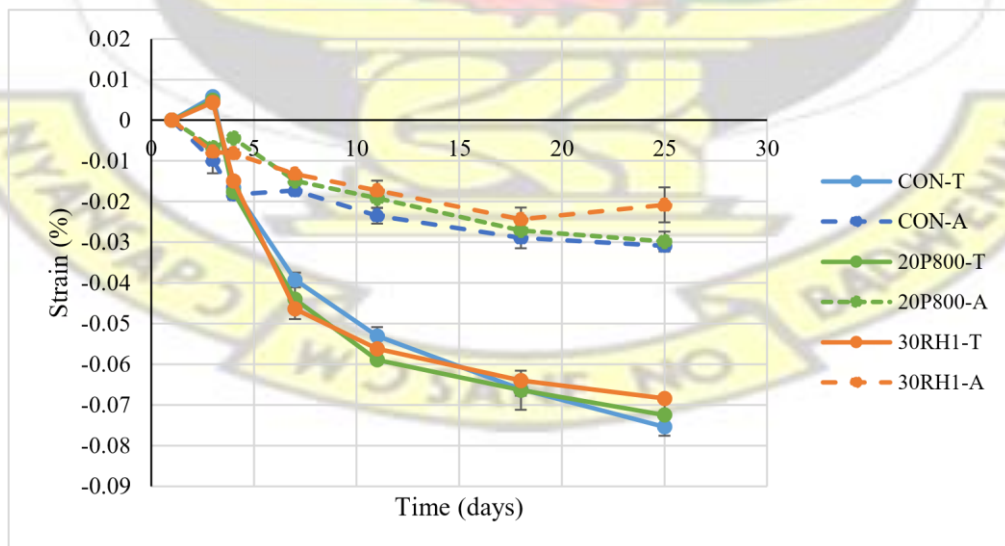


Figure 4.27: Average measured total and autogenous shrinkages of CON, 20P800 and 30RH1 mortars

Figure 4.28 presents the autogenous and total shrinkage of calcined clay/ maize cob (20MC1) compared with the control (CON) and calcined clay (20P800) mortar mixtures. Both autogenous and total shrinkages showed no significant effect among the mortar mixtures throughout the periods of exposure. This indicates that maize cob addition has little influence on calcined clay pozzolana with respect to shrinkage.

Figure 4.29 shows the autogenous and total shrinkage properties of calcined clay/sawdust mortar mixtures compared with CON and 20P800. The results show that 20SD2 had autogenous and total shrinkage values that were not statistically different from CON and 20P800. This indicates shrinkage properties are not very much affected by the addition of sawdust in a co-fired clay and sawdust pozzolan.

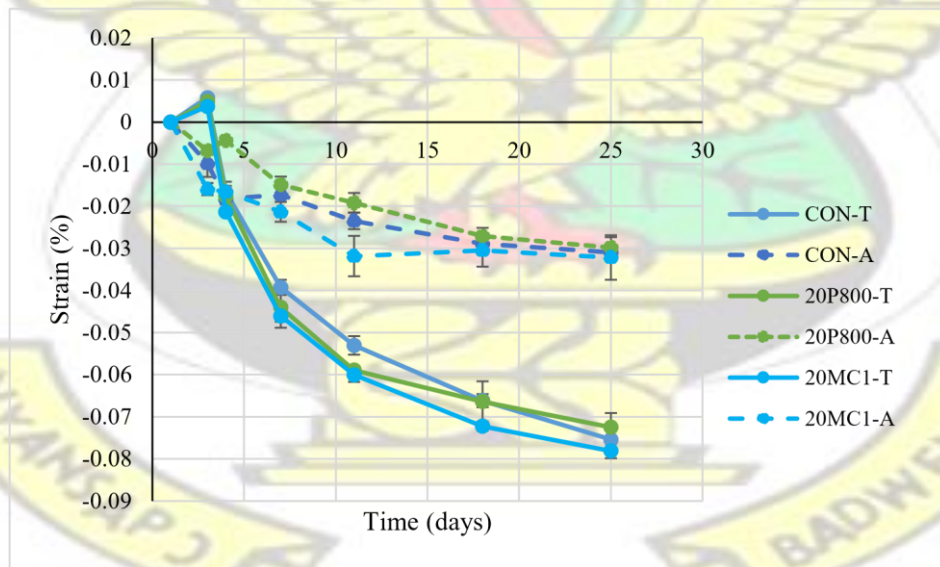


Figure 4.28: Average measured total and autogenous shrinkages of CON, 20P800 and 20MC1 mortar prisms

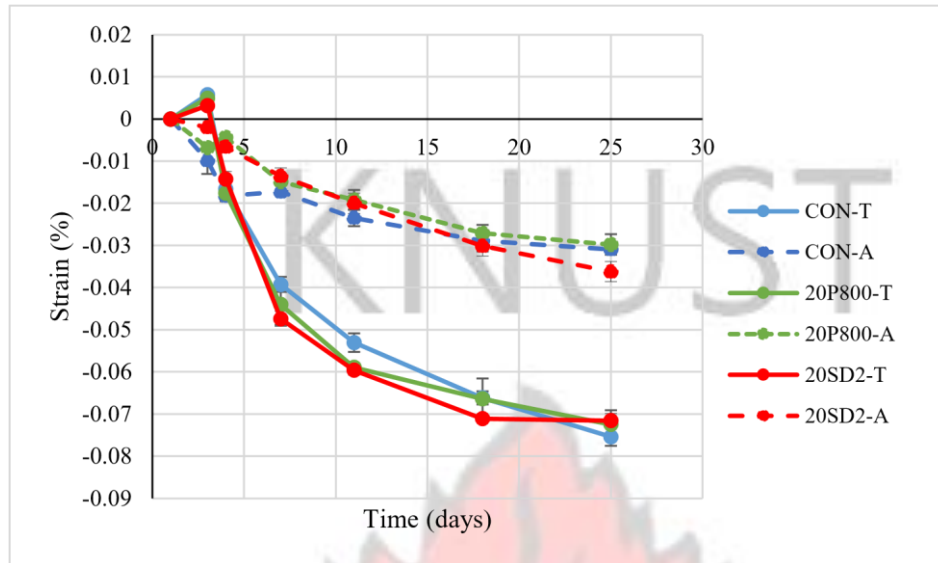


Figure 4.29: Average measured total and autogenous shrinkages of CON, 20P800 and 20SD2 mortar prisms

The results from the Figures 4.26-29 showed that almost all the biomass materials had little influence on calcined clay pozzolan in terms of shrinkage (autogeneous and total).

Many authors including Kosmatka and Wilson (2011), Tam et al (2012) and Kara et al (2014) have argued that sometimes the trend of hydration could be studied using shrinkage, however the trend of these results proved otherwise. These results suggest that shrinkage alone may misinform hydration trend unless there is corroboration with other parameters including strength and probably sorptivity.

4.8.2 Water Sorptivity

Figures 4.30-33 presents the sorptivity performance of calcined clay/ biomass pozzolan compared to the performance of the control mortar and calcined clay. It has already been stated in the literature that the slope of the linear part of the graph of i versus $t^{1/2}$ provides

information on Sorptivity (Sabir et al, 1998). The greater the slopes of the regressed graph the greater the ingress of ions through concrete.

Figure 4.30 provides the sorptivity of calcined clay/palm kernel shells (20PK2) compared with control (CON) and calcined clay (20P800). The initial sorptivity of 20PK2 was 0.0074, which is lower than 0.0107 for CON, however higher than 0.0028 for 20P800. The secondary sorptivity for 20PK2 was 0.0009, lower than the 0.0017 of CON but higher than that for 20P800 which was 0.0008. The results of the initial (S_i) and the secondary (S_s) sorptivity indicated that the addition of palm kernel shells had effect on sorptivity of calcined clays. The palm kernel shells addition raised the ingress of ions compared to calcined clay mortar. The reason could be attributed to the introduction of less reactive crystalline compounds from PKS calcined at 800°C into calcined clays (see Figure 4.1A). However, with respect to CON, there was a significant pore refinement of 20PK2 mortars which led to the decrease in sorptivity. This trend of pore refinement also influences the compressive strength of 20PK2 compared to CON which is shown in Figure 4.8.

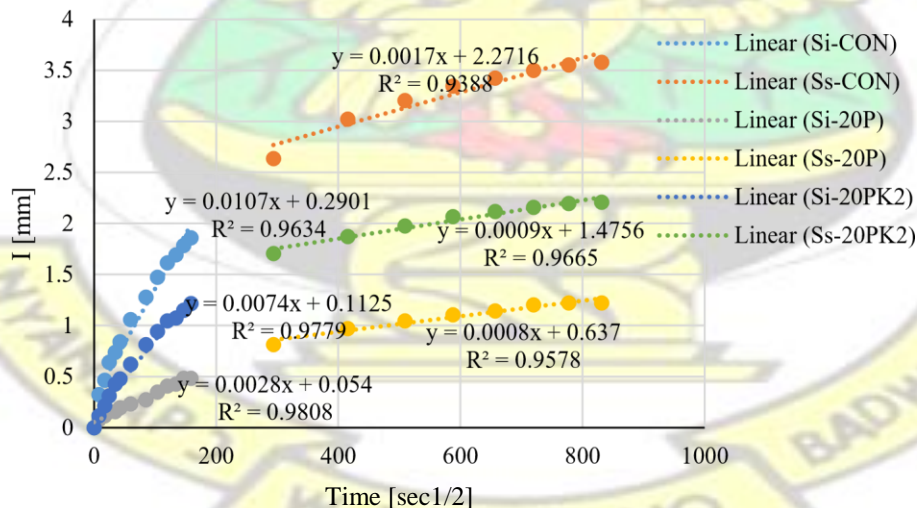


Figure 4.30: Sorptivity of control, calcined clay and calcined clay/palm kernel shells pozzolan mortars

Figure 4.31 provides the sorptivity of calcined clay/rice husk pozzolan compared with the control and calcined clay mortars. The initial and secondary slope values of 30RH1 were 0.0021 and 0.0007 respectively. Both values were significantly lower than CON ($S_i=0.0107$; $S_s=0.0017$) and 20P800 ($S_i=0.0028$; $S_s=0.0008$). The results indicated that addition of rice husk had a positive influence on pore size refinement thereby reducing sorptivity. These results further show that the composition of calcined rice husk at 800°C (see Figure 4.1B) were very reactive and improved the reactive phases in the calcined clay. This is also proven from the AI MAS NMR studies particularly at 28 days of curing which showed a high content of condensed hydrated products (see Figure 4.23A-C).

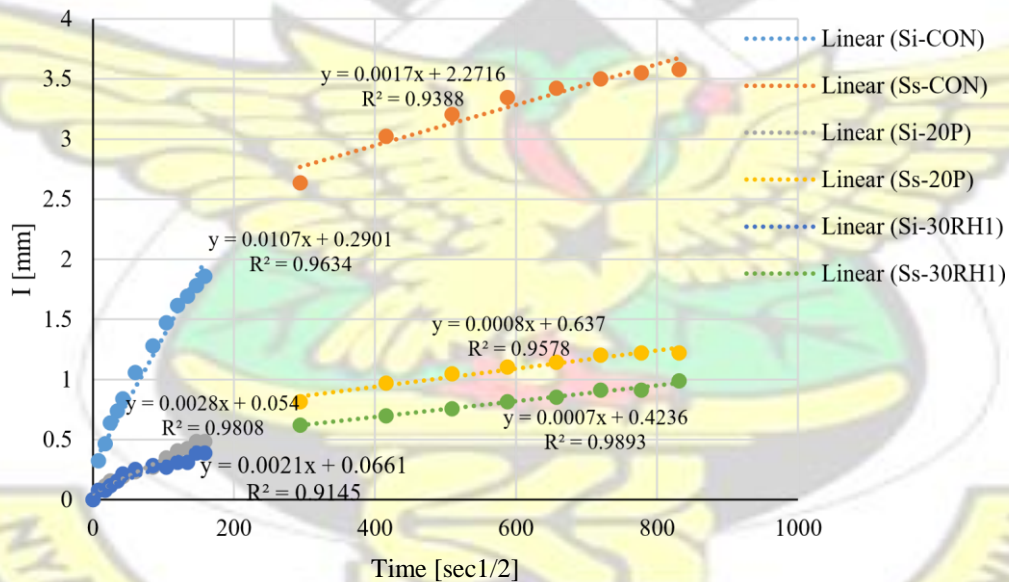


Figure 4.31: Sorptivity of control, calcined clay and calcined clay/rice husk pozzolan mortars

Figure 4.32 presents the sorptivity of calcined clay/maize cob pozzolan compared with the control and calcined clay pozzolan. Sorptivity, initial and secondary values of calcined clay/maize cob pozzolan (20MC1) were 0.0052 and 0.0009 respectively. These values were

higher than that for the calcined clay (20P800) but lower than control mortar (CON). The sorptivity performance of 20MC1 indicated that the extent of pore refinement due to pozzolanic activity was significant with respect to CON. However due to less reactive crystalline phases (see Figure 4.1C), reactivity of calcined clays was inhibited through the addition of maize cob hence affecting ion ingress through the mortar medium.

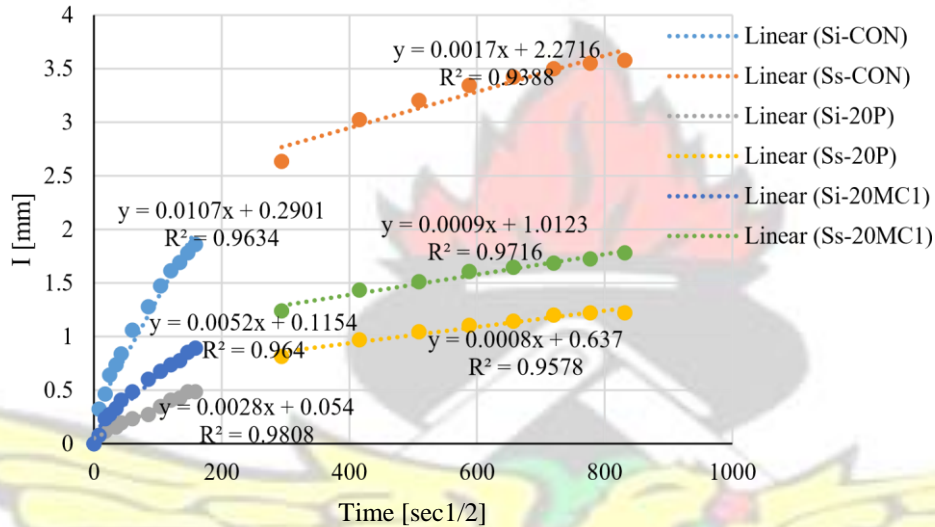


Figure 4.32: Sorptivity of control, calcined clay and calcined clay/maize cob pozzolan mortars

Figure 4.33 showed the the sorptivity of calcined clay/sawdust pozzolan compared with the control and calcined clay pozzolan mortars. The initial and secondary sorptivity values of 20SD2 were 0.0022 and 0.0005 respectively. These values were lower than the sorptivity value of 20P800 and the control indicating a higher resistance to the ingress of ion than 20P800 and CONT. This behavior of 20SD2 could be attributed to the high polymerized materials formed as indicated from the Al MAS NMR studies (see Figure 4.25A-C).

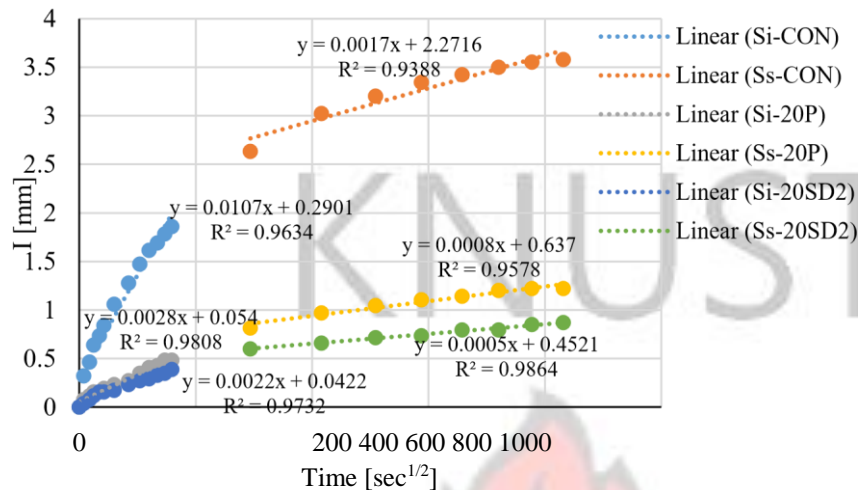


Figure 4.33: Sorptivity of control, calcined clay and calcined clay/sawdust pozzolan mortars

4.9 Sustainability analysis

It has already been indicated earlier that developments that embrace the principles of the triple bottom line (TBL) which include economics, environment and society usually fall in line with sustainability concept.

The sustainability analysis for this study assumed the following

1. Estimated annual consumption of cement as 4 million tonnes in Ghana as of 2014 (Global cement report, 2013)
2. A replacement proportion of cement by calcined products based on the annual consumption.
3. The average inflation rate as of April 2014 was 16.0%.
4. An ex-factory price of GHc28.00 per 50 kg bag of cement hence GHc560.00 per ton
5. An ex-factory price of GHc15.00 per 50 kg bag of calcined clay pozzolan hence GHc300.00 per ton.

6. An average amount of \$9.91 per ton is spent on solid waste collection by city authorities (Anon, 2010).
7. A tonne of cement consumed is to 1 tonne of CO₂ released in the atmosphere
8. A tonne of SCM consumed released approximately 0.4 tonnes CO₂ in the atmosphere (Smith, 2013)

Table 4.7 presents the consumption pattern of cement and supplementary cementitious materials (SCM) based on the assumed annual consumption of cement. The introduction of SCMs would reduce the quantity of cement consumption annually. The table shows that SCMs utilization introduces a volume increase between 28% and 57% compared to the same weight of cement. This indicates that given the same weight of Portland cement and blended cement incorporated with SCM, the SCM will cover more concrete or mortar works than Portland cement.

Table 4.8 shows the estimated cost and savings expected to gain from the use of SCMs in Ghana. The utilization of any of the SCMs in Portland cement would lead to a cost gain ranging between GHc208 Million and GHc312 Million which represent 9% and 14%.

Table 4.9 shows the consumption of calcined clay and biomass based on the annual consumption of Portland cement. The table showed that an SCM containing any of the biomass products could lead to a cost saving between \$0.12 Million and \$1.59 Million.

Table 4.10 shows the estimated amount of carbon emission of the baseline cement consumption and the cement containing the calcined materials. The table shows that the utilization of blended cement components could reduce carbon emission between 12% and 16%. This gives environmental sustainability credence to the project.

Table 4.7: Estimated annual Portland cement and SCM consumption

Mix name	Cement consumption (Million Tons)	SCM consumption (Million Tons)	(m ³)		% Total Volume change
			Volume	Total Volume (m ³)	
Control	4.0	0.0	1269841	1269841	0%
20P800	3.2	0.8	606061	1621934	28%
20PK2	3.2	0.8	647249	1663122	31%
30RH1	2.8	1.2	1102941	1991830	57%
20MC1	3.2	0.8	722022	1737895	37%
20SD2	3.2	0.8	728597	1744470	37%

NB: Total volume= the volume of cement and SCM

Table 4.8: Estimated cost of cement and SCM consumption

Mix name	Cost of cement consumption (Million GH¢)	Cost of SCM utilization (Million GH¢)		Total cost (Million GH¢)	Savings (Million GH¢)	% savings
		PK2	RH1			
Control	2240	0	0	2240	0.00	0%
20P800	1792	240	0	2032	208.00	9%
20PK2	1792	240	0	2032	208.00	9%
30RH1	1568	360	0	1928	312.00	14%
20MC1	1792	240	0	2032	208.00	9%
20SD2	1792	240	0	2032	208.00	9%

Table 4.9: Estimated annual consumption of calcined clay and biomass

Mix name	Calcined clay (Million-Tonnes)	Biomass Consumption (Million tonnes)				Biomass consumption (m ³)	Cost savings (million\$)
		PK2	RH1	MC1	SD2		
Control	0.00	0.000	0.000	0.000	0.000	0	0.00
20P800	0.80	0.000	0.000	0.000	0.000	0	0.00
20PK2	0.64	0.160	0.000	0.000	0.000	177,778	1.59
30RH1	1.18	0.000	0.024	0.000	0.000	150,000	0.24
20MC1	0.78	0.000	0.000	0.016	0.000	61,538	0.16
20SD2	0.79	0.000	0.000	0.000	0.012	57,143	0.12

Table 4.10: Estimated annual carbon emissions

Carbon emission

Mix name	Cement (MT)	Calcined material (MT)	Total emission (MT)
Control	4.0	0.00	4.0
20P800	3.2	0.32	3.5
20PK2	3.2	0.32	3.5
30RH1	2.8	0.48	3.3
20MC1	3.2	0.32	3.5
20SD2	3.2	0.32	3.5



CHAPTER FIVE

5.0 CONCLUSION AND RECOMMENDATIONS 5.1 Conclusion

The following conclusions are made based on the results and discussion of the studies and they are:

1. The optimum temperature of clay calcined from 600-1000°C that achieved the maximum strength activity was at 800°C. This was attributed to the complete dehydroxylation indicated on the TGA graph, the achievement of amorphous structure shown on the X-ray diffraction pattern and the increased intensity of ^{29}Si as detected by the MAS NMR.
2. The agriculture biomasses, palm kernel shells (PKS), rice husk (RH), sawdust (SD) and maize cob (MC) calcined at 800°C which was the optimum temperature for thermally activated clay yielded various forms of crystalline compounds indicated qualitatively by the XRD studies. This shows that the 800°C temperature for the pyro-processing of clay and biomass mixtures was too high for the biomass materials and thus impact negatively on the degree of amorphousness of the agriculture biomasses, a major boost for reactive silica component of calcined clay. Crystalline compounds generally inhibit pozzolanic reaction of calcined clays and are even worse when their presence is very high.
3. Calcined clay materials above 800°C indicated a reduction in the content of the superplasticizer or the high range-water reducer (HRWR). This was due to the formation of crystalline structures when clay is calcined at higher temperatures. Temperatures from 900°C to 1000°C rendered the calcined clay materials less porous.

4. Portland cement and calcined clay mortar mixture that yielded optimum compressive strength was obtained at 20% replacement of cement with clay calcined at 800°C.
5. The optimum strength activity index and replacement value for calcined clay/palm kernel shells were 20% content of the shells and 20% cement replacement, that for rice husk mix was 2% rice husk content and 30% cement replacement, maize cob mix was 2% content and 20% cement replacement and that for saw dust mix was 1.5% content and 20% cement replacement.
6. The clay obtained from Nyamebikyere was confirmed as a 1:1 kaolinitic type and clay minerals formed were obtained from the earth crust. This was confirmed using the MAS NMR.
7. The higher content of polymerized phases that occurred with Portland cement and calcined products resulted in more enhancement of strength of the cement and calcined product mixtures than Portland cement only.
8. The percentage lime (CH) content generated from Portland cement in the blended cement system between Portland cement and the calcined clay products generally reduced at the hardened state (28 days of curing) of the blended cements compared to the unblended cement system. This confirmed the occurrence of pozzolanic reaction.
9. The degree of pozzolanic reaction of calcined clay/rice husk was much higher than the calcined clay pozzolan at all periods of curing. This indicated that calcined rice husk introduced more pozzolanic active phases to the calcined clay therefore fixing a higher percentage of calcium hydroxide.

10. The degree of pozzolanic reaction of calcined clay/palm kernel shell mixtures occurred much more quickly than the calcined clay system. However, the amount of pozzolanic active phases of calcined clay/palm kernel shell system disappeared before (used-up at the early ages) the maximum age of 28 days and therefore had similar CH consumption pattern like the calcined clay.
11. The degree of pozzolanic reactions of calcined clay/maize cobs and calcined clay/sawdust were much lower compared to the control cement system. However, the fixated lime content surged up compared to the control and was almost similar to the calcined clay pozzolan at the maximum 28 days.
12. The shrinkage properties of Portland cement and the blended cement materials were not very significant and therefore shrinkage investigation cannot be used as a criterion to study degree of hydration and pozzolanic reaction in such type of investigations.
13. The influence of the biomasses on calcined clay in terms of shrinkage, both total and autogeneous were generally not statistically significant therefore shrinkage investigations cannot be a sole indicator for studies on degree of hydration and pozzolanic reaction.
14. The calcined clay and biomass products generally enhanced the pore structure refinement of Portland cement which has a positive bearing on the durability of blended cements.
15. Sorptivity characterization could be a good analytical tool to analyze the durability of calcined products on Portland cement.
16. The use of SCMs could reduce the amount of cement utilization in the country and save between 9% and 14% of the total cement cost annually.

17. The use of SCM could reduce carbon emission by between 12% and 16%, a major boost for environmental sustainability.
18. Supplementary cementitious materials utilization in Ghana could be a means to reduce the cost of solid waste collection by city authorities. The cost reduction is estimated between \$0.12 million and \$1.59 million depending on the type of biomass utilization.

5.2 Recommendations

From the study, the following recommendations are made:

1. A study on binary mixture formulations between thermally activated clay and pyrolyzed biomasses could be performed to optimize both materials utilization as supplementary cementitious materials.
2. Though the optimum temperature that achieved maximum strength was at 800°C, other temperatures such as 600°C and 700°C performed appreciably well compared to the control mortar. Studies regarding durability analysis on clay calcined at 600°C and 700°C are recommended since it may help to save energy cost.
3. Investigations into the properties of heat evolution regarding calcined clay/biomass mixtures are highly recommended. This wasn't determined in this study.
4. Investigations into the life cycle analysis (LCA) of the Portland cement containing the calcined materials and Portland cement

5. The study proposes the setting up of a plant for the production of a supplementary cementitious material using clay and biomass which include any of the following: palm kernel shells, rice husk, maize cob and sawdust.



REFERENCES

- Abon-Sekkina, M. M., Issa, R. M., Bastawisy, A. E. D. M., El-Helece, W. A. (2010), Characterization and Evaluation of thermodynamic parameters for Egyptian Heap Fired Rice Straw Ash (RSA), *International Journal of Chemistry* 2, pp 81
- ACI Committee 234 (1996), Guide for the use of silica fume in concrete ACI 234-96, American Concrete Institute, Farmington Hill, Michigan, pp 51
- ACI Committee 232 (1994), Proposed Report: Use of Pozzolana in concrete. *ACI Materials Journal* 91(4), pp 410 – 27
- Adesanya, D. A and Raheem, A. A. (2009), A study of the workability and compressive strength characteristics of corn cob ash blended cement concrete, *Construction and Building Materials* 23, pp 3111 -317
- Agarwal, S. K. (2006), Pozzolanic activity of various siliceous materials, *Cement and Concrete Res.* 36, pp 1735 – 9
- Agarwal, S. K. and Gulati, D. (2006), Utilization of industrial wastes and unprocessed micro-fillers for making cost effective mortars, *Construction and Building Materials*, vol. 20, no. 10, pp 999–1004.
- Al-Amondi, O. S. B. (2002), Attack on plain and blended cements exposed to aggressive sulfate environments, *Cement and Concrete Composites* 24, pp 305 – 316
- Al-Amoudi, O. S., Maslehuddin, M. and Saadi, M. M. (1995), Effect of magnesium sulfate and sodium sulfate on the durability performance of plain and blended cements, *ACI Material Journal* 92(1), pp 15 – 24
- Ali, M.S., Khan, I. A., and Hossain, M. I. (2008), Chemical analysis of ordinary Portland cement of Bangladesh, *Chemical Engineering Research Bulletin* 12, pp 7-10.
- Alonso, C., Fernandez, L. (2004), Dehydration and rehydration processes of cement paste exposed to high temperature environments, *J Mater Sci* 39, pp 3015-3024
- Al-Rawas, A. A. & Hago, A. W. (2006), Evaluation of field and laboratory produced burnt clay Pozzolans, *Applied Clay Science* 31, pp 29 – 35
- AL-Salami, A.E., Morsy, M.S., Taha, S., and Shoukry, H. (2013), Physico-mechanical characteristics of blended white cement pastes containing thermally activated ultrafine nano clays, *Construction and Building Materials* 47, pp 138–145

- Altwair, N. M., Megat Johari, M. A. and Saiyid Hashim, S. F. (2011), Influence of calcinations temperature on characteristics and pozzolanic activity of Palm oil waste ash, *Australian Journal of Basic and Applied Sciences*, 5(11), pp 1010 – 18
- Alwood, J. M., Cullen, J. M., Milford, R. L. (2010), Options for achieving a 50% Cut in industrial emissions by 2050. *Environmental Science & Technology* 44(6), 1888 – 1894
- Alver, B.E., Alver, O. (2012), The investigation of the effect of thermal treatment on bentonites from Turkey with Fourier transform infrared and solid state nuclear magnetic resonance spectroscopic methods. *Spectrochim. Acta A* 94, pp 331–333
- Amin, M.S., Abo-El-Enein, S.A., Abdel Rahman, A., Alfalous Khaled, A. (2012), Artificial pozzolanic cement pastes containing burnt clay with and without silica fume, *J. Therm. Anal. Calorim* 107, pp 1105–1115
- Anand, S., & Sen A. (2000), Human development and economic sustainability, *World Development* Vol. 28(12), pp 2029-49
- Anderson, M. W., Teisl, M. and Noblet, C. (2012), Giving voice to the future in Sustainability: Retrospective assessment to learn prospective stakeholder engagement, *Ecological Economics*, Vol. 84, Scopus, pp 1-6
- Andersen M.D., Jakobsen H.J., Skibsted J. (2006), A new aluminium-hydrate species in hydrated Portland cements characterized by ^{27}Al and ^{29}Si MAS NMR spectroscopy, *Cem Concr Res* 36, pp 3-17
- Andersen M.D., Jakobsen H.J., Skibsted J. (2003), Incorporation of aluminium in the calcium silicate hydrate (C–S–H) of hydrated Portland cements a high field ^{27}Al and ^{29}Si MAS NMR investigation, *Inorg Chem* 42, pp 2280–2287
- Anonymous (1990), Human Development Report, UNDP report, Oxford Printing Press, pp 6-20
- Anonymous (2001), Kaolinite group, U.S Geological Survey- File Report 041
- Anonymous (2010), More local limestone for Ghacem's cement production, *Chronicle newspaper*, Ghana, 12th February
- Anonymous (2010), National Environmental Sanitation Strategy and Action Plan (NESSAP) 2010 – 2015, MWRWH MINT, Ghana
- Anonymous (2011), Agriculture in Ghana, Facts and Figures 2010, Ministry of Food and Agriculture Statistics, Research and Information Directorate (SRID), pp 5-25

Anonymous (2013), Dangote cement to meet most West African demand, Graphic newspaper.

Antiohos, S., Papageorgiou, A., and Tsimas, S. (2006), Activation of fly ash cementitious systems in the presence of quicklime. Part II: Nature of hydration products, porosity and microstructure development, *Cement Concr Res* 36, pp 2123–31.

Arakshita, M., Shama, Y. K. and Naik, D. V. (2012), Blending optimization of Hempel distilled bio-oil with commercial diesel, *Fuel* 96, pp 264 – 269

Atiemo, E. (2009), Production of pozzolana from some local clays- prospects for application in housing construction, *Journal of Building and Road Research*, Vol 9, pp 34-39

Awal Abdul, A.S.M. and Shehu, I.A. (2013), Evaluation of heat of hydration of concrete containing high volume palm oil fuel ash, *Fuel* 105, pp 728-731

Awal, A.S.M.A. & Nguong, S.K (2010), A short-term investigation on high volume palm oil fuel ash (POFA) concrete: In proceeding of 35th conference on our world in concrete and structures, Singapore

Ayres, R. U., Van den Bergh, J. C. J. M. and Gowdy, J. M. (2001), Strong versus weak sustainability: Economic natural sciences, and consilience: *Environment Ethics*, 28(2), pp 155-168

Badogiannis, E., Kakali, G., Dimopoulou, G., Chaniotakis, E., Tsvivilis, S. (2005), Metakaolin as a main cement constituent: exploitation of poor Greek kaolins, *Cement & Concrete Composites* 27, 197–203

Bao-guo, M.A., Xiao-dong, W., Ming-yuan, W., Jia-jia, Y., Xiao-jin, G. (2007), Drying shrinkage of cement-based materials under conditions of constant temperature and varying humidity, *J China Univ Mining & Technology* 17(3), 0428-0431

Balat, M. and Balat, H. (2009), Recent trends in global production and utilization of bioethanol fuel, *Applied Energy* 86, pp 2273 – 2282

Batterham, R. J. (2003), Ten years of sustainability: where do we go from here, *Chemical Engineering Science* 58, pp 2167-2179

Bediako, M. and Osei Frimpong, A. (2013), Alternative Binders for Increased Sustainable Construction in Ghana—A Guide for Building Professionals, *Materials Sciences and Applications* 4, pp 20-28

Bediako, M., Gawu, S.K.Y. and Adjaottor, A.A. (2012), Suitability of Some Ghanaian Mineral Admixtures for Masonry Mortar Formulation, *Construction and Building Materials*, 29, pp 667-671

Bergmann, J.C., Tupinamba, D.D., Costa, O.Y.A, Almeida, J.R.M., Barreto, C.C., Quirino, B.F. (2013), Biodiesel production in Brazil and alternative biomass feedstocks, *Renewable and Sustainable Energy Reviews*, pp 411-420

Bentz DP, Sato T, de la Varga I, Weiss WJ. (2012), Fine limestone additions to regulate setting in high volume fly ash mixtures. *Cem Concr Compos* 34, pp 11-7

Biricik, H., Akoz, F., Berktaç, I and Tulgar, A. N. (1999), Study of pozzolana properties of wheat straw ash, *Cement and Concrete Res.* 29, pp 637-643

Binici, H., Yuçegök, F., Aksogan, O. and Kaplan, H. (2008), Effect of corn cob, wheat straw, and plane leaf ashes s mineral admixtures on concrete durability, *Journal of Materials in Civil Engineering* 20(7), pp

Bond, A. & Morrison-Saunders, A. (2011), Re-Evaluating Sustainability Assessment: Aligning the Vision and the Practice. *Environmental Impact Assessment Review* 31(1), pp 1-7

Boycheva, S., Zgureva, D., Vassitev, V. (2013), Kinetic and thermodynamic studies on the thermal behavior of fly ash from lignite coals, *Fuel* 108, pp 639 – 646

Brough, A.R., Dobson, C.M., Richardson, I.G. and Groves, G.W. (1996), Alkali activation of reactive silicas in cements: in situ ²⁹Si MAS NMR studies of the kinetics of silicate polymerization, *J. Mater. Sci.* 31, pp 3365–3373.

Brooks, J.J., Megat Johari, M.A. and Mazloom, M (2000), Effects of admixtures on the setting times of high strength concrete, *Cement and Concrete Composites* 22, Elsevier publication, London, pp 293-301

Brooks, J.J. and Johari, M.M.A. (2001), Effect of metakaolin on creep and shrinkage concrete, *Cement and Concrete Composites* 23, pp 495- 502

Brouwers, H. J. H. (2005), The work of Powers and Brownyard revisited: Part 2, *Cement and Concrete* 35, Elsevier, pp 1922 – 1936

Brunet, F., Charpentier, T., Chao, C.N., Peycelon, H., Nonat, A. (2010), Characterization by Solid-state NMR and selective dissolution techniques of anhydrous and hydrated CEM V cement pastes, *Cem Concr Res* 40, pp 208-219

Bullard, J. W. (2008), A determination of hydration mechanisms for tricalcium silicate using a kinetics cellular automation model, *Journal of Ceramic Society* 91, pp 2088 – 2097

- Buchwald, A., Hohmann, M., Posern, K., and Brendler, E. (2009), The suitability of thermally activated illite/smectite clay as raw material for geopolymer binders, *Applied Clay Science* 46, pp 300-304
- Burger, P. & Christen, M. (2011), Towards a capability approach of sustainability, *Journal of Cleaner Production*, Vol. 19(8), pp 787 – 795
- Cabrera, J. & Rojas, M.F. (2001), Mechanism of hydration of the metakaolin-lime-water system. *Cement and Concrete Research* 31, pp 177-182
- Cam, W. C. N. (2013), Fostering interconnectivity dimension of low-carbon cities: the triple bottom line re-interpretation, *Habitat International*, pp 1 – 7
- Castellote, M., Fernandez, L., Andrade, C., Alonso, C. (2009), Chemical changes and phase analysis of OPC pastes carbonated at different CO₂ concentrations, *Mater Struct* 42, pp 515-525
- Cavdar, A. and Yetgin, S. (2010), Investigation of abrasion resistance of cement mortar with different pozzolanic compositions and subjected to sulfated medium, *Construction and Building Materials*, pp 461 – 470
- Cercio, F., DeAngeli, B.A., Pagliolico, S. (1998), Metakaolin as a pozzolanic microfiller for high-performance mortars, *Cement and Concrete Res.* 28, pp 803-09
- Chan, S.Y.N., Ji., X. (1998), Water sorptivity and chloride diffusivity of oil shale ash concrete, *Const Build Mater*, Vol. 12 (4), pp 177-83
- Chatveera, B. and Lertwattanakul (2009), Evaluation of sulfate resistance of cement mortars containing black rice husk ash, *Journal of Environmental Management*, 90, pp 1435 – 1441
- Chauhan, B.S., Kumar, N., Cho, H.M. (2012), A study on the performance and emission of a biodiesel engine fueled with Jatropha biodiesel and its blends, *Energy* 37, pp 616- 22
- Cheah, C.B., Ramli, M. (2012), Mechanical strength, durability and drying shrinkage of structural mortar containing HCWA as partial replacement of cement, *Const Build Mater* 30, pp 320-329
- Chew, J-J. & Doshi, V. (2011), Recent advance in biomass pretreatment – torrefaction fundamentals and technology, *Renewable and Sustainable Energy Review*, 15, pp 42124222

- Chen, A., Chao, S-J, Lin, W-T. (2012), Effect of calcination temperature on Pozzolanic reaction of calcined shale mortar, *Applied Mechanics and Materials*, Vols. 174-177, pp 843-846
- Chen, H. Y., Ganesan S. & Jia, B. S. (2005), Environmental challenges of post reform housing in Beijing, *Habitat International* 29(3), pp 571 – 89
- Chen, J. K., Jiang, M-q and Zhu, J. (2008), Damage evolution in cement mortar due to erosion of sulphate, *Corrosion Science* 50, pp 2478 – 2483
- Chen, W., Brouwers, H. J. H., Shui, Z. H. (2007), Three-dimensional computer modeling of slag cement hydration, *J. Mater Sci*, 42, pp 9595 – 9610
- Cheng, A. (2012), Effect of incinerator bottom ash properties on mechanical and pore size of blended cement mortars, *Materials and Design* 36, pp 859–864
- Chenguang, H.U., Shuguang, H.U., Qingjun, D., Xiaoxin, F., Xiulin, H. (2014), Effect of Curing Regime on Degree of Al^{3+} Substituting for Si^{4+} in C-S-H Gels of Hardened Portland Cement Pastes, *Journal of Wuhan University of Technology-Mater.*, pp 546-552
- Cherif, M., Rocha, J.C and Pera, J (1999), Pozzolanic properties of pulverized combustion bottom ash, *Cem & Conc Res* 29, pp 1387-1391
- Chindaprasirt, P., Jaturapitakkul, C., Sinsiri, T. (2007), Effect of fly ash fineness on microstructure of blended cement paste, *Construction and Building Materials* 21(7), pp 1534 – 1541
- Chindaprasirt, P., Jaturapitakkul, C. and Rattanasak, U. (2009), Influence of Fineness of Rice Husk Ash and Additives on the Properties of Lightweight Aggregate, *Fuel*, 88(1), pp 158-162.
- Chindaprasirt, P., Homwuttiwong, S and Sirivivatnanon, V. (2004), Influence of fly ash fineness on strength, drying shrinkage and sulphate resistance of blended cement mortars, *Cem & Conc Res*. 34, pp 1087-1092
- Chindaprasirt, P., Buapa N. and Cao, H.T (2005), Mixed cement containing fly ash for masonry and plastering work, *Construction and Building Material*, Vol. 19, Elsevier publication, London, pp 612-618
- Collepardi, M. and Valente, M. (2006), Recent developments in superplasticizers, *Superplasticizers and other chemical admixtures in concrete*, SP-239, ACI, Farmington Hills, USA
- Coleman, N.J. and McWhinnie, W.R. (2000), The Solid State Chemistry of Metakaolin Blended Ordinary Portland Cement, *Journal of Materials Science* 35, pp 2701-2710.

- Cohen, J.E. (1995), How many people can the earth support? Norton & Company, New York. 532 p.
- Cordeiro, G. C., Toledo Filho, R. D., Tavares, L. M. Fairbain, E. M. R. (2009), Ultrafine grinding of sugarcane bagasse ash for application as pozzolanic admixture, *Cement and Concrete Research* 39, pp 110-115
- Cordeiro, G. C., Toledo Filho, R. D., Tavares, L. M. Fairbain, E. M. R. (2012), Experimental characterization of binary and ternary blended cement concrete containing ultrafine residual husk and sugarcane bagasse ashes, *Construction and Building Materials*, Vol. 29, pp 641 – 646
- Cordeiro, G. C., Toledo Filho, R. D., Tavares, L. M. and Farbrain, E. M. R. (2008), Pozzolanic activity and filler effect of sugarcane bagasse ash in Portland cement and lime mortars, *Cement and Concrete Composites* 30, pp 410 – 418
- Cordio, G. C., Toledo Filho, R. D., Tavares, L. M., Fairbairn, Ed MR., Hempel, S. (2011), Influence of particle size and specific surface area on the Pozzolanic activity of residual rice husk ash, *Cement and Concrete Composites* 33, pp 529 – 534
- Cruz, J. M., Fata, I. C., Soriano, L., Paya, J and Borrachero (2013), The use of electrical impedance spectroscopy for monitoring the hydration products of Portland cement mortars with high percentage of pozzolans, *Cement and Concrete Research* 50, pp 51 – 61
- Csizmadia, J., Balázs, G. and Tamás, F. D. (2000), Chloride ion binding capacity of aluminosilicates, *Cement and Concrete Research* 31, Pergamon, pp 577 – 588
- Costoya Fernandes, M. M. (2008), Effect of particle size on the hydration kinetics and microstructural development of Tricalcium silicate, PhD thesis, Ecole Polytechnic Federal de Lausanne, Switzerland.
- Curcio, F., DeAngelina, B.A., Pagliolico, S. (1998), Metakaolin as a pozzolanic microfiller for high-performance mortars, *Cem & Conc Res.* 28, pp 803-809
- Dabai, M. U., Muhammed, C., Baguds, B. U. and Musa, A. (2009), Studies on the effect of rice husk ash as cement admixture, *NJBAs* 17(2), pp 252 – 256
- Dai, Z., Tran, T.T., Skibsted J. (2014), Aluminum Incorporation in the C–S–H Phase of White Portland Cement–Metakaolin Blends Studied by ^{27}Al and ^{29}Si MAS NMR Spectroscopy, *J. Am. Ceram. Soc.* 97 (8), pp 2662–2671
- Danner, T (2013), Reactivity of Calcined Clays, PhD Thesis, Norwegian University of Science and Technology
- Day, R. L. (1990), Pozzolana for use in low-cost housing, Technical Report, International

Development Research Centers, Ottawa, Canada

Darquennes, A., Espion, B., Staquet, S. (2013), How to assess the hydration of slag concrete?, *Construction and Building Materials*, Vol. 40, pp 1012 – 1020

Dasgupta, P. (2001), *Human Well-Being and the Natural Environment*, Oxford University Press.

Dehwah, H. A. F. (2007), Effect of Sulfate concentration and associated action type on concrete deterioration and morphological changes in cement hydrates, *Construction and Building Materials*, 21, pp 29 – 39

Demibras, A. (2011), A competitive liquid biofuel from biomass, a review, *Applied Energy* 88, pp 17-28

Demiral, I., Eryazici, A., and Sevgi, S. (2012), Bio-oil production from pyrolysis of corncob (Zeamays), *Biomass and Bioenergy* 36, pp 43-49

Demis, S., Tapali J.G., and Papadakis V.G. (2014), An investigation of the effectiveness of the utilization of biomass ashes as pozzolanic materials, *Construction and Building Materials* 68, pp 291–300

Deschner, F., Winnefeld, F., Lothenbach, B., Seufert, S., Schwesig, P., Dittrich, S., Goetz-Neunhoeffler, F., Neubauer, J. (2012), Hydration of Portland cement with high replacement by siliceous fly ash, *Cem Concr Res* 42, pp 1389-1400

Dirakar, P, Reddy, M. K., Sharma, M. (2013), Behavior of self-compacting concrete using Portland Pozzolana cement with different levels of fly ash, *Materials and Design* 46, pp 609 – 616

Diamond, S. (2004), The microstructure of cement paste and concrete – a visual primer, *Cement and Concrete Composites* 26, pp 919-933

Donatello, S., Tyrer, M., and Cheeseman, C. R. (2010), Comparison of test methods to assess pozzolanic activity, *Cement and Concrete Composites*, Vol. 32(2), pp 121 – 127

Dong, C., Yanga, Y., Jinb, B., and Horioc, M. (2007), The pyrolysis of sawdust and polyethylene in TG and U-shape tube reactor, *Waste Management* Vol. 27, Issue 11, pp 1557–1561

Doughty, M. R. C. and Hammond, G. P. (2004), Sustainability and Built environment at and beyond the city scale, *Building and Environment* 39, pp 1223 – 1233

Drexhage, J. & Murphy, D. (2010), *Sustainability Development: From Brundtland to Rio 2012*, United Nations Headquarters report, New York, pp 1 – 26

- Duku, M.H., Gu, S., and Hagan, E.B. (2011), A comprehensive review of biomass resources and biofuels potentials in Ghana, *Renewable and Sustainable Energy Reviews* 15, pp 404-15
- Erberl, D.D. (1984), Clay mineral formation and transformation in rocks and soils, *Phil. Trans. R. Soc, Lond. A* 311, pp 241-257
- Elzen, B. and Wieczorek, A. (2005), "Transitions towards sustainability through system innovation." *Technological forecasting and social change* 72(6), pp 651-661.
- Edwin, R. and Dunstan Jr., P. E. (2011), How does Pozzolanic Reaction Make Concrete "Green"? *World of Coal Ash (WOCA) Conference*, pp 1-14
- Eom, I-Y., Kim, J-Y., Kim, T-S., Lee, S-M., Choi, D, Choi, I-G (2012), Effect of essential inorganic metals on primary thermal degradation of lignocellulosic biomass, *Bioresource Technology* 104, pp 687-694
- Elliot JA. 1999. *Introduction to Sustainable Development*. 2nd Edition. Taylor & Francis: New York.
- Elinwa, A.U., Mahmood, Y.A. (2002)", Ash from timber waste as cement replacement material", *Cement and Concrete Composites*, vol 24(2), pp. 219-222
- Elkington, J. (1998), *Cannibals with Forks: the TBL of the 21st century Business*: Oxford, Capstone
- Escalera, E., Antti, M.L., Oden, M. (2012), Thermal treatment and phase transformation in kaolinite and illite based clays tropical regions of Bolivia. 6th EEIGM International Conference on Advanced Materials Research, IOP Publishing. *IOP Conf. Series: Materials Science and Engineering* (31), pp 8
- Esteves, L.P. (On the hydration of water-entrained cement- silica systems: Combined SEM, XRD and thermal analysis in cement pastes, *Thermochimica Acta* 518, pp 27-35
- Ezziane, K., Bougara, A., Kadri, A., Khelafi, H. and Kadri, E. (2007), Compressive strength of mortar containing natural pozzolan under various curing temperature, *Cement and Concrete Composites* 29(8), pp 587-593
- Faludi, J. (2004), *Concrete: A Burning Issue*. *World Changing*. www.worldchanging.com. [date accessed: 23rd June 2014]
- Fairbairn, E. M. R., Americano, B. B., Condeiro, G. C., Paula, T. P., Toledo Filho, R. D., Silvano, M. M. (2010), Cement replacement by sugarcane bagasse ash: CO₂ emissions reduction and potential for carbon credits, *Journal of Environment Management* 91, pp

1844 – 1871

Fernández, C., Mercedes, M., Karen, S., and Emmanuel, G. (2008), Effect of particle size on the hydration kinetics and microstructural development of tricalcium silicate, Published Thesis, EPFL infoscience

Fernandez, R., Martinez, F., Scrivener, K.L. (2011), The origin of the pozzolanic activity of calcined clay minerals: A comparison between kaolinit, illite and montmorillonite, *Cem & Conc Res* 41, pp 113-22

Feret, B. and Feret, C.F. (1999), CemQUANT ® software Mathematical modeling in quantitative phase analysis of Portland cement, *Cement and Concrete Research* 29(10), pp.1627-1633

Frais, M., Martinez-Ramirez, S., Blasco, T., Rodriguez, M.F. (2013), Evolution of mineralogical phases by Al and Si NMR in MK-Ca(OH)₂ system cured at 60°C, *J. Am. Ceram. Soc.* 96(7), pp 2306-2310

Frais, M., Villar, E., and Savastano, H. (2011), Brazilian sugarcane baggase ashes from the cogeneration industry as active pozzolans for cement manufacture, *Cement and Concrete Composites* 33, pp 490 – 496

Frais, M., Savastano, H., Villar, E. de Rojas, M. I. S. and Santos, S. (2012), Characterization and properties of blended cement matrices containing activated bamboo leaf wastes, *Cement and Concrete Res.* 34, pp 311 – 317

Frais, M., Villar-Cocina, E. and Valencia-Morales, E. (2007), Characterization of sugarcane straw waste as pozzolanic material for construction: calcining temperature and kinetic parameters, *Waste Management* 27, pp 533 – 538

Fu, X., Wang, Z., Tao, W., Yang, C., Hou, W., Dong, Y and Wu, X (2002), Studies on blended cement with large amount of fly ash, *Cement and Concrete Research* 22, pp 1153-1159

Fu, P., Hu, S., Xiang, J., Yi, W., Bai, X., Sun, L., and Su, S. (2012), evolution of char structure during steam gasification of the chars produced from rapid pyrolysis of rice husk, *Bioresource Technology* 114, pp 691-97

Gallucci, E., Mathur, P. and Scrivener, K. (2010), Microstructural development of early age hydration shells around cement grains, *Cement and Concrete Research*, Vol. 40(1), pp 4 – 13

Gallucci, E. & Scrivener, K. (2007), Crystallisation of calcium hydroxide in early age model and ordinary cementitious systems, *Cement & Concrete Res.* 37, pp 1418 – 1426

- García-Serna, G., Pérez-Barrigón, L. and Cocero, M.J. (2007), New trends for design towards sustainability in chemical engineering: green engineering, *Chemical Engineering Journal*, pp 133:7-30
- Ghana Statistical Service (2012), 2010 Population and Housing Census, GSA publication, pp 1-103
- Ganesan, K., Rajagopal, K. and Thangavel K. (2007), Evaluation of bagasse ash as supplementary cementitious material. *Cement and Concrete Composites* 29, pp 515-524.
- Gartner, E.M., Macphee, D.E. (2011), A physico-chemical basis for novel cementitious binders. *Cement Concrete Res.* 41, pp 736–749.
- Ghani, W.A.W.A.K., Mohd, A., da Silva, G., Bachmann, R.T. Tanfiq-Yap, Y.H., Rashid, U., Al-Muhtseb, A.H. (2013), Bio-char production from waste rubber-wood-sawdust and its potential use in C sequestration: Chemical & Physical characterization, *Industrial Crops and Products* 44, pp 18-24
- Gao, N., Li, A., Quan, C., Du, L., and Duan, Y. (2013) “TG–FTIR and Py– GC/MS analysis on pyrolysis and combustion of pine sawdust,” *Journal of Analytical and Applied Pyrolysis* 100, pp 26–32
- Gimenez, C., Sierra, V. & Rodon, R. (2012), Sustainable operation: Their impact on the triple bottom line, *International Journal of Production Economics*, Elsevier, pp 149 – 159
- Gleize Philippe, J. P., Martin C., and Gilles, Es. (2007), Effects of metakaolin on autogenous shrinkage of cement pastes, *Cement and Concrete Composites*, Vol. 29, pp 80-87
- Global Cement Report: International cement Review (2013) [<http://www.cement.com>] (Accessed 2013 April 9)
- Gómez-Zamorano, L.Y., Escalante-García, J.I. (2010), Effect of curing temperature on the nonevaporable water in Portland cement blended with geothermal silica waste, *Cement and Concrete Composites* 32(8), pp 603-610.
- Gottlieb, R.S. (1996), *This Sacred Earth: Religion, Nature, Environment*. New York: Routledge, Psychology Press, 762 p.
- Grim, R.E. (1962), *Applied Clay Mineralogy*, McGraw Hill, New York, NY
- Guest, R. (2010), The economics of sustainability in the context of climate change: An overview, *Journal of World Business* 45, pp 326-335

Guggenheim, S., and Martin, R.T. (1995), Definition of clay and clay minerals: Joint report of the AIPEA nomenclature and CMS nomenclature committee, *Clays and Clay minerals* 43 (2), pp 255-56

Guggenheim, S., Adams, J.M., Bain, D.C., Bergaya, F., Brigatti, M.F., Drits, V.A., Formoso, M.L.L., Galan, E., Kogure, T., and Stanjek, H. (2006), Summary of recommendations of nomenclature committees relevant to clay mineralogy: report of the Association Internationale Pour L'etude des Argiles (AIPEA) nomenclature committee 2006. *Clays Clay Miner.* 54, 761–772

Gu, S., Zhou, J., Luo, Z., Wang, Q., Ni, M. (2013), A detailed study of the effects of pyrolysis temperature and feedstock particle size on the preparation of nanosilic from rice husk, *Industrial Crops and Product* 50, pp 540-49

Güneyisi, E., Gesog̃lu, M. and Mermerdas, K. (2008), Improving strength, drying shrinkage, and pore structure of concrete using metakaolin, *Mater Struct* 41, pp 937–49

Hall, C. (1989), Water sorptivity of mortars and concretes: a review, *Magazine of oncrete Research* 41, pp 51-61

Hammond, A.A. (1987), Hydration products of bauxite-waste pozzolana cement, *The international journal of cement composites and lightweight concrete*, Vol 9(1), pp 19-31

Hanson, S. O. (2010), Technology and the notion of Sustainability, *Technology in Society*, Vol. 52(4), pp 274 – 279

Hanna, R.A., Barrie, P.J., Cheeseman, C.R., Hills, C.D, Buchler, P.M., Perry, R. (1995), Solid state Si and Al NMR and FTIR study of cement pastes containing industrial wastes and organics, *Cem Concr Res* 25, pp 1435-1444

Hardjilo, D. (2007), The use of fly ash to reduce the environmental impact of concrete, In *Proceedings of Encon 2007, 1st Engineering Conference on Energy and Environment*, Malaysia, pp 101

Harris, J. (2000), "Basic Principles of Sustainable Development." *Global Development and Environment Institute*, Tufts University, Working paper 00-004

Hedger, M. (2011). Climate finance in Bangladesh: Lessons or development cooperation and climate finance at the national level. EDC 2020 Policy Brief. Retrieved from [http://www.edc2020.eu/fileadmin/publications/EDC 2020 Policy Brief no 14 Climate Finance in Bangladesh](http://www.edc2020.eu/fileadmin/publications/EDC_2020_Policy_Brief_no_14_Climate_Finance_in_Bangladesh). [accessed on 23rd June 2014]

Heal, G. (1999), *Valuing the Future: Economic Theory and Sustainability*, Columbia

University Press

Hekal, E. E., Kishar, G. and Mostafa, H. (2002), Magnesium sulfate attack on hardened blended cement pastes under different circumstances, *Cement and Concrete Research* 32, pp 1421 C– 1427

Hesse, C., Goetz-Neunhoeffer, F. and Neubauer, J. (2010), A new approach in quantitative insitu XRD of cement paste: Correlation of heat flow curves with early hydration reactions, *Cement and Concrete Research* 41, pp 123 – 128

Hellar-Kallai, L. (2006), Thermally modified clay minerals. In: Bergaya Theng, B.K.G., Legaly, G. (Eds), *Handbook of clay science, development in clay science*: Elsevier, pp 289-308

Helmuth, R. (1987), *Fly ash in Cement and Concrete*, Portland cement Association, Illinois, pp 203

Heikal, M., El-Didamony, H., Sokkary, T.M., Ahmed, I.A. (2013), Behavior of composite pastes containing microsilica and fly ash at elevated temperature, *Cons. Build. Mat.* 38, pp 1180-1190

Hill, J. and Sharp, J. H. (2002), The mineralogy and microstructure of three composite cements with high replacement levels, *Cement and Concrete Composites* 24, pp191 – 199

Hjorth, J., Skibsted, J., Jakobsen, H.J. (1998), Si MAS NMR studies of Portland cement components and effects of microsilica on the hydration reaction, *Cem Concr Res* 18, pp 789-798

Howarth, R. B. (2007), Towards an operational sustainability criterion, *Ecological Economics*, Vol. 63, Issue 4, pp 656-663

Hooton, R. D. (1993), Influence of silica fume replacement on cement on physical properties and resistance to sulfate attack, freezing and thawing, and alkali silica reactivity, *ACI Material Journal* 90(2), pp 143 – 51

Hong H., Fu, Z., and Min, X. (2001), *Cem. Concr. Res.* 31 (2), pp 287–290

Hosseini, H. M. & Kaneko, S. (2011), Dynamic sustainability assessment of countries at the macro level: A principal component analysis, *Ecological Indicators*, pp 811 – 823

Hosseini, M. M., Shao, Y. and Whalen, J. K. (2011), Bio-cement production from Silicon-rich plant: Perspectives and future potential in Canada, *Bio-systems Engineering*, Vol. 110, Issue 4, pp 351 – 362

- Idris, S. S., Rahman, N. A., Ismail, K., Alias, A. B., Rashid, Z. A. and Aris, J. M. (2010), Investigation on thermochemical behavior of low rank Malaysian coal, oil palm biomass and their blends during pyrolysis via thermogravimetric analysis (TGA), *Bioresource Technology* 101, pp 4584 – 4592
- Itim, A., Ezziane, K., Kadri, E-H. (2011), Compressive strength and shrinkage of mortar containing various amounts of mineral additions, *Construction and Building Materials* 25, pp 3603-3609
- Ilic, B.R., Mitrovic, A.A., Milicic, L.R. (2010), Thermal Treatment of Kaolin Clay to Obtain Metakaolin, Institute for Testing of Materials, Belgrade, Serbia, pp 351-356
- Indrawati, V. and Manaf, A. (2008), Mechanical strength of trass as supplementary cementing material, *Journal of Physical Science*, Vol. 92(2), pp 51 – 59
- Ioannidou, O., Zabaniotou, A., Antonakou, E.V., Papazsi, K.M., Lappas, A.A., Athanassion, C. (2009), Investigating the potential for energy, fuel, materials and chemical production from corn residues (cobs and stalks) by non-catalytic and catalytic pyrolysis in two reactor configurations, *Renewable and Sustainable Energy Reviews* 13, pp 750-62
- Isaia G.C., Gastaldini A.L.G., and Moraes, R. (2003), Physical and pozzolanic action of mineral additions on the mechanical strength of high-performance concrete. *Cem. Concr. Compos* 25, pp 69
- James, J. and Rao, S. (1986), Reactivity of rice husk ash, *Cement and Concrete Res.* 16, pp 329 – 336
- Jansen, D., Goetz-Neunhoeffler, F., Lothenbach, B. and Newbaver, J. (2012), The early hydration of ordinary Portland cement (OPC): An approach comparing measured heat flow with calculated heat flow from QXRD, *Cement and Concrete Research* 42, pp 134 – 138
- Jain, N. (2012), Effect of nonpozzolanic and pozzolanic mineral admixtures on the hydration behavior of ordinary Portland cement. *Construct.Build. Mater.* 27, pp 39-44
- Jalkanen, A. & Nygren, P. (2005), Sustainable use of renewable natural resources — from principles to practices. University of Helsinki Department of Forest Ecology Publications 34, pp 3
- Jenkins, B.M., Baxter, L.L., Miles Jr, T.R., and Miles, T.R. (1998), Combustion properties of biomass, *Fuel Processing Technology* 54, pp 17-46
- Jensen, O.M., Hansen, P.H. (1996), Autogenous deformation and change of relative humidity in silica-fume modified cement paste, *ACI Material J* 93, pp 539-43

Jo, B-W., Kim, C-H., Tae, G-h and Park, J-B. (2007), Characteristics of cement mortar with nano – SiO₂ particles, *Construction and Building Materials*, 21, pp 1351 – 1355

Kadri, E. H., Duval, R. (2009), Hydration heat kinetics of concrete with silica fume, *Construction and Building Material* 23(11), pp 3388 – 3392

Kadri, E. H., Kenai, S., Ezziane, K., Siddique, R. and De Schulte, G. (2012), Influence of metakaoline and silica fume on the heat of hydration and compressive strength development of mortar, *Applied Clay Science* 53, pp 704 – 708

Kakali, G., Perraki, T., Tsivilis, S., and Badogiannis, E, (2001), Thermal treatment of kaolin: the effect of mineralogy on the pozzolanic activity, *Applied Clay Science* 20(1), pp.73-80

Kates, R. W. & Parris, T. M. (2003), Long-term trends and sustainability transition, *PNAS*, Vol. 100, pp 8062 – 67

Kara, P., Borosnyoi, A., Fenyvesi, O. (2014), Performance of waste glass powder (WGP) supplementary cementitious material (SCM)- Drying shrinkage and early age shrinkage cracking, *Journal of Silicate Based and Composite Materials*, Vol. 66, pp 18-22

Kartina, K (2011), Rice husk ash- pozzolanic material for sustainability, *International Journal of Applied Science and Technology*, Vol. 1(6), pp 169-178

Kesse, G.O. (1985). *The Mineral and Rock Resources of Ghana*. A.A. Balkema, Rotterdam, Netherlands, pp. 95-156.

Kevern, J.T. and Wang, K. (2010), Investigation of Corn Ash as a Supplementary Cementitious Material in Concrete, In: *Proceedings of the second international conference on sustainable materials and technology*, J. Zachar, P. Claisse, T.R Naik, E. Ganjain, June 28-30, Italy

Khatib, J.M. (2004), Absorption characteristics of metakaolin concrete, *Cem Concr Res* 34 (1), pp 19-29

Khatib, J.M. and Hibbert, J.J. (2005), Selected engineering properties of concrete incorporating slag and metakaolin, *Construction and Building Mat.* 19, pp 460-472

Khosla, A. (1995), Foreword. In *a Sustainable World*, T.C. Tryzna (ed). Sacramento: IUCN.

Kim, S-J., Jung, S-H., and Kim, J-S. (2010), Fast pyrolysis of palm kernel shells: Influence of operation parameters on the bio-oil yield of phenol and phenolic compounds, *Bioresource Technology* 10, pp 9294-300

Klimesch, D.S., Lee, G., Ray, A., Wilson, M.A. (1998), Metakaolin addition in autoclaved cement-quartz pastes: A Si and Al MAS NMR investigation, *Adv. Cem. Res.*, 30 (2), pp 93-99

Kjellsen, K. O. and Justnes, H. (2004), Revisiting the microstructure of hydrated tricalcium silicate – a comparison to Portland cement, *Cement and Concrete Composites* 26, pp 947 – 956

Korobeinichev, O.P., Paletsky, A.A., Gonchikzhapov, M.B., Shundrina, I.K., Chen, H., and Liu, N. (2013), Combustion chemistry and decomposition kinetics of forest fuels, *Procedia Engineering* 62, pp 182-93

Korpa, A., Kowald, T., Trettin, R. (2008), Hydration behavior structure and morphology of hydration phases in advanced cement – based system containing micro and nano scale Pozzolana additions, *Cement and Concrete Research* 38, pp 955 – 962

Korpa, A., Kowald, T., Trettin, R. (2008), Phase development in normal and ultra high performance cementitious systems by quantitative X-ray analysis and thermo-analytical methods, *Cement and Concrete Research* 39, pp 69 – 76

Kosmatka, S., Kerkhoff, H., Beatrix, Pananese, W. C. (2002), Design and control of concrete mixtures, 14th Edition, Portland Cement Association, Skokie, IL, pp 39

Kosmatka, S.H., and Wilson, M.L. (2011), Design and Control of Concrete Mixtures, 15th Edition, EB001-15, Portland cement Association, Skokie, Illinois, USA, 460 pp.

Kumar, M., Singh, S.K. and Singh, N.P (2012), Heat evolution during the hydration of Portland cement in the presence of fly ash, calcium hydroxide and super plasticizer, *Thermochemica Acta*, Vol. 548, pp 27 – 32

Kumar, M., Singh, N. P., Singh, S. K. and Singh, N. B. (2012), Tertiary biocomposite cement and its hydration, *Construction and Building Materials* 29, pp 1-6

Kumbhar, G. M., Vasandani, A. G. M., Shah, S. W. and Bhangar, M. I. (2003), Differential thermal analysis of lignite coals/ Mineral admixtures and decomposition studies of carbonate minerals in coal ashes by isothermal thermogravimetry, *Journal of Chemistry Soc. Palc*, Vol. 254), pp 265 – 268

Kurecic, M. and Smole, M.S. (2012), Polymer nanocomposite hydrogels for water purification, In: *Nanotechnology and Nanomaterials, Nanocomposites- New Trends and Deveolpments*

Lam, L., Wong, Y.L. and Poon, C.S. (2000), Degree of hydration and gel/space ratio of high-volume fly ash/cement systems, *Cement and Concrete Research* 30, pp 747-756

- Langan, B. W., Weng, K., Ward, M. A. (2002), Effect of silica fume and fly ash on heat of hydration of Portland cement, *Cement and Concrete Res.* 32, pp 1045 – 1051
- Lea, F.M. (1998), *The Chemistry of Cement and Concrete*, Third edition, Arnold, London.
- Leach, A. R. (2001), *Molecular Modeling Principles and applications*, 2nd Ed., Practice Hall
- Lehtonen, M. (2004), The environmental–social interface of sustainable development: capabilities, social capital, institutions, *Ecological Economics* 49 (2004) 199 – 214
- Li, H., Liu, X., Legros, R., Bi, X.T., Lim, C.J., Sokhanoamy, S. (2012), Torrefaction of sawdust in a fluidised bed reactor, *Bioresource Technology* 103, pp 453-458
- Li, Z. G. (2006), A new life cycle impact assessment for buildings, *Built Environment* 41 (10), pp 1414 – 22
- Liu, X., Zhang N., Sun, H., Zhang, J., Li, L. (2011), Structural investigation relating to the cementitious activity of bauxite residue — Red mud, *Cement and Concrete Research* 41, 847–853
- Lin, K-E., Chen, B-Y., Chiou, C-S., Chen, A. (2010), Waste Brick's potential for use as a pozzolana in blended cement, *Waste and Management Research*, pp 647-652
- Li, Y., Junling, B., Yulin, G. (2010), The relationship between autogeneous shrinkage and pore structure of cement paste with mineral admixtures, *Const Build Mater* 24, pp 1855-60
- Lockington, D., Parlange, J-Y., Dux, P. (1999), Sorptivity and the estimation of water penetration into unsaturated concrete, *Materials and structures*, Vol. 32, pp 342-347
- Lopez-Gonzalez, D., Fernandez-Lopez, M., Valverde, L. (2013), Thermogravimetric mass spectrometric analysis on combustion of lignocellulosic biomass, *Boiresource technology* 143, pp 562-574
- Lothenbach, B., Winnefeld, F., Alder, C., Weiland, E. and Lunk, P. (2007), Effect of temperature on the pore solution, microstructure and hydration products of Portland cement pastes, *Cement and Concrete Research* 37, pp 978 – 987.
- Lothenbach, B., Matschei, T., Moschner, G. and Glasser, F. P. (2008), Thermodynamic modeling of the effect of temperature on the hydration and porosity of Portland cement, *Cement and Concrete Res.* 38, pp 1 – 18
- Lothenbach, B, Scrivener, K., Hooton R.D. (2011), Supplementary cementitious materials, *Cement and Concrete Research* 41, pp 1244-56

- Luxan, M. P., Madruga, F. and Saavedra, J. (1989), Rapid evaluation of pozzolanic activity of natural pits by conductivity measurement, *Cement and Concrete Res.* 19(1), pp 63 – 68
- MacCarter, W.J., Ezirim, H., Emerson, M. (1992), Properties of concrete in the cover zone: water penetration, sorptivity and ionic ingress, *Magazine of Concrete Research* 48, pp 149-156
- MacLaren, D.C., White, M.A. (2003), *Cement: Its chemistry and properties*, *J Chem Edu* 80, pp 623-635
- Mandandoust, R., Mohammad Ranjbar, M., Ahmadi Moghadan, H. and Yasin Mousavi, S. (2011), Mechanical properties and durability assessment of rice husk ash concrete, *Biosystems Engineering*, pp144 – 152
- Magat-Johar, M. A., Brooks, J. J., Kabir, S., and Rivand, P. (2011), Influence of supplementary cementitious materials on engineering properties of high Strength Concrete, *Construction and Building Materials* 25, Elsevier, pp 2639 – 2648
- Maghanaki, M.M., Ghobadian, B., Najafi, G. and Galogah, R.J. (2013), Potential of biogas production in Iran, *Renewable and Sustainable Energy Reviews* 28, pp 702-14
- Malvar, L. J., and Lenke, L. R. (2006), Efficiency of fly ash in mitigating alkali – silica reaction based on chemical composition, *ACI Materials Journal* 103, pp 310 – 319
- Malquori, G. (1960). In: *Proceedings of the Fourth International Symposium on Chemistry of Cement*. Washington DC, pp 983-88
- Martinelli, L. A. and Filoso, S. (2008), Expansion of sugarcane ethanol production in Brazil environmental and social challenges, *Ecological Application* 18, pp 885 – 98
- Maia, A.Á.B., Angélica, R.S., de Freitas Neves, R., Pöllmann, H., Straub, C., Saalwächter, K. (2014), Use of ^{29}Si and ^{27}Al MAS NMR to study thermal activation of kaolinites from Brazilian Amazon kaolin wastes, *Applied. Clay Science* 87, pp 189–196
- Maiconi, G. (2010), *Sustainability – Driven Innovation in the Society of the Future*: Ancona, Italy
- Mainguy, M., Tognazzi, C., Torrenti, J-m., Adenot, F. (2000), Modelling of leaching in pure cement paste and mortar, *Cement and Concrete Research* 30, pp 83-90
- Mamlouk, M.S. and Zaniewski, J.P. (2006), *Materials for Civil and Construction Engineers*. Prentice Hall Publishers, Upper Saddle River.

Mansaray, K.G., and Ghaly, A. (1998), Thermal degradation of rice husk in nitrogen atmosphere, *Bioresource Technology* 65, pp 13-20

Massaza, F. (1993), Pozzolanic cements, *Cement and Concrete Research* 41, pp 1244-1256

Mathur, P. C. (2007), Study of cementitious materials using transmission electron microscopy, PhD thesis Ecole Polytechnic Federal de Lausanne, Switzerland.

Matschei, T., Skapa, R.; Lothenbach, B.; Glasser, F.P. (2007), The distribution of sulfate in hydrated Portland cement paste. Proceedings of the 12th Intern. Congress on the Chemistry of Cements, Montreal

Mbiti, J.S. (1996), African Views of the Universe. In: Gottlieb, R.S. (ed.), *This sacred earth*, New York: Routledge.

McCarter, W.J., Ezirim, H., Emerson, M. (1992), Absorption of water and chloride into concrete. *Magazine of Concrete Research* 44(158), pp 31-7.

McCarter, W. J. and Tran, D. (1996), monitoring pozzolanic activity by direct activation with calcium hydroxide, *Construction and Building Materials*, pp 179 – 184

Mckendry, P. (2002), Energy Production from biomass (Part 1): Overview of biomass, *Bioresource Technology* 83, pp 37-46

Mebratu, D. (1998), Sustainability and sustainable development: Historical and conceptual review, *Environmental Impact Assessment* 18, pp 493-520

Mehta, P. K. (2009), Global Concrete Industry Sustainability, *ACI Concrete Int.* 31(2), pp 45-48

Mendelovici, E (1997), Comparative study of the effect of thermal and mechanical treatments on the structures of clay mineral, *Journal of thermal analysis* 49(3), pp 1385-97

Mendess, A., Gates, W.P., Sanjayan, J.G., Collins, F (2011), NMR, XRD, IR and synchrotron NEXAFS spectroscopic studies of OPC and OPC/ slag cement paste hydrates, *Materials and Structures* 44, pp 1773-1791.

Mendoza, O. and Tobon, J.I. (2013), An alternative thermal method for identification of pozzolanic activity in Ca(OH)₂/ pozzolan pastes, *J. Therm Anal Calorim* 114, pp 589-596

Mensah, M. (2010), More local limestone for Ghanaian's cement production, *Chronicle newspaper Ghana*

Mindess, S., Young, J. F., and Darwin, D. (2003). *Concrete*. 2nd Ed., Prentice-Hall Inc., Englewood Cliffs, New Jersey.

Mirza, J., Riaz, M., Naseer, A., Rehman, F., Khan, A.N., Ali, Q. (2009), Pakistani bentonite in mortars and concrete as low cost construction material. *Appl. Clay Sci.* 45, 220–226

Mofijur, M., Masjuki, H.H., Kalam, M.A., Atabani, A.E., Shahabuddin, M. (2013), Effect of biodiesel from various feedstock on combustion characteristics, engine durability and materials compatability: A review, *Renewable and Sustainable Energy Reviews* 28, pp 441-55

Mohammed, Y.S., Mokhtar, A.S., Bashir, N., Saidur, R. (2013), An overview of agricultural biomass for decentralized rural energy in Ghana, *Renewable and Sustainable Energy Review* 20, pp15-22

Mohammed, B. M. & Sharp, J. H. (2002), Kinetics and mechanism of formation of tricalcium aluminate $\text{Ca}_3\text{Al}_2\text{O}_6$, *Thermochimica Acta* 388, Elsevier, pp 105 – 114

Momade, Z.G., Atiemo, E. (2004), Evaluation of pozzolanic activity of some clays in Ghana, *Journal of Science and Technology*, Vol. 24 (1), pp 76-83

Montakarntiwong, K., Chulsip, N., Tangchirapat, W., Jaturapitakkul, C. (2013), Strength and heat evolution of concretes containing bagasse ash thermal power plants in sugar industry, *Materials and Design* 49, pp 414 – 420

Moodi, F., Ramezaniapour, A.A., Safavizadeh, A.Sh. (2011), Evaluation of the optimal process of thermal activation of kaolins, *Scintia Iranica A*, Vol 18 (4), pp 906-912.

Morbi, A., Cargiano, S. and Borgerello, E. (2010), Cements based materials for sustainable development: In Proceedings of 2nd International Conference on Sustainable Construction Materials and Technologies, Arizona, Italy

Morbid, A., Cargiano, S. and Borgarello, E. (2010), Cement based materials for sustainable development: In Proceeding of Sustainable Construction Materials and Technologies, Ancona, Italy

Mori, K., & Christodoulou, A. (2012), Review of sustainability indices and indicators: Towards a new City Sustainability Index (CSI). *Environmental Impact Assessment Review*, 32(1), 94-106

Morales, E. V., Villar-Cocina, E., Fraix, M., Santos, S. F., Savastano Jr., H. (2009), Effect of calcining conditions on the microstructure of sugarcane waste ashes (SCWA), Influence in the pozzolanic activation, *Cement and Concrete Composites* 31, pp 22-28

- Moriconi, G. (2010), Sustainability-Driven Innovation in the Society of the Future, In: Proceedings of the second international conference on sustainable construction materials and technology, J. Zacher, P. Claisse, T.R Naik, E. Ganjan, June 28-30, Ancona, Italy
- Moropoulou, A., Bakolas, A. and Aggelakopoulou, E. (2004), Evaluation of pozzolanic activity of natural and artificial pozzolans by thermal analysis, *Thermochimica Acta* 420, pp 135-140.
- Morsy, M.S., Abo- El- Enein, S.A and Hanna, G.B. (1997), Microstructure and hydration characteristics of artificial pozzolana- cement pastes containing burnt kaolinite clay, *Cem & Conc Res.* 27(9), pp 1307- 1312
- Mostafa, N. J., El-Hemaly, S. A. S, Al-Wakeel, E. I., El-Korashy, S. A., Brown, P. W. (2002), Characterization and evaluation of the pozzolanic activity of Egyptian industrial by – products I: Silica fume and dealuminated kaolin, *Cement and Concrete Res.*, pp 467 – 474
- Mostafa, N. Y. and Brown, P. W. (2005), Heat of hydration of high reactive pozzolans in blended cements: Isothermal conduction calorimetry, *Thermochimica Acta* 435, pp 162 – 167
- Muhmood, L., Vilita, S. and Venkateswaran (2009), Cementitious and pozzolanic behavior of electric arc furnace steel slags, *Cement and Concrete Res.* 39, pp 102 – 109
- Munir, S., Daood, S. S., Himmo, W., Canliffe, A. M. and Gibbs, B. M. (2009), Thermal analysis and devolatilization kinetics of cotton stalk, sugarcane bagasse, and shea meal under nitrogen and air atmospheres, *Biosource technology* 3, pp 1413 – 1418
- Murgier, S., Zanni, H., Gouvenant, D. (2004), Blast furnace slag cement: a ^{29}Si and ^{27}Al NMR study, *Comptes Rendus chimie* 7, pp 389-394
- Murray, H.H. (1999), Applied clay mineralogy today and tomorrow, *Clay Minerals* 34, pp 39-49
- Naciri, A. and Chikouche Hamina, M. (2009), Use of brick as a partial replacement of cement mortar, Elsevier publication, *Waste management* 29, pp 2378- 2384
- Nair, D. G., Fraij, A., Klaasen, A. A. K. and Kentgens, A. P. M. (2008), A structural investigation relating to the pozzolana activity of rice husk ashes, *Cement and Concrete Res.* 38, pp 861 – 869
- Ness, B., Urbel-Piirsalu, E., Anderberg, S., Olsson, L. (2007), Categorising tools for sustainability assessment, *Ecological Economics* 60, pp 498–508.
- Neville, A. (2003), *Neville on Concrete*, ACI, Farmington Hills, MI, USA,

Neville, A. (2004), The confused world of sulfate attack on concrete, *Cement and Concrete Research* 34, pp 1275 – 1296

Ng, W.P.Q., Lam, H.L., Ng, F.Y, Kamal, M., Lim, J.H.E (2012), Waste-to-wealth: Green potential from palm biomass in Malaysia, *Journal of Cleaner Production*, pp 57-65

Nimyat, P.S., Tok, Y. (2013), Effect of saw dust ash (SDA) pozzolana on the performance of blended cement paste concrete at high temperatures, *Civil and Environment Research* Vol. 3(11), pp 2224-9

Ninduangdee, P., & Kuprianov, V. (2013), Study on burning oil palm kernel shell in a conical fluidized-bed combustor using alumina as the bed material, *Journal of the Taiwan Institute of Chemical Engineers* 44, pp 1045-53

Norton, B. (2011), *Intergenerational Equity*, Berkshire encyclopedia of Sustainability, Vol. 3, Great Barrington, Massachusetts, USA.

Nwoko, V.O. and Hammond, A.A. (1978), Pozzolana from Bauxite waste, *Construction and Recycling*, Vol. 2, pp 43- 47

Obernberger, I., Biedermann, F. Wiemann, W, Riedl, R. (1997), Concentration of inorganic elements in biomass fuels and recovery in the different ash fractions, *Biomass Bioenergy* 12, pp 211-224

OECD/IEA (2003), *Policies to Reduce Greenhouse Gas Emissions in Industry Successful Approaches and Lessons Learned: Workshop Report*, OECD and IEA Information Paper, pp 1-51

Ofori-Boateng, C., Lee, K. T, Mensah, M. (2013), The prospects of electricity generation from municipal solid waste (MSW) in Ghana: A better waste management option, *Fuel Processing Technology* 110, pp 94–102

Oliveira de Paula, G, & Cavalcanti, R. N. (2000), Ethics: essence of sustainability, *Journal of Cleaner Production*, pp 109-117

Olutoge, F.A., Quadri, H.A., and Olafusi, O.S. (2012), Investigation of the strength properties of palm kernel shell ash concrete, *Engineering Technology and Applied Science Research*, Vol. 2, pp 315-19

Okoroigee, E.C., Shaffron, C.M (2012), Determination of bio-energy potential of palm kernel shell by physicochemical characterization, *Nigeria Journal of Technology*, pp 32935

Oriol, M. and Pera, J. (1995), Pozzolanic activity of metakaolin under microwave treatment, *Cement and Concrete Research* Vol. 25 (2), pp 265–270

- Parnphumeup, P., Kerr, S.A. (2011), Stakeholder preferences towards the sustainable development of CDM Projects: Lessons from biomass (rice husk). CDM Project in Thailand, Energy Policy 39, pp 3591 – 3601
- Parande, A. K., Babu, B. R., Pandi, K., Karthikeyan, M. S., Palaniswamy, W. (2011), Environmental effects on concrete using Ordinary and Pozzolana Portland cement, Construction and Building Materials, 25, pp 288 – 297
- Park, D.K., Kim, S.D., Lee, H.S., Lee, J.G. (2010), Co-pyrolysis characteristics of sawdust and coal blend in TGA and a fixed bed reactor, Bioresource Technology 101, pp 6151-56
- Patel, M., Karera, A., Prasanna, P. (1987), Effect of thermal and chemical treatments on carbon and silica contents in rice husk, Journal of Material Science 22, pp 2457-64
- Paya, J., Borracheto, M. V., Monzo, J. Peris-Mora, E. and Amah-Jour, F. (2001), Enhanced conductivity measurement techniques for evaluation of fly ash pozzolanic activity, Cement and Concrete Res. 31, pp 179 – 84
- Pekmezci, B.Y. and Akyuz, S. (2004), Optimum usage of a natural pozzolan for the maximum compressive strength of concrete, Cem & Conc Res.34, pp 2175- 2179
- Perraki, T., Kontori, E., Tsivilis, S. and Kakali, G. (2010), The effect of zeolite on the properties and hydration of blended cements, Cement and Concrete Composites 32(2), pp 128-133
- Pena, P., Rivas Mercury, J.M., de Aza, A.H., Turrillas, X., Sobrados, I., Sanz, J. (2008), Solid state Al and Si NMR characterization of hydrates formed in calcium aluminatesilica fume mixtures, J. Solid State Chem. 181 (8), pp 1744-52
- Peterson, V. K., Neumann, D. A. and Livingston, R. A. (2006), Hydration of cement: the application of quasielastic and inelastic neutron scattering, Physica B, Elsevier, pp 481 – 486.
- Poon, C.S., Lam, L., Kou, S.C., Lin, Z.S. (1999), A study on the hydration rate of natural zeolite blended cement pastes, Construction and Building Materials 13(8), pp.427-432
- Potgieter, J. H. (2012), An overview of cement production: How green and sustainable is the industry, Environmental Management and Sustainable Development, Vol. (2), pp 14 – 37
- Poulsen, S. L. (2009), Methodologies for measuring the degree of reaction in Portland cement blends with supplementary cementitious materials by ^{29}Si and ^{27}Al MAS NMR spectroscopy, Published PhD thesis, Aarhus Universitet.

Quennoz, A. & Scrivener, K. L. (2012), Hydration of C₃A gypsum systems, *Cement & Concrete Res.* 42, Elsevier, pp 1032 – 1041

Quyung, D., Xu, W., Lo, T. Y. and Shan, J. F. C. (2011), Increasing mortar strength with the use of activated kaolin by-products from paper industry, *Construction and Building Materials* 25(4), pp 1537 – 1545

Rao, G. A. (2003), Investigations on the performance of silica fume – incorporated cement pastes and mortars, *Cement and Concrete Research* 33, pp 1765 – 1770.

Raheem, A.A. and Sulaiman, O.K. (2013), Saw dust ash as partial replacement for cement in the production of sandcrete hollow blocks, *Ijera*, Vol 3 (4), pp 713-21

Rahhal, V. and Talero, R. (2004), Influence of two different fly ashes on the hydration of Portland cements, *J. Therm Anal Calorim* 78, pp 191 - 205

Ramadhansyah, P.J., A.W. Mahyun, M.Z. Salwa, B.H. Abu Bakar, M.A. Megat Johari and Wan M.H. Ibrahim (2012), Thermal analysis and pozzolanic index of rice husk ash at different grinding time. *International Conference on Advances Science and Contemporary Engineering 2012, Procedia Engineering*, pp 1-9.

Razak, H.A, Chai, H.K., Wong, H.S. (2004), Near surface characteristics of concrete containing supplementary cementing materials. *Cement Concrete Compos* 26, pp 883–9

Richardson, I. G. (1999), The nature of the hydration products in hardened cement pastes, *Cement and Concrete Composites* 22, pp 97 – 113

Robinson, J. (2004), Squaring the circle? Some thoughts on the idea of sustainable development, *Ecological Economics* 48, pp 369-384

Robinson, A. L., Junker, H., Baxter L. L. (2002), Pilot –scale investigation of the influence of coal-biomass cofiring on ash deposition, *Energy Fuel* 16, pp 343-533

Roewell, R.M. (1984), *The chemistry of solid*, America Chemical Society, Washington D.C

Rosalyn, M. (2002), *Education for Sustainable Development tool kit*, center for Geography & Environment Education, University of Tennessee, USA.

Rowland, ID., Howe, (2006), *The Ten Books of architecture*, Cambridge University Press, UK

- Roziere, E., Loukili, A., El Hachem, R., and Grondin, F. (2009), Durability of concrete exposed to leaching and external sulfate attacks, *Cement and Concrete Research* 39, pp. 118 – 1198
- Rukson, S. and Chindapasirt, P. (2012), Utilization of bagasse ash in high – strength concrete, *Materials and Design* 34, pp 45 -50
- Sabil, K.M., Aziz, M.A., Lal, B., Uemura, Y. (2013), Effects of torrefaction on the physiochemical properties od oil palm empty fruit bunches, mesocarp fibre and kernel shell, *Biomass and Bioenergy* 56, pp 351-60
- Sabir, B. B., Wild, S., and Bai, J. (2001), Metakaolin and calcined clays as pozzolans for concrete: a review, *Cement and Concrete Composites* 23, pp 441 – 454
- Sabir, B.B., Wild, S., O’Farrell, M. (1998), A water sorptivity test for mortar and concrete, *Materials and Structures*, Vol 31, pp 568-574
- Salla, A., Delvasto, S., De Gutierrez, R. M., and Lange, D. (2009), Comparison of two processes for treating rice husk ash for use in high performance concrete, *Cement and Concrete Res.* 39, pp 773 – 778
- Samet, B., Mnif, T and Chaaboni, M. (2007), Use of kaolinitic clay as a pozzolanic material for cements: Formulation of blended cement, *Cement and Concrete Composite* 29, Elsevier publication, London, pp 741-749
- Sandberg, P. and Roberts, L. R. (2008), Studies of cement-admixture interaction related to aluminate hydration control by isothermal calorimetry, *Am. Concr Inst.* 217, pp 529 – 542
- Sata, V., Jaturapitakkal, C. and Kiattikomol, K. (2007), Influence of pozzolan from various by-products materials on mechanical properties of high-strength concrete, *Construction and Building Materials* 21, pp 1589 – 1598
- Scriver, K. L. (1984), Development of microstructure during the hydration of Portland cement, PhD thesis, University of London.
- Scrivener, K. L. and Pratt, P. (1984), Backscattered electron images of polished cement section in the scanning electron microscope In: Bayles J., editor, *Proceedings 6th International Conference on cement microscopy*, pp 145 – 155, Texas, USA
- Scrivener, K. L. (2004), Backscattered electron imaging of cementitious microstructures: understanding and quantification, *Cement and Concrete Composites* 26, pp 935 – 945
- Schneider, J., Cincotto, M.A., Panepucci, H. (2001), Si and Al high resolution NMR characterization of calcium silicate hydrate phases in activated blast-furnace slag pastes, *Cem Concr Res* 31, pp 993-1001

Seyfang, G. (2003), Environmental mega-conferences—from Stockholm to Johannesburg and beyond, *Global Environmental Change*, pp 223-228

Senadheera, S. (2010), Materials Systems for Sustainable Civil Engineering Design: A course Syllabus, Delivery and student Feedback, In proceedings of 2nd International Conference on Sustainable Construction Materials & Technologies, Ancona, Italy.

Setina, J., Gabrene, A. and Juhnevica, I. (2013), Effect of Pozzolanitic additives on structure and chemical durability of concrete, *Procedia Engineering* 57, pp 1005 – 1012

Sharon, H., Karuppasamy, K., Kumar, S., Sundaresan, D.R. (2012), A test on DI diesel engine fueled with methy esters of used palm oil, *Renewable Energy* 47, pp 160-66 Shadangi, K.P., and Mohanty, K. (2014), Kinetic study and thermal analysis of the pyrolysis of nonoedible oilseed powders by thermogravimetric and differential scanning calorimetric analysis, *Renewable Energy* 63, pp 337-44

Shi, G., Wu, T. Reifler, C. and Wang, H. (2005), Characteristics and pozzolanitic reactivity of glass powders, *Cement and Concrete Res.* 35, pp 987 – 993

Shia, C., Wua, Y., Rieflerb, C., Wang, H. (2005), Characteristics and pozzolanitic reactivity of glass powders, *Cement and Concrete Research* 35, pp 987– 993

Shvarzman, A., Kovler, K., Grader, G. S., and Shter, G. E. (2003). The effect of dehydroxylation/amorphization degree on pozzolanitic activity of kaolinite, *Cement and Concrete Research*, 33, 405–416.

Siddique, R. and Klaus, J. (2013), Influence of metakaolin on the properties of mortar and concrete: A review, *Applied Clay Science* 43, pp 392–400

Simionato, D., Block, M.A, La Rocca, N., Jouhet, J., Maréchal, E., Finazzi, G. and Morosinotto, T. (2013), The Response of *Nannochloropsis gaditana* to Nitrogen Starvation Includes De Novo Biosynthesis of Triacylglycerols, a Decrease of Chloroplast Galactolipids, and Reorganization of the Photosynthetic Apparatus, *Eukaryotic cell*, 12(5), pp 665-676.

Smag, Al., Uskan, B., and Gülbay, S. (2011), Detailed characterization of the pyrolytic liquids obtained by pyrolysis of sawdust, *Journal of Analytical and Applied Pyrolysis* 90, pp 48–52

Singh, N. B., Singh, V. D. and Rai, S. (2000), Hydration of bagasse ash blended cement, *Cement and Concrete Res.* 30(9), pp 1485 – 1488

Singh, M. and Garg, M. (2006), Reactive pozzolana from India clays-their use in cement mortars, *Cement and concrete research* 36, Elsevier publications, UK, pp 1903-1907

Sinthaworn, S. and Nimityogskul (2009), Quick monitoring of pozzolanic reactivity of waste ashes, *Waste Management* 29(5), pp 1526 -1531

Sinsiri, T., Kroehong, W., Jaturapitakkul, C. and Chindaprasirt, P. (2012), Assessing the effect of biomass ashes with different fineness on the compressive strength of blended cement paste, *Materials and Design* 42, pp 424 – 433

Skibsted, J., Hall, C. (2008), Characterization of cement minerals, cement and their reaction products at the atomic and nano scale, *Cem Concr Res* 38, pp 18-19

Skibsted J., Henderson E., Jakobsen H.J. (1993), Characterization of calcium aluminate phases in cements by ²⁷Al MAS NMR spectroscopy, *Inorg Chem* 32, pp 1013–1027
Sneddon C, Howarth RB, Norgaard RB (2006) Sustainable development in a postBrundtland world, *Ecological Economics* 57(2), pp 253–268.

Sobolev, K., Tturker, P., Soboleva, S., and Iscioglu, G. (2007), “Utilization of waste glass in eco-cement: strength properties and microstructural observations”. *Waste Management*, 27, pp 971-976.

Solow, R.M. (2000), Sustainability: and economist’s perspective. In Starvins, pp 131-138

Sperinck, S., Raiferi, P., Marks, N., Wright, K. (2011), Dehydroxylation of kaolinite to metakaolin- a molecular dynamic study, *J. Mater. Chem* 21, pp 2118-2125

Stark, J. (2011), Recent advances in the field of cement hydration and microstructure analysis, *Cement and Concrete Research* 41, pp 666 – 678

Stebbins, J.F. and Kanzaki, M. (1991), Local Structure and Chemical Shifts for Six Coordinated Silicon in High-Pressure Mantle Phases, *Science, New Series*, Vol. 251 (4991), pp. 294-298

Sutherland, K. (2006), Opinion: Sustainability – moving forward?, *Filtration & Separation*, Vol. 43(3), pp 40 – 42

Svinning, K. and Høskuldsson, A. (2006), Design and manufacture of Portland cement— application of sensitivity analysis in exploration and optimization Part II. Optimisation, *Chemometrics and Intelligent Laboratory Systems* 84, pp 188–194

Swart, R. J., Raskin, P. & Robinson, J. (2004), The problem of the future sustainability science and scenario analysis, *Global Environmental Change* 14, Elsevier, pp 137 – 146

Sudo, S., Takahashi, F., & Takenchi, M. (1989), Chemical properties of biomass, In: O. Kitani, C. W. (Eds), *Biomass Handbook*, Gordon and Breach, New York, pp 133-141

- Talero, R. (2005), Performance of metakaolin and Portland cements in ettringite formation as determined by ASTM C452 – 68: Kinetic and morphological differences. *Cement and Concrete Res.* 35, pp 1269 – 84
- Tam, C.M., Vivian, W.Y., Tam and Ng, K.M. (2012), Assessing drying shrinkage and water permeability of reactive powder concrete produced in Hong Kong 26, pp 79-89
- Taylor, H. F. W. (1997), *Cement chemistry*, Thomas Telford Publication, 2nd Ed., London
- Taylor, H.F.W. (1998) *Cement Chemistry*. 2th Edition, Thomas Telford Publication, London
- Taylor-Lange, S.C., Lamon, E.L., Riding, K.A., Juenger, M.C.G. (2015), Calcined kaolinite–bentonite clay blends as supplementary cementitious materials, *Applied Clay Science* 108, pp 84–93
- Thomas, J. J., Biernaki, J. J., Bullard, J. W., Bishnoi, S., Dolado, J. S., Scherer, G. W. and Luttge, A. (2011), Modelling and simulation of cement hydration kinetic and microstructure development, *Cement and Concrete Research* 41, pp 1257 – 1278
- Tikalsky, P. J., Carras, quillo, R. L. (1992), Influence of fly ash on the sulfate resistance of concrete, *ACI Material Journal* 89(1), pp 69 – 75
- Tironi, A., Terezza, M. A., Scian, A. N. and Irassar, E. F. (2013), Assessment of Pozzolanic activity of different calcined clays, *Cement & Concrete Composites* 37, pp 319 – 327
- Toledo Filho, R.D., Gonclaves, J.P., Americano, B.B. and Fairbairn, E.M.R. (2007), Potential for use of crushed waste calcined clay brick as supplementary cementitious material in Brazil, *Cement & Concrete Res.* 37(9), pp 1357-1365
- Turkmenoglu, A. G. & Tankut, A. (2002), Use of tuffs from central Turkey as admixture in Pozzolana cements assessment of their petrographical properties, *Cement and Concrete Res.* 32, pp 629 – 637
- Twidell, J. & Weir.T, (2005), *Biomass and Biofuel*. In: *Renewable energy resources*, 2nd edition, Spoon Press, pp 351-399
- Umar, M. S., Jennings, P., Urme, T. (2014), Generating renewable Energy from Oil Palm Biomass in Malaysia: The Feed-in Tariff policy framework. *Biomass and Bioenergy* 62: pp 37–46.
- Uzal, B., Turanli, H, Yucel, H., Guncuoglu, M. C. and Culfaz, A. (2010), Pozzolanic activity of clinoptilolite: A comparative study with silica fume, fly ash and non-zeolitic natural pozzolan, *Cement and Concrete Res.* 40(3), pp 398 – 404

- Uzal, B. and Turanli, L. (2003), Studies on blended cements containing a high volume of natural pozzolans, *Cem & Conc Res.*33, pp 1777- 17811
- Uzan, B.B., and Sarioglu, N. (2009), Rapid and catalytic pyrolysis of corn stalks, *Fuel processing Technology* 90, pp705-16
- Van, V. F. A., Ropler, C., Bui, D. D., Ludwig, H. M. (2013), Mesoporous structure and pozzolana reactivity of rice husk ash in cementitious system, *Construction and Building Materials* 43, pp 208 – 216
- Van, V-T-A., Robler, C., Bui, D. D., Ludwig, H. M. (2013), Mesoporous structure and pozzolanic reactivity of rice husk ash in cementitious system, *Construction and Building Materials*, pp 208 – 216
- Vassilev, S.V., Baxter D., Andersen L. K., Vassileva, C.G, Morgan T.J. (2012), An overview of the organic and inorganic phase composition of biomass, *Fuel* 94, pp, 1-33
- Velosa, A. L., Veiga, R., Coroado, J., Ferreira, V. M. & Rocha, F. (2010), Characterization of Ancient pozzolanic mortars from Roman Times to the 19th Century: Compatibility Issues of New Mortars with substrates and ancient Mortars, In *Materials, Technologies and Practice in History heritage*. pp 235 – 36
- Voinor & Farley (2007), Reconciling sustainability, systems theory and discounting, *Futures*, Vol. 42(7), pp 743 – 748
- Wab Ab Karim Ghani, W.A., Abdullah, M.S.F., Matori, K.A., Alias, A.B, da Silva, G. (2010), Physical and thermochemical characterization of Malaysian biomass ashes, *Journal- The institution of Engineers, Malaysia* 71 (3), pp 9-18
- Wanson, S., Jarja turaphan, S. and Sinthupinyo, S. (2010), Characterizing pozzolanic activity of rice husk ash by impedance spectroscopy, *Cement and Concrete Res.* 40, pp 1714 – 22
- Wackernagel, M. and Rees, W.E. (1996), *Our Ecological Footprint: Reducing Human Impact on the Earth*, Gabriola Press New Society Publishing, B.C.
- Wassermann, R., Katz, A., and Bentur, A. (2009), Minimum cement content requirements: a must or a myth? *Materials and Structures* 42, pp 973–982
- WCED (World Commission on Environment and Development) (1987), *Our Common Future*. Oxford University Press, Oxford
- Williams, A., Jones, J.M., Ma, L., Pourkashanian, M. (2012), Pollutants from the combustion of solid biomass fuels, *Progress in Energy and Combustion Science* 38, pp113-37

Wilson, J. W. and Ding, T. C. (2007), A comprehensive report on pozzolana admixtures, the cement industry, Market and Economic Trends and major companies operating in the Far East with reference to Pagan Island, pp 1 – 60

Wilin´ska, I., Pacewska, B. (2014), Calorimetric and thermal analysis studies on the influence of waste aluminosilicate catalyst on the hydration of fly ash–cement paste, *J. Therm Anal Calorim* 116, pp 689-697

Worasuwannarak, N., Sonobe, T., Tanthapanichakoon, W. (2007), Pyrolysis behaviors of rice straw, rice husk and corn cob by TG-MS technique, *J. Anal. Appl. Pyrolysis* 78, pp 265-271

Wright, S. D. & Lund, D. A. (2000), Gray and green, stewardship and sustainability in an aging society, *Journal of Aging Studies*, Vol. 14 (3), pp 229 – 249

Xiamong, L., Na, Z., Henghu, S., Jixlu, Z. and Longtu, L. (2011), Structural investigation relating to the cementitious activity of bauxite residue red mud, *Cem. Conc Res* 41, pp 847-853

Xiujuan, G., Shurong, W., Qi, W., Zuogang, G. and ZZhongyang, L. (2011), Properties of bio-oil from fast pyrolysis of rice husk, *Biotechnology and Bioengineering* 19 (1), pp 116-121

Xu, W., Lo, T. U., and Menon, S. A. (2012), Microstructure and reactivity of rich husk ash, *Construction and Building Materials*, pp 541 – 547

Yu, L., Zhou, X., Deng, W. (2015), Pozzolanic activity of volcanic rocks from Southern Jiangxi Province, China, *Journal of Sustainable Cement-based Materials*, pp 1-23

Yuzer, N., Cinar, Z., Akoz, F., Biricik, H., Gurkan, Y. Y., Kabay, N., and Kizikanat, A. B. (2013), Influence of raw rice husk addition on structure and properties of concrete, *Construction and Building Materials* 44, pp 54 – 62

Zhang, D., Zhou, C-H., Lin, C-X., Tong, D-S & Yu, W-H. (2010), Synthesis of clay minerals, *Applied Clay Science* 50, pp 1-11

Zhang Y.M., Sun W., Yan H.D., (2000), Hydration of high-volume fly ash cement pastes. *Cem Concr Compos* 22, pp 445–52

Zhang, T., Yu, Q., Wei, J. and Zhang, P. (2012), Efficient utilization of cementitious materials to produce sustainable blended cement, *Cement and Concrete* 34, pp 692 – 699

Zhou, C.H., and Keeling, J. (2013), Fundamental and applied research on clay minerals: From climate and environment to nanotechnology, Applied Clay Science 74, pp 3-9

Zivica, V. and Bajza, A. (2001), Acidic attack of cement based materials- a review Part 1, Principle of acidic attack, Construction and Building materials, Vol. 15, Elsevier publication, UK, pp 331-340.

KNUST

APPENDICES

Appendix 3.1: Chemical composition of Ashgrove and Ghacem cements

Item	Ordinary Portland Cement	
	Ash grove	Ghacem
SiO ₂	20.49	19.7
Al ₂ O ₃	4.26	5
Fe ₂ O ₃	3.14	3.16
CaO	63.48	63.03
MgO	2.11	1.75
SO ₃	2.9	2.8
Na ₂ O	0.18	0.2
K ₂ O	0.47	0.16
LOI	2.2	2.58
C ₃ S	56	59.6
C ₂ S	17	12.6
C ₃ A	6	7.86
C ₄ AF	9	9.49

Appendix 3.2: t-Test on Portland cements

Two-Sample Assuming Unequal Variances

Ash grove	Ghacem
-----------	--------

Mean	14.40230769	14.45615385
Variance	445.0807526	463.291309
Observations	13	13
Hypothesized	Mean	
Difference	0	
df	24	
t Stat	-0.006441611	
P(T<=t) one-tail	0.49745681	
t Critical one-tail	1.71088208	
P(T<=t) two-tail	0.99491362	
t Critical two-tail	2.063898562	

Appendix 4.1(a): Compressive strength values of blended cement and clay pozzolana mortars

Mix name	3d			7d			28d		
	1	2	3	1	2	3	1	2	3
control	27.6	29.4	29.4	33.6	32.4	31.6	44.1	44.4	44.0
10P800	29.8	28.8	28.8	33.2	32.4	34.2	38.8	39.6	40.5
20P800	31.4	30.5	30.5	40.3	41.3	38.8	47.2	48.5	46.9
30P800	21.8	21.2	21.2	28.3	28.8	26.8	36.3	34.0	34.2
40P800	18.1	18.6	18.6	22.9	22.5	26.6	30.4	30.3	29.5
50P800	15.2	15.1	15.1	19.7	19.3	19.3	26.9	27.3	26.7

Appendix 4.1(b): Mean, standard deviation and coefficient of variance of strength values in a

Mix name	3d			7d			28d		
	Mean	ST.D	COV	Mean	ST.D	COV	Mean	ST.D	COV
control	28.8	1.0390	3.61%	32.5	1.0	3.03%	44.14	0.20	0.45%
10P800	29.1	0.5812	1.99%	33.2	0.9	2.72%	39.65	0.82	2.06%
20P800	30.8	0.5215	1.69%	40.1	1.3	3.13%	47.55	0.86	1.81%
30P800	21.4	0.3463	1.62%	27.9	1.1	3.79%	34.82	1.30	3.72%

40P800	18.5	0.3105	1.68%	24.0	2.3	9.41%	30.07	0.49	1.61%
50P800	15.1	0.0796	0.53%	19.4	0.2	1.14%	26.95	0.32	1.17%

N.B:ST.D- standard deviation; COV-coefficient of variance

Appendix 4.2: Student t-test analysis between RH1 and RH2

t-Test: Two-Sample Assuming Unequal Variances

	<i>7d</i>	<i>28d</i>
Mean	117	117.5
Variance	2	4.5
Observations	2	2
Hypothesized Mean Difference	0	
df	2	
t Stat	-0.277350098	
P(T<=t) one-tail	0.403774955	
t Critical one-tail	2.91998558	
P(T<=t) two-tail	0.80754991	
t Critical two-tail	4.30265273	

Appendix 4.3: Student t-test analysis between 20RH1 and 30RH1 t-Test:

Paired Two Sample for Means

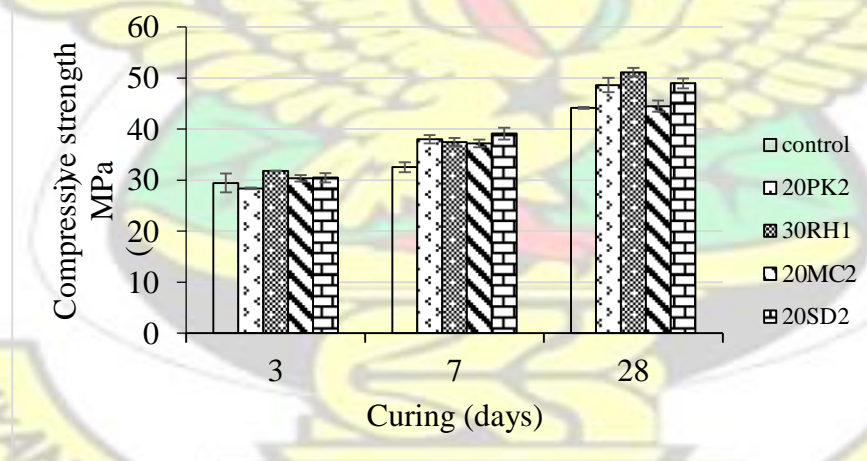
	<u>20RH1</u>	<u>30RH1</u>
Mean	40.33333333	40
Variance	114.3333333	97
Observations	3	3
Pearson Correlation	0.997050141	
Hypothesized Mean Difference	0	2
t Stat	0.5	
P(T<=t) one-tail	0.333333333	t Critical one-tail
	2.91998558	P(T<=t) two-tail
	0.666666667	t
Critical two-tail	4.30265273	

Appendix 4.4: Student t-test analysis between 10MC2 and 20MC2

t-Test: Paired Two Sample for Means

	10MC2	20MC2
Mean	37	37
Variance	43	49
Observations	3	3
Pearson Correlation	0.991240707	
Hypothesized Mean Difference	0	
df	2	
t Stat	0	
P(T<=t) one-tail	0.5	
t Critical one-tail	2.91998558	
P(T<=t) two-tail	1	
t Critical two-tail	4.30265273	

Appendix 4.5: Comparison of strength performance of control and mortar mixes



Appendix 4.6: Anova outcome of control and optimum mortar mixes

Source of Variation	SS	df	MS	F	P-value	F crit
Rows	42.4	4	10.6	3.2	0.08	3.8
Columns	765.8	2	382.9	115.4	1.26E-06	4.5

Error	26.5	8	3.3
Total	834.8	14	

Appendix 4.7: Anova test for shrinkage of CON, 20P800 and 20PK2 at 7, 11, and 18 days

<i>Source of Variation</i>	<i>SS</i>	<i>df</i>	<i>MS</i>	<i>F</i>	<i>P-value</i>	<i>F crit</i>
Curing period Mortar mixtures	46.96412975	3	15.65470992	0.993695765	0.438811569	3.862548358
Error	699.9895609	3	233.3298536	14.81080701	0.00079342	3.862548358
Total	141.7862431	9	15.75402701			
Total	888.7399338	15				

